Optimal Configuration of Distributed Energy Systems with Hydrogen as Energy Carrier under Sustainability Criteria

Juan Fonseca

École Doctorale SIMPPÉ - Sciences et Ingénierie des Molécules des Produits des Procédés et de l'Énergie

Configuration optimale des systèmes d'énergie distribuée avec l'hydrogène comme vecteur d'énergie selon les critères de durabilité

Thèse présentée et soutenue publiquement pour l'obtention du titre de :

Docteur de l'Université de Lorraine

Mention : Génie des Procédés, des Produits et des Molécules

Par :

Juan David FONSECA GAMBOA

Avec le soutien de :

Soutenue publiquement le 3 Décembre 2020 à Nancy, France

Membres du jury :

Rapporteurs :	Prof. Andrea RAMIREZ	Delft University of Technology
	Prof. Stéphane NEGNY	Université de Toulouse
Examinateurs :	Prof. Melika HINAJE	Université de Lorraine
	Prof. Paulo César NARVAEZ	Universidad Nacional de Colombia
	Prof. Julio César VARGAS	Universidad Nacional de Colombia
Invité :	Prof. Jean-Marc COMMENGE	Université de Lorraine
Directeur :	Prof. Mauricio CAMARGO	Université de Lorraine
Co-directeur :	Prof. Laurent FALK	Université de Lorraine
Co-directeur :	Prof. Iván Darío GIL	Universidad Nacional de Colombia

This work was developed under a joint supervision agreement with the

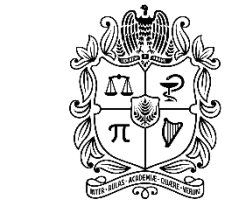

UNIVERSIDAD
NACIONAL
DE COLOMBIA

Optimal Configuration of Distributed Energy Systems with Hydrogen as Energy Carrier Under Sustainability Criteria

Doctoral dissertation presented in partial fulfillment of the requirements for the degree of:

Doctor of Philosophy – Chemical Engineering

By:

Juan David Fonseca Gamboa

Research Group:

Grupo de Procesos Químicos y Bioquímicos

Universidad Nacional de Colombia

Facultad de Ingeniería, Departamento de Ingeniería Química y Ambiental

Bogotá, Colombia, 2020

Acknowledgments

First, I would like to thank to my advisors, Professors Mauricio Camargo, Laurent Falk and Iván Gil for their kind guidance, suggestions, and support throughout the development of this work. Also, I would like to express my great gratitude to the Professor Jean-Marc Commenge. He was not my advisor for the administrative issues, but he was involved in the project as much as the other advisors. With all of them, I am especially grateful for their patience, time, encouragement, and for given me as diverse as valuable perspectives to address this project. Thanks to their enthusiasm, kindness, and constructive feedback, they made of this work an experience full of learnings for my professional and personal life.

This thesis was developed under a joint supervision agreement between Universidad Nacional de Colombia and Université de Lorraine. Thus, I want to express my deep and sincere gratitude to:

- Professor Alvaro Orjuela for his guide and support during my first research experiences. Also, for his advices and motivation to undertake this adventure.
- María Fernanda Acevedo and Luis Carlos López who collaborated in the project during their international internships.
- All the members of the Grupo de Procesos Químicos y Bioquímicos, especially to Sandra Arroyave, César Sánchez, Andrés Herrera, Jesús Jaime, Nicolás Correa, Felipe Martínez, Jesús Quintero, Rodrigo Ibarra, Sergio López, and Jean Pimentel. All of them made part of this project in some way.
- All the members of the Équipe de Recherche sur les Processus Innovatifs (ERPI), especially to Diana Cárdenas for kindly allowing me to perform some simulations in her computer. Also, to Cindy Neves, Thomas Didier, Julie Creusat, Laëtitia Laurent, and Alexandra Melon for their help with the administrative issues.

Also, I want to thank to Lorraine Université d'Excellence, since this work was developed within the IMPACT project Université de Lorraine Hydrogène Science et Technologies (ULHyS), and it was supported partly by the french PIA project « Lorraine Université d'Excellence », reference ANR-15-IDEX-04-LUE.

Abstract

This work focuses on the conceptual design of distributed energy systems considering the sustainability dimensions. The design problem is addressed by means of an optimization-based strategy that enables to integrate different energy vectors and multiple technological units as possible solutions. The modeling approach considers the time-varying operation of the energy conversion units along with the seasonal behavior of the storage system. Meanwhile, the multi-objective optimization problem simultaneously addresses economic, environmental, and social aspects for the design of the energy system. Total annualized cost, levelized cost of energy, CO_2 emissions, water consumption, grid dependence, and inherent safety are the selected indicators to evaluate the sustainability dimensions. Two case studies are analyzed to illustrate the proposed framework. The first case study is in France and corresponds to a grid-connected energy system conceived to satisfy the electricity and hydrogen needs of a neighborhood of 1500 inhabitants. The second case study is an isolated energy system located in a remote region in the Colombian Amazon. In such a case, the objective is to design a self-sufficient energy system with the capacity for supplying electricity and methane to a community of 4200 inhabitants. Initially, the impact of the sustainability indicators on the optimal design of the energy systems is investigated through single-objective optimizations. Besides, the time-varying operating conditions and the seasonal behavior of the energy storage units are also analyzed. Subsequently, different multi-objective optimization problems are addressed considering different combinations of the sustainability indicators. In such a way, the compromise among the objective functions is identified, and the obtained Pareto solutions are explored for elucidating the changes in the design and operating conditions throughout the non-dominated solutions. Broadly, these results constitute a valuable information about the relationships between the sustainability dimensions in terms of design and operation variables. Accordingly, the proposed approach represents a useful tool for decision-makers to make informed decisions from early stages in the energy system design.

Keywords: Hydrogen, sustainability assessment, renewable energy, energy system design, power-to-gas, multi-objective optimization.

Resumen

Este trabajo se centra en el diseño conceptual de sistemas descentralizados de energía considerando las dimensiones de la sostenibilidad. El problema se aborda mediante una estrategia basada en la optimización que permite integrar diferentes formas de energía y múltiples unidades tecnológicas como posibles soluciones. El enfoque de modelación considera el funcionamiento variable en el tiempo de las unidades de conversión de energía y el comportamiento estacional del sistema de almacenamiento. Mientras tanto, la optimización multiobjetivo aborda simultáneamente los aspectos económicos, ambientales y sociales para el diseño del sistema de energía. El costo total anualizado, el costo nivelado de la energía, las emisiones de CO_2, el consumo de agua, la dependencia de la red y la seguridad inherente son los indicadores seleccionados para evaluar las dimensiones de la sostenibilidad. Se analizan dos estudios de caso para ilustrar el marco propuesto. El primer estudio de caso se encuentra en Francia y corresponde a un sistema de energía conectado a la red concebido para satisfacer las necesidades de electricidad e hidrógeno de un barrio de 1500 habitantes. El segundo estudio de caso es un sistema de energía aislado ubicado en una región remota de la Amazonia colombiana. En este caso, el objetivo es diseñar un sistema energético autosuficiente con capacidad para suministrar electricidad y metano a una comunidad de 4200 habitantes. Inicialmente, se investiga el impacto de los indicadores de sostenibilidad en el diseño óptimo de los sistemas energéticos mediante optimizaciones mono-objetivo. Además, se analizan los perfiles de operación (en función del tiempo) y el comportamiento estacional de las unidades de almacenamiento de energía. Posteriormente, se abordan diferentes problemas de optimización multi-objetivo considerando diferentes combinaciones de los indicadores de sostenibilidad. De esta manera, se identifican las relaciones entre las funciones objetivo, y se exploran las soluciones de Pareto para dilucidar los cambios en el diseño y las condiciones de operación a lo largo de las soluciones no dominadas. En general, estos resultados constituyen una valiosa información acerca de las relaciones entre las dimensiones de la sostenibilidad en términos de variables de diseño y operación. En consecuencia, el enfoque propuesto representa un instrumento útil para que los encargados de la adopción de decisiones tomen decisiones informadas desde las primeras etapas del diseño.

Palabras clave: Hidrógeno, evaluación de sostenibilidad, energía renovable, diseño del sistema de energía, optimización multi-objetivo.

Résumé

Ce travail se concentre sur la conception de systèmes énergétiques distribués en tenant compte des dimensions de durabilité. Le problème de la conception est abordé au moyen d'une stratégie basée sur l'optimisation qui permet d'intégrer différents vecteurs énergétiques et de multiples unités technologiques comme solutions possibles. L'approche de modélisation prend en compte le fonctionnement variable dans le temps des unités de conversion d'énergie ainsi que le comportement saisonnier du système de stockage. Parallèlement, le problème de l'optimisation multi-objectifs aborde simultanément les aspects économiques, environnementaux et sociaux de la conception du système énergétique. Le coût total annualisé, le coût nivelé de l'énergie, les émissions de CO_2, la consommation d'eau, la dépendance au réseau et la sécurité inhérente ont été les indicateurs choisis pour évaluer les dimensions de la durabilité. Deux études de cas ont été analysées pour illustrer le cadre proposé. La première étude de cas est en France et correspond à un système énergétique connecté au réseau conçu pour satisfaire les besoins en électricité et en hydrogène d'un quartier de 1500 habitants. La seconde étude de cas est un système énergétique isolé situé dans une région reculée de l'Amazonie colombienne. Dans un tel cas, l'objectif était de concevoir un système énergétique autonome capable de fournir de l'électricité et du méthane à une communauté de 4200 habitants. Dans un premier temps, l'impact des indicateurs de durabilité sur la conception optimale des systèmes énergétiques a été étudié par le biais d'optimisations à objectif unique. En outre, les conditions de fonctionnement variables dans le temps et le comportement saisonnier des unités de stockage d'énergie ont également été analysés. Par la suite, différents problèmes d'optimisation multi-objectifs ont été abordés en combinant les indicateurs de durabilité. De cette manière, le compromis entre les fonctions objectives a été identifié, et les solutions de Pareto obtenues ont été explorées pour élucider les changements dans la conception et les conditions d'exploitation à travers les solutions non dominées. Dans l'ensemble, ces résultats constituent une information précieuse sur les relations entre les dimensions de durabilité en termes de variables de conception et d'exploitation. En conséquence, l'approche proposée représente un outil utile pour les décideurs afin de prendre des décisions éclairées dès les premières étapes de la conception du système énergétique.

Mots-clés : Hydrogène, évaluation de la durabilité, énergie renouvelable, conception de systèmes énergétiques, électricité-gaz, optimisation multi-objectifs.

Content

List of Figures

Page

List of Tables

Page

List of Symbols and Abbreviations

Nomenclature

Symbol	Definition	Units
PV_T	Power generated by photovoltaics	kW
n_{PV}	Efficiency of photovoltaics	-
I	Solar irradiance	kW/m^2
A	Area of photovoltaics	m^2
n_s	Panel efficiency at reference conditions	-
β	Temperature coefficient	-
T_a	Ambient temperature	°C
T_{ref}	Temperature at reference conditions	°C
T_{NOCT}	Nominal operating cell temperature	°C
I_{NOCT}	Irradiance at nominal operating conditions	kW/m^2
W_T	Power generated by wind turbine	kW
v_w	Wind speed	m/s
v_{cut-in}	Speed at which turbine starts to generate electricity	m/s
$v_{cut-out}$	Speed at which turbine shuts-down	m/s
v_{rated}	Speed for the maximum electricity generation	m/s
El_{in}	Input power to the electrolyzer	kW
El_{out}	Output power of the electrolyzer	kW
n_{el}	Efficiency of electrolyzer	-
LHV_{H2}	Low heating value of hydrogen	kJ/kg
$H_{2,El}$	Mass flow rate of hydrogen from electrolyzer	kg/s
H_2O_{El}	Mass flow rate of water to the electrolyzer	kg/s
$O_{2,El}$	Mass flow rate of oxygen from the electrolyzer	kg/s
PM_{O2}	Molecular weight of oxygen	kg/kmol
PM_{H2}	Molecular weight of hydrogen	kg/kmol
PV_{H2}	Photovoltaic electricity used in electrolysis	kW
W_{H2}	Wind electricity used in electrolysis	kW
EG_{H2}	Electricity from the grid used in electrolysis	kW
FC_{in}	Input power to the fuel cell	kW
FC_{out}	Output power of the fuel cell	kW
n_{FC}	Efficiency of the fuel cell	-
$H_{2,FC}$	Mass flow rate of hydrogen to the fuel cell	kg/s
$O_{2,FC}$	Mass flow rate of oxygen to the fuel cell	kg/s
H_2O_{FC}	Mass flow rate of water from the fuel cell	kg/s
FC_{th-out}	Output thermal power from the fuel cell	kW
S_B	Energy stored in the battery	kWh
S_{H2}	Energy stored in the pressurized tank	kWh
n_{ch}	Charging efficiency of the battery	-
n_{dch}	Discharging efficiency of the battery	-
B_{in}	Input power to the battery	kW
B_{out}	Output power of the battery	kW

Symbol	Definition	Units
$S_{H2,in}$	Input power to the pressurized tank	kW
$S_{H2,out}$	Output power of the pressurized tank	kW
$CH_{4,AD}$	Volumetric flow rate of methane from digester	m^3/s
AD_{out}	Output power of the digester	kW
AD_{in}	Mass flow rate of biomass to the digester	kg/s
n_{AD}	Yield to methane of the digestion process	-
n_{VS}	Fraction of volatile matter in biomass	-
n_{up}	Recovery fraction of biogas upgrading	-
LHV_{CH4}	Low heating value of methane	kJ/m^3
$CO_{2,AD}$	Carbon dioxide from anaerobic digestion	m^3/s
R_{in}	Input power to the reformer	kW
R_{out}	Output power of the reformer	kW
n_R	Efficiency of the reforming process	-
AD_{H2}	Biomethane fed to the reformer	kW
NG_R	Natural gas from the network fed to the reformer	kW
$CH_{4,R}$	Mass flow rate of methane to the reformer	kg/s
$H_{2,R}$	Mass flow rate of hydrogen from the reformer	kg/s
$CO_{2,R}$	Mass flow rate of carbon dioxide from the reformer	kg/s
H_2O_R	Mass flow rate of water to the reformer	kg/s
M_{in}	Input power to the methanation	kW
M_{out}	Output power of the methanation	kW
n_M	Efficiency of the methanation	-
$CH_{4,M}$	Mass flow rate of methane from methanation	kg/s
$H_{2,M}$	Mass flow rate of hydrogen to the methanation	kg/s
$CO_{2,M}$	Mass flow rate of carbon dioxide to the methanation	kg/s
H_2O_M	Mass flow rate of water from the methanation	kg/s
M_{th-out}	Output thermal power from the methanation	kW
D_{el}	Demand of electricity	kW
PV_D	Photovoltaic electricity used for the demand	kW
W_D	Wind electricity used for the demand	kW
EG_D	Electricity from the grid for the electricity demand	kW
NG_D	Natural gas taken from the network for the demand	kW
EG_T	Total electricity taken from the grid	kW
NG	Total natural gas taken from the network	kW
Q_{th}	Total output of thermal power	kW
C	Capital cost	€/ kW – €/ kWh
Cap	Capacity	kW – kWh
r	Discounting rate	%
$O\&M_F$	Fixed operational and maintenance costs	€
OC_V	Variable operational cost	€
C_{EG}	Price of grid electricity	€/ kWh
C_{NG}	Price of natural gas from the network	€/ kWh
C_{Bio}	Price of gathering biomass	€/ ton
TE	Total energy supplied	kWh
AGE	Annual carbon dioxide emissions	ton/year
AGE_P	Carbon dioxide emissions from process operations	ton/year
AGE_G	Carbon dioxide emissions from grid energy	ton/year
AGE_B	Carbon dioxide emissions from biomass processing	ton/year
$H_{2,ref}^{f,m}$	Hydrogen from fossil-based reforming process	kg
BE_{AD}	Carbon dioxide emissions from digestion	ton/year
BE_{ref}	Carbon dioxide emissions from biomethane reforming	ton/year

Symbol	Definition	Units
$H_{2,ref}^{b,m}$	Hydrogen from biomass-based reforming process	kg
IG	Energy imported from the grid	kWh
IST	Total inherent safety index	-
I_C	Chemical safety index	-
I_P	Process safety index	-
I_{FL}	Flammability score	-
I_{EX}	Explosiveness score	-
I_{TOX}	Toxicity score	-
I_{COR}	Corrosiveness score	-
I_R	Reaction score	-
I_I	Inventory score	-
I_T	Temperature score	-
I_{Pr}	Pressure index	-
J	Performance criterion	-
El_{out}^R	Electrolytic hydrogen produced by renewables	kW
El_{out}^G	Electrolytic hydrogen produced by the grid	kW
$D_{el,M}$	Electricity demand not directly covered by renewables	kW
Re_{H2}	Renewable-based electricity used in electrolysis	kW
Re_S	Surplus electricity from renewables	kW
$S_{B,max}$	Maximum capacity of the battery	kWh
$S_{H2,max}$	Maximum capacity of the pressurized tank	kWh
Bio_D	Biomass available for digestion	ton/year
u	Decision variables	-
x	State variables	-

Greek Letters

Symbol	Definition	Units
τ	Self-discharging parameter of the battery	-
ρ_{CH4}	Density of methane	kg/m^3
ρ_{CO2}	Density of carbon dioxide	kg/m^3
λ_{ref}	Emission factor of reforming process	$kgCO_2/kgH_2$
λ_{EG}	Emission factor of grid electricity	$kgCO_2/kWh$
λ_{NG}	Emission factor of natural gas	$kgCO_2/kWh$
λ_{AD}	Emission factor of anaerobic digestion	$kgCO_2/m^3CH_4$
ψ_{El}	Water consumption in electrolysis	kgH_2O/kgH_2
ψ_{AD}	Water consumption in anaerobic digestion	kgH_2O/kg biomass
ω	Deforestation rate	%
θ	Source of hydrogen	-
φ	Source for supplying the electricity demand	-
δ	Electricity storage option	-
γ	Source of methane for reforming	-
σ	Source for supplying the methane demand	-

Abbreviations

Abbreviation	Name
DES	Distributed energy systems
MES	Multi-energy system
CHP	Combined heat and power
HES	Hybrid energy systems
PSA	Pressure swing adsorption
PEM	Polymer electrolyte membrane
SOEC	Solid oxide electrolyte cell
MILP	Mixed integer linear programming
SSG	Solution structure generation
P-graph	Process graph
TBL	Triple bottom line
TAC	Total annualized cost
LCOE	Levelized cost of energy
CAPEX	Capital expenditure
OPEX	Operational expenditure
WC	Water consumption
GD	Grid dependence
HAZOP	Hazard and operability
P&ID	Piping and instrumentation diagram
PIIS	Prototype index of inherent safety
ISI	Inherent safety index
EISI	Enhanced inherent safety index
CISI	Comprehensive inherent safety index
LP	Linear programming
GCC	Grand composite curve
PV	Photovoltaic
NIG	National interconnected grid
NIZ	Non-interconnected zones
TRL	Technological readiness level

Introduction

The expansion of the global economy, and the growing demand for heating and cooling led to an increase of 2.3% in the worldwide energy consumption and of 1.7% in CO_2 emissions in 2018 [1]. These results represent a significant concern for the energy sector, since the raising emissions trends of the last few years are not aligned with the Paris agreement for keeping the global temperature rise below 2°C [2]. In this regard, the main issues to deal with are the elevated reliance on fossil-derived fuels and the high energy intensity of certain industries. In fact, currently around 82% of worldwide energy needs are covered by fossil sources [2,3]. As a response to this scenario, and to satisfy the continuous increase in the energy consumption and to meet the world environmental goals, a global energy transformation is undergoing. This necessary change lies upon three main pillars: (i) to increase the share of renewable resources, (ii) to rise the participation of low-carbon electricity as end-use energy form, and (iii) to deploy the distributed energy generation [2–4].

In addition to mitigate the climate change effects, the use of renewable energies is boosted by concerns about air quality and energy security. In this sense, renewable sources represent a great alternative for reducing health problems derived from air contamination, for handling the finite character of fossil sources, and for providing electricity to isolated regions. Overall, the largest contribution of renewables is in the power sector, since in 2018 about 25% of electricity generation was renewable-based [1,2]. In fact, nowadays, electricity appears as one of the preferred energy carriers for supporting the deployment of renewables and facing the current environmental challenges.

Moreover, transport and residential sectors are identified as the pillars for the growth of the electricity consumption in the upcoming years [3,5]. The former, driven by using electricity in passenger rail, buses, and light vehicles in addition to the use of hydrogen (derived from renewable electricity) as transport fuel. The latter, due to the migration of communities from rural to urban areas, the rising personal income, and the increase in the access to electricity in developing countries.

Distributed generation refers to small-scale systems, typically with a capacity lower than 1000 kW and located close to the end-consumers, i.e. distributed/decentralized energy systems (DES) [6,7]. This kind of energy plants are focused on covering local demands, e.g. building, neighborhood, isolated zones, university campus or hospitals, by using specific on-site energy sources. In addition to a variety of resources, that can be renewable or conventional, DES include multiple conversion and storage technologies for supplying different demands (e.g. power, heating, cooling, fuel). In that sense, distributed generation represents a shift in the paradigm from the traditional decoupled energy systems, towards those ones including various energy forms. DES also reduce the energy losses in transmission and delivery (characteristic of centralized plants), promote the use of renewable energies (which are location-dependent and not easily transported), favor the coupling between different energy forms, boost the energy self-sufficiency, and support the energy security [7–9].

Among the variety of energy carriers involved in DES, hydrogen has the potential to play a key role in energy transition. Hydrogen offers an environmentally friendly alternative for a range of sectors including transport, chemical and power generation. It is a versatile compound that can be obtained from a variety of sources such as fossil fuels, renewables, nuclear and biomass [10]. Additionally, hydrogen as storage medium can enhance the renewables deployment by providing a mid-term (weeks) or even long-term (months) alternative to trade-off the mismatch between electricity availability and demand [11,12]. In this application, hydrogen offers an option with reduced self-discharge rate that could be reconverted into electricity when required, but also into methane (biomethane) through the power-to-gas pathway [13]. Besides storing energy over long periods, hydrogen is a promising alternative for the transport of energy from renewables through long distances. For example, hydrogen could be obtained at regions rich in solar and/or wind resources as Latin America or Australia, and then, being transported and delivered where required [11]. Broadly, hydrogen can contribute to a reliable, secure, resilient, and decarbonized energy system by enabling the sector coupling, and exploiting the synergies among different energy forms [7,11,12,14].

Despite the potential benefits of using hydrogen as energy carrier, and in general of decentralized generation, the design and operation of this kind of plants are a challenging task. At conceptual design stage, the objective is to select the process units for energy conversion and storage, their capacities and operation conditions. Besides, the interconnections between those units for transforming the energy sources into useful energy forms is also defined at this stage. Thus, the complexity lies upon three main issues:

(i) the uncertainty of input data, (ii) the great number of decisions to be made, and (iii) the need to involve different and usually contradictory objectives. The first is due to the variability and time-dependent nature of energy sources and demands, the second is due to the co-existence of multiple energy conversion and storage technologies and, the last is due to the necessity of developing a global industry in a sustainable way [15,16]. Figure 0-1 schematically depicts the framework for the conceptual design of energy systems.

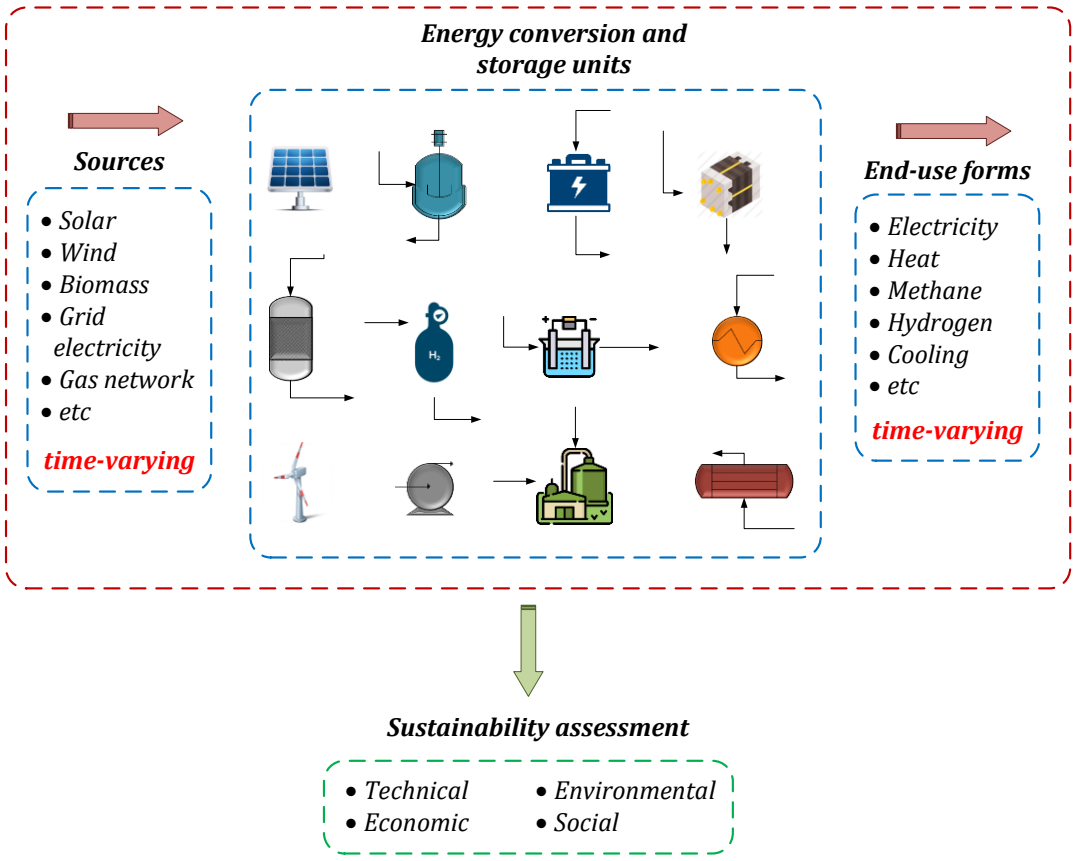

Figure 0-1: Global framework for the conceptual design of energy systems.

In general, it is well recognized that decisions made at conceptual design stage are of paramount importance because they have the greatest level of freedom, and consequently, the highest opportunity for enhancing the sustainability performance of a process [17–19]. Moreover, energy is a key component of human life since it drives many aspects of the economic and social growth (e.g. jobs, food production, incomes) [20]. The use of energy is also linked with environmental issues, as it accounts for over two thirds of worldwide greenhouse gas emissions [20,21]. Accordingly, energy could be considered as nearly the prime challenge and opportunity the world has to deal with towards sustainable development [20].

Sustainable development promotes the balance of three aspects: economic success, social acceptance, and environmental protection [22]. Thus, engineering activities must no longer be performed in isolation, since it is necessary to consider the interactions among industrial processes, society and ecosystem at every stage of an engineering project [17,23]. Therefore, sustainability analysis demands a holistic approach, and to expand the traditional system boundaries for including the economic, environmental and societal needs and constraints in the decision-making process [19,23]. Indeed, this multi-criteria evaluation typically introduces stakeholders with conflicting objectives, which represents additional difficulties during the design process [16,24].

A common strategy for evaluating process alternatives at conceptual design step is through modeling and optimization tools. Process models enable to perform a virtual representation of the reality, so that they provide a cheap, fast, and safe way for studying the impact of design decisions on the sustainability performance of a system. Nonetheless, the problem of the design and operation of energy systems potentially has many possible solutions. On the one hand, because there is a variety of process units and operating conditions that could be implemented for converting the sources into the required energy forms. On the other hand, because the sustainability assessment entails to include multiple and contradictory objectives, so that the obtained system design and operating conditions could vary as a function of each dimension of sustainability. In such a way, enumerating, evaluating, and classifying all alternatives would be an extremely time-consuming task. Then, a suitable approach is to use mathematical methods for finding the best candidate solution without explicitly testing the entire set of alternatives, i.e. to solve an optimization problem.

Optimization problems for the design of energy systems have been featured as multi-modal problems as they have multiple local solutions [25]. Also, it is recognized that single-objective optimization eases the computational burden for solving the design problem [24]. However, in such a case, as the focus is on a single criterion, the obtained result leaves aside the impact of the other criteria on the design decisions. In this regard, mono-objective optimization seems to be a suitable strategy for starting to know the search space, and to identify some extreme points within the design options. Nevertheless, as aforementioned, the sustainability assessment lies on balancing economic, environmental, and social aspects, so that it requires to simultaneously integrate multiple criteria. Accordingly, the sustainable design of energy systems turns into a multi-objective optimization problem.

In addition to deal with various objectives at the same time, multi-objective optimization enables to identify the compromise among them and provides to decision-maker a valuable information to make an informed decision. Indeed, through the exploration of the trade-offs among the sustainability dimensions, decision-maker can recognize the effect of design decisions in terms of design variables and performance criteria.

Broadly, the current state in the literature shows that the design of energy systems is predominantly performed based upon economic and environmental criteria, thus neglecting the impact of the social dimension. In fact, when included, social aspects are accounted for after to solve the optimization problem, so that they are not a criterion during the system design [25]. Nonetheless, further than being economically feasible and environmentally friendly, industrial activities must agree with social requirements, i.e. to improve the quality of life [26,27]. Moreover, even though the energy system design is primarily a technical challenge, social aspects can become the most important factors for its successful implementation in the community [28].

DES are featured as complex socio-technical systems since they involve different stakeholders in a close relation with a set of technological devices [29]. In this respect, it is paramount to promote an intense participation of all stakeholders and to integrate their perspectives into the decision-making process [30]. Indeed, this integration could enhance the community ownership with the energy technologies and to have a positive impact on their implementation [31,32]. On the contrary, the lack of stakeholders' involvement can produce resistance, and consequently, to constraint the deployment of technologically promising solutions [32]. To address this issue, it is necessary to develop methodological tools that enable to analyze these socio-technical systems within the framework of sustainable development, i.e. considering their economic, environmental, and social aspects [24,28,30].

Taking this into account, this project is envisaged to provide a comprehensive framework for the analysis and assessment of distributed energy systems considering the sustainability dimensions from the early design stages. Thus, the aim and specific objectives of this research are presented as follows.

Research Objectives

Considering the foregoing overview, the aim of this thesis is to propose and implement a modeling and optimization-based approach to support the conceptual design of distributed energy systems. Moreover, to promote the participation of stakeholders and to support the

decision-making process, the proposed framework includes the sustainability dimensions for the assessment of the technological alternatives.

Thus, the specific objectives of this research are to:

- Build a mathematical model to represent the operation of the energy system considering different conversion technologies.
- Set up two distributed energy system application cases, one in Colombia and another in France.
- Simulate and evaluate the case studies under economic, technical, environmental, and social indicators.
- Determine the systems configuration and their operational regime by means of optimization tools including sustainability criteria.

Accordingly, this document is divided in six chapters for responding to the proposed objectives and to elucidate the conclusions of the research. A summary of the contents is presented below.

Outline of the Thesis

Initially, in Chapter 1, a general context of the topic is presented. This includes a world energy outlook for identifying and point out the current state, challenges, and perspectives of the sector for the upcoming years. Then, some features of the decentralized energy systems are discussed. Also, the main technologies and the different energy forms that can be integrated in such systems are introduced. Thereafter, the focus will be on the properties of hydrogen as energy carrier and its potential applications in decentralized power plants. This chapter concludes highlighting the challenges and opportunities in the conceptual design of DES.

Chapter 2 is divided into two main parts: (i) the mathematical modeling of a base-case energy system, and (ii) the definition of the sustainability indicators for the performance assessment. In such a way, the first part includes a detailed description of the base-case energy system, and the mass and energy balances through the energy conversion and storage units. Besides, the main considerations of the proposed model are stated. Subsequently, the sustainability assessment is introduced. In this part, the main characteristics of the economic, environmental, and social dimension of sustainability are

displayed. This chapter ends by presenting the mathematical formulation of the indicators for assessing the energy system performance.

Thereafter, based upon the proposed energy system model and the selected indicators, Chapter 3 presents an optimization approach for the design and operation of energy systems. In this respect, aiming to illustrate such an approach, a case of application is developed. The case study corresponds to a neighborhood of 1500 inhabitants near Marseille – France. Accordingly, five single-optimization problems are solved including the sustainability indicators. From this chapter, a set of optimal energy system configurations and operating policies are obtained for the analyzed case study.

Next, aiming to investigate the trade-offs among the performance criteria, the multi-objective optimization is addressed in Chapter 4. Thus, based on the previous knowledge from the single-objective optimization, four multi-objective optimization problems for the optimal design and operation of the energy system are solved. Such optimization cases include different combinations of the sustainability indicators. Also, the set of Pareto solutions is explored and analyzed for identifying the changes in the design and operating conditions across the optimization results.

Chapter 5 deals with the optimal design of an isolated energy system in the Colombian Amazon region. To do so, initially, a brief context about the energy sector of Colombia is introduced. Then, the case study is presented including the base-case flowsheet, the parameters, and the constraints of the energy system according to the specific context conditions. Subsequently, four single-objective and three multi-objective optimization problems are solved for analyzing the conceptual design of the energy system.

Finally, in Chapter 6, the results of this thesis are summarized, and main conclusions are drawn. Besides, some perspectives of future work are presented.

1. Trends in Design of Distributed Energy Systems

The current situation derived from the coronavirus pandemic (Covid-19) has represented great impacts on global health, economy, energy use and CO_2 emissions. On the one hand, at 15 of June, the World Health Organization had reported 7.7 million of confirmed cases of Covid-19 and 430000 deaths due to the virus [33]. Consequently, governments have adopted measures aiming to slow the spread of the illness. Broadly, restrictions included the public gatherings and the closure of frontiers, educational institutions, and non-essential business. In fact, about 54% of global population have been affected by complete or partial lockdowns during the first semester of 2020. Otherwise, because of these unprecedent circumstances, the economic curtailment has led to a decline in energy demand of 3.8% with respect to the first quarter of 2019. In this respect, according to the perspectives of the International Energy Agency, the annual energy demand will decrease between 4 and 6%. In the same line, it is expected the CO_2 emissions push down by 8% relative to the 2019 [34].

Before the coronavirus pandemic, global energy demand grew by 2,3% in 2018, and it was expected to increase by 30% until 2040 with respect to the current world consumption. This growth is equivalent to add the consumption of China and India to the current energy demand [35]. Nevertheless, although this increase is slower than in the past, when a rise of 40% from 2000 to 2017 was registered, according to perspectives, only in Europe, United States and Japan the energy consumption will decrease in the upcoming years (Figure 1-1) [35]. This behavior is mainly driven by the constant expansion of world economy and population, and the growing demand for heating and cooling in some parts of the world. Indeed, in 2018 around 20% of the increase in energy consumption was the consequence of some extreme weather conditions (cold and hot snaps), which led to high heating and cooling needs [1].

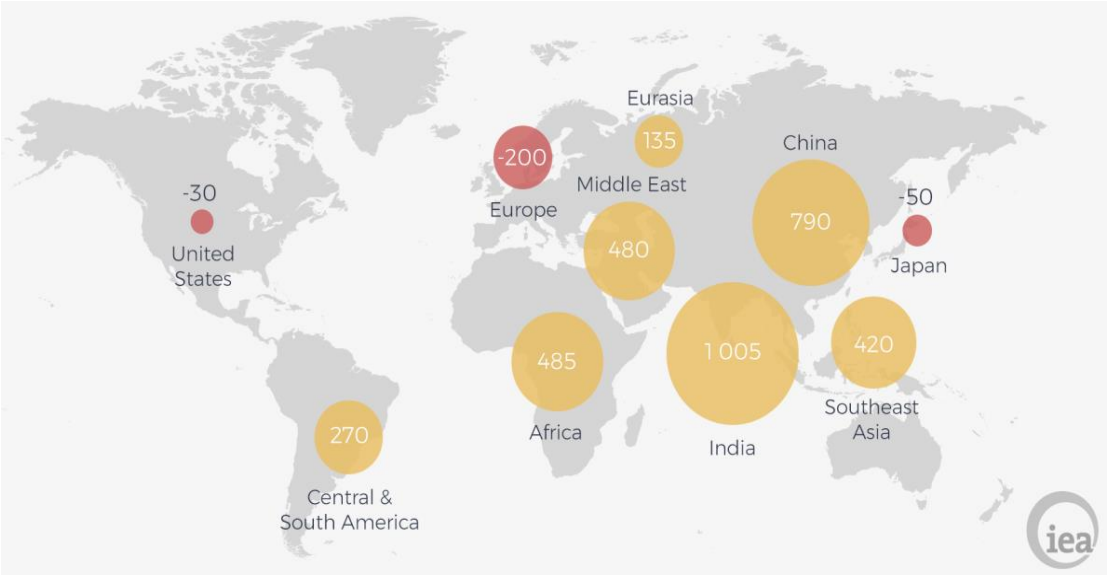

Figure 1-1: Change in energy demand 2016 – 2040 (Mtoneq) [35].

As a consequence of this growing energy demand, the CO_2 emissions also increased by 1.7% in 2018 [1]. This represents a significant concern for the energy sector, since the raising emissions trends of the last few years are not aligned with the Paris agreement for keeping the global temperature rise below 2°C [2]. In this regard, the main issues to deal with are the elevated reliance on fossil-derived fuels, and the high energy intensity of certain industries. In fact, currently around 82% of worldwide energy needs are covered by fossil sources [2,3]. Broadly, industry appears as the most challenging sector to decarbonize because of its energy and non-energy-related carbon dependence. In the former case, due to the massive energy consumption and the high temperatures that some processes demand (mainly chemical, petrochemical, and steel). In the latter case, due to the high carbon footprint of some widespread products (e.g. additives, solvents, polymers, plasticizers) [2].

Further than industry, power and transport sectors represent additional dares towards emission reduction and decarbonization objectives. On the one hand, because of power sector is responsible of the biggest part of CO_2 emissions (≈ 38%) and, on the other hand, because of transport sector has the highest reliance upon fossil fuels (≈ 94%) [2]. As a response to this scenario, and in order to both satisfy the continuous increase in the energy consumption and meet the world environmental goals, a global energy transformation is undergoing. This necessary change lies upon three main pillars: (i) to increase the share of renewable resources, (ii) to rise the participation of low-carbon electricity as end-use energy form, and (iii) to deploy the distributed generation of energy [2–4].

Besides mitigating the climate change effects, the use of renewable energies is boosted by concerns about air quality and energy security. In this sense, renewable sources represent a great alternative for reducing health problems derived from air contamination, for handling the finite character of fossil sources, and for providing electricity to isolated regions. In 2018, renewables grew by 4%, met almost one-quarter of the growth in global energy demand, and represented around 11 million of jobs worldwide [1,2]. Overall, the largest contribution of renewables is in the power sector, since in 2018 about 25% of electricity generation was renewable-based [1,2]. Indeed, electricity appears as one of the preferred energy carriers for supporting the deployment of renewables and facing the current environmental challenges. For that reason, a significant electrification of transport, industry and residential sectors is expected in order to rise the consumption of electricity as end-use energy form up to 40% by 2050 (20% currently) [2].

Transport and residential sectors emerge as the pillars for the growth in electricity consumption in the upcoming years [3,5]. The first, driven by using electricity in passenger rail, buses, and light vehicles in addition to the use of hydrogen (derived from renewable electricity) as transport fuel. The latter, due to the migration of communities from rural to urban areas, the rising personal income, and the increase in the access to electricity that developing countries are experiencing. Moreover, beyond specific sector-oriented actions, the energy transition also relies on having more flexible energy systems, i.e. capable to manage the variability of demand and supply, while ensuring instantaneous stability and long-term security of energy supply [4]. In this regard, distributed generation has the potential for providing system flexibility, and for enhancing the electricity coverage and the integration of renewable resources [2–4].

1.1 Distributed Energy Systems

Energy consumption is intrinsically decentralized, but transmission and distribution depend upon the location of the energy sources, and the place where they are converted into useful energy forms [6,36]. Thus, a typical centralized energy system consists of large generation plants, followed by transmission and distribution networks for delivering the energy to end-users. Conversely, distributed or decentralized energy systems (DES) correspond to smaller power plants, which are characterized by working with local resources and being placed (conversion and storage technologies) close to energy consumers [6,36]. Figure 1-2 depicts a schematic representation of centralized and distributed energy systems.

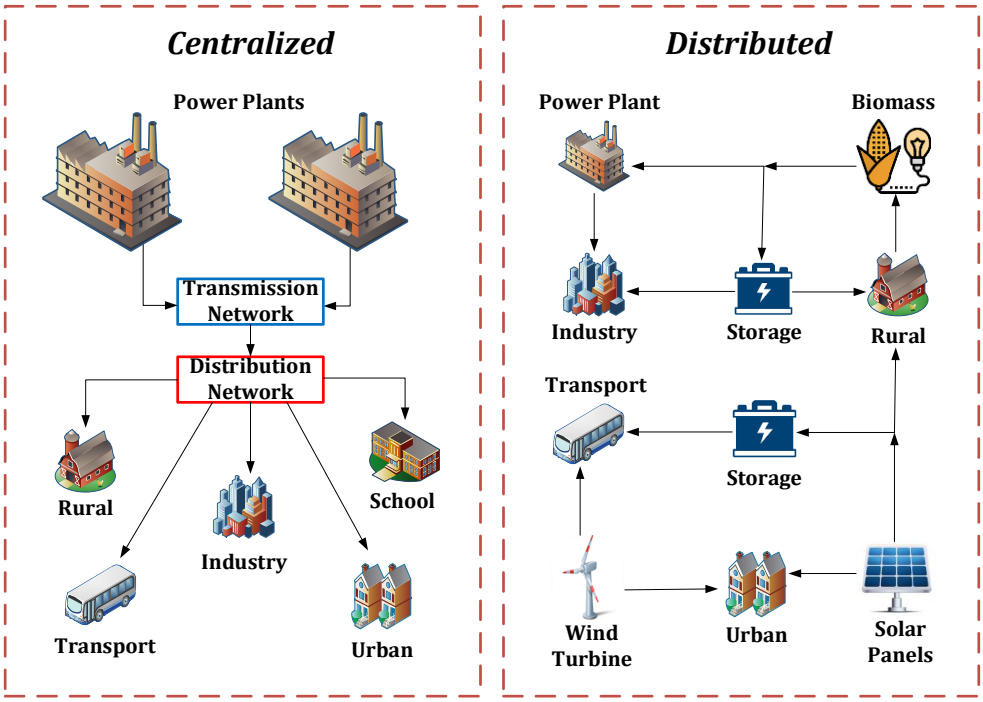

Figure 1-2: Scheme of centralized and distributed energy systems.

As aforementioned, DES refer to small-scale generation units, i.e. typically with a capacity lower than 1000 kW, and located close to the end-consumers [6,7]. This kind of energy plants are focused on covering local demands, e.g. building, neighborhood, university campus or hospitals, by using the specific on-site energy sources. In addition to the variety of resources, that can be renewable or conventional, DES include multiple conversion and storage technologies for supplying different demands (e.g. power, heating, cooling, fuel). Distributed generation offers a reliable, flexible, and efficient alternative for the energy transition. DES also reduce the energy losses in transmission and delivery (characteristic of centralized plants), promote the use of renewable energies (which are location-dependent and not easily transported), favor the coupling between different energy forms, boost the energetic self-sufficiency, and support the energy security [7–9].

Some common applications of this kind of systems are located at remote zones such as islands, which are not connected to the main grid and typically depend upon diesel generators for energy supply. For instance, at the Isabella island, that belongs to the Galapagos Islands (Ecuador), and at the Ventotene island (Italy), Siemens designed and procured decentralized power plants for covering the local energy needs [37,38]. Other examples of these systems are those ones developed by Hydro Tasmania at King Island and Coober Pedy in Australia [39]. In the same line, the European Commission has funded several projects such as GOFLEX, GRIDSOL, IElectrix, InteGrid, among others, for

supporting the integration of renewables and energy storage technologies within distributed energy systems [40].

As a result of the increasing interest on DES, a diversity of aggregation concepts and approaches have emerged for referring to this kind of systems. In the following, some of these are defined with the aim to clarify the framework of this document. However, it is important to highlight that there is no complete consensus about this terminology, and in some cases, it is used indistinctly.

1.1.1 Energy Hub

This approach represents an interface between energy sources (fossil fuels, biomass, solar, wind) and demands (electricity, cooling, heating, fuels). Energy hub is based on considering the energy system as a unit where multiple energy carriers can be converted, stored and distributed [41]. This is characterized by a black-box approach oriented to obtain an optimal arrangement among energy vectors, and where the components relationships are modelled through coupling matrices composed of efficiencies and conversion factors [36,42].

1.1.2 Microgrid

A microgrid is a local power system composed of distributed generation and storage units, in addition to clearly delimited energy loads [43,44]. Microgrids have the capability to operate in isolated (self-sufficient) and grid-connected modes, and are generally operated by means of a control center that is in charge of managing energy supply and demands in real-time [45]. One of the key advantages of microgrids lies on their distributed generation based on local resources, since besides to improve the resilience of the system, they enable the integration of renewable energies [29].

1.1.3 Multi-energy Systems

These are based on the idea of changing the paradigm where sector-oriented (electricity, heating, fueling) energy systems just have few interactions, or are even planned and operated in a completely independent way [46]. Thus, this approach intends to expand the system boundary beyond a specific energy sector in order to take advantage of the synergies provided by the integration (also called integrated energy systems) of different energy networks [45]. Regarding scale, it is important to point out that in contrast with

microgrids, multi-energy systems (MES) can be addressed for both centralized and decentralized generation.

1.1.4 Polygeneration

From the most general point of view, it consists in the generation of more than one energy vector from a single process [47]. However, the concept can be used for referring to a unit as well as to the whole system. The most common examples of polygeneration units are the combined heat and power plants (CHP) and fuel cells, where heat and electricity can be obtained from a unique fuel and process. Nonetheless, when all the energy system is considered, polygeneration represents a case of MES [45].

1.1.5 Hybrid Energy Systems

These systems represent the kind of applications where more than one energy conversion device or source are involved to supply an energy requirement [9,48]. Unlike polygeneration definition, which is based on the products, the concept of hybrid energy systems (HES) is addressed to energy sources and transformation units. For instance, a power plant fed by wind and sun, or simultaneously employing batteries and hydrogen for energy storage, can be considered as a hybrid system. Nevertheless, HES are not constrained by the products of the system (more than one could be considered), whereby they can be considered as a sub-case of MES as well.

As previously stated, one of the main characteristics of DES lies upon the integration of multiple energy forms. In that sense, distributed generation represents a shift in the paradigm from the traditional decoupled energy systems, towards those ones including various energy forms (e.g. electricity, heat, cooling, hydrogen). In this regard, the emergence of technologies such as CHP, fuel cells, electric heat pumps, and electricity-based transport appears as alternative for sector coupling [43,45,46]. Overall, further than promoting the electrification as end-use energy form, the integration of different energy vectors could lead to technical (increased efficiency), economic (reduced operating costs), environmental (reduced emissions), and social (self-sufficiency) advantages with respect to sector-oriented energy systems [4,36,43,45,46].

Among the variety of energy carriers that can be involved in DES, hydrogen has the potential to play a key role in energy transition. Hydrogen offers an environmentally friendly alternative for a range of sectors including transport, chemical and power

generation. It is a versatile compound that can be obtained from a variety of sources such as fossil fuels, renewables, nuclear and biomass [10]. Additionally, hydrogen as storage medium can enhance the renewables deployment by providing a mid-term (weeks) or even long-term (months) alternative to trade-off the mismatch between electricity availability and demand [11,12]. In this application, hydrogen offers an option with reduced self-discharge rate that could be reconverted into electricity when required, but also into methane (biomethane) through the power-to-gas pathway [13]. Broadly, hydrogen can contribute to a reliable, secure, resilient, and decarbonized energy system by enabling the sector coupling, and exploiting the synergies among different energy forms [7,11,12,14].

1.2 Hydrogen as Energy Carrier

Hydrogen is an energy carrier with a wide range of properties to be used as fuel, as raw material or as interface between electricity and chemical energy forms through the power-to-gas process. In the latter, it can be used either as storage medium to absorb the renewables fluctuation, or as feedstock for synthetic natural gas production through methanation reaction, with the key feature of offering a completely emission-free pathway [49,50]. Besides storing energy over long periods, hydrogen is a promising alternative for the transport of energy from renewables through long distances. For example, hydrogen could be obtained at regions rich in solar and/or wind resources as Latin America or Australia, and then, being transported and delivered where required [11]. Moreover, hydrogen has a high content of energy per mass (higher heating value 142 MJ/kg), which is around three times larger than common fossil-derived fuels, namely natural gas (53.6 MJ/kg), diesel (45.4 MJ/kg) and gasoline (46.4 MJ/kg). Additionally, its capability to enable the decarbonization of some chemical processes (e.g. steelmaking, oil reforming, fertilizers production) and the transport sector, makes hydrogen a key energy carrier to face the current energy and environmental challenges [10,14].

Hydrogen is not an energy source but an energy carrier, i.e. despite being the most common element on earth, it is not present by itself in nature but combined mainly with carbon and oxygen. Hence, it needs to be extracted and/or separated. In this regard, there are several sources such as biomass, fossil fuels, solar and wind energies, and different pathways, including reforming, electrochemical and biochemical processes for obtaining hydrogen.

1.2.1 Production Processes

For 2018, the world demand of pure hydrogen was around 70Mton, mainly for hydrotreating in refineries and ammonia synthesis [11,51]. This demand was almost entirely satisfied by using fossil-derived sources, 75% from natural gas and 23% from coal. The remainder was produced by oil gasification and electrolysis of water. Consequently, worldwide hydrogen production was responsible of emitting 830 MtonCO_2/year, which is equivalent to 2.8 times the annual emissions of France, or 11 times the annual emissions of Colombia [11].

As follows, a general overview including the main characteristics, strengths, weaknesses, and perspectives of the most common hydrogen production processes is presented. A summary is also presented in Table 1-1.

- *Reforming*:

Steam methane reforming (SMR) is the most mature technology and common process to produce hydrogen around the world [52]. It consists in the catalytic reaction of methane with steam to produce syngas (Equation 1.1), which is a mixture composed of H_2 and CO. In general, this reaction is carried out using a nickel-based catalyst, and under temperature and pressure ranging between 700-900°C and 3-25 bar, respectively. Then, in order to increase the amount of hydrogen, the syngas is submitted to water-gas shift reaction (Equation 1.2), where H_2 and CO_2 are the products. Finally, the resulting gas stream (rich in H_2) is subjected to separation/purification by means of pressure swing adsorption (PSA) process, to obtain the desired hydrogen purity according to its end-use [52].

$$CH_4 + H_2O \leftrightarrow 3H_2 + CO \quad (1.1)$$

$$CO + H_2O \leftrightarrow H_2 + CO_2 \quad (1.2)$$

Usually, reformer units are conceived to operate at large-scale (150-300 MW), mainly to supply refining and chemical industry requirements, with mature technologies that reach efficiencies around 70-85% [49]. However, in order to respond to the current energy trends towards decentralized systems, and the expected deployment of hydrogen as fuel in transport applications, the reforming technology is being adapted to small scales (0.15-15 MW) for on-site hydrogen production [49,52].

Furthermore, from the process perspective, it is well known that the packed-bed reactors used in large-scale plants have to deal with problems such as the diffusional limitations produced by the size of catalyst particles (needed to avoid excessive pressure drop), the

low heat-transfer rates, and the thermodynamic constraints intrinsic to equilibrium reactions [53]. Meanwhile, small-scale hydrogen production systems are operated by using process intensification principles. This kind of processes is carried out in micro-reactor reformers, which allows the deployment of on-site and portable hydrogen infrastructure. These units are composed of a set of plates with parallel channels (diameter between 10 and 500 μm), where the catalyst is charged or coated, and where the reaction occurs. As a result, this configuration provides the process with a higher surface area to volume ratio than large reactors, which leads to overcome their heat and mass transfer limitations [53,54]. As consequence of the decreasing influence of transport phenomena, in micro-reformers the process becomes kinetically controlled, and thus, it achieves additional improvement by acting over the catalyst. In this respect, it has been identified that noble metals (mainly Pt, Pd and Rh) are more active, more resistant to sulfur, and less prone to coke deposition than nickel-based ones [52,54,55]. Currently, the main challenges of these miniaturized systems concern to the sensitivity to fouling, pressure drop and difficulties in sealing, which are expected to be solved in the near future through research in the materials selection and equipment design [54].

- *Electrolysis*:

This electro-chemical process consists in splitting water into oxygen and hydrogen by using electrical energy (Equation 1.3). The electrolyzer is composed of a cathode, an anode, and an electrolyte that acts as the medium for ions transport. The process is based on the transfer of electrons through an electrical circuit and ionic species across the electrolyte, from the anode (oxidation) to the cathode (reduction), i.e. a redox reaction occurs [56]. Currently, there are three main electrolysis technologies: alkaline, polymer electrolyte membrane (PEM) and solid oxide electrolyzer cell (SOEC), which differ in the material of the electrolyte, the conversion efficiency, and the operating conditions.

$$2H_2O \rightarrow 2H_2 + O_2 \qquad (1.3)$$

Alkaline electrolyzers are the most mature technology. They use a solution of sodium or potassium hydroxide (20-40% wt.) as electrolyte, and operate at temperatures between 60-90°C with a resulting efficiency of 70-80% [52]. Unlike alkaline ones, PEM devices have an acidic and solid electrolyte, and a platinum-based catalyst is needed to make the reaction proceeds. These electrolyzers have efficiencies of 65-80%, and their working temperatures are 25-80°C [49]. Some advantages of PEM technology are its higher power density and hydrogen purity, the short response time, and its capability to operate in a wider load range and at more elevated pressures with respect to alkaline ones [52].

However, they are limited by the lifetime of the membrane and the cost of the catalyst [49]. Meanwhile, SOEC with a solid ceramic electrolyte are considered as high-temperature electrolysis units, since the reaction is carried out at 700-900°C, which allows to achieve efficiencies up to 90% [49]. Nowadays, despite the promising potential of this electrolysis alternative, SOEC is the least mature technology and its current development is still restricted at lab-scale processes [13,52,57], whereas alkaline and PEM electrolyzers systems are already available at megawatt scale [57,58]. From the economic point of view, challenges for the electro-chemical process remain. For instance, considering a price of 27 €/MWh for the natural gas, in Europe the cost for producing hydrogen from methane reforming is about 1.6 €/kg, which can be between two and five times lower than the cost of electrolysis, due to the current prices of equipment and electricity [57]. Nevertheless, thanks to the continuous research and technological developments on electrolyzers and the installation of larger plants, a significant decrease in their investment and operating costs is expected in the upcoming years [57].

- *Gasification:*

This process consists in the thermo-chemical conversion of solid or liquid carbon-formed materials (fossil fuels or biomass) into hydrogen and carbon monoxide (syngas). However, depending on the feedstock and operating conditions, CH_4, H_2S, CO_2 and NH_3 can be produced as well [59]. Gasification is a process involving different steps. The first one is the moisture removal (drying); then, a chemical decomposition by heating in absence of oxygen (pyrolysis) is done to release volatile compounds (mainly CH_4, CO, H_2). In the next step, an oxygen-controlled environment is supplied to the system for the combustion of the volatile matter, which helps to increase the process temperature and provides the medium for the subsequent operation. Finally, the gasification ends with the reactions (Equations 1.4-1.7) between the char coal and a gas phase mainly composed of CO_2, H_2O and O_2 under temperatures of 800-1300°C [59].

Subsequently, depending on the end-use of the syngas produced, it is further subjected to water-gas shift reaction and/or purification processes to employ it as fuel, or raw material for methanol or synthetic natural gas production (methanation) [59].

$$C_{(s)} + O_2 \rightarrow CO_2 \quad (1.4)$$

$$2C_{(s)} + O_2 \rightarrow 2CO \quad (1.5)$$

$$C_{(s)} + H_2O \leftrightarrow H_2 + CO \quad (1.6)$$

$$C_{(s)} + 2H_2O \leftrightarrow 2H_2 + CO_2 \quad (1.7)$$

In general, gasifiers can be classified according to a wide variety of characteristics such as bed temperature and type, pressure, oxidant flow through the equipment and ash formations [59,60]. The most conventional classification considers entrained-flow, fixed-bed, and fluidized-bed gasification technologies. Currently entrained-flow gasifiers are the most efficient alternative and have the smallest environmental impact and the largest production capacity. Hence, they represent the major part of the commercial market for centralized syngas plants [60]. This technology is characterized by operating at high temperatures (1100-1500°C), which allows good conversions in short reaction times, and to avoid technical limitations in the feedstock type. Fluidized-bed equipment offers a homogeneous temperature environment promoting the heat and mass transfer between the reactants. The main advantages of these gasifiers are their easy scale-up and adaptation to changes in the feedstock, as well as the better temperature control, whereas their drawbacks are related to the need of specific particle size and lower conversion with respect to other gasification options [59,60]. Otherwise, fixed-bed reactors are commonly used for biomass gasification, and are divided into co-current (downdraft) and counter-current (updraft) gasifiers. From these alternatives, downdraft gasifiers are the preferred option for small-scale and on-site applications due to their relatively easy design, fabrication and operation, as well as their low tar content in the product [60,61]. However, there are some drawbacks such as the channeling, and the limitations to obtain good performances with feedstock moisture over 20% that still need to be overcome [61].

- *Biochemical Processes*:

There are several pathways to produce hydrogen from microorganisms and/or biomass (waste, wood, agricultural crops, and human or animal residues) including dark fermentation, direct and indirect biophotolysis, photofermentation, and even the biogas synthesis through anaerobic digestion and its subsequent reforming process [62]. Among these, dark fermentation and digestion processes exhibit the major developments and offer the most promising options for biochemical production of hydrogen [52,62].

Table 1-1: Summary of characteristics and challenges of hydrogen production technologies. Adapted from [63–66].

Technology	Strengths	Weaknesses	Perspectives/ Challenges
Steam Reforming	Established and mature technology	High energy consumption and operating costs	Improve product purification
	High thermal efficiency	CO_2 emissions	Renewable feedstocks (biofuels, biogas, bioethanol)
	Cheapest production method (currently)	Catalyst deactivation	Process intensification (membranes, on-site units)
Electrolysis	No pollution - decarbonized pathway	High electricity consumption	Improve efficiency
	Hydrogen purity	Low system efficiency	Renewable sources integration
	Link between electrical and chemical energy	High capital cost	Durable and cheap materials
Gasification	Abundant and cheap feedstock (organic waste)	High reactor costs	Product purification
	CO_2-neutral (biomass)	System efficiency	Handle with feedstock variability
	Favorable for large-scale production	Greenhouse gas emissions (coal)	Process cost and efficiency
Dark Fermentation	Simple reactor technology	Low hydrogen yield	Research in metabolic engineering
	No light and oxygen dependence	Large quantity of side products is formed	Materials science breakthrough
	Wide variety of carbon sources can be used	Reactor-to-reactor variation	Improve hydrogen selectivity

In dark fermentation, the process is performed by an anaerobic bacterium that acts over the organic matter to produce a gas stream composed of H_2 and CO_2. The main advantages of this process are the possibility to use a wide variety of waste as feedstock and its simple reactor technology, making even nonsterile conditions and impurities acceptable without negative effect on the performance of the process [14]. However, the process constraint due to the accumulation of by-products in the reactor and the difficulties of hydrogen purification are some drawbacks that need to be further studied. Otherwise, anaerobic digestion is a biochemical process where different types of microorganisms metabolize the organic compounds of biomass to produce biogas (mixture of CH_4 and CO_2), which is then subjected to a reforming process for hydrogen synthesis [62].

1.2.2 Storage and Safety

Besides synthesis alternatives, the reliable deployment of hydrogen as energy carrier is strongly connected to the performance of its storage [67]. In this regard, hydrogen has the capability to be stored as compressed gas or in liquefied cryogenic form (physical), and through metal hydrides (chemical) in solid state. Among these alternatives, the high pressure system for gaseous hydrogen storage is the most common method, and it offers capacities up to several GWh [68,69]. However, due to the low density of hydrogen as gas (0.08 kg/m^3), pressures up to 700 bar are used to avoid excessive volume of the tanks, which implies challenges for vessel materials and safety concerns [67,70]. Otherwise, liquid hydrogen storage is carried out by cryogenic process to condense the hydrogen from gas to liquid state using temperatures around -253°C. This method allows higher energy densities (capacity up to 100 GWh), and is the preferred option for transport, short-term storage and in space applications. Nevertheless, the main limitations lie on the energy consumption and isolation conditions that the process demands, along with the product losses by boil-off (0.3% per day) [49,56,67].

Considering these hydrogen storage technologies, the cryo-compressed alternative has been developed to trade-off their properties. In this option, the hydrogen is stored under cryogenic temperature (-253°C) and elevated pressure (> 300 bar) to avoid evaporation losses keeping high energy density, and with the key advantage of being compatible with hydrogen in gas and liquid state [67]. Nonetheless, a significant amount of energy is required to cool and compress hydrogen up to those conditions. Moreover, this storage alternative demands a great technological effort for designing a vessel able to contain

hydrogen at such pressure and temperature for a long time. Accordingly, work is in progress to address these issues and to make this technology feasible on the market [71].

Furthermore, hydrogen can be also stored as solid by means of metal hydrides formation in a physicochemical process. In this alternative, the hydrogen atoms are chemically bonded to the host material (e.g. sodium, lithium, aluminum, or magnesium) during the adsorption phase (charging), and subsequently released by heating through the desorption process (discharging). This is a promising technology because it provides high volumetric densities with operating conditions that do not entail the safety concerns of pressurized and cryogenic processes [67,70]. However, this is the least mature technology, and some issues such as the material volume expansion due to the stress produced by the adsorption/desorption cycles still need to be solved [72].

Besides reducing the environmental impacts, increasing the efficiency, and promoting the deployment of renewable sources, energy systems must be safe along the whole supply chain, which includes production, storage, transport, delivery and end-use [65,67]. In this regard, hydrogen energy systems (particularly in distributed applications) have to deal with the limited operative experience of this kind of plants, and with the public reputation of hydrogen for some unfortunate accidents that implied significant societal and economic costs in the history [73,74]. However, from the safety point of view, hydrogen is not more or less dangerous than other fuels, e.g. gasoline or natural gas, but like all the fuels, it must be manipulated responsibly and according to specific standards and procedures [65,75]. Leaking is one of the main challenges that hydrogen must tackle due to its difficult detection, since it is a colorless, odorless, and tasteless gas. Other safety concerns are its low ignition energy and its capability to have a wide range of combustible concentrations with air [52,75]. Nevertheless, these issues can be addressed with a well-defined framework including standards, community education, and technology improvement and certification, in order to ease the consumer acceptability and the integration of hydrogen solutions in energy systems [65,75].

Despite the potential benefits of using hydrogen as energy carrier, and in general of decentralized generation, the design of this kind of plants is a challenging task. Broadly, this complexity lies upon three main issues: (i) the uncertainty of input data, (ii) the great number of decisions to be made, and (iii) the need to involve different and usually contradictory objectives. The first because of the variability and time-dependent nature of energy sources and demands, the second due to the co-existence of multiple energy

conversion and storage technologies and, the last due to the necessity of developing a global industry in a sustainable way [15,16].

Taking this into account, the next section of this document is dedicated of depicting a general overview about the different stages of an energy system project. Special focus is on the conceptual design stage because of its notable impact on the progress of the project. Additionally, the main challenges in the conceptual design of DES are stated and a brief research background about these issues is presented.

1.3 Energy Systems Design

Overall, as for a chemical or biochemical transformation plant, developing an energy system project implies certain design and engineering stages. In this sense, whereas chemical process synthesis starts with the market analysis for manufacturing a new product (product design), the design of an energy transformation plant begins with the recognition of energy needs (electricity, cooling, heat, fuel). Once the objective of the new plant has been identified, the preliminary or conceptual process design is undergone. At this stage, the main goal is to obtain a process flowsheet, to do so, many alternatives are generated and evaluated aiming to determine how they perform in terms of economics, safety, and environmental issues. Then, based upon the selected process flowsheet, the basic and detailed design are carried out. During this step, mass and energy balances are refined in order to evaluate the process controllability and establish the equipment specifications for their buying and/or construction, which at the same time leads to a refined version of the process performance. Subsequently, procurement and commissioning of the equipment are done, followed by the final step of the project that is the operation of the plant [76,77].

It is well known that decisions made at conceptual design stage are responsible for the largest part of the cost for a process plant. Indeed, even if the fraction of this activity in the total project cost is very limited, around 2-3%, it could fix up to 80% of the investment and operational expenses of the final plant [22,76]. Thus, it is noted that these decisions have a major impact during the entire life of the project. In this regard, Figure 1-3 illustrates a schematic representation for the evolution of the economic factor across the different stages of a project. As observed, cost reduction opportunity falls while the total cost rises throughout each phase of the project. For example, basic and detailed design add 12% of the expenses and decrease the margin of cost reduction from 30 until near 10%. In the same line, procurement and construction of equipment account for 80% of the project cost,

but these permit saving opportunities lower than 10%. Broadly, this fact highlights the importance of decisions made at early design stages for either, impacting positively the project economics or avoiding costs for correcting misconceptions [22,76].

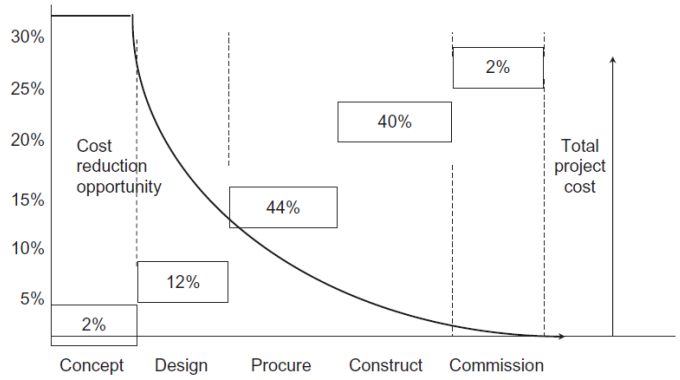

Figure 1-3: Cost reduction opportunity through the different stages of process design and engineering [22].

1.3.1 Conceptual Design of DES

Conceptual design refers to the screening of alternatives aiming to find the best process flowsheet. Specifically, for an energy system, this design stage consists in selecting the process units, their capacities and operation conditions, and the interconnections between them for transforming energy sources into useful energy forms. Beyond its technical feasibility, the selection of the process architecture should be done upon sustainability criteria, i.e. integrating economic, environmental and social dimensions for its assessment [22,78]. In fact, like for the economic aspect, the opportunity for enhancing the sustainability performance of the system is greater in preliminary design that in later stages of the project [17].

In general, once a design problem has been formulated, process synthesis entails four main activities: gather of information, generation of process options, assessment of preliminary designs, and selection of the most performant alternative [76,79]. The problem statement for the design of a DES requires both, the specification of the energy needs and the definition of the placement of the plant. This information determines the desired products of the energy system and the context wherein the project will be developed. Then, the data gathering task involves a more detailed knowledge of the energy demands, e.g. time-dependent profiles, purity required for fuels and temperature for heating. Additionally, during this activity the available energy sources and their potential are identified (e.g. solar

irradiance, wind speed, biomass production), as well as the possibility or not to be connected to the main grid and its corresponding price.

Having gathered this information, the next step in the design is to generate process flowsheets for converting the energy sources into the desired energy forms. Thus, this activity consists in proposing system structures and performing their corresponding mass and energy balances based upon a set of energy conversion and storage units. Subsequently, the assessment of the energy system alternatives is carried out. In this task, the objective is to determine the performance of the flowsheets under sustainability dimensions, i.e. considering economic, environmental, and social aspects. Finally, decision-making process is undertaken for ranking the energy system alternatives and selecting the most adequate one based on the project objectives and decision-makers preferences.

1.3.2 Challenges in Conceptual Design of DES

Considering the foregoing and the characteristics of DES, different challenges can appear at each step of the energy system design. Firstly, the strongly fluctuating and unpredictable behavior of renewable resources over time, and the need to satisfy multiple and variable energy demands simultaneously, which require special attention for considering a temporal resolution according to the design objectives [15]. Besides, the evaluation of a variety of energy sources, technologies for energy conversion and storage, and their interconnections contribute to the problem complexity [15,16]. Furthermore, from a project perspective, due to the close interaction of DES with community and the need to accomplish sustainable development objectives, the design of this type of systems implies the assessment of the socio-political dimension in addition to the economic and environmental aspects [2,44]. This multi-criteria evaluation typically introduces stakeholders with conflicting objectives and preferences, which represents additional difficulties during the decision-making process [16].

Aiming to state a research background about the main challenges in the conceptual design of DES, these were classified in three main issues: the uncertainty of data, the time resolution for the energy system representation, and the objectives considered for evaluating the performance of the system.

- *Uncertainty*

As aforementioned, one of the first steps in the design of an energy system is the gathering of data related with the power demands, weather conditions, resources availability, energy

price and cost of technologies. Considering the intermittent and unpredictable behavior of some of these data (demands, climate conditions, and electricity prices), a wide amount of research has included these uncertainties in the energy system design. Indeed, some research has been done for comparing different optimization techniques under uncertainty in order to evaluate their impact on the objective function and DES configuration [80]. Broadly, the research addressing the uncertainty issue differs in the parameters assessed, and the employed methods. For example, Akbari et al., Gabrielli et al., and Kang and Wang deal with this issue under the concept of robust optimization. In those studies, uncertainty in energy demands [81]; weather conditions and energy demands [82]; and a Monte Carlo method to simulate the ucertainty of energy price and demand, in combination with a generic approach for quantifying the equipment degradation along the life cycle of the system were included [83]. Recently, Mavromatidis et al. formulated a two-stage stochastic mixed integer linear programming (MILP) problem including energy demand patterns, solar energy availability, energy carrier prices and emission factors as uncertain parameters [84]; and Jing et al. considered uncertainty in energy demands, and introduced a hierarchical based approach to decompose the district-level problem into neighborhood-level sub-problems by a clustering technique [85].

- *Time Resolution*

A significant amount of research about the design and operation of distributed energy systems has been done considering different simulation periods or time-steps, and single objective functions. For example, Mehleri et al. developed an economic optimization dividing the full year calendar into 18 different periods (6 periods per day for 3 seasons) for the selection of the system components among several candidate technologies to satisfy the heat and power demands of a small neighborhood [86]. Yang et al. included cooling demand in the design of a district-scale system, and considered three types of typical days per year (winter, summer, and mid-season days), each one divided into 12 periods [87]. In those studies, only the economic criterion was considered for designing the system, and energy storage was not included. In another research, Khalid et al. performed an energetic and exergetic analysis along with the economic optimization of an energy system using hydrogen for energy storage [88]. Other works have employed decomposition methods for reducing the computational requirements to solve the optimization problem. In this line, Schütz et al. compared a compact and distributed methodologies to optimize building energy systems within local neighborhoods using twelve typical demand days with hourly time resolution [89]; and Pan et al. proposed a two-stage method considering an integrated

demand-response program for planning and designing multi-energy systems, which is evaluated in three typical days of the year (winter, summer and transition season) [90].

Although these approaches are very useful for reducing the complexity of the optimization problem, they are not able to represent the seasonal behavior of the system due to the discontinuity between the used characteristic periods. To tackle this issue, only few works have been reported contemplating simultaneously a yearly horizon and the seasonal cycle of the energy storage. In this respect, the whole year has been modeled by using hourly time steps for designing district heating and cooling systems [91,92], and urban energy systems under the energy hub concept [93]. Apart from that, some approaches have considered the whole year but reducing the complexity of the system, e.g. decomposing the optimization problem (separating the design and the operation) [94], coupling typical design days [95], considering typical periods [96], or employing time steps of 4 hours [97].

- *Assessment Objectives*

As previously referred, the planning of DES requires the consideration of criteria beyond the economic one. In this sense, some works have included multi-objective functions for designing and/or operating these systems. Those objective functions comprise mainly economic (cost, profit), environmental (CO_2 emissions) and energy quality (exergy) criteria. On the one hand, some works have focused on the design of DES according to economic and environmental/exergetic criteria by using different representative periods. For instance, Pelet et al. modeled the electrical needs with 12 representative days, and considered five busy days for representing the peak demand in the design of integrated energy systems under economic and ecological criteria [98]; Li et al. developed a mixed integer linear programming (MILP) model for the optimal design of DES considering the total annualized cost and the CO_2 emissions as objective functions [99]; and Di Somma et al. carried out the optimization employing four representative season days, and included economic and exergetic assessments in the design of DES [100]. In another work, Fazlollahi et al. addressed the MILP optimization problem by using two optimization techniques, the integer cut constrain (ICC) algorithm combined with the epsilon constraint method, and a multi-objective evolutionary algorithm [101]. Other works have focused on optimizing the operation of the system either by formulating deterministic multi-objective linear programming (MOLP) problems [102,103], or through stochastic models for including uncertainties on energy demand and supply [104]. The latter uses Monte Carlo method and roulette wheel mechanism for modeling the uncertainty of energy price, solar availability, and user energy demand.

Otherwise, some studies have also addressed multi-criteria optimization problems, but considering energy storage and the whole year as time horizon. In this respect, Dorotić et al. implemented economic, environmental and exergetic criteria for designing district heating systems [91], and a multi-objective problem based on minimizing the total costs and the CO_2 emissions in the design of heating and cooling systems [92]. Unlike those papers, that addressed the multi-objective problem by using the weighted sum method, other works have employed MILP and the epsilon constraint method for the optimal design of DES. In this regard, Maroufmashat et al. employed the energy hub approach and focused on the energy exchange between hubs [93], whereas Gabrielli et al. emphasized on the seasonal energy storage within the system [95]. Conversely, Dufo-López et al. used evolutionary and genetic algorithms to solve a triple-objective optimization problem including cost, pollutant emissions and unmet load as objective functions [105]. Moreover, Eriksson and Gray, considered a semi-quantitative socio-political index that represents the expected public satisfaction of a particular energy system in addition to the economic and environmental objectives [106]. Meanwhile, some studies have been mainly focused on the implementation and/or comparison of decision-aid methods, aiming to integrate the decision-maker preferences in the DES design [107–109].

This overview shows the great diversity of research already done regarding the design and operation of decentralized energy systems. However, to have a deeper perspective over DES involving hydrogen as energy carrier, a specific and systematic literature review was performed. Overall, including a particular energy form does not have any effect on the uncertainty of information and the time resolution of a DES. In fact, these are intrinsic characteristics of the system, and the same approaches could be employed for a diversity of energy forms. Nevertheless, the technologies for energy conversion and storage would be quite different depending on the involved energy carriers. Therefore, the objectives of the literature review were twofold: (i) to identify the technologies employed when introduced hydrogen into DES, and (ii) to obtain a more exhaustive state of how the performance is assessed in this kind of systems.

The literature review was based on three main stages: (i) definition of a search strategy, (ii) classification of the documents, and (iii) their subsequent analysis. As follows, the results regarding the hydrogen-related technologies and the evaluated criteria in the system design are presented over the 106 documents analyzed. Further details about methodology and additional results can be found in our paper " *Trends in design of distributed energy systems using hydrogen as energy vector: A systematic literature review* ".

This is one of the products of this thesis project, and it is published in the *International Journal of Hydrogen Energy* [11].

- *Hydrogen Technologies*

The set of technological alternatives includes electrolyzers (EL), fuel cells (FC), methanation and reforming reactors, gasification units and hydrogen storage options (gas, liquid, metal hydride adsorption). Figure 1-4 shows that EL and FC are the preferred technologies to involve hydrogen in energy systems. In this regard, alkaline electrolyzers are selected because of their higher capacity and technological maturity, whereas PEM and SOEC options are chosen when response to operational conditions (frequent start-up and shut down) or energy efficiency are privileged.

The distribution of EL and FC technologies is also presented, where PEM type represents the most widely used technology for both EL and FC. Regarding the methanation process, the employed gas comes either from gasification, or from an electrolyzer powered by wind turbines or photovoltaic panels. Hence, the whole methane produced in the system proceeds from renewable sources. In the case of reforming process, natural gas (NG), biogas or bioethanol are used as raw materials.

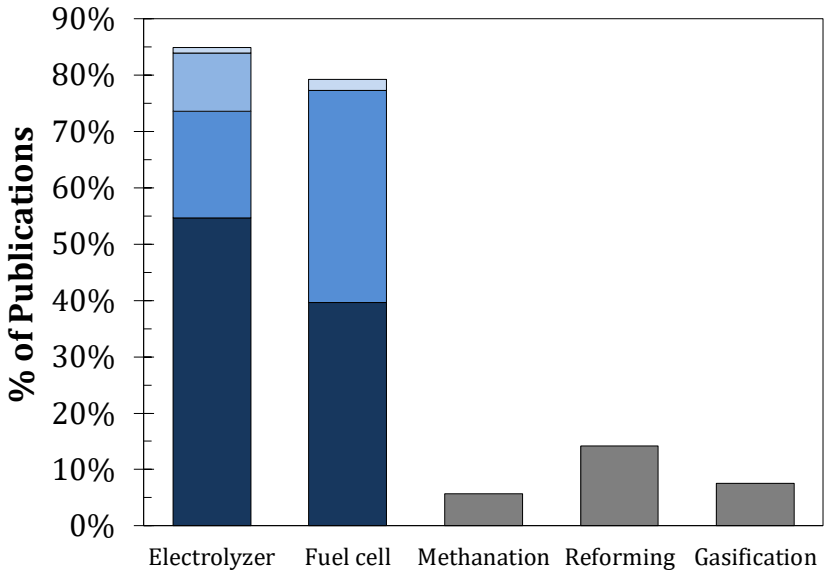

Figure 1-4: Publication distribution as a function of hydrogen technologies. (■) solid oxide technology; (■) alkaline electrolyzers;(■) PEM technology; (■) not specified.

- *Performance Objectives*

Economic, technical, and environmental aspects are the focus of research to evaluate the energy systems involving hydrogen as energy vector. Among economic objectives, net present value, levelized ($/kWh) and operational costs are the most used. In a few cases, environmental and human health impacts (produced by emissions) were also addressed in economic terms [110–114]. Exergy analysis, energy efficiency, technological feasibility and experimental validations were considered as technical targets. Meanwhile, the life cycle assessment and greenhouse gas emissions represent the main goals with respect to environmental aspects.

Figure 1-5 depicts the distribution of publications according to their evaluated objective. As observed, there is a strong prevalence of economic issues, which are involved in almost 80% of studies. It is also important to note that around 45% of documents include multi-objective analysis, and 9% of works address economic, technical, and environmental goals simultaneously.

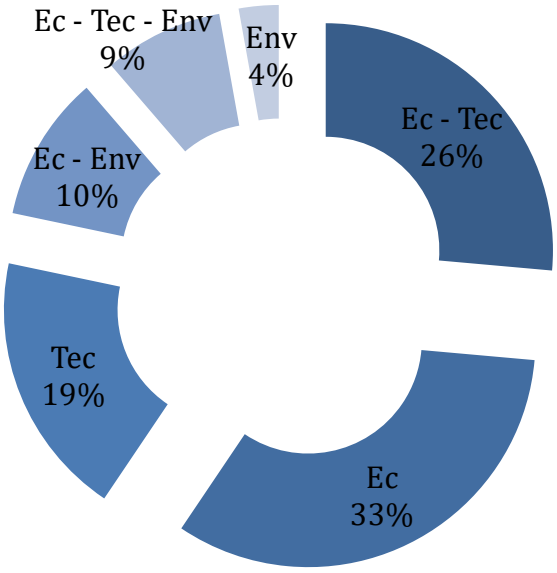

Figure 1-5: Publication distribution of performance objectives evaluated for the design of distributed energy systems. (Ec-economic, Tec-technical, Env-environmental)

1.4 Summary and Conclusions

Because of the constant increase in the population and energy consumption, and aiming to meet the world environmental goals, a global energy transformation is undergoing. This transition lies on increasing the renewables share, the electrification in end-use consumption, and the deployment of distributed and flexible energy systems. In this sense, there is a need of including energy carriers as hydrogen, which could enhance the

renewables integration and to enable the sector coupling for exploiting the synergies among the different energy forms.

Regarding the design of DES, typically it is formulated as a MILP optimization problem, where binary variables are used for specifying whether a technology is installed or not, and for representing their on/off status at each time step. Besides, the analysis has been predominantly focused on economic and environmental criteria, thus neglecting the influence of the social dimension in the design of DES [7]. However, DES are socio-technical systems because of the close interaction of multiple stakeholders with the technological devices. In such a way, there is a need to develop methodological frameworks considering the different aspects of the sustainability, i.e. economic, environmental, and social dimensions. Also, this kind of approaches can promote the participation of the stakeholders during the decision-making process and to enhance the adoption of technological solutions for dealing with the current challenges of the energy sector [24,28,30].

2. Energy System Representation and Assessment

As stated in Chapter 1, the conceptual design of a DES begins with the definition of the plant location, which at the same time leads to establish the energy needs and the availability of resources. All this information is collected during the data gathering task, that corresponds to the first activity of the process synthesis. Then, the generation of process alternatives and their assessment are performed. For doing that, it is necessary to represent the different system structures, to carry out the mass and energy balances, and to define the assessing criteria. In this regard, this chapter focuses on three main objectives: (i) to define a base-case flowsheet for the energy system, (ii) to formulate a mathematical model for representing the energy system, and (iii) to establish the criteria for evaluating its performance. Thus, the remainder of the chapter is structured as follows. Initially, the base-case structure of the energy system is described, and the energy sources, conversion units, and energy demands are identified. Then, the main features of energy system modeling are presented. Afterwards, based upon the base-case configuration, a mathematical model for representing the energy system is developed. Subsequently, the sustainability issue is introduced highlighting the importance of addressing the three dimensions (economic, environmental, and social) during the energy system design. Finally, the criteria for assessing the energy system performance under the sustainability dimensions are formulated.

2.1 Flowsheet of the System

At the conceptual design step many decisions to be made are related to discrete variables, such as the location of the conversion units within the flowsheet and the choice among different technologies for a specific function. This leads to consider a very large spectrum of design alternatives, and consequently contributes to the complexity of the process synthesis task. Specifically, the multiple energy forms included in DES imply a massive amount of options for energy transformation and storage. As a result, a great number of process flowsheets could be generated. However, performing a complete representation of

all available technologies in DES, and the exhaustive evaluation of all possible system configurations are beyond the scope of this work.

Taking this into account, a set of candidate technologies was selected to build a base-case process flowsheet. The choice of this group of energy conversion and storage units was based upon the results of our review paper [11], and from literature regarding DES design. Thus, the base-case energy system considered in this thesis is depicted in Figure 2-1. The proposed base-case structure includes the most common renewable sources used in this kind of systems, i.e. solar, wind and biomass. Moreover, the connection to the main electricity grid and gas network is also considered. Regarding the energy storage options, electrical battery and hydrogen system are studied because these offer the possibility to analyze both, the short-term and long-term energy storage. Meanwhile, as presented in Table 1-1, the electrolyzer constitutes a decarbonized pathway to obtain hydrogen, and it represents a link between electrical and chemical energy forms. Methanation reactor is included because it can be coupled to the electrolyzer and to CO_2 capture system to produce methane through the power-to-gas route. Besides, the reformer is analyzed because it represents the cheapest and most mature technology for producing hydrogen (Table 1-1). The anaerobic digester is studied as an alternative to use the biomass for obtaining biomethane and to replace or complement the gas network.

As observed in Figure 2-1, the energy inputs are converted and/or managed within the system for satisfying electricity, hydrogen, and methane demand. Electricity is supplied through photovoltaic panels, wind turbines or the electricity grid. For tackling the mismatch between the energy availability from renewables and the demand, during periods of high electricity production from photovoltaics or wind turbine, the surplus power can be stored either in an electrical battery or in hydrogen form by using an electrolyzer and a pressurized tank. In the latter storing option, hydrogen might be reconverted into electricity when required by employing a fuel cell. Regarding hydrogen, it can be obtained by water electrolysis or steam methane reforming processes. In the former, the process is powered by both renewable or grid-derived electricity, and the latter employs methane obtained from anaerobic digestion or the gas network. Moreover, the methane demand can be supplied from the biomass transformation, the methanation reaction or the natural gas network. For the methanation unit, the reactants are CO_2 and hydrogen from water electrolysis. The CO_2 can be obtained from various sources including operations within the system such as the biogas upgrading (anaerobic digestion) and the reforming reaction, but also can be captured from the air, or directly imported from the industry releases (e.g. cement).

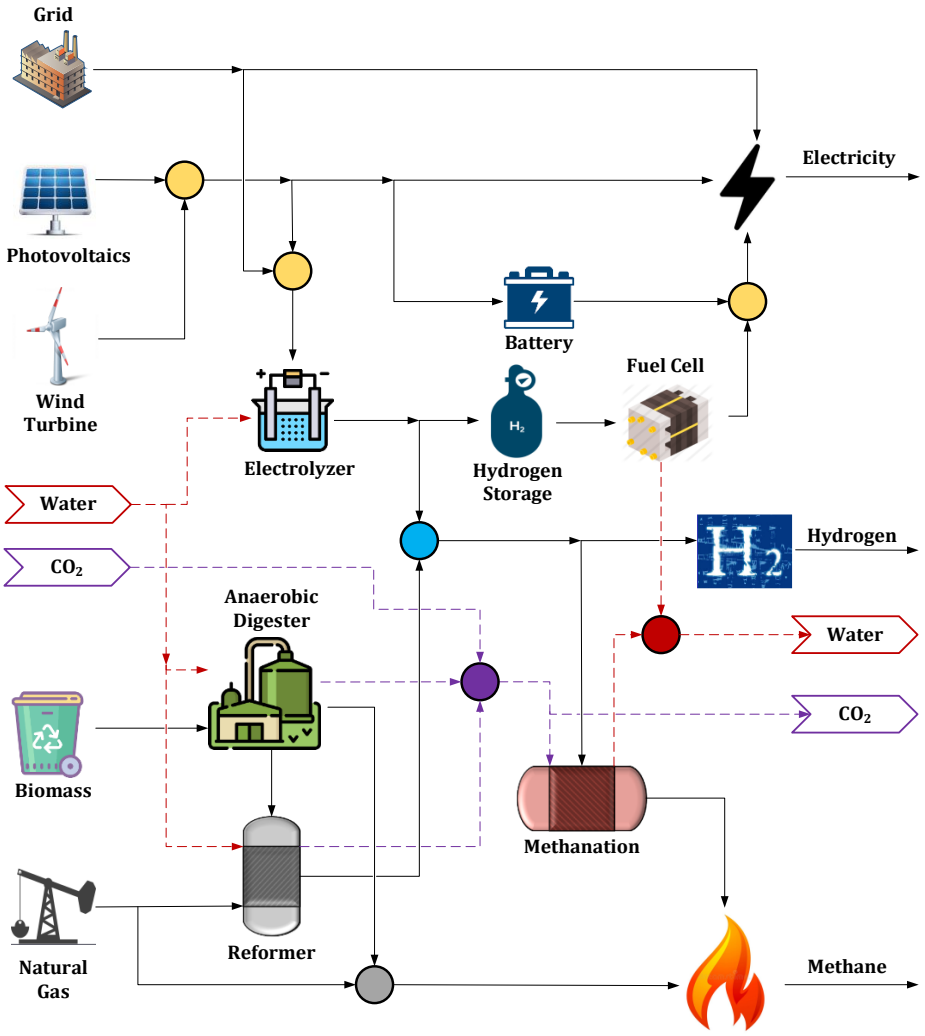

Figure 2-1: Base-case flowsheet of the energy system. (●) electricity, (●) hydrogen, (●) water, (●) CO_2, (●) methane.

Note that the proposed energy system structure is based upon energy vectors rather than on end-use utilities. Hence, the energy products of the system could be used whatever needed. Also, it is worth to note that the proposed flowsheet represents a wide amount of process alternatives, but it is not a superstructure itself. In this regard, Table 2-1 presents a simple analysis between the sources and the products of the system for elucidating some considerations.

Table 2-1: Connections between sources and products within the base-case energy system.

Inputs / Outputs	Electricity	Hydrogen	Methane
Grid electricity	Directly	Electrolyzer	Electrolyzer - Methanation
Natural gas	Reformer - Fuel cell (not considered)	Reformer	Directly
Biomass	Digester - Reformer - Fuel cell (not considered)	Digester - Reformer	Digester
PV -Wind	Directly	Electrolyzer	Electrolyzer - Methanation

As depicted, two pathways of energy conversion are not considered in the base-case structure. They consist in the conversion of natural gas and biomass into electricity. The reason of that decision lies on the fact that the fuel cell makes part of the hydrogen storage system. Then, under this assumption, the fuel cell can be exclusively fed by hydrogen from the storage tank. In fact, these two units are closely related, since the whole hydrogen leaving the pressurized tank is sent to the fuel cell. This decision implies that there is no connection for taking hydrogen from the tank and use it for supplying the hydrogen demand. This choice was taken because of the pressurized tank is supposed to be only employed for storing the surplus electricity from renewables.

Taking this into account, a brief analysis was carried out through the Process-graph (P-graph) approach for quantifying the number of alternatives considered/neglected. To do that, two scenarios were evaluated within the P-graph studio software by using the solution structure generation (SSG) algorithm [115,116]. The first scenario corresponded to the proposed base-case structure (Figure 2-1). Meanwhile the second case was a configuration including all the connections presented in Table 2-1, and the possibility to use the hydrogen stored in the pressurized tank for supplying the hydrogen demand. Thus, by using the SSG algorithm, it was possible to generate all the combinatorial feasible flowsheets covered by each scenario. According to these results, the proposed structure contains 1035 process alternatives, whereas the second scenario comprises 2499 structures. Broadly, these results depict the impact of decisions made during process synthesis and the complexity of designing this kind systems, since there are many alternatives to be evaluated.

Thus, once the base-case flowsheet is defined, the next step is to carry out the mass and energy balances of the energy system. This set of equations involves both, the specific representation of each process unit and the relation among the different technologies

within the system. Then, the results of this task are employed for sizing the plant, determining how it operates and evaluating its performance.

2.2 Process Modeling

2.2.1 General Aspects

Process modeling is a useful tool for understanding/predicting the behavior of chemical plants or energy systems. It relies upon the abstraction of reality for representing the phenomena occurring either in a process unit or in the whole system. Therefore, process models are commonly employed in activities such as research and development, design, scale-up, operation, control, and optimization of processes. Hence, modeling enables for experiments planning, operational fault detection and troubleshooting, evaluation of process alternatives, definition of control strategies and training of people, among others [117,118]. At design stage, process models offer a safe, cheap and fast way for analyzing the effect of design variables on the system performance [119]. Nevertheless, it is important to point out that process models are a powerful tool for carrying out virtual experiments and evaluate scenarios, but they are not the reality itself. Then, the model user must evaluate the reliability of results according to the model accuracy [22].

Broadly, one important issue in the process modeling is to determine a level of detail, so that the formulation is able to capture the key features of the system according to the envisaged application of the results [120]. Therefore, the required accuracy of a model for fitting experimental results would be considerably different to that one employed for optimizing the operation of industrial-scale units, or for designing a new production plant. In fact, along the different design and engineering stages for developing a chemical plant or energy system project, different kinds of models are used. Thus, as the objective at conceptual design is to screen multiple process units and system architectures, models capable to quickly perform the mass and energy balances of the system are necessary. Hence, the employed mathematical expressions are relatively simple and with low degree of detail. Meanwhile, at basic and detailed engineering stage, more complex and rigorous models are required for establishing all the characteristics for buying and/or constructing the process units.

2.2.2 Features of Energy System Modeling

As presented in Chapter 1 (section 1.3.2), one of the most challenging issues for designing energy systems is related to the time-dependence in the availability of renewable resources (solar and wind) and the energy demands. This fact leads to the need of considering the time dimension when designing an energy system capable of managing this characteristic. In this regard, a process model for representing an energy system is intrinsically transient. However, a common practice in literature consists in neglecting the dynamic behavior of the energy converters because of their fast response. Indeed, the modeling approaches addressing the energy system design typically employ time steps of one hour or higher, whereas the time constant of some energy transformers such as electrolyzers and fuel cells are in the order of a few seconds or minutes. Consequently, concerning the time dependence issue, energy system design is commonly performed by means of pseudo-steady state models, i.e. the time evolution of the whole system is considered but the process units are supposed to have instantaneous response.

Regarding the linearity issue, the approach has been predominantly focused on the development of linear models for representing the energy systems. This happens due to two main reasons, (i) the availability of methods for solving this kind of problems, and (ii) because of the required computational capacity is considerably lower with respect to that needed for solving non-linear problems. In general, these non-linearities appear when part-load efficiencies and economic power-law functions are included. However, for avoiding the mathematical complexity that non-linearities imply, the dominant approaches are either assuming constant conversion efficiencies and linear cost functions, or approximating them through linear piecewise functions (e.g. Gabrielli et al. [95] and Mavromatidis [121]).

Additional aspects are focused on the uncertainty and continuity of the model variables. The former has been already discussed in Chapter 1, and it was noted that different techniques have been employed for addressing the fluctuant and unpredictable behavior of some variables such as energy demands, climate conditions, and electricity prices. The latter is mainly associated to the capacities of energy converters, which ideally must be selected taking into account the options available in the market. Nevertheless, a common practice is to consider them as continuous variables due to the modularity of some technological units, and in order to reduce the complexity of the model formulation.

About the level of process knowledge, mathematical models are classified as first principle or empirical [122]. On the one hand, first principle or mechanistic models, correspond to those ones based on the fundamental understanding of the physicochemical phenomena, so that the relation between input and output variables is represented by means of conservation laws (mass, energy and momentum). On the other hand, empirical or data-driven models rely on the mapping of input/output data rather than on the process knowledge, which can lead to results without physical sense. Accordingly, first principle models are typically employed in process design activities since mass and energy balances are pillars of this task, whereas empirical models are preferred in applications for process control because a high computational speed is privileged [117,122]. Nevertheless, the kinetic and thermodynamic relationships used in first principle models involves non-linear expressions, and consequently increase the complexity of the problem. In this line, a common approach for process design is to fix the operational conditions (temperature and pressure) and approximate the behavior of the process units through linear equations [77].

Considering the foregoing and keeping in mind that the objective of this work is focused on the conceptual design stage, in the next subsection (2.2.3) a mathematical model for representing the base-case flowsheet of the energy system (Figure 2-1) is presented.

2.2.3 Energy System Model

The proposed model aims to be used for conceptual design of energy systems. In this line, the objective is to build a mathematical formulation capable of capturing the main characteristics of the system (relations among the process units, time-dependent behavior, energy storage), and then to perform the mass and energy balances for the subsequent performance evaluation of the system. Therefore, the energy system model has four main features:

1. It is a pseudo-steady state model, so that the time-dependence is considered but process units with instantaneous responses are assumed. Hence, accumulation within the energy converters is neglected. Moreover, the evolution of the energy stored is addressed by discretization of the temporal variable.
2. The operational conditions of energy converters are fixed, then the input/output variables are related by means of constant efficiencies and linear expressions.
3. There are no energy losses across the connection lines.
4. It is a deterministic model, and all the sizes of equipment are considered as continuous variables.

Thus, the mathematical formulation for representing each one of the process units within the base-case flowsheet is described as follows. For clarity, Figure 2-2 depicts the energy flows throughout the system.

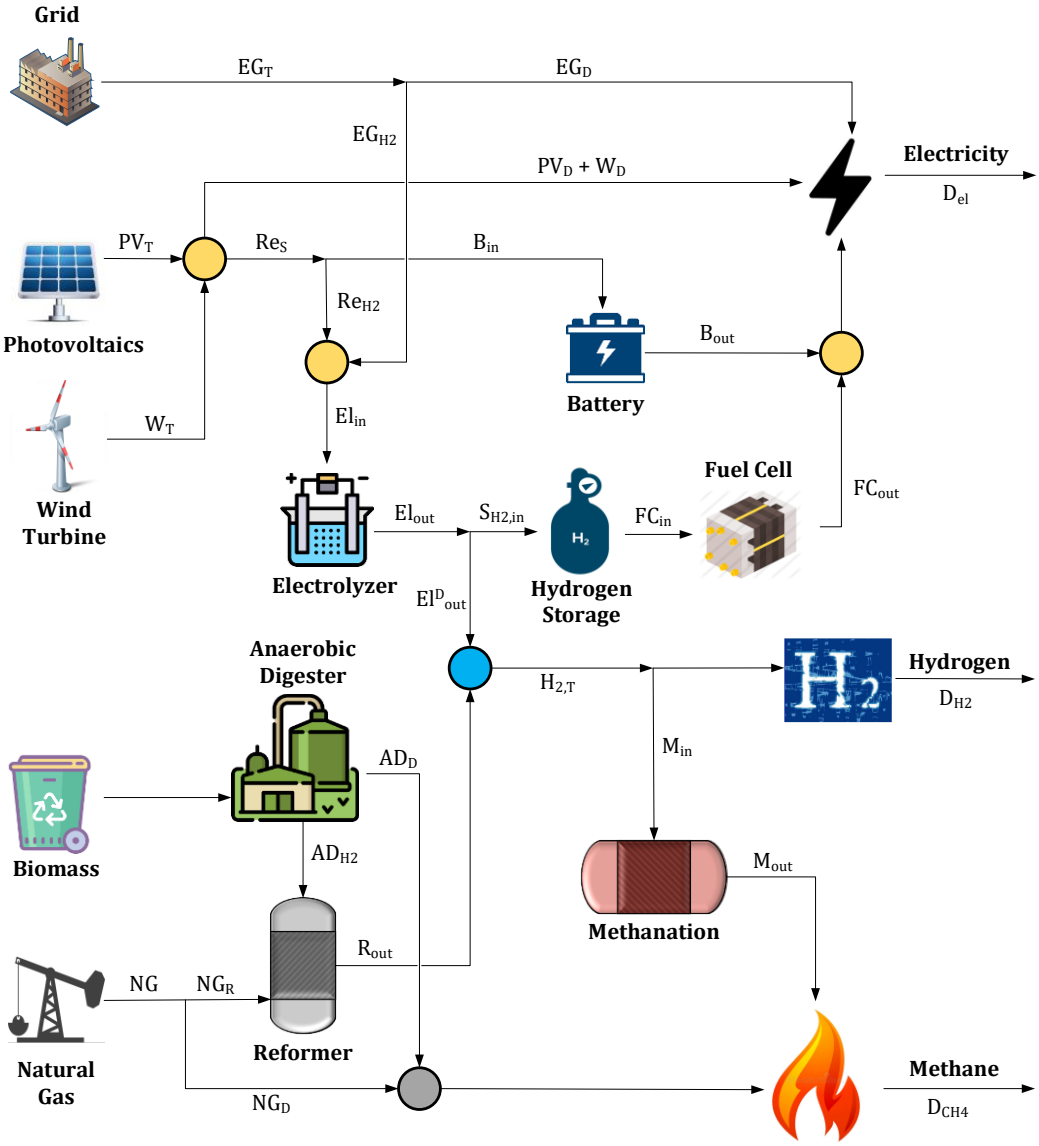

Figure 2-2: Base-case flowsheet of the energy system including energy flows. (●) electricity, (●) hydrogen, (●) water, (●) CO_2, (●) methane.

- *Photovoltaics:*

This device converts the sunlight into electricity by means of the photoelectric effect within the photovoltaic cell. Thus, the instantaneous power obtained from solar panels as a function of time is presented in Equation 2.1. Additionally, Equation 2.2 describes the dependence of the conversion efficiency upon the solar irradiance and the ambient temperature [123].

$$PV_T(t) = n_{PV}(t)I(t)A \tag{2.1}$$

$$n_{PV}(t) = n_s\left(1 - \beta\left[T_a(t) - T_{ref} + (T_{NOCT} - T_a(t))\frac{I(t)}{I_{NOCT}}\right]\right) \tag{2.2}$$

Here, PV_T is the electrical power generated [kW], n_{PV} the panel efficiency, I the solar irradiance [kW/m^2], and A represents the installed area [m^2]. n_s is the panel efficiency at reference conditions, β the characteristic temperature coefficient, T_a the ambient temperature [°C], and T_{ref} the temperature at reference conditions. Meanwhile, T_{NOCT} denotes the nominal operating cell temperature and I_{NOCT} its corresponding irradiance.

- *Wind turbine:*

  This equipment transforms the kinetic energy of wind into electricity through the rotation of the propellers around a rotor that is connected to the generator. Hence, the power produced by a wind turbine is a function of the wind speed as stated in Equation 2.3. Typically, the operation of a wind turbine is characterized by three zones depending upon the characteristic power curve of the device [124].

$$W_T(t) = \begin{cases} 0 & ; \quad v_{cut-in} \geq v_w \; or \; v_w \geq v_{cut-out} \\ f_1(v_w) & ; \quad v_{cut-in} \leq v_w \leq v_{rated} \\ f_2(v_w) & ; \quad v_{rated} \leq v_w \leq v_{cut-out} \end{cases} \tag{2.3}$$

Where $W_T(t)$ is the power generated [kW], v_w is the wind speed [m/s], and v_{cut-in}, $v_{cut-out}$ and v_{rated} are parameters provided by the manufacturer and represent the speed at which the turbine starts to generate electricity, the speed at which the generator shuts-down for avoiding damage, and the wind speed for the greatest electricity generation, respectively.

- *Electrolyzer:*

In this unit, electricity is used to convert water into hydrogen and oxygen. This energy conversion is expressed in terms of input-output power as presented in Equation 2.4. In that equation, El_{in} is the input electrical power [kW], El_{out} the hydrogen produced [kW], and n_{el} the efficiency of electrolysis. Then, using the hydrogen low heating value (LHV_{H2}), the hydrogen mass flowrate ($H_{2,El}$) is obtained as stated in Equation 2.5.

$$El_{out}(t) = El_{in}(t)n_{El} \tag{2.4}$$

$$H_{2,El}(t) = \frac{El_{out}(t)}{LHV_{H2}} \tag{2.5}$$

Moreover, considering the stoichiometry expressed in Equation 1.3, the mass balance around the electrolyzer can be expressed by means of Equation 2.6.

$$H_2O_{El}(t) = H_{2,El}(t) + O_{2,El}(t) \tag{2.6}$$

$$O_{2,El}(t) = \frac{PM_{O2}}{2PM_{H2}} H_{2,El}(t) \tag{2.7}$$

Where H_2O_{El} corresponds to the inlet mass flow rate of water [kg/s], $O_{2,El}$ is the oxygen leaving the electrolyzer [kg/s], and PM_{O2} and PM_{H2} are the molecular weights of the oxygen and hydrogen, respectively.

It is worth noting that according to the proposed energy system scheme (Figure 2-1), the power supplied to the electrolyzer could come from the photovoltaic panels (PV_{H2}), the wind turbine (W_{H2}) and/or the electricity grid (EG_{H2}). Hence, the total input power (El_{in}) considers the contribution of these three sources as stated in Equation 2.8.

$$El_{in}(t) = PV_{H2}(t) + EG_{H2} + W_{H2}(t) = Re_{H2}(t) + EG_{H2} \tag{2.8}$$

- *Fuel cell:*

Here takes place the reverse process of the electrolyzer, i.e. hydrogen and oxygen are fed to produce electricity and water (Equation 2.9). In this work, the fuel cell is employed for obtaining electricity from hydrogen, if available in the storage system, and if there is not enough production from photovoltaics. As for the electrolyzer, the fuel cell performance is described by a characteristic efficiency (Equation 2.10), where FC_{in} is the input power [kW], FC_{out} the electricity produced [kW], and n_{FC} the efficiency of the fuel cell.

$$2H_2 + O_2 \rightarrow 2H_2O \tag{2.9}$$

$$FC_{out}(t) = FC_{in}(t)n_{FC} \tag{2.10}$$

Thus, from the reaction stated in Equation 2.9, the corresponding mass balance of the fuel cell is described by Equations 2.11-2.13. In those expressions, $H_{2,FC}$, $O_{2,FC}$ and H_2O_{FC} are the mass flow rate [kg/s] of hydrogen, oxygen and water, respectively.

$$H_{2,FC}(t) = \frac{FC_{in}(t)}{LHV_{H2}} \tag{2.11}$$

$$H_{2,FC}(t) + O_{2,FC}(t) = H_2O_{FC}(t) \tag{2.12}$$

$$O_{2,FC}(t) = \frac{PM_{O2}}{2PM_{H2}} H_{2,FC}(t) \quad (2.13)$$

Fuel cells are cogeneration units, i.e. they produce at the same time electrical and thermal power, which are related by means of the first principle to electrical efficiency ratio (n_{fr}) as expressed in Equation 2.14. In that equation, FC_{th-out} represents the thermal power [kW] generated in the fuel cell.

$$FC_{th-out}(t) = FC_{out}(t)(n_{fr} - 1) \quad (2.14)$$

- *Energy storage:*

In this study, the electrical battery and the pressurized hydrogen tank are the two storing energy alternatives. In both systems, the cycle energy losses are considered. For the battery, these losses depend on the charging/discharging efficiencies and the self-discharge, which is characteristic of these devices. Meanwhile, the loss of energy through the hydrogen system is due to the conversion efficiencies of the electrolyzer and fuel cell.

Taking this into account, Equations 2.15 and 2.16 present the time-dependent balance for the battery and hydrogen storage systems, respectively.

$$S_B(t) = (1 - \tau)S_B(t - \Delta t) + \left(B_{in}(t)n_{ch} - \frac{B_{out}(t)}{n_{dch}}\right)\Delta t \quad (2.15)$$

$$S_{H2}(t) = S_{H2}(t - \Delta t) + \left(S_{H2,in}(t) - S_{H2,out}(t)\right)\Delta t \quad (2.16)$$

Here, S_B and S_{H2} represent the amount of energy stored [kWh] at each time *t* in the battery and hydrogen system, respectively. τ is the self-discharging parameter of the battery; n_{ch} and n_{dch} the corresponding charging and discharging efficiencies; B_{in} and B_{out} the input and output power to the battery [kW]; and $S_{H2,in}$ and $S_{H2,out}$ the corresponding input and output energy flowrates [kW] to the hydrogen storage tank.

- *Anaerobic digester:*

In this biochemical process, biogas (mixture of CH_4 and CO_2) is obtained as the result of the action (in absence of oxygen) of microorganisms over the organic compounds of biomass. In addition to biogas, a solid residue (so-called digestate) results from the process, which after a treatment can be used as bio-fertilizer. Typically, methane represents around of 70% (v/v) of the biogas, hence it needs to be upgraded for removing the undesired impurities (mainly CO_2). At commercial level, there is a wide range of options for biogas

clean-up, with physical, chemical, and pressure-based operations offering gas losses below 2%. Among them, the most widespread technologies are PSA, water or amine scrubbing, and membrane or cryogenic separations [125,126].

Thus, the volumetric flow rate [m^3/s] of biomethane ($CH_{4,AD}$) as a function of time can be described by means of Equation 2.17. Meanwhile, the corresponding output power [kW] of the anaerobic digestion process (AD_{out}) is presented in Equation 2.18.

$$CH_{4,AD}(t) = AD_{in}(t) n_{AD} n_{VS} n_{up} \tag{2.17}$$

$$AD_{out}(t) = CH_{4,AD}(t) LHV_{CH4} \tag{2.18}$$

Here, AD_{in} represents the input mass flow rate of biomass [kg/s], n_{AD} is the yield to methane of the digestion process [m^3/kg volatile solid], n_{VS} is the fraction of volatile matter in the biomass [kg volatile solid/kg biomass], n_{up} the recovery fraction of upgrading operation; and LHV_{CH4} the low heating value of methane [kJ/m^3].

Moreover, assuming that biogas is only composed of methane (70% v/v) and CO_2 (30% v/v), the mass balance over the anaerobic digester is described by Equations 2.19 and 2.20.

$$CO_{2,AD}(t) = \frac{0.3}{0.7} CH_{4,AD}(t) \tag{2.19}$$

$$AD_{in}(t) = CH_{4,AD}(t)\rho_{CH4} + CO_{2,AD}(t)\rho_{CO2} + Dig(t) \tag{2.20}$$

Where, $CO_{2,AD}$ represents the CO_2 released [m^3/s], ρ_{CH4} and ρ_{CO2} correspond to the density [kg/m^3] of methane and CO_2, respectively, and Dig is the digestate.

- *Reforming reactor:*

The steam reforming of methane is the dominant worldwide process for producing hydrogen. Broadly, it consists of three main steps: firstly, the catalytic reaction of methane with steam to produce syngas (Equation 2.21); then, the water-gas-shift reaction (Equation 2.22); and finally, the pressure swing adsorption (PSA) in order to purify the hydrogen.

$$CH_4 + H_2O \leftrightarrow 3H_2 + CO \tag{2.21}$$

$$CO + H_2O \leftrightarrow H_2 + CO_2 \tag{2.22}$$

In this work, the unit called *reformer* in Figure 2-1 represents the whole process, and it is used for obtaining hydrogen from methane taken from the gas network (NG_R) or from the anaerobic digestion (AD_{H2}). The performance is described by a global efficiency, which relates the methane supplied with the hydrogen produced as expressed in Equation 2.23.

In that equation, n_R is the efficiency of the reforming process, and R_{in} and R_{out} the input of methane and output of hydrogen in terms of power [kW], respectively.

$$R_{out}(t) = R_{in}(t)n_R \tag{2.23}$$

Additionally, Equation 2.24 represents the contribution of the two sources of methane for the reforming process. Here, AD_{H2} corresponds to the biomethane [kW] and NG_R to the methane [kW] from the network.

$$R_{in}(t) = AD_{H2}(t) + NG_R(t) \tag{2.24}$$

Besides, according to the reactions stated by Equations 2.21 and 2.22, the mass flow rate of the components through the reformer reactor are expressed by means of Equations 2.25-2.28.

$$CH_{4,R}(t) = \frac{R_{in}(t)\rho_{CH4}}{LHV_{CH4}} \tag{2.25}$$

$$H_{2,R}(t) = \frac{R_{out}(t)}{LHV_{H2}} \tag{2.26}$$

$$CO_{2,R}(t) = \frac{PM_{CO2}}{4PM_{H2}} H_{2,R}(t) \tag{2.27}$$

$$H_2O_R(t) = \frac{2PM_{H2O}}{4PM_{H2}} H_{2,R}(t) \tag{2.28}$$

Where $CH_{4,R}$, $H_{2,R}$, $CO_{2,R}$ and H_2O_R represent the mass flow rate [kg/s] of methane, hydrogen, CO_2 and water, respectively.

- *Methanation:*

This operation is commonly known as the *Sabatier* reaction (Equation 2.29) and corresponds to the opposite to the reforming process. In the studied configuration (Figure 2-1), this reaction is employed for getting methane through the reaction of electrolysis-derived hydrogen and CO_2. This is a highly exothermic reaction, consequently, a reliable thermal management is required to avoid the thermodynamic limitation in the CO_2 conversion and to shift the reaction towards methane production. Typically, temperature ranges between 200 and 700°C, and pressure from 1 to 100 bar [127].

$$4H_2 + CO_2 \leftrightarrow CH_4 + 2H_2O \tag{2.29}$$

The generated methane in terms of power (M_{out}) and mass flowrate ($CH_{4,M}$) is expressed as presented in Equations 2.30 and 2.31, respectively. Besides, n_M represents the efficiency of the operation, and M_{in} the input power [kW].

$$M_{out}(t) = M_{in}(t) n_M \tag{2.30}$$

$$CH_{4,M}(t) = \frac{M_{out}(t)\rho_{CH4}}{LHV_{CH4}} \tag{2.31}$$

Moreover, the corresponding mass balance is described by Equation 2.32. In that expression, $CH_{4,M}$, $H_{2,M}$, $CO_{2,M}$ and H_2O_M represent the mass flow rates [kg/s] through the methanation reactor.

$$H_{2,M}(t) + CO_{2,M}(t) = CH_{4,M}(t) + H_2O_M(t) \tag{2.32}$$

$$H_{2,M}(t) = \frac{4PM_{H2}}{PM_{CH4}} CH_{4,M}(t) \tag{2.33}$$

$$CO_{2,M}(t) = \frac{PM_{CO2}}{PM_{CH4}} CH_{4,M}(t) \tag{2.34}$$

Additionally, aiming to improve the efficiency of the process, the heat released can be recovered and reused as high-temperature utility. Thus, assuming a recovery of 90%, the potential heat available from methanation reactor (M_{th-out}) can be computed by means of Equation 2.35.

$$M_{th-out}(t) = M_{in}(t)(1 - n_M) * 0.9 \tag{2.35}$$

- *Overall energy balance:*

As aforementioned, the objective of the proposed energy system is to satisfy the specific time-dependent demands of electricity and hydrogen. Taking this into account, and considering the system configuration depicted in Figure 2-1, the energy balance over each energy demand at each time step *t* is expressed in Equations 2.36-2.38.

$$D_{el}(t) = PV_D(t) + W_D(t) + FC_{out}(t) + B_{out}(t) + EG_D(t) \tag{2.36}$$

$$D_{H2}(t) + M_{in}(t) = El^D_{out}(t) + R_{out}(t) = H_{2,T}(t) \tag{2.37}$$

$$D_{CH4}(t) = M_{out}(t) + AD_D(t) + NG_D(t) \tag{2.38}$$

Here, D_{el}, D_{H2} and D_{CH4} represent the demand of electricity, hydrogen, and methane [kW], respectively. EG_D and NG_D denote the power [kW] taken from the electricity and natural gas grid for satisfying the corresponding energy demands. Additionally, the total power of electricity and natural gas imported from the grid at each time step are presented in Equations 2.39 and 2.40. In these equations, EG_{H2} represents the electricity imported from

the grid for producing hydrogen by means of water electrolysis, and NG_R the natural gas taken from the network for the steam reforming process.

$$EG_T(t) = EG_D(t) + EG_{H2}(t) \tag{2.39}$$

$$NG(t) = NG_R(t) + NG_D(t) \tag{2.40}$$

Moreover, the total thermal energy (Q_{th}) that is available for valorization is described by Equation 2.41. It is worth noting that the heat from the fuel cell is a low-temperature utility, whereas the heat recovered from methanation is a high-temperature one.

$$Q_{th}(t) = FC_{th-out}(t) + M_{th-out}(t) \tag{2.41}$$

Having completed the mass and energy balances through the process model, the next step is to define the criteria for evaluating the performance of the process flowsheet. Historically, this assessment had been focused on determining the technical feasibility and the economic profitability of processes [17]. However, these practices can lead to operations with a high energetic intensity and an inefficient use of the materials, which at the same time conducts to the exhaustion of resources, elevated greenhouse gas emissions and health problems derived from pollution of air and water [22]. In this regard, sustainable development aims to equilibrate the human activities with the ecosystem capacity, so that activities of the present do not compromise the ability of future generations to meet their own needs [22,78]. Therefore, sustainable development lies on the equilibrium of economic, environmental, and social dimensions.

In this line, the next section of this chapter is dedicated to describe each one of the sustainability dimensions and to present the mathematical expressions for assessing the performance of the process flowsheet based on the mass and energy balances.

2.3 Sustainability Evaluation

Sustainable development promotes the balance of three aspects: economic success, social acceptance, and environmental protection [22]. Firstly, economic sustainability relies on the efficient use of raw materials and natural resources. Hence, the utilization of novel technologies and alternative resources, as well as the recycling of waste are paramount. Second, social sustainability is based on the well-being of people, the social justice, and the rights of individuals. In this regard, it is crucial to consider the public perception, and to raise the awareness about fossil resources depletion and climate change for obtaining the commitment of people to preserve the natural resources. Lastly, environmental

sustainability relies on retaining the capacity of ecosystems for supporting the life and industrial activity. Thus, the employment of renewable resources and the reduction of environmentally harmful waste are the pillars of this aspect [19,22,78]. Figure 2-3 depicts a schematic representation of the three dimensions of sustainability, also referred in literature as the triple bottom line (TBL), and their interactions.

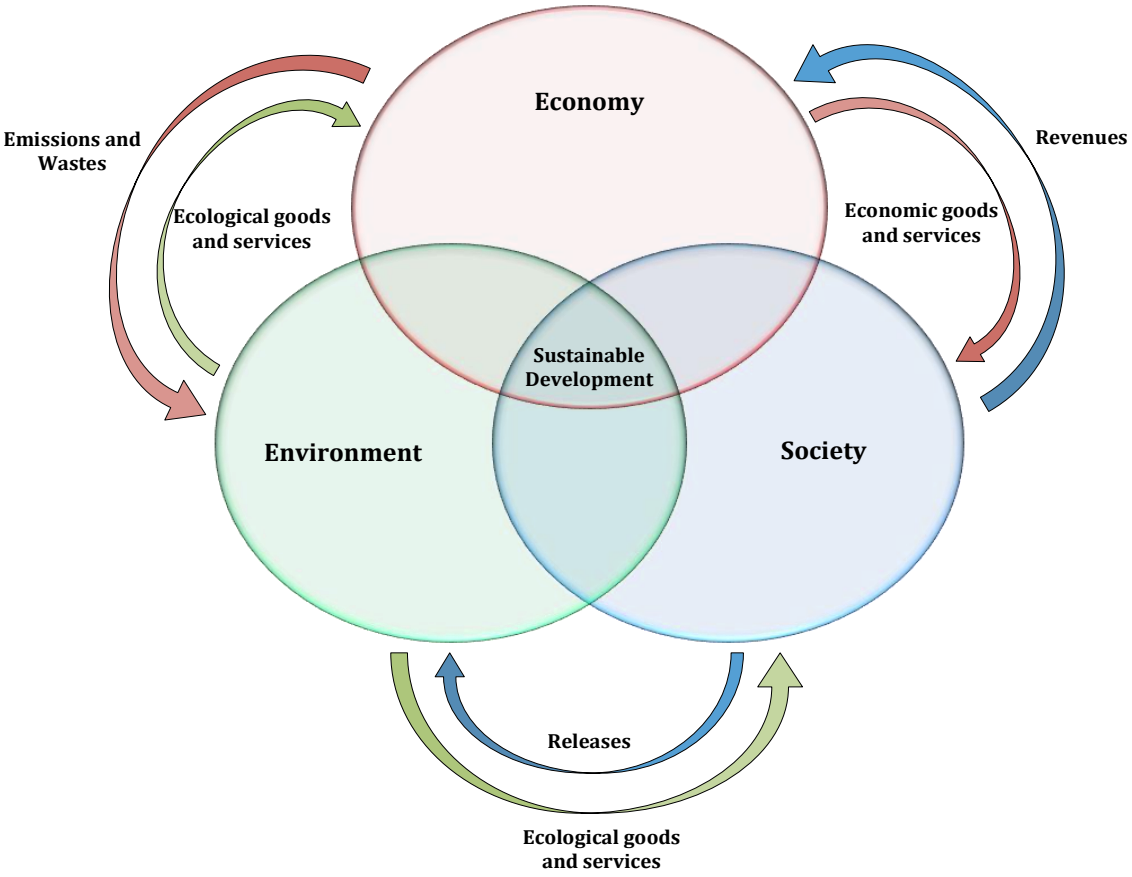

Figure 2-3: Dimensions of sustainable development. Adapted from [18,128,129].

Achieving this sustainable development goal requires a shift of current engineering practices, and rethinking the way to design, build, operate, and evaluate industrial products and processes [17,23]. Thus, engineering activities must no longer be performed in isolation, since it is necessary to consider the interactions among industrial processes, society and ecosystem at every stage of an engineering project [17,23]. Therefore, sustainability demands a holistic approach, and to expand the traditional system boundaries for including the economic, environmental and societal needs and constraints over the entire life cycle of products and processes [19,23].

Nevertheless, assuming that either a product is needed, or some end-use energy form is required, the way wherein they are obtained has the greatest influence on their

sustainability performance. For example, early decisions purely based on techno-economic aspects could involve hazardous raw materials or extreme operational conditions that can lead to safety or environmental problems. In that case, given that the structure of the process is already set, subsequent engineering stages would require complex and expensive solutions, but the margin for improving the performance of the process has been considerably reduced. Accordingly, it is well recognized that decisions made at conceptual design stage are of paramount importance because they have the greatest level of freedom, and consequently, the highest opportunity of enhancing the sustainability performance of a process [17–19].

Moreover, energy is a key component of the human life since it drives many aspects of economic and social growth (e.g. jobs, food production, incomes) [20]. Additionally, energy is also linked with the environmental issues, as it accounts for over two thirds of worldwide greenhouse gas emissions [20,21]. Therefore, energy could be considered as nearly the prime challenge and opportunity the world has to deal with towards sustainable development [20]. Thus, according to the TBL considerations, energy systems should have four main characteristics: cost-efficiency, reliability, safety, and environmental-friendliness [6,47]. In principle, DES seem to be a suitable alternative to the aforementioned challenges, since they fit well with the features of sustainable energy systems. DES rely on the energy consumption close to the generation site, so that energy efficiency is increased because losses in long-distance transmission lines are avoided [47]. Distributed generation also promotes the use of local and renewable resources, then enhancing self-sufficiency and energy security, and offering energy with low-carbon emissions [44,47].

Taking this into account, the aim of this section of the manuscript is to identify a set of indicators covering the three sustainability dimensions, and to integrate them with the process model. This will enable to carry out the assessment of energy system alternatives under TBL considerations from conceptual design stage, and hence, to take advantage of the highest opportunity for increasing their sustainability performance.

It is worth to point out that indicators are part of a hierarchy which also comprises principles and criteria. In this respect, the first instance are the principles, which are the premises or attributes that define sustainability. On the second level, criteria correspond to specific objectives and measurable conditions (quantitative or qualitative) that denote the degree of application of the principles. Then, the third instance comprises the indicators, which are variables and descriptors for objectively elucidate the features of a

system and infer the status of a criterion [130,131]. Figure 2-4 shows an example of the three levels of the conceptual framework for evaluating the performance.

In general, indicators should be able to capture essential features so that they enable to discriminate among different alternatives. Additionally, indicators also must be: consistent with the objective, easy to analyze and communicate, understandable and relevant for decision-makers and stakeholders, based on timely and reliable information, and few and manageable in number [130,132–134].

In this regard, a common practice is to conduct a survey with experts, stakeholders and/or decision-makers for selecting the appropriate criteria and indicators according to their specific requirements. For instance, Bautista et al. and Buchholz et al. performed a survey with experts aiming to validate a framework of indicators for the sustainability assessment of biodiesel production and bioenergy systems, respectively [135,136]. Moreover, Stamford and Azapagic, based upon literature and direct contact with stakeholders and experts, proposed 43 sustainability indicators for the assessment of energy systems [137]. To address the energy planning issue, Neves and Leal developed a framework of 18 sustainability indicators for energy planning from literature analysis and feedback from local authorities and experts [138]. In another work, Shaaban and Scheffran implemented a systematic approach for selecting the most relevant indicators and their applicability in the assessment of electricity production technologies in Egypt [134].

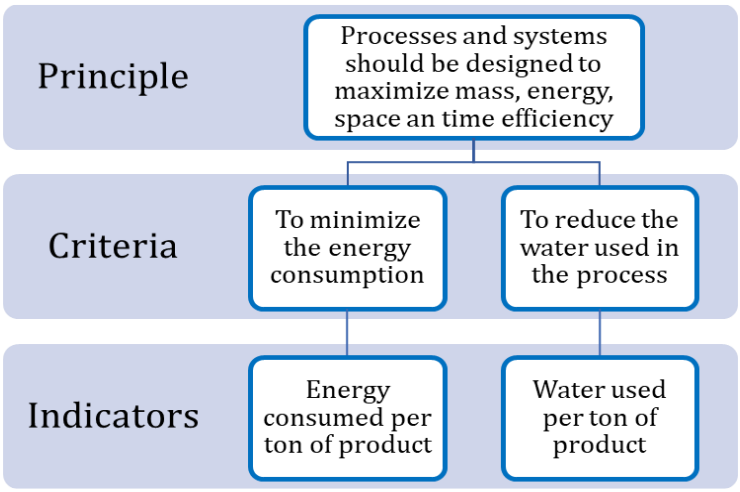

Figure 2-4: Instances for the performance assessment. Adapted from [17,139].

Nonetheless, that type of exhaustive analysis for a huge number of indicators is beyond the scope of this thesis. Accordingly, in this work, the choice of the indicators was based upon literature information. Thus, the selected indicators have four main characteristics: (i) cover the three sustainability dimensions, (ii) they are directly related with conceptual

design decisions, (iii) they can be defined through the information from mass and energy balances, and (iv) they have been identified as relevant for the evaluation of energy systems.

In the next subsections, each one of sustainability dimensions is addressed, and the corresponding indicators are presented. According to the energy system model formulated in section 2.2.3, as the proposed approach focuses on the early design of the energy system, only the main energy conversion and storage technologies are included. In such a way, intermediate units such as heat exchangers, pumps and compressors are not considered within the energy system model. Accordingly, the impact of the utilities required for those pieces of equipment is not taken into account for the system analysis.

2.3.1 Economic Dimension

In a competitive market, economic feasibility is vital for a new project. Indeed, unfavorable financial viability is not sustainable. In this respect, the indicators within the economic dimension must describe the profitability and costs of the energy system. As a result, total annualized cost (TAC) and levelized cost of energy ($LCOE$) were selected as the most relevant indicators for evaluating the economic performance of energy systems [134,137,138,140–143].

- *Total Annualized Cost:*

This indicator is the result of the contribution of capital and operational expenditures as stated in Equation 2.42. This indicator reflects the decisions made at conceptual design stage, since it relies on the type, size, and operation of the technologies within the system.

$$TAC = CAPEX + OPEX \tag{2.42}$$

$$CAPEX = \sum_{k}^{K} C_k Cap_k CRF_k \tag{2.43}$$

$$CRF_k = \frac{r(1+r)^{Lk}}{(1+r)^{Lk} - 1} \tag{2.44}$$

$$OPEX = O\&M_F + OC_V \tag{2.45}$$

$$O\&M_F = \sum_{k}^{K} O\&M_k \quad ; \quad O\&M_k = f(C_k) \tag{2.46}$$

$$OC_V = C_{EG}\int_{t0}^{tf} EG_T dt + C_{NG}\int_{t0}^{tf} NG dt + C_{Bio}\int_{t0}^{tf} AD_{in} dt \quad (2.47)$$

As stated in Equation 2.43, *CAPEX* depends upon the capital cost (C_k), the capacity (Cap_k), and the annuity factor (CRF_k) of each technology k. Besides, r represents the discount rate (7%) and L_k the lifetime of the equipment. Note that as the proposed framework focuses on small-scale equipment (distributed generation), typical power functions are not used for accounting the economies of scale. Nevertheless, if required, this kind of expressions can be easily integrated for computing the capital cost of the technologies. Meanwhile, *OPEX* comprises the fixed operational and maintenance costs ($O\&M_F$) and the variable operation costs (OC_V), as expressed in Equation 2.45. In this study, $O\&M_k$ are considered as a percentage of the annual investment cost of the corresponding energy conversion and storage alternative (Equation 2.46), and they account for the fixed maintenance and labor costs. Moreover, variable operational costs rely upon the amount of electricity and natural gas imported from the grid during the evaluated period t_f, and their corresponding prices C_{EG} and C_{NG} (Equation 2.47). Also, variable costs include the cost of gathering the biomass for anaerobic digestion (C_{Bio}).

Considering the stated assumptions, this corresponds to a preliminary economic analysis, which fits well with the accuracy expected at conceptual design stage [22]. Nevertheless, as the project proceeds, the proposed approach can be easily adapted to perform a more detailed evaluation of the energy system. For instance, the cost of land, and additional equipment (e.g. heat exchangers, pumps) and their utilities can be included to enhance the economic assessment [79].

- *Levelized Cost of Energy:*

This indicator represents the cost per unit of energy produced within the system. Hence, it corresponds to the minimum price that end-users would pay for the investor to break even [137]. As observed in Equation 2.48, *LCOE* is the ratio between the *TAC* and the total amount of energy generated in one year (*TE*). The latter is equivalent to the total energy demanded, as presented in Equation 2.49.

$$LCOE = \frac{TAC}{TE} \quad (2.48)$$

$$TE = \int_{t0}^{tf} D_{el} dt + \int_{t0}^{tf} D_{H2} dt + \int_{t0}^{tf} D_{CH4} dt \quad (2.49)$$

2.3.2 Environmental Dimension

Conventional energy systems are strongly dependent on fossil fuels. As a consequence, energy is the dominant contributor to climate change, accounting for more than 80% of CO_2 emissions in 2018 [21]. Therefore, energy systems must be designed in order to reduce or eliminate these releases, since they are one of the key variables for defining the sustainability of a process [137,138,141,143–146].

Moreover, currently billions of people worldwide still lack of water for drinking and hygiene [147]. Also, water shortages due to climate change effects, make the use of water another issue of supreme importance for assessing industrial activities [144]. As a result, high water consumptions in energy conversion processes should be avoided since they are not sustainable [18,134,143,144,148].

Taking this into account, CO_2 emissions and water consumption were selected as the indicators for evaluating the environmental dimension during the energy system design.

- *CO_2 emissions:*

Annual CO_2 emissions (AGE) are expressed in Equation 2.50 as a function of three contributions: the process operations that release CO_2 (AGE_P), the electricity and natural gas imported from the grid (AGE_G), and the processing of biomass (AGE_B). As stated in Equation 2.51, process emissions correspond to those produced from reforming reaction by using methane from the network, i.e. only fossil-derived CO_2 emissions are considered. In that equation, λ_{ref} represents the emission factor of reforming process [$kgCO_2/kgH_2$], and $H_{2,ref}^{f,m}$ is the total amount of hydrogen produced [kg] by means of steam methane reforming of natural gas (Equation 2.52).

Meanwhile, CO_2 emissions due to the imports of energy from the grid are described in Equation 2.53. This value depends upon the total amount of electricity and natural gas taken from the grid and their corresponding emission factors λ_{EG} and λ_{NG} [$kgCO_2/kWh$], respectively.

$$AGE = AGE_P + AGE_G + AGE_B \tag{2.50}$$

$$AGE_P = \lambda_{ref} H_{2,ref}^{f,m} \tag{2.51}$$

$$H_{2,ref}^{f,m} = \frac{n_R}{LHV_{H2}} \int_{t0}^{tf} NG_R dt \tag{2.52}$$

$$AGE_G = \lambda_{EG} \int_{t0}^{tf} EG_T dt + \lambda_{NG} \int_{t0}^{tf} NG dt \quad (2.53)$$

In general, it is well recognized the benefit of using the organic waste to produce biogas through anaerobic digestion instead of leaving it in landfills. In this respect, in addition to the reduction of waste itself, some advantages are the replacement of fossil-based by biogenic CO_2 emissions from the biogas burning, the possibility to avoid the methane emissions from landfilling, and the production of a fertilizer rich in nutrients (digestate) [149–151]. Moreover, anaerobic digestion of organic waste can also contribute to mitigate deforestation, since the firewood could be substituted by biomethane [152].

Taking this into account, the CO_2 derived from processes employing biomass correspond to biogenic emissions and are accounted as expressed in Equation 2.55. That expression includes the emissions from the anaerobic digestion of biomass (BE_{AD}), the subsequent reforming of biomethane (BE_{ref}), and the factor ω, which represents the deforestation rate. Indeed, the quantification of these emissions depends upon the location wherein the energy system would be implemented. For example, considering the low deforestation in France, it can be assumed that the CO_2 emitted by biomass processing is equivalent to that captured by biomass in the photosynthesis process (carbon neutrality). In that case, the term AGE_B can be neglected in the global balance, i.e. the deforestation rate (ω) is zero. However, in countries with high deforestation rate, those emissions are not compensated so that their contribution must be accounted. In this work, the deforestation rate is estimated as the relative change in the forest area over the last twenty years since this is the average lifetime of the energy system. This variable was used because forest represents a long-term carbon stock, and it has a higher capacity for storing carbon per unit of land area compared with crop-based plants [153–155].

Equation 2.55 presents the emissions derived from anaerobic digestion process as a function of the emission factor λ_{AD} [$kgCO_2/m^3CH_4$], and the total amount of biomethane produced. In Equation 2.56, $H_{2,ref}^{b,m}$ represents the hydrogen obtained via reforming of biomethane [kg], which can be computed by means of Equation 2.57.

$$AGE_B = \omega\left(BE_{AD} + BE_{ref}\right) \quad (2.54)$$

$$BE_{AD} = \lambda_{AD} \int_{t0}^{tf} CH_{4,AD} dt \quad (2.55)$$

$$BE_{ref} = \lambda_{ref} H_{2,ref}^{b,m} \tag{2.56}$$

$$H_{2,ref}^{b,m} = \frac{n_R}{LHV_{H2}} \int_{t0}^{tf} AD_{out} dt \tag{2.57}$$

As noted from the Equations 2.50-2.57, in this work the CO_2 emissions are assessed through a gate-to-gate analysis. This approach is used because the focus of this research is on the early design of the energy system, and because of the information available from the proposed energy system model. Therefore, this evaluation does not include the impacts throughout the whole life cycle of the products delivered by the energy system. This implies that the use of some technologies such as the photovoltaics, the electrolyzer and fuel cell is considered as an emission-free option. In this regard, in a later design stage, a cradle-to-grave analysis could be performed by means of a life cycle assessment to include all the impacts from the acquisition of the raw materials employed for the fabrication of these units until their recycling and final disposal [156,157].

- *Water Consumption:*

As aforementioned, the impact of utilities is not considered in this work. Thus, the water consumption indicator is focused on the use of process water. According to the energy system model, water is consumed in two operations: electrolysis of water and steam methane reforming. Nevertheless, water is also obtained from operation of fuel cell and as byproduct in methanation reactor. In this respect, whereas water produced in fuel cell is commonly recycled and reused in the electrolyzer, water from methanation is treated and discharged as wastewater since it may contain traces of heavy metals [158,159]. Additionally, water is also required for biomass processing. In this case, it is mixed with the biomass for obtaining the slurry that is fed to the anaerobic digester. It is noteworthy that electrolyzer requires water of high purity for its optimal operation. Nonetheless, this issue is not particularly addressed in the analysis since the manufacturers of equipment typically include reverse osmosis and deionization units as standard to pretreat the feeding water (e.g. Hydrogenics and Areva H_2Gen).

Thus, the net water consumption (WC) of process water by the operation of the energy system can be described through the Equation 2.58. It is worthy to note that from the stoichiometry of reaction (Equation 1.3), 9kg of water are needed to produce 1kg of hydrogen. However, in practice around of 11 kgH_2O/kgH_2 are required [160], which is represented by the factor ψ_{El}. Moreover, ψ_{AD} represents the water consumption of the anaerobic digestion process [kgH_2O/kg biomass].

$$WC = \psi_{El} \int_{t0}^{tf} H_{2,El} dt + \int_{t0}^{tf} H_2O_R dt + \psi_{AD} \int_{t0}^{tf} AD_{in} dt - \int_{t0}^{tf} H_2O_{FC} dt \qquad (2.58)$$

2.3.3 Social Dimension

In addition to the economic viability and the environmental friendliness, industrial activities must agree with social requirements, i.e. improving the quality of life [26,27]. In this regard, public perception and acceptability have a prime importance, since these could define whether an energy solution is implemented or not, and represent the intangible cost associated with the image of the project [18,142].

Broadly, quality of life can be associated to two main aspects: equity and health. Regarding energy, social equity involves the level of fairness and inclusiveness for energy resources distribution [26]. Indeed, this issue is addressed in one of the sustainable development goals proposed by United Nations (Goal 7), which consists in ensuring access to affordable, reliable, sustainable and modern energy for all [20]. Moreover, the health aspect refers to the potential pollution, accidents, injuries, or fatalities derived from energy generation. On the one hand, pollution issue commonly falls into environmental dimension, as it is quantified with variables such as gas emissions, particulate matter, or contamination of water. On the other hand, occupational accidents and public hazards are related with the inherent risk derived from the operation of conversion technologies (e.g. temperature and pressure conditions), and the properties of chemical compounds (e.g. flammability, toxicity) employed within energy systems [26,134,137,142,143,148].

Accordingly, the energy import dependency, and the inherent safety index are the selected indicators for assessing the energy system performance.

- *Energy Import Dependency:*

Access to energy has implications on poverty, education, health and welfare issues [26,161]. Therefore, reliable energy supply is essential for improving quality of life. However, there are still around 800 million people worldwide, mainly in developing countries, without access to electricity [20]. In fact, lack of access to modern energy implies that people depend on inefficient and pollutant technologies for cooking and electrification (mainly based upon traditional biomass, kerosene, and diesel) [20]. In addition to that, depletion and uncertain prices of fossil energy sources, risks derived from extreme weather conditions due to climate change, and possible political conflicts could affect the energy security even for people already connected to the grid [44,142]. Taking this into

account, it is essential to design energy systems that promote the diversification of energy sources, the use of low-carbon technologies, and the reduction of import dependency in order to secure the energy provision [26,29,142,162–164]. In this respect, the energy grid dependency has been recognized as a suitable indicator for assessing energy security since it is able to account for both, the amount of imported energy potentially avoided and the degree of self-sufficiency for providing access to energy [137,142,162,164].

Besides of increasing the security of supply, energy autonomy could also lead to the creation of local jobs, economic growth, and community ownership [29,165]. Indeed, either in developed or developing regions, local communities are changing from their traditional passive role as energy consumers for being active prosumers, i.e. they participate in both, energy production and consumption [28,29]. Moreover, autonomous energy systems lead to opportunities of self-regulation and self-governance [165]. In this respect, energy independency enables the engagement of people for addressing global common goals such as the CO_2 emission reduction and the renewable technologies deployment [29,165]. In such a way, this kind of systems can represent a fair and inclusive alternative since they increase the awareness and willingness of communities to participate in the market, and allow them to get benefit from the financial reward offered by governments [29,165].

In this work the energy security issue is quantified as the dependence (GD) on the main networks of electricity and natural gas, which is expressed as the ratio between total energy imported from the grid (IG) and total energy demanded by users (TE), as stated in Equation 2.59. The former is accounted by adding the electricity and natural gas imported from the grid (Equation 2.60). The latter was already presented in Equation 2.49.

$$GD = \frac{IG}{TE} * 100 \tag{2.59}$$

$$IG = \int_{t0}^{tf} EG_T dt + \int_{t0}^{tf} NG dt \tag{2.60}$$

- *Inherent Safety:*

Power plants involve hazardous materials and processes that can lead to accidents, and negatively impact the health of workers and the wellbeing of communities. Therefore, aiming to avoid or reduce those accidents, a variety of methods can be implemented for evaluating the safety issue during the whole life cycle of the project [166]. Broadly, these methods differ on the aspects considered, the required information, and the output data type [167]. For example, some of the most common and popular approaches are the Hazard and Operability method (HAZOP), the Dow chemical/fire and exposure indexes (C&EI and

F&EI), and the Mond index [167,168]. However, these methods are not suitable for conceptual design stage since, they rely upon information from basic and detailed engineering such as the P&ID (piping and instrumentation diagram) of the process [166–168].

Moreover, some methodologies are based upon the assessment of the inherent safety of the processes. The essence of this perspective is to avoid and/or eliminate hazards rather than controlling them through add-on systems [169–172]. Indeed, these approaches rely on the fact that the potential risks of a process are related with the intrinsic characteristics of the chemical substances and operation units [172,173]. In this line, inherent safety analysis fits well with conceptual design decisions, since the selection of chemistry routes, conversion technologies and process conditions could be rated according to their intrinsic properties [167,174].

Inherent safety comprises four main principles: intensification, substitution, attenuation, and simplification. Intensification or minimization refers to quantities of materials and size of equipment within the plant. Thus, safer processes are those ones with lower amount of hazardous substances and smaller operation units. Substitution relies on replacing hazardous materials for safer ones, e.g. using non-flammable and/or non-toxic refrigerants or solvents instead of flammable and/or toxic compounds. Attenuation or moderation seeks to modify process conditions (e.g. temperature, pressure, concentration) for avoiding flammable limits or reactions close to runaway temperatures. Meanwhile, simplification lies on the fact that processes with less equipment lead to fewer opportunities for error, so that simpler plants are inherently safer [171,172,174].

Considering the foregoing, the inherent safety assessment is typically quantified as the contribution of two sub-indices: the chemical and the process inherent safety index. The former includes properties such as heat of reaction, flammability, explosiveness, and toxicity. In contrast, the latter focuses on process conditions such as pressure and temperature. In this respect, a variety of methods have been proposed aiming to evaluate the inherent safety of processes. For example, Edwards and Lawrence proposed the prototype index of inherent safety (PIIS) which is mainly focused on the selection of raw materials and reaction steps [175]. Nonetheless, this is a reaction-oriented method and is not suitable for the safety evaluation of the whole process plant. In another work, Heikkilä proposed the inherent safety index (ISI), which permits to compare between different process alternatives [171]. Despite that, this method has some limitations because it is based on the worst-case scenario and does not consider neither the quantity of materials

nor the number of equipment within the process. Indeed, the evaluation of the worst-case scenario could lead to similar results even if considerably different processes are analyzed [173,176].

To overcome this issue, Li et al. proposed the enhanced inherent safety index (EISI), which includes all the chemicals and their amount by multiplying the flow rate with the severity factor (e.g. explosiveness or toxicity) [173]. Additionally, for process inherent safety index, the scores of the equipment are multiplied by their number and are added all together. In a similar direction, recently Gangadharan et al. introduced the comprehensive inherent safety index (CISI) adopting and object-oriented approach [176]. In this method, each equipment corresponds to a separate entity so that the inherent safety index is calculated for individual operations units. Moreover, this approach considers the severity of reactions based on the combination of chemicals, and a connection score between two units as a function of their individual safety scores.

In this thesis, the inherent safety for the energy system design is quantified based upon the comprehensive inherent safety index. However, the severity of reaction and the connection score are not included. The former because the score of reaction is considered as a function of the heat of reaction (already included), and the latter because as stated by Gangadharan et al., such score could change depending on the judgement and/or experience of the method user. Accordingly, the total inherent safety index for evaluating the energy system can be calculated as stated in Equations 2.61-2.64.

$$IST = \sum_{k}^{K} I_{E,k} \tag{2.61}$$

$$I_{E,k} = I_{C,k} + I_{P,k} \tag{2.62}$$

$$I_{C,k} = \frac{\sum_{n}^{N}(I_{FL,n} + I_{EX,n} + I_{TOX,n} + I_{COR,n})F_n + I_{R,k}\sum_{n}^{N} F_n}{1000} \tag{2.63}$$

$$I_{P,k} = I_{I,k} + I_{T,k} + I_{Pr,k} \tag{2.64}$$

Where, IST is the total inherent safety index, $I_{E,k}$ is the individual equipment safety index, $I_{C,k}$ is the chemical index, and $I_{P,k}$ is the process index of the equipment k. Additionally, $I_{FL,n}$, $I_{EX,n}$, $I_{TOX,n}$ and $I_{COR,n}$ are the flammability, explosiveness, toxicity and corrosiveness scores, respectively. F_n represents the mass flow rate, $I_{R,k}$ is the reaction sore, the subscript n denotes each chemical substance through the equipment k and the factor 1000 is the basis flow rate. Meanwhile, $I_{I,k}$, $I_{T,k}$ and $I_{Pr,k}$ correspond to the inventory, temperature,

and pressure scores, respectively. Detailed information for computing the inherent safety index is presented in Annex A.

2.4 Summary and Conclusions

In this chapter, a process model for representing the energy system was built, and the indicators for the assessment of system structures during conceptual design were formulated. Initially, a base-case flowsheet for the energy system was proposed based upon a literature review, so that the most common technologies within energy systems were included. Broadly, this base-case flowsheet comprises electricity, hydrogen, and methane as potential energy demands, which can be satisfied by means of renewable resources or importing energy from electricity and natural gas grids. Additionally, energy storage in electrical battery and hydrogen form are considered. Subsequently, the mass and energy balances were formulated for each operation unit according to the base-case system structure. Thereafter, the approach for assessing the energy system performance was introduced including the sustainability dimensions. In that part, the main characteristics of each dimension, as well as the relation among them were highlighted. Finally, a set of indicators were defined including economic, environmental, and social dimensions for evaluating the energy system configurations during conceptual design stage. Aiming to summarize, Figure 2-5 depicts the proposed framework based on principles, criteria, and indicators.

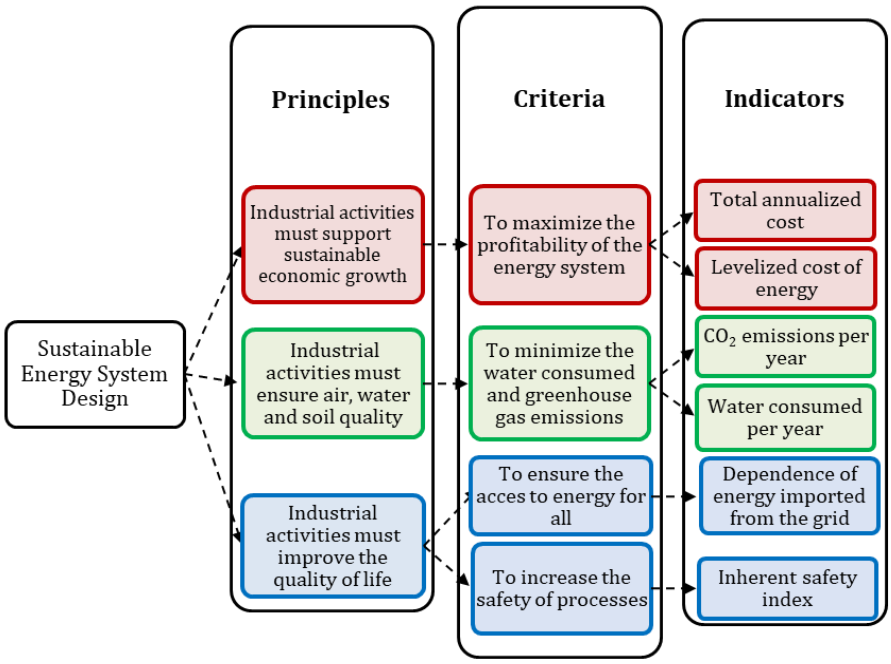

Figure 2-5: Triple bottom line framework for the sustainability assessment of energy systems.

3. Optimal Energy System Design Considering the Sustainability Dimensions

Once the base-case flowsheet is represented and the evaluation criteria are defined, the next task in conceptual design is to find the best process structure. This implies to assess the possibilities covered within the base-case flowsheet, and to select the set of equipment, their capacities, and the operating policy that provides the most effective option. Indeed, that choice lies on rating the process alternatives according to one or more performance criteria, i.e. solve an optimization problem. Thus, the selected process layout corresponds to the one that yields the maximum or minimum value of the assessed indicator. In this respect, based upon the process model and the sustainability indicators already proposed, this chapter focuses on formulating and solving the optimization problem for the design of energy systems.

3.1 Process Optimization

3.1.1 General Aspects

Typical problems in process design and operation have many possible solutions, since there is a variety of process units and/or operating conditions that could be implemented for the conversion of raw materials into the desired product. In such a way, enumerate, evaluate, and classify all alternatives would be an extremely time-consuming task. In this regard, and from the most general perspective, optimization lies on the use of mathematical methods for finding the best candidate without explicitly testing the entire set of alternatives [119,177]. In fact, beyond process design and operation, the use of optimization techniques can take place at any level wherein decisions based upon an objective and quantitative evaluation of options are required [177,178]. For instance, optimization could be applied in decisions to be made at the management level such as the evaluation of a new project and the definition of an investment plan, until the definition of

hourly guidelines for improving the operation of an equipment within a production process.

Mathematically, an optimization problem consists of three main elements: the performance criterion, the decision variables, and the system model [119,179,180]. The first is commonly stated as the objective function, and it is a numerical value that represents the basis wherein the alternatives are evaluated. In this line, the best candidate corresponds to the solution that provides the maximum or minimum value of the assessed index. Then, decision/optimization variables constitute the degrees of freedom of the problem, i.e. the decisions to be made. This implies that optimization problems are underspecified ones, as the number of variables is higher that the number of equations. Lastly, the system model is the set of mathematical relationships that describes how all the variables are related. These relations could be either equality (e.g. mass and energy balances) or inequality (e.g. system bounds, allowable conditions) expressions that represent the physical phenomena occurring within the system. Thus, a general optimization problem can be formulated as presented in Equations 3.1-3.5.

$$min_{x,y} \quad f(x,y) \tag{3.1}$$

$$subject\ to \quad h(x,y) = 0 \tag{3.2}$$

$$g(x,y) \leq 0 \tag{3.3}$$

$$x \in X \subseteq \mathcal{R}^n \tag{3.4}$$

$$y \in Y \quad integer \tag{3.5}$$

In these expressions, f represents the objective function, h the equality constraints and g the inequality constraints. All of them are functions of the continuous variables x and integer variables y. Indeed, this formulation contains a great number of types of optimization problems. For instance, if the set of integer variables is non-empty and the objective function and constraints are non-linear, it is a mixed-integer nonlinear programming (MINLP) problem, but if the set of integer variables is empty and all system equations are linear, it becomes a linear programming (LP) problem, and so on [180].

Broadly, optimization problems can be classified according to a variety of aspects such as the existence or no of process constraints, the linearity of objective function and system constraints, the continuity of decision variables, and the number of objective functions. In fact, depending on the type of problem, different algorithms or strategies could be used for its solution. Nonetheless, the discussion about all classes of optimization problems and

solution algorithms is not within the aim of this work. Therefore, if interested, the reader is referred to the books by Ravindran et al. [119], Floudas [180], Edgar and Himmelblau [177], Dutta [179], or Pandu Rangaiah [181] for a more detailed information.

3.1.2 Optimization in Energy Systems Design

Conceptual design of energy systems requires three decisions to be made: selecting the process units (conversion and storage), defining their capacities, and establishing how they operate. In fact, these three decisions influence each other, so that they need to be appraised simultaneously for obtaining a suitable system structure [182]. Additionally, unlike steady state processes wherein the mass and energy flows are constant along time, the time-varying behavior of energy availability and loads must be considered for determining the operating policy of an energy system.

As presented in the first chapter (section 1.3.2), the optimal design of DES is commonly formulated as a MI(N)LP problem, where binary variables are used for specifying whether a technology is installed or not, and for representing their on/off status at each time step. Moreover, continuous variables are employed for establishing the energy flows within the system. In this regard, there is a consensus in literature about the complexity of solving the problem of the optimal design of DES. In general, this complexity resides on the number of decisions to be made, the diversity of energy sources and technologies to be considered, the time-dependency of variables, and the variety of objectives to be addressed. Indeed, although there are different techniques for addressing MI(N)LP problems such as branch-and-bound, cutting plane or decomposition methods, it is also recognized that the difficulty of solving this type of problems is higher than that one of a model only based on continuous variables [177,180].

In general, the complexity of problems involving binary variables lies on its combinatorial nature. In fact, any choice over the binary domain leads to a continuous problem that must be solved. In such a way, as the number of binary variables gets bigger, the quantity of possible solutions exponentially increases, and consequently, the required computational effort for solving the problem gets greater. In this respect, MI(N)LP is classed as a NP-hard problem since there is no algorithm running in polynomial time for solving it [180,182].

Taking this into account, the following passages of this work are dedicated to proposing an optimization approach for the design of DES only employing continuous variables.

Afterwards, based on the energy model and the sustainability indicators presented in Chapter 2, an application case is developed to illustrate the proposed framework.

3.2 Optimization Approach

As stated before, an optimization problem comprises three components: the objective function, the decision variables, and the equality and inequality constraints (process model). Thus, the next subsections will present each one of these elements and the formulation of the optimization problem for the design of energy systems considering the sustainability dimensions.

3.2.1 Objective Functions

The objective functions correspond to the economic, environmental, and social indicators defined in Chapter 2 (section 2.3). Therefore, six performance criteria (J) are considered as presented in Equation 3.6.

$$Obj.functions \qquad J \ni \{TAC, LCOE, AGE, WC, GD, IST\} \tag{3.6}$$

Nonetheless, in practice there are five objective functions since the total annualized costs are embedded within the levelized cost of energy.

3.2.2 Decision Variables

About the decision variables, as mentioned above, design of energy systems has been mainly addressed by employing integer binary variables, which are used to select the energy conversion technologies and to describe their on/off status. Conversely, in this work the implemented optimization approach only uses continuous variables. This was performed by considering that, once the energy demands are specified, and for a set of given performance parameters (conversion efficiencies), all the power inputs can be formulated as a function of the desired power outputs. For instance, taking as reference the requirement of hydrogen ($H_{2,T}$), there are three options for supplying it, renewable electricity, grid electricity and reforming process (El^{R}_{out}, El^{G}_{out} and R_{out}). Then, each one of these alternatives can be interpreted as a fraction of the total demand, as stated in Equations 3.7-3.10.

$$El_{out}^{R}(t) = \theta_1(t)H_{2,T}(t) \tag{3.7}$$

$$El_{out}^{G}(t) = \theta_2(t)H_{2,T}(t) \tag{3.8}$$

$$R_{out}(t) = \theta_3(t)H_{2,T}(t) \tag{3.9}$$

$$H_{2,T}(t) = El_{out}^{R}(t) + El_{out}^{G}(t) + R_{out}(t) = \sum_{i}^{I=3} \theta_i(t)H_{2,T}(t) \tag{3.10}$$

Where θ_1, θ_2 and θ_3 represent the fraction of hydrogen coming from renewable energy, the electricity of the grid and the steam methane reforming process, respectively. Meanwhile, *I* corresponds to the number of alternatives for supplying hydrogen.

Similarly, this approach can be extended for the remainder of decisions required across the energy system, i.e. the source for supplying the electricity demand, the electricity storage alternative, the source of methane for reforming process, the source of electricity for water electrolysis, and the source for supplying the methane demand. Regarding the electricity demand, as observed in Figure 2-2, the power supplied by photovoltaics and wind turbine (when available) is directly sent to satisfy the whole or a fraction of the electricity demand. Therefore, it is not a decision variable of the system. Taking this into account, the decision must be made over the energy not covered by such sources ($D_{el,M}$). Thus, Equation 2.36 can be transformed into Equation 3.11. In such a way, the three alternatives for covering the remaining demand are the fuel cell, the battery, and the electricity grid (Equation 3.12). In that Equation, φ represents the fraction of electricity supplied by each alternative *i.*

$$D_{el}(t) = PV_D(t) + WT_D(t) + D_{el,M} \tag{3.11}$$

$$D_{el,M}(t) = FC_{out}(t) + B_{out}(t) + EG_D(t) = \sum_{i}^{I=3} \varphi_i(t)D_{el,M}(t) \tag{3.12}$$

With respect to the storage alternative for the surplus electricity (Re_S), a pressurized tank with hydrogen and a battery are considered (Equation 3.13). In that expression, Re_{H2} and B_{in} are the renewable power sent to the electrolyzer and the battery [kW], respectively. Accordingly, δ represents the corresponding fraction of surplus electricity directed to each storage option.

$$Re_S(t) = Re_{H2}(t) + B_{in} = \sum_{i}^{I=2} \delta_i(t)Re_S(t) \tag{3.13}$$

Likewise, Equations 3.14-3.15 represent the sources for the steam methane reforming and for supplying the demand of methane.

$$R_{in}(t) = AD_{H2}(t) + NG_R(t) = \sum_{i}^{I=2} \gamma_i(t) R_{in}(t) \tag{3.14}$$

$$D_{CH4}(t) = AD_D(t) + NG_D(t) + M_{out}(t) = \sum_{i}^{I=3} \sigma_i(t) D_{CH4}(t) \tag{3.15}$$

Where γ represents the fraction of methane coming from the natural gas network or the anaerobic digester for the reforming process, and σ is the fraction of methane demand supplied by the anaerobic digester, the gas network and the methanation process. Additionally, I represents the number of alternatives for each decision within the system. For clarity, the reader is referred to the Figure 3-1, where the energy flows of the energy system are depicted.

Summarizing, the set of optimization variables comprises the fractions θ, φ, δ, γ and σ. Thus, according to Equations 3.10 and 3.12-3.15, there are thirteen decision variables by time step. However, by adding a consistency relationship for each decision (Equation 3.16), the number of optimization variables is reduced to eight by time step.

$$\sum_{i}^{I} S_i(t) = 1 \qquad S \ni \{\varphi, \theta, \delta, \gamma, \sigma\} \tag{3.16}$$

Then, from the proposed approach, optimization variables correspond to operating profiles since they are associated to the energy flows within the system. Meanwhile, design variables (i.e. capacity of energy converters) are determined by picking the highest energy flow rate through the corresponding unit. In such a way, the capacity of fuel cell is equivalent to the highest value of its output flow rate (FC_{out}), the capacity of the reforming reactor is given by the maximum flow rate R_{out} and so on. In the same line, if there is no flow rate through a technology along the whole evaluated period, it means that such equipment does not need to be installed within the system. Additionally, it is worth to note that Figure 3-1 depicts two electrolyzers, one powered by renewables, and another one by the electricity grid. Nevertheless, this was done just for illustrating the electricity sources for obtaining hydrogen, and to show that hydrogen sent to the pressurized tank only comes from renewable electricity. In fact, in practice there is only one electrolyzer and its capacity is defined by the sum of energy flow rates Re_{H2} and EG_{H2}.

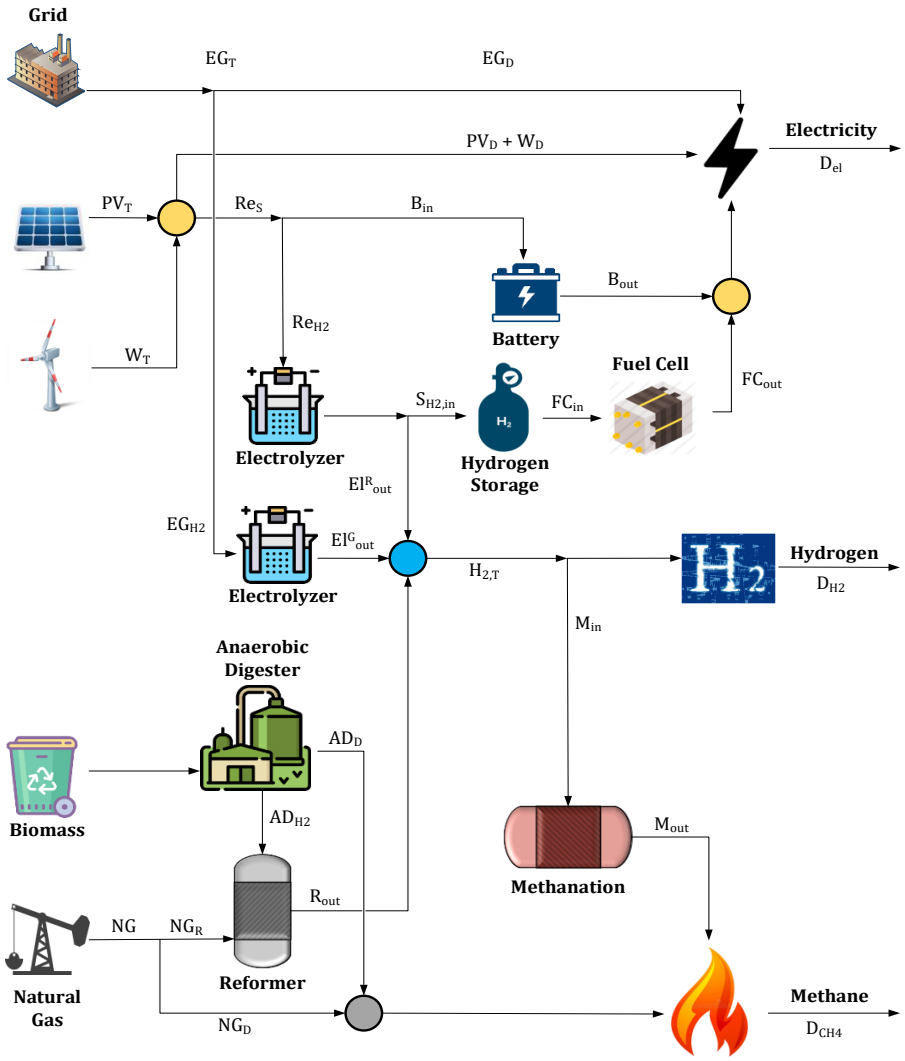

Figure 3-1: Energy system flowsheet for representing the decision variables of the optimization problem.

3.2.3 Constraints

The intrinsic constraints of any optimization problem rely on the process model. For the energy system case, these constraints lie on the mass and energy conservation principles and correspond to the system model developed in Chapter 2. In addition to that, other constraints needed for the problem are related to the physical sense of the energy storage systems. In such a way, Equations 3.17 and 3.18 are employed for assuring non-negative values of those variables (S_B and S_{H2}). Besides, these expressions also include upper limits for restricting the amount of energy stored ($S_{B,max}$ and $S_{H2,max}$). Meanwhile, Equation 3.19 imposes a limit on the amount of biomass available for anaerobic digestion (Bio_D).

$$0 \leq S_B(t) \leq S_{B,max} \tag{3.17}$$

$$0 \leq S_{H2}(t) \leq S_{H2,max} \tag{3.18}$$

$$\int_{t0}^{tf} AD_{in}\,dt \leq Bio_D \tag{3.19}$$

Another constraint of the storage systems lies on their periodic behavior, so that the storage level must be the same at the beginning and at the end of the evaluated period, i.e. there is no net accumulation of energy over the evaluated time horizon, as described in Equations 3.20-3.21.

$$S_B(t_0) = S_B(t_f) \tag{3.20}$$

$$S_{H2}(t_0) = S_{H2}(t_f) \tag{3.21}$$

Regarding decision variables (u), they are constrained by lower and upper limits as presented in Equation 3.22.

$$0 \leq u(t) \leq 1 \quad ; \quad u \ni \{\varphi_1, \varphi_2, \theta_1, \theta_2, \delta_1, \gamma_1, \sigma_1, \sigma_2\} \tag{3.22}$$

3.2.4 Optimization Problem

Considering the energy system model, the objective functions, the decision variables, and the constraints previously defined, the optimization problem for the design of energy systems considering the sustainability dimensions can be formulated as presented in Equations 3.23-3.35.

$$Minimize \qquad J_1(u,x,t) = TAC \tag{3.23}$$

$$J_2(u,x,t) = AGE \tag{3.24}$$

$$J_3(u,x,t) = WC \tag{3.25}$$

$$J_4(u,x,t) = GD \tag{3.26}$$

$$J_5(u,x,t) = IST \tag{3.27}$$

$$Subject\ to \qquad h = f(u(t),x(t),p,t) \quad ,system\ model \tag{3.28}$$

$$0 \leq S_B(t) \leq S_{B,max} \quad ,battery\ storage \tag{3.29}$$

$$S_B(t_0) = S_B(t_f) \quad ,periodicity \tag{3.30}$$

$$0 \leq S_{H2}(t) \leq S_{H2,max} \quad ,hydrogen\ storage \tag{3.31}$$

$$S_{H2}(t_0) = S_{H2}(t_f) \quad , periodicity \tag{3.32}$$

$$\int_{t0}^{tf} AD_{in}\,dt \leq Bio_D \quad , biomass\ available \tag{3.33}$$

$$0 \leq u(t) \leq 1\ ;\ u \ni \{\varphi_1, \varphi_2, \theta_1, \theta_2, \delta_1, \gamma_1, \sigma_1, \sigma_2\} \quad , decision\ variables \tag{3.34}$$

$$\sum_{i}^{I} S_i(t) = 1 \quad S \ni \{\varphi, \theta, \alpha, \delta, \gamma, \sigma\} \quad , consistency \tag{3.35}$$

In these expressions, J represents each performance criterion, i.e. total annualized costs, CO_2 emissions, water consumption, grid dependence, and inherent safety. h is a vector that contains the equations of the energy system model, i.e. those presented in Section 2.2.3 (Chapter 2). As noted, these expressions are function of the decision variables (u), the state variables (x), the parameters (p), and the time (t). Moreover, the constraints are stated in Equations 3.28-3.35 and include the model of the energy system, the upper and lower limits of the storage units, the periodicity relations, and the availability of biomass. Meanwhile, u denotes the optimization variables, which are linked to the energy flows FC_{out} (φ_1), B_{out} (φ_2), El^R_{out} (θ_1), El^G_{out} (θ_2), Re_{H2} (δ_1), AD_{H2} (γ_1), AD_D (σ_1) and NG_D (σ_2).

3.3 Case of Application

Considering the proposed energy system modeling (Chapter 2) and the optimization approach (section 3.2), the required input information for designing the DES is:

a) The time-dependent weather conditions, i.e. ambient temperature, solar irradiance, and wind speed.
b) The time-dependent profiles of electricity, hydrogen, and methane demands.
c) The prices of taking energy from the electricity grid and natural gas network.
d) The emission factor of the electricity and natural gas coming from the grid.
e) The technical parameters of each technology. These values refer to the conversion efficiencies, pressure, and temperature.
f) The cost parameters of each technology, i.e. lifetime, investment, and fixed operation and maintenance costs.
g) The properties for the safety evaluation of chemical compounds, i.e. flammability, explosiveness, toxicity, corrosiveness, and heat of reaction (Annex A).
h) The energy system constraints, which correspond to the upper limits for the capacity of battery and hydrogen systems. Additionally, the total amount of biomass available is required.

3.3.1 Case Study

The case study is a hypothetical community of 1500 inhabitants near Marseille – France. This case of application considers electricity grid, photovoltaics, biomass, and gas network as energy inputs. Meanwhile, the energy demands correspond to electricity and hydrogen. Thus, the base-case structure of the energy system can be reduced (with respect to the general case Figure 2-1) since wind turbine and methane demand are not included. Therefore, the corresponding base-case flowsheet of the energy system is depicted in Figure 3-2. Moreover, as there is no demand of methane within the system, the number of optimization variables decreases from eight to six by time step, since Equation 3.15 does not need to be considered.

It is noteworthy that this case study is used to illustrate the proposed approach for the design and analysis of DES considering the sustainability dimensions, so that it is not an exhaustive assessment of all available technologies. Nevertheless, the approach could be easily extended to evaluate other technological units (e.g. wind energy, gasification) or energy forms (e.g. methane demand).

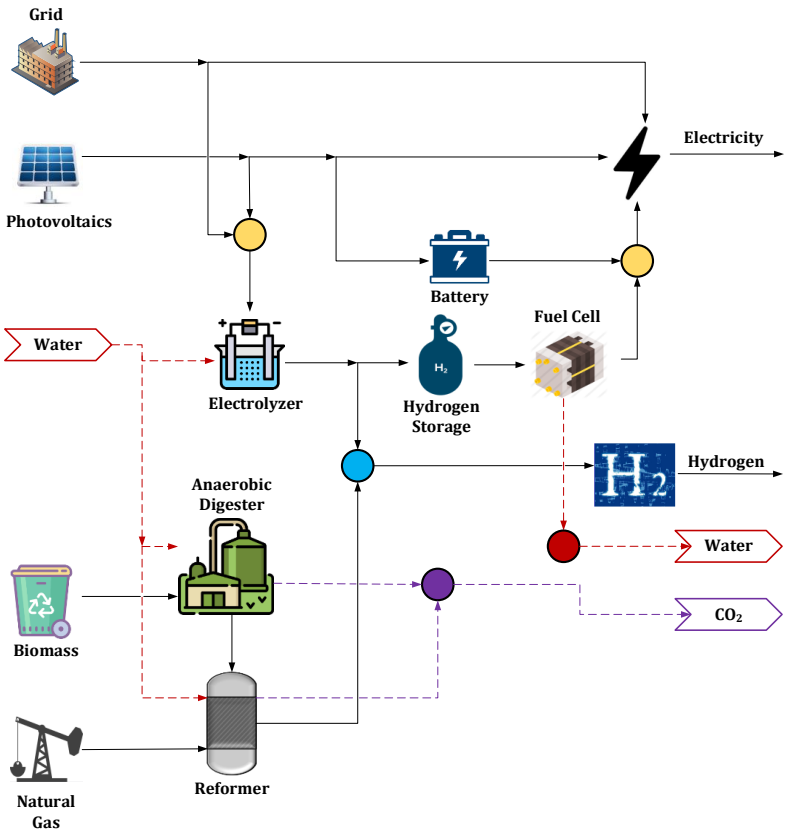

Figure 3-2: Base-case flowsheet of the energy system for the case study.

Weather data, namely solar irradiance (Figure 3-3a) and ambient temperature (Figure 3-3b) were gathered from Solcast webpage [183]. The time-dependent profile of electricity demand (Figure 3-3c) was obtained for 2018 from the Open Data Réseaux Énergies (ODRÉ) [184]. Regarding hydrogen, it is supposed to be used in mobility with a peak demand of 160 kW, which corresponds approximately to a capacity for supplying 60 kg of hydrogen by day (i.e. ≈ 12 cars by day). For this demand, a daily periodic behavior was assumed as presented in Figure 3-3d.

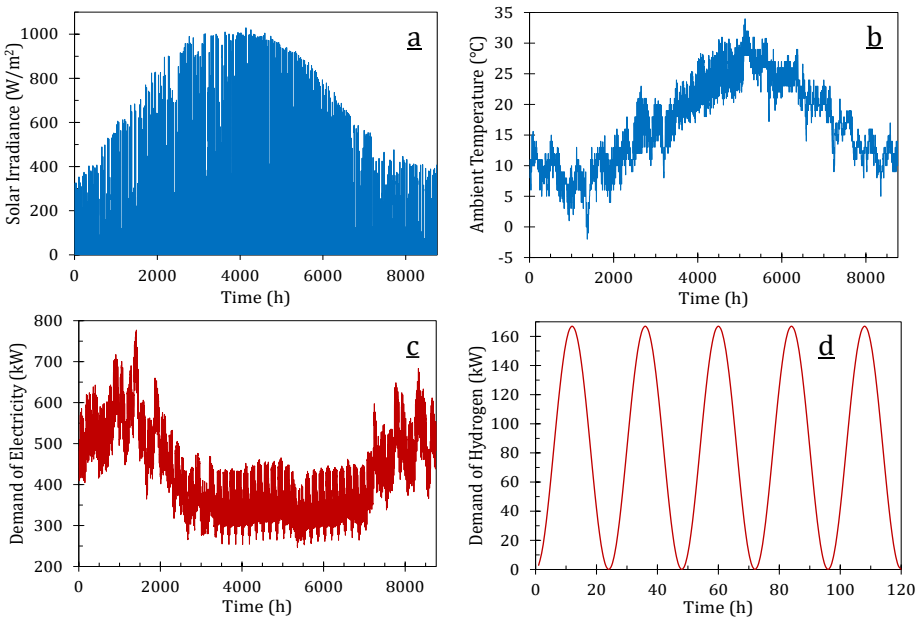

Figure 3-3: Profiles of input data for designing the energy system. (a) Solar radiation, (b) ambient temperature, (c) electricity demand, (d) hydrogen demand.

3.3.2 Parameters

The selected prices for importing electricity (C_{EG}) and natural gas (C_{NG}) from the grid are 0.10 €/kWh and 0.037 €/kWh, respectively, which correspond to the values reported by the French energy market in 2018 [185]. Besides, 0.054 €/kg is the cost of gathering the feedstock for anaerobic digestion process (C_{Bio}). Otherwise, the emission factor of electricity (λ_{EG}) and natural gas (λ_{NG}) according to the French energy matrix are 0.057 and 0.040 $kgCO_2/kWh$, respectively [186]. Furthermore, the emission factors of reforming and anaerobic digestion processes are 10 $kgCO_2/kgH_2$ and 0.92 $kgCO_2/m^3CH_4$, respectively. Regarding the water consumption factor, the corresponding value for the electrolyzer (ψ_{El}) is 11 kgH_2O/kgH_2 [160]. Meanwhile, in literature is reported that water added to biomass corresponds to 15-40% of the total mass of the digester [187]. Accordingly, in this

work a water consumption factor (ψ_{AD}) of 0.25 kgH_2O/kg biomass is used. All these values are considered constant along time.

Moreover, technical and cost parameters for the set of evaluated technologies are presented in Tables 3-1 and 3-2. These include the energy conversion efficiency, lifetime, and capital, operation, and maintenance costs of each technology.

Table 3-1: Energy conversion efficiencies of the technologies considered in the distributed energy system.

Technology	Value in literature (%)	Selected value (%)	Reference
Photovoltaics	16 – 22	20	[188–190]
Electrolyzer [a]	56 – 69	65	[11,51,191]
Fuel cell [a]	37 – 58	55	[49]
Battery self-discharge (daily)	0.1 – 0.3	0.2	[192]
Battery charge/discharge	75 – 97	95	[69,192,193]
Reforming (small scale)	51	51	[49]
Anaerobic digestion [b]	0.42 – 0.53	0.48	[126]
Upgrading	99	99	[125]

[a] Polymer electrolyte membrane technology

[b] Using domestic waste (m^3CH_4/kg volatile solid). ≈ 23% of volatile solid in the biomass.

Table 3-2: Cost parameters of energy conversion and storage technologies.

Technology	CAPEX	O&M (% CAPEX)	Lifetime (years)	Reference
Photovoltaics (€/m^2)	220	5	20	[194]
Electrolyzer [a] (€/kW)	1600	2	8	[11,49,195]
Fuel Cell [a] (€/kW)	2700	7	8	[196]
Battery [b] (€/kWh)	520	2	15	[192,193,197]
Pressurized tank (€/kWh)	7.2	5	20	[49]
Reforming (€/kW)	3000	4.7	15	[49,198]
Anaerobic digestion [c] (€/kW)	1600	2.5	20	[194,199]

[a] Polymer electrolyte membrane technology

[b] Li-ion battery

[c] Includes the upgrading operation

Table 3-3: Operating conditions and heat of reaction of the energy conversion and storage technologies.

Technology	Temperature (°C)	Pressure (MPa)	Heat of Reaction (kJ/mol)	Reference
Electrolyzer	80	4	286	[11,51,160]
Fuel cell	80	4	-286	[11,51]
Pressurized tank	25	4	-	[11,51,160]
Reforming reactor	800	3	165	[52]
Anaerobic digestion	40	0.1	-	[126]

Polymer electrolyte membrane (PEM) technology was selected for the electrolyzer because of its higher operating pressure (up to 80 atm) and smaller area requirement with respect to the alkaline one [11]. The former enables to store the hydrogen without any additional compression step. The latter could be an advantage for the implementation of such a system in places where there are restrictions over the area available. Moreover, PEM technology offers an option to produce hydrogen at purity up to 99.99% with high flexibility and fast dynamics, which translate into a better coupling with intermittent resources as renewables [127,191]. Meanwhile, Li-ion battery was the technology used for the battery because of its high energy density and cycle efficiency, its low self-discharge rate, and its fast response time [69,192,193].

3.3.3 Energy System Constraints

As mentioned in section 3.2.3, the level of energy stored in battery and hydrogen units is constrained by upper limits in their capacities $S_{B,max}$ and $S_{H2,max}$, respectively. Overall, the definition of those limits depends upon the time scale of application (i.e. short-term for battery and long-term for hydrogen), and the generation and consumption profiles of electricity within the energy system. On the one hand, concerning the storage time scale, batteries are identified as a suitable option for storing electricity during days, whereas hydrogen system has the potential for reserving energy by months (seasonal storage) [68,69,192,200].

On the other hand, the electricity generated by photovoltaics is a function of the panel efficiency, the solar irradiance, and the installed surface as stated in Equation 2.1. In this respect, efficiency and irradiance are defined from the input data registered in Table 3-2, and in Figures 3-3a and 3-3b. Meanwhile, three different values of photovoltaic surface are considered in this work. The minimum area corresponds to that one capable to satisfy the peak electricity demand, which according to the Figure 3-3c is approximately 800 kW. In such a way, photovoltaic area was computed by dividing the peak demand into the nominal capacity factor of panels, which is around 0.16 kW/m^2 as specified by some manufacturers [188–190]. Therefore, the minimum surface required for satisfying the peak electricity demand is equal to 5000 m^2. The other evaluated values represent scenarios with 50 and 100 % of additional area, i.e. 7500 and 10000 m^2.

These scenarios make possible to analyze the impact of this variable on the energy system performance, which is difficult based on a single optimal value obtained from an optimization algorithm. Additionally, this analysis enables to consider possible future

modifications of the energy system, i.e. evaluate a system that already exists, or the forecast for different stages of a project. Nevertheless, if required, the proposed framework can be easily adapted for including the PV surface as a decision variable.

Taking this into account, the upper limits $S_{B,max}$ and $S_{H2,max}$ were defined for the scenario with the highest electricity production, i.e. with a photovoltaic area of 10000 m^2. Thus, the maximum capacities of the storage systems were determined considering an isolated system through the pinch analysis and the grand composite curves (GCC) as proposed by Bandyopadhyay [201]. Then, assuming that the battery is able to store energy up to ten days, and the pressurized hydrogen tank up to two months, the upper limits $S_{B,max}$ and $S_{H2,max}$ are 30 MWh and 300 MWh, respectively. The corresponding GCC are depicted in Figure B-1 of the Annex B.

Additionally, the total amount of biomass available (Bio_D) was estimated considering that in France each inhabitant generates 568 kg/year of domestic waste. From such rubbish, around 30% corresponds to organic matter that can be used in the digestion process, so that the biomass available is 255.6 ton/year for the considered system [202,203].

3.4 Optimization Results

Based on the proposed approach, the optimization problem formulated in Equations 3.23-3.35 was solved for the case study described in Section 3.3. This includes the evaluation of the three surfaces of photovoltaic panels, and the optimization of each criterion individually. Hence, five optimization problems were solved for minimizing the total annualized cost, the CO_2 emissions, the water consumption, the grid dependence, and the inherent safety index.

The optimization problem was solved considering a period of one year, and using a time step of 12 hours, i.e. $\Delta t = 12h$, $t_0 = 0h$ and $t_f = 8760h$. This time step enables both, to describe the daily fluctuations of energy demand and availability, and to decrease the number of optimization variables from 52860 (using 1h time step) to 4380 (12h time step), which leads to reduce the CPU time for solving the problem. Indeed, the optimizations lasted up to 24 h in a computer with an Intel® Xeon® Silver processor and were performed within MATLAB® software using the *fmincon* function and the sequential quadratic programming (*SQP)* algorithm. This algorithm was selected because of its speed of convergence. Moreover, *SQP* algorithm can be effectively used if nonlinearities are included in the objective functions and/or the constraints, e.g. by adding part-load efficiencies or

economies of scale within the energy system model. Additionally, it is noteworthy that the aim of this work was focused on the conceptual design stage of the energy system, hence the detailed simulations, which could be easily implemented by modifying the time step, are beyond the scope of this study.

Taking this into account, the next sections present the main optimization results for each one of the sustainability dimensions.

3.4.1 Economic Optimization

As stated before, the evaluated economic indicators were the total annualized cost (TAC) and the levelized cost of energy (LCOE). Nevertheless, only the TAC was addressed as objective function since it is embedded within LCOE. Figure 3-4 depicts the obtained energy system configuration for the three photovoltaic (PV) surfaces.

In general, through the obtained configurations, results show the influence of the PV surface on the selection of technologies for satisfying the energy needs. Indeed, the optimal set of technologies with 5000 m^2 of PV differs from the one obtained when the area is 7500 or 10000 m^2. As observed in Figures 3-4a and 3-4b, the most significant difference concerns the storage unit. Thus, for the smallest size of panels (5000 m^2), there is no need of storing a large amount of electricity during long periods, and hence just the battery is employed (Figures 3-4a). Conversely, for 7500 and 10000 m^2 of PV the pressurized tank is included since the renewable electricity production increases. Moreover, as depicted in Figure 3-4, these energy system structures are characterized by the production of the whole hydrogen from electricity supplied by PV, and the steam methane reforming of gas from the network. Hence, according to the optimization results, the anaerobic digester is not included within the system, and the electricity grid is only used for supplying the electricity demand when required. Indeed, as the objective is focused on minimizing the cost, these results are explained by two main reasons: (i) the reduction in the number of equipment, and (ii) because the price of the natural gas is lower than the electricity.

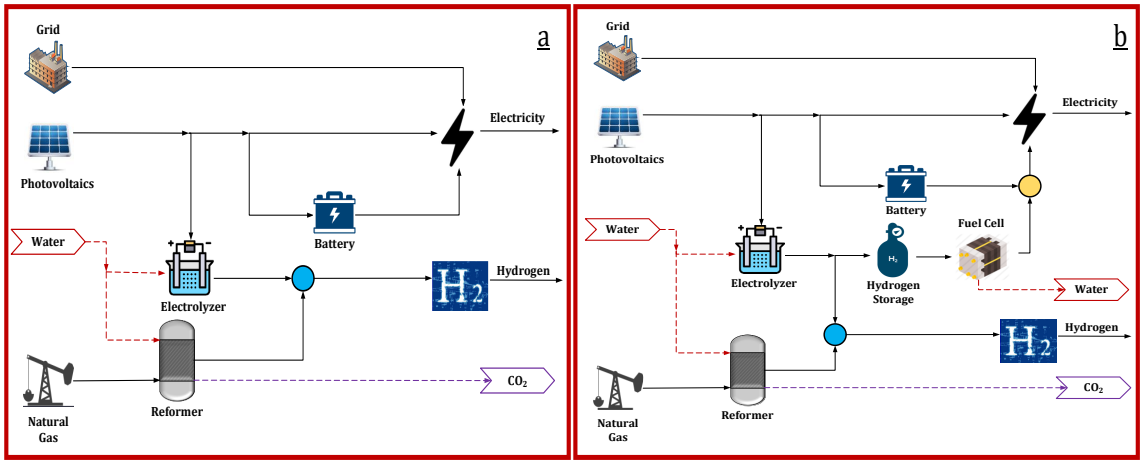

Figure 3-4: Optimal configuration of the distributed energy system for minimizing the total annualized costs. Photovoltaic surface (a) 5000 m^2 (b) 7500-10000 m^2.

Table 3-4 presents the optimization results for the three evaluated areas of PV. These include the six sustainability indicators and the contribution of different factors to each one of them (CAPEX, OPEX, grid and process emissions, the type of energy imported, etc.). Besides, the optimal size and investment cost of each technology installed within the energy system are depicted in Table 3-5. From these results, the direct relation between the economic indicators and the area of PV is observed. In this respect, for a given demand of energy, the LCOE increases as the PV surface gets larger. This happens because, as observed in Table 3-5, a higher PV production also implies a larger size of equipment for conversion of the surplus energy (electrolyzer and fuel cell) and larger capacities of the storage units (battery and pressurized tank). Indeed, according to optimization results, the storage devices represent about 60-65% of the CAPEX.

Moreover, it is also noted the low water consumption of the energy system, that according to results is between 145 and 245 m^3/year. This result can be explained by analyzing the expression used to estimate the water consumption (Equation 2.58). First, note that this indicator exclusively accounts the process water, i.e. the water used for steam and cooling utilities is not included. Besides, water consumption due to the energy storage in hydrogen form is reduced because the water obtained from the fuel cell is recycled to the electrolyzer.

Table 3-4: Optimization results of the distributed energy system for minimizing the total annualized costs.

Variable	Area of photovoltaics (m²)		
	5 000	7 500	10 000
LCOE (€/kWh)	0.18	0.37	0.49
TAC (M€/year)	0.9	1.8	2.4
CAPEX (% TAC)	73	90	93
OPEX (% TAC)	27	10	7
CO_2 emissions (ton/year)	345.1	227.7	176.0
Grid emissions (%)	43	37	34
Process emissions (%)	57	63	66
Biogenic (ton/year)	-	-	-
Water consumption (m³/year)	114.9	174.0	244.4
Electrolysis (%)	23	66	81
Reforming (%)	77	34	19
Dependence (%)	63	40	30
Imported electricity (%)	57	56	53
Imported natural gas (%)	43	44	47
Inherent Safety	10.3	18.8	19.4
Chemical Index	0.4	1.4	2.0
Process Index	9.9	17.4	17.4

Table 3-5: Optimal size and investment cost of equipment within the energy system for the economic optimization.

Equipment	PV area = 5 000 m²		PV area = 7 500 m²		PV area = 10 000 m²	
	Size	Investment (k€/year)	Size	Investment (k€/year)	Size	Investment (k€/year)
Photovoltaics	-	103.8	-	155.8	-	207.7
Electrolyzer (kW)	257	68.9	790	211.2	1 544	413.6
Battery (MWh)	7.1	406.5	17	965.6	21.9	1 249.5
Reformer (kW)	167	55.0	167	55.0	167	55.0
Hydrogen Storage (MWh)	-	-	125.4	85.2	150	101.9
Fuel Cell (kW)	-	-	270	122.1	386	174.4
Digester (kW)	-	-	-	-	-	-

The profiles of energy stored in the battery and the pressurized tank are presented in Figure 3-5. Roughly, the battery (Figure 3-5a) follows a short-term pattern, which is represented by the continuous oscillations on the level of energy stored. Conversely, the hydrogen system (Figure 3-5b) exhibits a long-term behavior, wherein the tank is discharged along cold periods (winter) and is charged during sunny seasons (spring and summer). Besides, it is worth to note that in no case the amount of energy stored reach the upper limits imposed in the optimization problem, i.e. 30 and 300 MWh for the battery and hydrogen system, respectively. This is explained by the important share of the storage units

on the total cost. Therefore, when the economic optimization is addressed, the system seeks to keep the size of such units as small as possible.

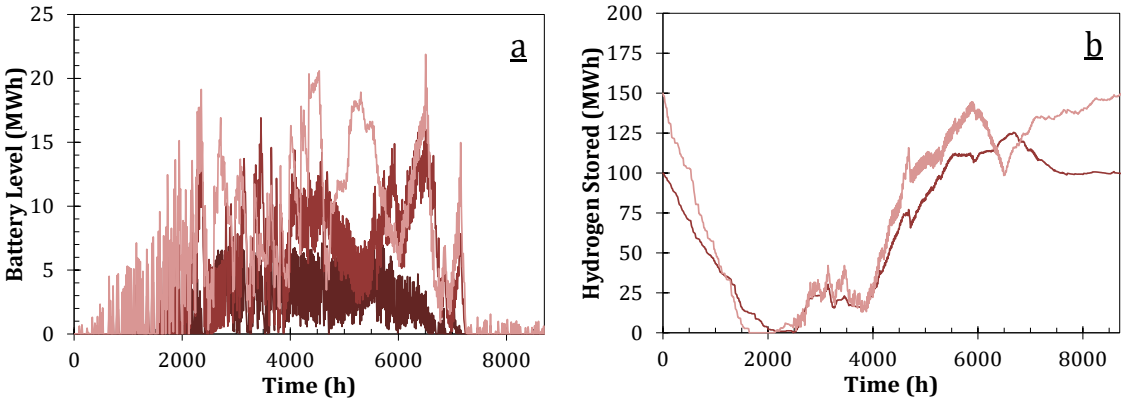

Figure 3-5: Optimal profiles of energy stored. (a) battery, (b) pressurized tank. Photovoltaic surface (—) 5000 m² (hydrogen is not used), (—) 7500 m² and (—) 10000 m².

Moreover, Figure 3-6 presents the average fraction of electricity supplied by the battery, the fuel cell, the main electricity grid, and the PV panels for the different seasons of the year. In general, it is shown that the share of fuel cell (power-to-power system) increases along with the PV surface (Figure 3-6b), since the long-term energy storage becomes more used. Indeed, short and long-term storage systems enable to meet up to 76% of electricity needs at winter, and up to 56% at fall with energy coming from PV. In addition to that, as observed in Figure 3-6c, the system is completely autonomous during spring and summer when a PV surface of 10000 m² is employed. Note that the fraction supplied by photovoltaics (Figure 3-6d) corresponds to the electricity delivered to users at the time that it is obtained, i.e. without passing through storage systems.

Regarding hydrogen demand, according to optimization results, the steam methane reforming of natural gas from the network, and the electrolysis process powered by PV electricity are the best alternatives from the economic perspective (Figure 3-7). Thus, Figure 3-7 depicts the fraction of hydrogen supplied by each one of these options along the year. Broadly, reforming process provides 90, 60 and 48% of hydrogen for the different areas of PV evaluated, 5000, 7500 and 10000 m², respectively. In fact, this process represents more than 80% of hydrogen produced during winter and fall seasons (Figure 3-7b). On the contrary, as presented in Figure 3-7a, the electrolyzer is mainly employed at sunny periods, i.e. spring and summer seasons.

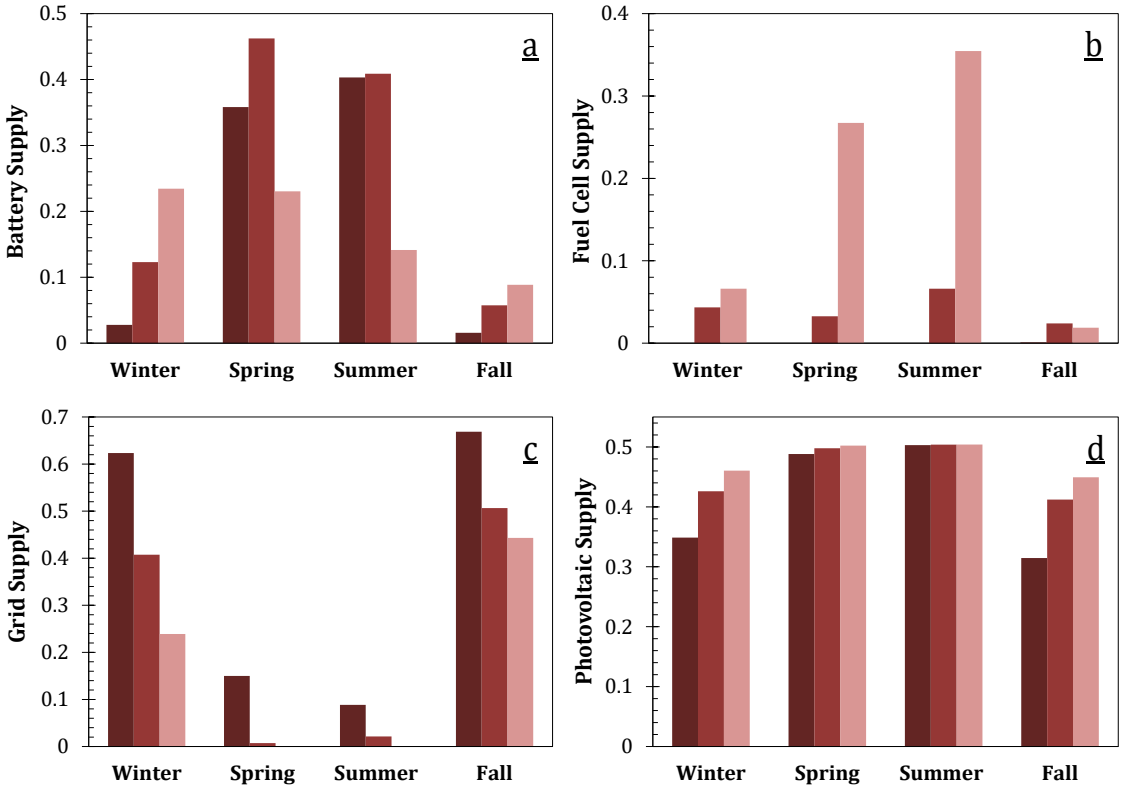

Figure 3-6: Optimal fraction of electricity supplied by the distributed energy system. Photovoltaic surface (■) 5000 m², (■), 7500 m² and (■) 10000 m². Sources (a) battery, (b) fuel cell, (c) grid and (d) photovoltaic panels.

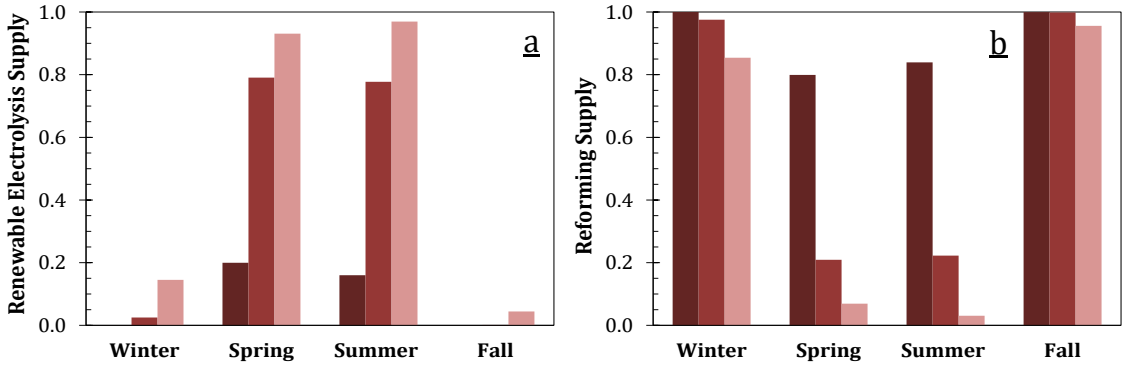

Figure 3-7: Optimal fraction of hydrogen supplied by the distributed energy system. Photovoltaic surface (■) 5000 m², (■), 7500 m² and (■) 10000 m². Sources (a) electrolysis powered by renewable electricity, (b) reforming process.

3.4.2 Environmental Optimization

The environmental dimension was addressed through the premise of minimizing the CO_2 emissions and the water consumption. Hence, the obtained system configurations and their main characteristics are described in the next passages.

- *CO_2 emissions*

Figure 3-8 presents the optimal energy system structure for minimizing the CO_2 emissions. It is noted that similarly to the economic optimization, the long-term storage is only required for larger areas of PV (7500 and 10000 m^2). Nevertheless, the remainder of the system structure is quite different. First, the electrolyzer is powered by both PV and grid electricity. Secondly, the reformer reactor is fed by biomethane and the natural gas network is not required by the system. On the one hand, this happens because, when the electrolyzer is used, environmental impact only depends on the emission factor of the electricity grid, which in the case of France is relatively low due to the massive electricity production from nuclear plants. On the other hand, as the case study is in France, a negligible deforestation rate was assumed. Then, all the CO_2 emissions from anaerobic digestion and the subsequent reforming of biomethane are biogenic. Consequently, as stated in Equation 2-54, such emissions are not accounted in the global indicator. Thus, according to the energy system flowsheets depicted in Figure 3-8, the whole of CO_2 emissions is derived from the imported electricity.

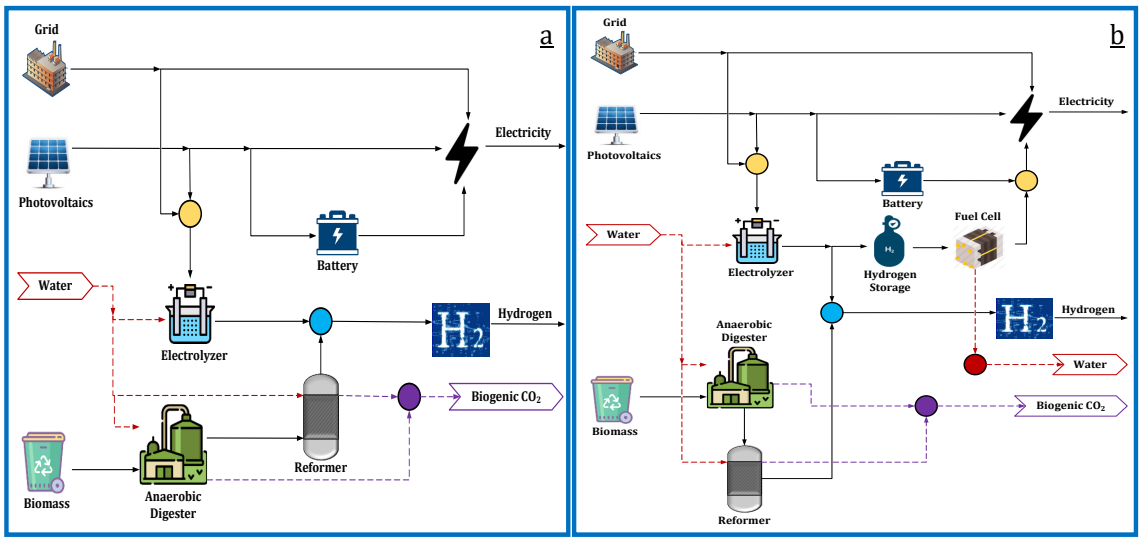

Figure 3-8: Optimal configuration of the distributed energy system for minimizing the CO_2 emissions. Photovoltaic surface (a) 5000 m^2 (b) 7500-10000 m^2.

As depicted in Table 3-6, the CO_2 emissions decrease as the PV surface gets bigger, since lower amount of energy must be imported from the grid. Also, note that the whole biomass available (255.6 ton/year) is employed in all the cases, as it offers a completely emission-free pathway for obtaining hydrogen. Moreover, as presented in Table 3-7, minimization of CO_2 emissions leads to use the biggest storage units without considering the costs that such decision implies. This occurs because of the energy stored corresponds to renewable

one, thus, as the capacity for storing this energy increases, less energy must be imported from the grid, and consequently emissions can be reduced.

Table 3-6: Optimization results of the distributed energy system for minimizing the CO_2 emissions.

Variable	Area of photovoltaics (m²)		
	5 000	**7 500**	**10 000**
LCOE (€/kWh)	0.30	0.52	0.59
TAC (M€/year)	1.5	2.5	2.8
CAPEX (% TAC)	74	91	94
OPEX (% TAC)	26	9	6
CO_2 emissions (ton/year)	145.6	81.7	51.2
Grid emissions (%)	100	100	100
Process emissions (%)	-	-	-
Biogenic (ton/year)	62.9	62.9	62.9
Water consumption (m³/year)	278.4	291.7	337.8
Electrolysis (%)	70	72	76
Reforming (%)	7	6	5
Digestion (%)	23	22	19
Dependence (%)	52	30	19
Imported electricity (%)	100	100	100
Imported natural gas (%)	-	-	-
Inherent Safety	10.7	18.8	19.4
Chemical Index	0.5	1.1	1.7
Process Index	10.2	17.7	17.7

Table 3-7: Optimal size and investment cost of equipment within the energy system for minimizing the CO_2 emissions.

Equipment	PV area = 5 000 m²		PV area = 7 500 m²		PV area = 10 000 m²	
	Size	**Investment (k€/year)**	**Size**	**Investment (k€/year)**	**Size**	**Investment (k€/year)**
Photovoltaics		103.8		155.8		207.7
Electrolyzer (kW)	257	68.9	766	205.3	1 409	377.6
Battery (MWh)	14	801.4	30	1 712.8	30	1 712.8
Reformer (kW)	166	54.7	134	44.2	134	44.2
Hydrogen Storage (MWh)	-	-	176	119.7	300	203.9
Fuel Cell (kW)	-	-	108	48.9	200	90.7
Digester (kW)	327	49.2	258	39.0	258	39.0

In the same way that in the economic optimization, the level of energy stored in the battery is characterized by its continuous oscillations (Figure 3-9a), whereas the hydrogen storage follows a seasonal pattern (Figure 3-9b). Thus, the pressurized tank starts to be charged at spring ($t \approx 2500$ h), and a significant change in the slope of the curve is observed at the beginning of summer season ($t \approx 4000$ h). Then, during fall and winter seasons the tank is

discharged for covering the lack of electricity from photovoltaics (t < 2000 h and 7500 h < t < 8760 h).

As a result of the high availability of electricity during summer season, if the photovoltaic surface is 10000 m², the amount of energy stored reaches up to the limits imposed in the optimization problem, i.e. 30 and 300 MWh for the Li-ion battery and the pressurized hydrogen tank, respectively. In this respect, a sensitivity analysis on the values of the storage limits was performed aiming to evaluate their impact on the optimization results. Thus, the optimization problem was solved by modifying the storage capacities ± 10%, i.e. 27 and 33 MWh for the battery, and 270 and 330 MWh for the pressurized tank. According to the results, such modifications represent changes lower than 2% on the objective function, as depicted in Table 3-8.

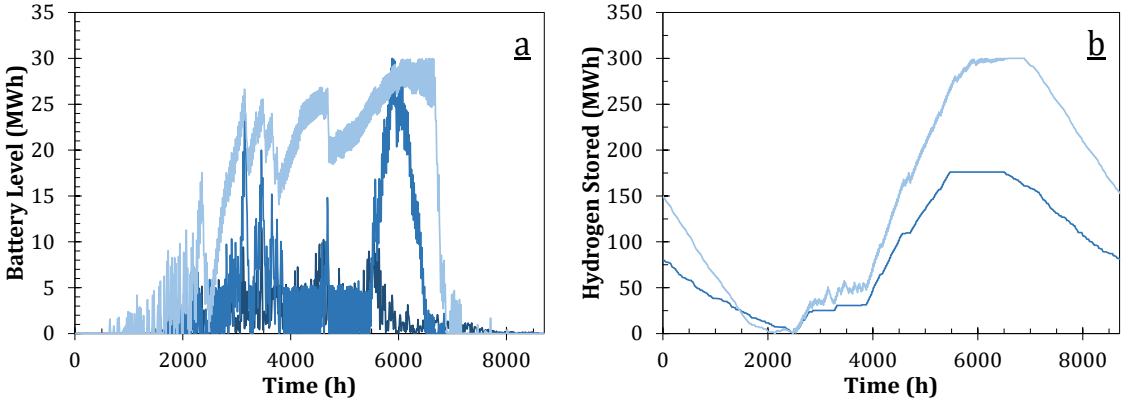

Figure 3-9: Optimal profiles of energy stored. (a) battery, (b) pressurized tank. Photovoltaic surface (—) 5000 m² (hydrogen is not used), (—) 7500 m² and (—) 10000 m².

Table 3-8: Results of the sensitivity analysis with respect to the storage capacities.

Storage option	Max. capacity (MWh)	CO_2 emissions (ton/year)	Relative difference* (%)
Pressurized tank	330	50.2	-1.9
	270	52.1	1.9
Battery	33	51	-0.4
	27	51.3	0.4

*The reference case corresponds to 51.2 tonCO_2/year

The optimal distribution of the electricity supplied by the battery, the fuel cell, the grid, and the PV are presented in Figure 3-10. In general, it is noted the great importance of the storage units for reducing the energy imported from the grid, and consequently the CO_2 emissions. On the one hand, short and long-term storage can meet up to 16 and 20% of energy needs at fall and winter seasons, respectively. On the other hand, results show that when the area of PV is 10000 m², storage units enable to satisfy the whole electricity

demand during sunny periods by means of renewable resources and without generating CO_2 emissions.

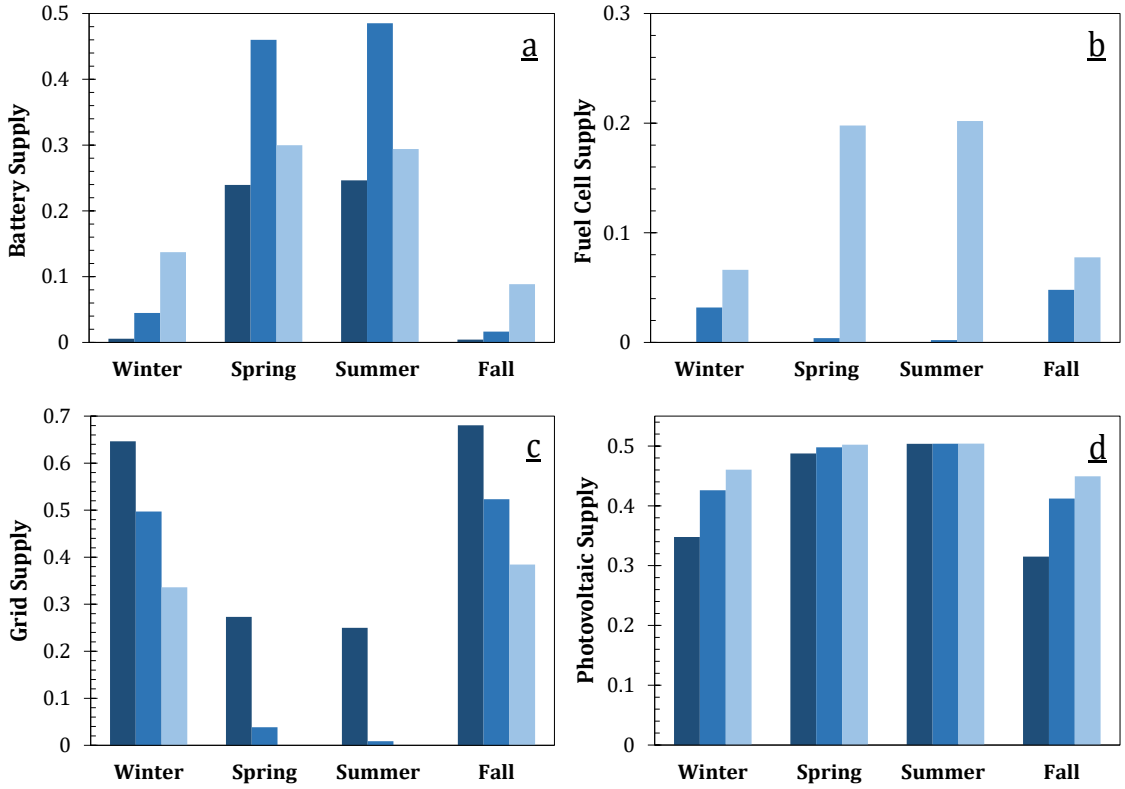

Figure 3-10: Optimal fraction of electricity supplied by the distributed energy system. Photovoltaic surface (■) 5000 m², (■), 7500 m² and (■) 10000 m². Sources (a) battery, (b) fuel cell, (c) grid and (d) photovoltaic panels.

Concerning the demand of hydrogen, as depicted in Figure 3-8, it can be supplied by an electrolyzer powered by either the PV or the grid, and by the reforming of biomethane. According to optimization results, about 83% of hydrogen is obtained by water electrolysis when the objective is to minimize the CO_2 emissions. As expected, the fraction covered by renewable electricity is predominantly important at spring and summer seasons (Figure 3-11a). Indeed, for the cases with larger PV areas (7500 and 10000 m²), solar-based electricity can supply between 92-99% of hydrogen demand during such periods. Meanwhile, grid electricity and reforming reactor are mainly used at fall and winter. In this respect, biomethane reforming seems to be an interesting alternative for enhancing the production of green hydrogen at cold seasons. Since, as observed in Figure 3-11c, this process can supply between 24-40% of hydrogen during such periods.

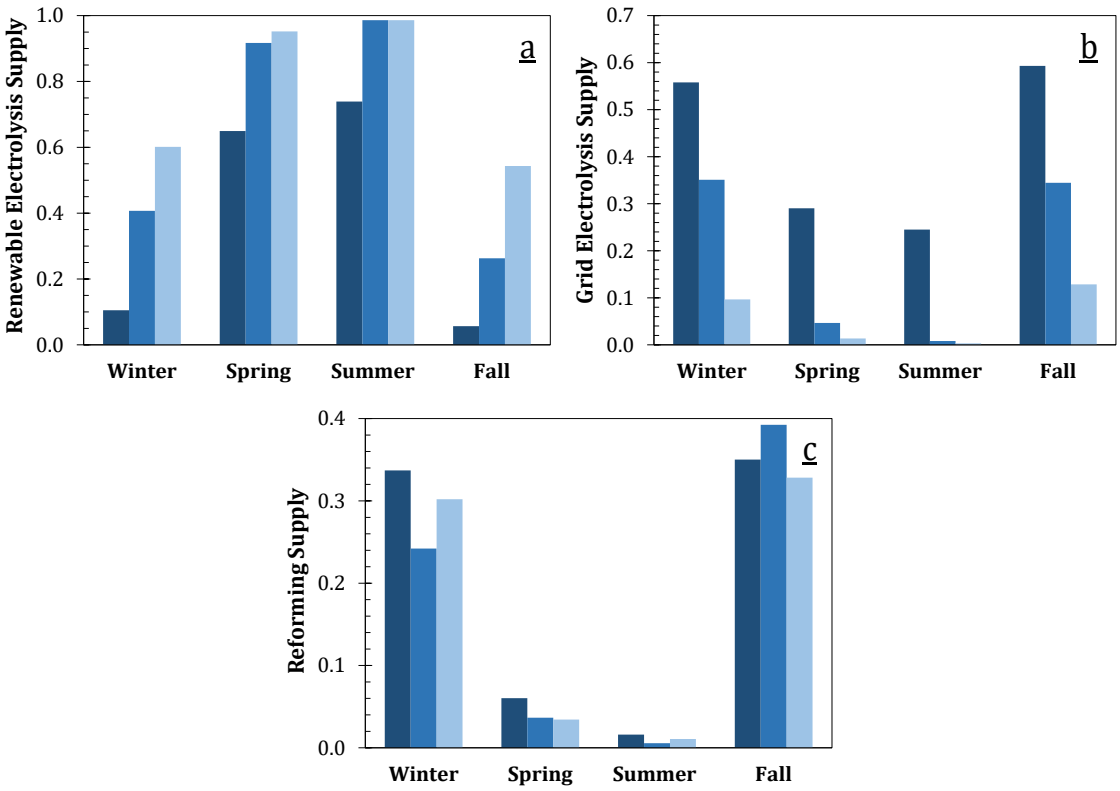

Figure 3-11: Optimal fraction of hydrogen supplied by the distributed energy system. Photovoltaic surface (■) 5000 m², (■), 7500 m² and (■) 10000 m². Sources (a) electrolysis powered by renewable electricity, (b) electrolysis powered by the grid, (c) reforming process.

- *Water Consumption*

In addition to the CO_2 emissions, the water consumption indicator was also evaluated within the environmental dimension. In this respect, Figure 3-12 shows the optimal flowsheet of the system by minimizing such indicator. Note that, similarly to the previous optimization cases, hydrogen storage is only used for larger PV surfaces. Moreover, the electrolyzer is only powered by PV electricity, and all the hydrogen produced by this process is sent to the pressurized tank, as depicted in Figure 3-12b. Therefore, the whole demand of hydrogen is supplied by the steam methane reforming process for the three evaluated areas of PV. Also note that the anaerobic digester is not included within the system, hence, only gas from the main network is fed to the reformer reactor.

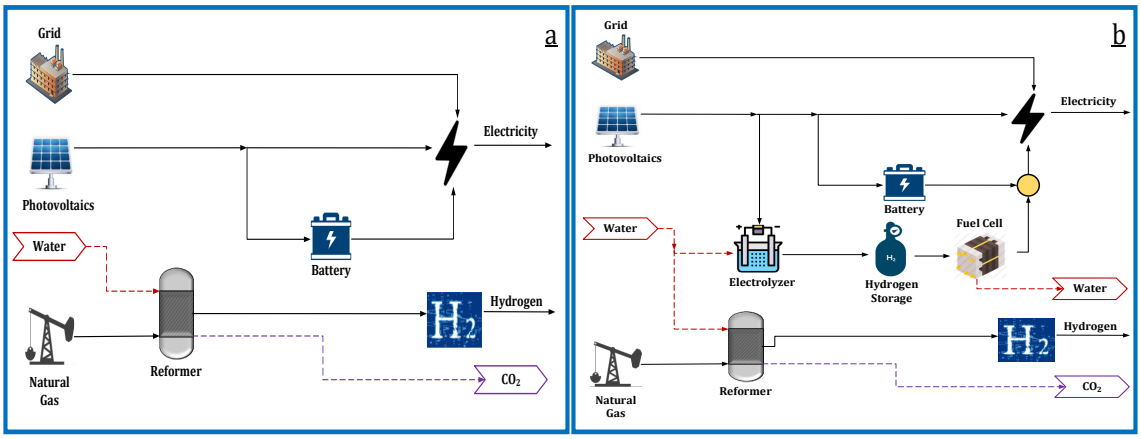

Figure 3-12: Optimal configuration of the distributed energy system for minimizing the water consumption. Photovoltaic surface (a) 5000 m² (b) 7500-10000 m².

On the one hand, the fact of sending all electrolytic hydrogen to the storage tank can be explained by analyzing the Equation 2.58. In that expression, it is noted that the employment of the system electrolyzer-tank-fuel cell offers the possibility of recovering the water produced in the fuel cell to be reused in the electrolyzer. In contrast, if such hydrogen is sent to supply the demand, there is no way of recuperating the water, and therefore its net consumption will increase. On the other hand, the selection of reforming instead of electrolysis process lies on the stoichiometry of reactions. Thus, by considering the stochiometric relation of each process, water electrolysis requires 9 kgH_2O/kgH_2, whereas the reforming reaction needs 4.5 kgH_2O/kgH_2. Consequently, as the objective is to minimize the water consumption, steam reforming process provides a better performance than water electrolysis.

Table 3-9 presents the results for the six sustainability indicators when the water consumption is minimized. Interestingly, such results show a competitive behavior between the two indicators considered for evaluating the environmental dimension. Thus, the lowest water consumption implies the highest CO_2 emissions (PV = 5000 m²). In contrast, as the PV surface increases, lower emissions can be achieved but at the cost of a more elevated water consumption. This happens because of such areas of PV (7500 and 10000 m²) entail to use the power-to-power system for the seasonal energy storage, which includes water consumption for the electrolysis step. Moreover, Table 3-10 depicts the optimal size and investment cost of equipment installed within the energy system.

Table 3-9: Optimization results of the distributed energy system for minimizing the water consumption.

Variable	Area of photovoltaics (m^2)		
	5 000	**7 500**	**10 000**
LCOE (€/kWh)	0.44	0.57	0.63
TAC (M€/year)	2.1	2.7	3.0
CAPEX (% TAC)	88	92	94
OPEX (% TAC)	12	8	6
CO_2 emissions (ton/year)	362.3	329.5	310.3
Grid emissions (%)	42	33	29
Process emissions (%)	58	67	71
Biogenic (ton/year)	-	-	-
Water consumption (m^3/year)	98.7	134.1	193.4
Electrolysis (%)	-	26	51
Reforming (%)	100	74	49
Digestion (%)	-	-	-
Dependence (%)	63	49	42
Imported electricity (%)	54	39	29
Imported natural gas (%)	46	61	71
Inherent Safety	6.4	19.1	19.9
Chemical Index	0.2	1.7	2.5
Process Index	6.2	17.4	17.4

Table 3-10: Optimal size and investment cost of equipment within the energy system for minimizing the water consumption.

Equipment	PV area = 5 000 m^2		PV area = 7 500 m^2		PV area = 10 000 m^2	
	Size	**Investment (k€/year)**	**Size**	**Investment (k€/year)**	**Size**	**Investment (k€/year)**
Photovoltaics		103.8		155.8		207.7
Electrolyzer (kW)	-	-	828	222.9	1 640	439.4
Battery (MWh)	30	1 712.8	30	1 712.8	30	1 712.8
Reformer (kW)	167	55.0	167	55.0	167	55.0
Hydrogen Storage (MWh)	-	-	300	203.9	300	203.9
Fuel Cell (kW)	-	-	390	176.0	462	209.2
Digester (kW)	-	-	-	-	-	-

As shown in Table 3-10 and Figure 3-13, minimization of water consumption implies to use the biggest available storage units for both battery and pressurized tank. Overall, this occurs because there is no connection between PV production and hydrogen demand (Figure 3-12). Therefore, the whole surplus electricity must be sent to the storage units. Then, the system seeks to reduce the water consumption by employing the battery as much as possible. Indeed, the pressurized tank only starts to be used when battery is completely charged. This fact can be observed by analyzing Figures 3-13a and 3-13b. For instance, considering the PV surface of 10000 m^2, the pressurized tank begins to be charged at around 2000h, which corresponds to the time wherein the battery has reached its

maximum capacity. Similarly, when the PV area is 7500 m², the battery is filled at 2500h so that the hydrogen system must start to be charged.

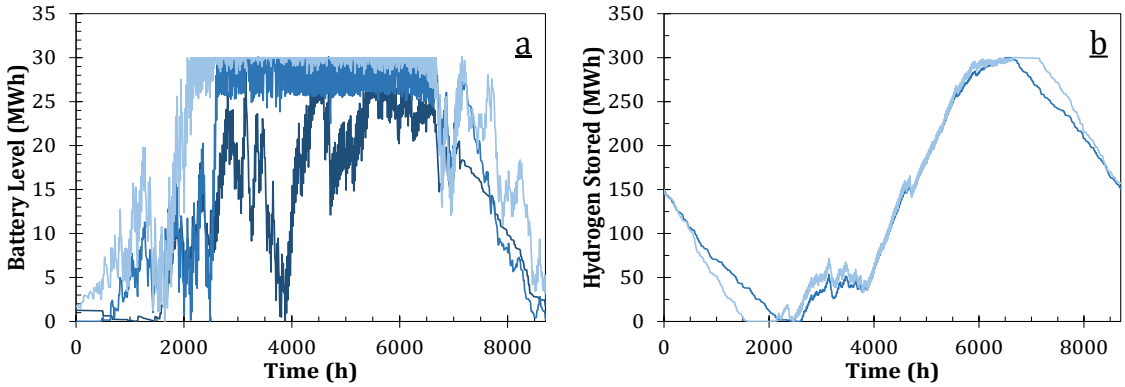

Figure 3-13: Optimal profiles of energy stored. (a) battery, (b) pressurized tank. Photovoltaic surface (—) 5000 m² (hydrogen is not used), (—) 7500 m² and (—) 10000 m².

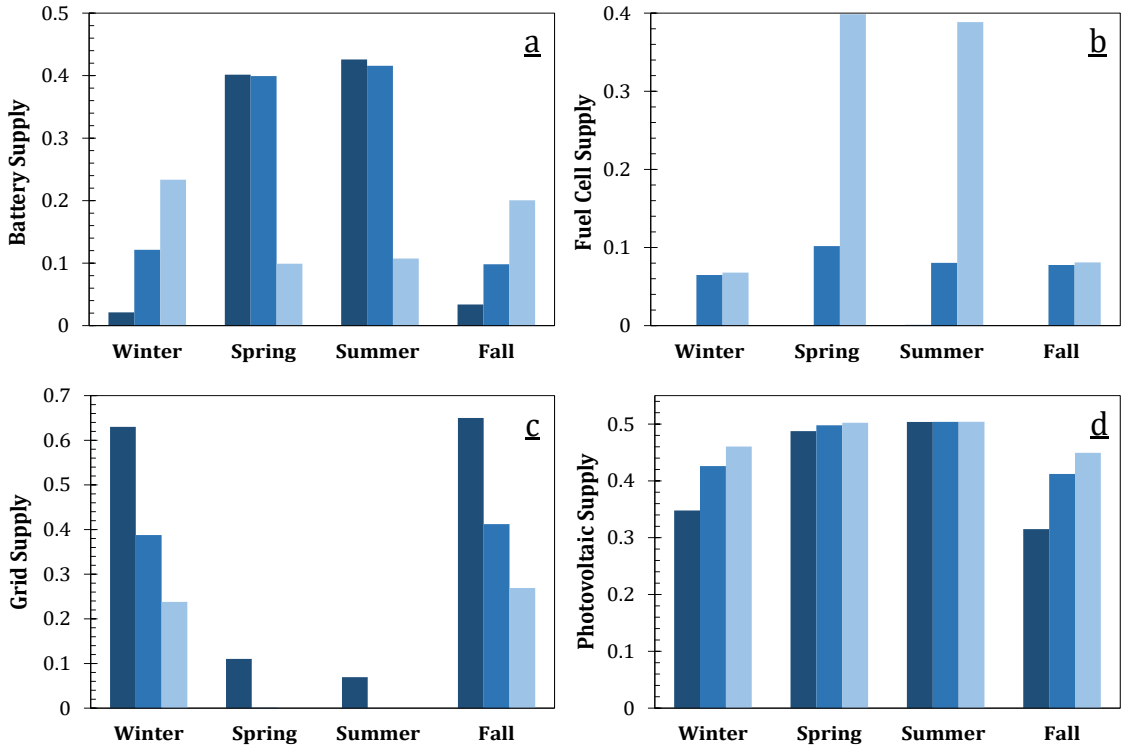

Figure 3-14: Optimal fraction of electricity supplied by the distributed energy system. Photovoltaic surface (■) 5000 m², (■), 7500 m² and (■) 10000 m². Sources (a) battery, (b) fuel cell, (c) grid and (d) photovoltaic panels.

Moreover, the different sources for supplying the electricity demand are presented in Figure 3-14. Note the high utilization of storage units. On the one hand, when the smallest PV surface is considered, battery enables to supply up to 90% of electricity demand from PV-based electricity at spring and summer seasons. On the other hand, when short and long-term energy storage is used, the system is completely self-sufficient during sunny

periods (Figure 3-14c), and up to 75% of electricity can be supplied from renewable resources at winter and fall seasons.

3.4.3 Social Optimization

The social dimension was assessed under the principle that industrial activities must improve the quality of life. In this regard the evaluated criteria are focused on ensuring the access to energy for all and on increasing the safety of processes. Thus, the corresponding indicators of these criteria are the dependence on the main energy grid, and the inherent safety index.

- *Grid Dependence*

Figure 3-15 depicts the optimal energy system structure for minimizing the dependency on the main grid. Interestingly, the obtained configurations are identical to those when CO_2 emissions are minimized (Figure 3-8). Also, the global performance of these two optimization cases is the same, as observed by comparing Tables 3-6 and 3-11. In this regard, it is worth noting that this result strongly relies upon the considered context and some technical parameters (e.g. conversion efficiency). Thus, as the case study of this work is in France, and negligible deforestation was assumed, biomass represents the best alternative when the objective is to minimize either the CO_2 emissions or the grid dependence. This happens because biomass does not imply any CO_2 emission and is not grid reliant. However, in a context with significative deforestation rate, or an energy matrix based on fossil resources, the optimization of these objectives could lead to different system structures. Indeed, this issue was verified by carrying out a sensitivity analysis with those two parameters, i.e. the deforestation rate and the emission factor of the electricity grid.

On the one hand, the influence of the deforestation rate (ω) was studied by solving the optimization problems for three different values of this parameter 10, 20 and 30%. The objective function addressed was the minimization of CO_2 emissions, and the scenario with a PV surface of 10000 m^2 was considered.

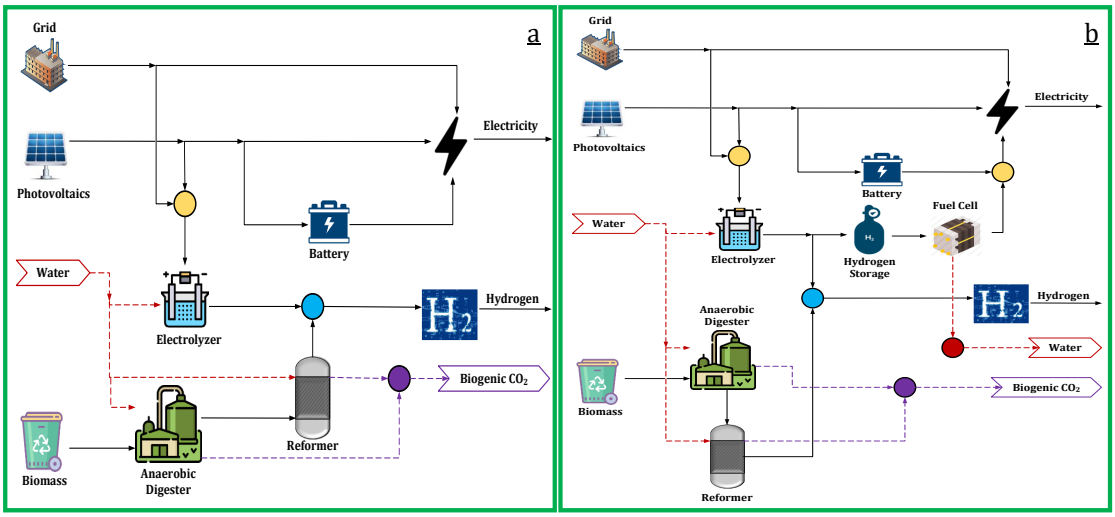

Figure 3-15: Optimal configuration of the distributed energy system for minimizing the grid dependence. Photovoltaic surface (a) 5000 m² (b) 7500-10000 m².

The results of sensitivity analysis are presented in Table 3-12 and Figure 3-16. As observed, in scenarios with lower deforestation rate (A and B), the energy system structure remains the same for the CO_2 emissions and the grid dependence objective functions (Figure 3-16a). Nonetheless, as the deforestation rate increases, the minimization of CO_2 emissions leads to an energy system without the employment of biomass (Figure 3-16b). This happens because at those deforestation rates (20 and 30%), the best option from the environmental perspective is to produce hydrogen via water electrolysis. Meanwhile, when the grid dependence is minimized the result remains the same, like on the scenarios A or B, because biomass is not grid reliant. This fact can be explained by analyzing the CO_2 emissions of both alternatives for producing hydrogen, either through anaerobic digestion followed by biomethane reforming, or by means of water electrolysis. Thus, considering the emission factors of anaerobic digestion and reforming processes, the production of hydrogen from biomass represents around 17 $kgCO_2/kgH_2$ (accounting digestion and reforming). Meanwhile, water electrolysis process has an emission factor of 2.9 $kgCO_2/kgH_2$ by using the French electricity grid. According to this, the CO_2 emission from electrolysis process represents around 17% of those derived from biomass processing. Therefore, as obtained from the sensitivity analysis results, if the deforestation rate is higher than 17%, water electrolysis is preferred instead of anaerobic digestion and biomethane reforming when the objective is to minimize the CO_2 emissions.

Table 3-11: Optimization results of the distributed energy system for minimizing the grid dependence.

Variable	Area of photovoltaics (m^2)		
	5 000	**7 500**	**10 000**
LCOE (€/kWh)	0.30	0.52	0.59
TAC (M€/year)	1.5	2.5	2.8
CAPEX (% TAC)	74	91	94
OPEX (% TAC)	26	9	6
CO_2 emissions (ton/year)	145.6	81.7	51.2
Grid emissions (%)	100	100	100
Process emissions (%)	-	-	-
Biogenic (ton/year)	62.9	62.9	62.9
Water consumption (m^3/year)	278.4	291.7	337.8
Electrolysis (%)	70	72	76
Reforming (%)	7	6	5
Digestion (%)	23	22	19
Grid Dependence (%)	52	30	19
Imported electricity (%)	100	100	100
Imported natural gas (%)	-	-	-
Inherent Safety	10.7	18.8	19.4
Chemical Index	0.5	1.1	1.7
Process Index	10.2	17.7	17.7

Table 3-12: Results for the minimization of CO_2 emissions considering different deforestation rates.

Scenario	Deforestation Rate (%)	CO_2 emissions (ton/year)			Grid Dependence (%)
		Fossil-derived	Biomass-derived	Total	
A	0	51.2	-	51.2	19
B	10	51.2	6.3	57.5	19
C	20	61.9	-	61.9	23
D	30	61.9	-	61.9	23

Otherwise, the impact of the electricity grid emission factor was evaluated by assuming the one of Germany, which was roughly 0.48 $kgCO_2/kWh$ in 2018 [204]. In this case, CO_2 emission and grid dependence objectives were evaluated for determining the influence of this value on the system configuration. According to these optimization results, when the environmental objective is evaluated, the system configuration is quite different to that obtained with the emission factor of the French grid. This fact is observed by comparing the Figures 3-15b and 3-17a. Indeed, the difference lies on the sources for supplying the hydrogen demand, since due to the high emission factor of the electricity from the grid (German grid), the electrolyzer is only powered by photovoltaic panels (Figure 3-17a). Thus, when the French grid is employed, water electrolysis (≈2.9 $kgCO_2/kgH_2$) is preferred instead of methane reforming (≈12 $kgCO_2/kgH_2$), as presented in Figure 3-15b. Conversely, if the electricity grid of Germany is used (≈24 $kgCO_2/kgH_2$), steam methane reforming

would be privileged by using both, biomethane and gas natural from the network (Figure 3-17a).

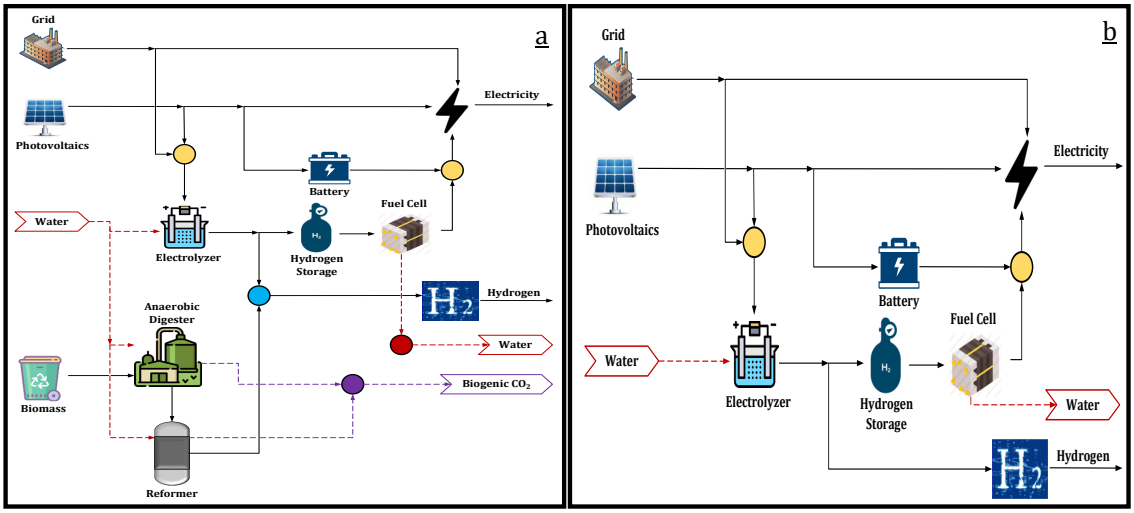

Figure 3-16: Energy system flowsheet for minimizing the CO_2 emissions. Deforestation rates (a) 0-10%, (b) 20-30%.

Moreover, it is also noted that the conversion efficiency is the key parameter for selecting the electricity grid instead of methane for obtaining hydrogen when the objective is to decrease the energy imported from the grid (Figure 3-15). This happens because for producing 1 kg of hydrogen, the energy consumption of the electrolyzer and methane reforming units are 51.3 and 65.4 kWh, respectively. Thus, even though using the German electricity grid, the optimal system structure is the same to that which uses the French grid (Figure 3-17b). Nevertheless, in such case the environmental performance (CO_2 emissions) is quite different with respect to the base case. In this regard, Table 3-13 depicts the comparison between the base case and the scenario assuming the electricity grid of Germany.

Table 3-13: Optimization results for environmental and social objectives considering the emission factor of the electricity grid of Germany.

Case	Objective	CO_2 emissions (ton/year)	Grid Dependence (%)
Base	Env -Soc	51.2	19
German Grid	Environmental	363.9	21
	Social	431	19

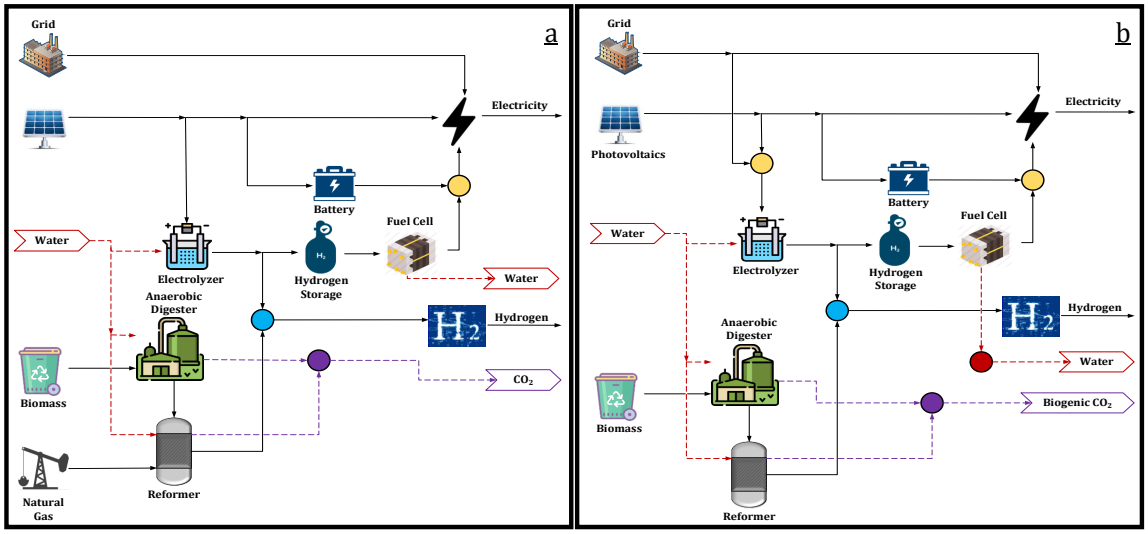

Figure 3-17: Optimal energy system flowsheet considering the emission factor of the electricity grid of Germany. Objective functions (a) minimization of CO_2 emissions, (b) minimization of grid dependence.

Summarizing, through this sensitivity analysis it was verified that the identical results for CO_2 emissions and grid dependence optimization are specific for the evaluated context, since by modifying some of the case study parameters, these optimizations lead to results considerably different.

- *Inherent Safety*

As stated above, in addition to the grid dependence, the inherent safety index was used for assessing the performance of the energy system in the social dimension. In this respect, the first step consisted in analyzing the results of this index through the previous optimization cases. Thus, Table 3-14 shows for each equipment, the detailed information of the chemical and process safety indexes for every optimization case. Note that a lower index corresponds to a safer system structure.

First, as expected, the hazards potential of the system increases as the size of the plant becomes larger, i.e. the PV surface augments. Secondly, it is also noted the impact of including the seasonal storage, since this implies to include at least two new pieces of equipment (pressurized tank and fuel cell), and to increase the size of the electrolyzer. Nevertheless, according to the values presented in Table 3-14, there are some unexpected results. On the one hand, when a PV surface of 7500 and 10000 m^2 is used, the process index for the pressurized tank is almost the same to that of the electrolyzer and fuel cell. In this regard, as stated by the intensification principle, safer processes are those ones with lower amount of hazardous substances and smaller operation units. Therefore, even though these units have quite similar operating conditions, the score of the tank should be

higher due to the size of such unit and the accumulation of hydrogen. On the other hand, when seasonal storage is included, the total index for the economic optimization is expected to be different to that of the CO_2 emission/grid dependence minimization. In fact, by comparing the results of such optimizations, the total score for the TAC minimization was expected to be lower because of the smaller size of the storage unit and the less amount of equipment.

Table 3-14: Inherent safety of the energy system for different objective functions.

Equipment	Index	PV area = 5 000 m²				PV area = 7 500 m²				PV area = 10 000 m²			
		TAC	AGE	DEP	WC	TAC	AGE	DEP	WC	TAC	AGE	DEP	WC
Electrolyzer	Chemical	0.2	0.2	0.2	-	0.6	0.5	0.5	0.6	1.0	1.0	1.0	1.2
	Process	3.7	3.7	3.7	-	3.7	3.7	3.7	3.7	3.7	3.7	3.7	3.7
Fuel Cell	Chemical	-	-	-	-	0.5	0.2	0.2	0.8	0.7	0.4	0.4	0.9
	Process	-	-	-	-	3.7	3.7	3.7	3.7	3.7	3.7	3.7	3.7
Digester	Chemical	-	0.1	0.1	-	-	0.1	0.1	-	-	0.1	0.1	-
	Process	-	0.3	0.3	-	-	0.3	0.3	-	-	0.3	0.3	-
Reformer	Chemical	0.2	0.2	0.2	0.2	0.2	0.2	0.2	0.2	0.2	0.2	0.2	0.2
	Process	6.2	6.2	6.2	6.2	6.2	6.2	6.2	6.2	6.2	6.2	6.2	6.2
Hydrogen Tank	Chemical	-	-	-	-	0.1	0.1	0.1	0.2	0.1	0.1	0.1	0.2
	Process	-	-	-	-	3.8	3.8	3.8	3.8	3.8	3.8	3.8	3.8
Total	Chemical	0.4	0.5	0.5	0.2	1.4	1.1	1.1	1.8	2.0	1.8	1.8	2.5
	Process	9.9	10.2	10.2	6.2	17.4	17.7	17.7	17.4	17.4	17.7	17.7	17.4
IST TOTAL		10.3	10.7	10.7	6.4	18.8	18.8	18.8	19.2	19.4	19.5	19.5	19.9

* Objective functions, (TAC) total annualized cost, (AGE) CO_2 emissions, (DEP) grid dependence and (WC) water consumption.

The explanation of these results lies on the fact that the original inventory index is not discriminant for small-scale equipment. Indeed, as observed in Table 3-15, the traditional index is conceived for evaluating large-scale units. For instance, by taking as reference the pressurized tank, that is the biggest unit within the energy system, its maximum inventory is 9 ton (300 MWh of hydrogen). Such capacity corresponds to a score of 1, that is the same even though the inventory is 4.5 ton (economic optimization). Consequently, as depicted in Table 3-14, the process index for the pressurized tank is the same for all optimization cases. Therefore, although this result can be acceptable in the evaluation of a large-scale plant, it is not accurate for assessing small-scale units since it does not permit to distinguish between capacities considerably different.

Table 3-15: Inventory index for the inherent safety assessment [171].

Inventory (ton)	Score
0 -1	0
1 – 10	1
10 – 50	2
50 – 200	3
200 – 500	4
500 - 1000	5

Considering the foregoing and the key role of the storage unit within the energy system, a transformed scale is proposed in this work. This new scale is focused on inventories from zero up to 10 tons and is described by a linear expression, as depicted in Figure 3-18. As observed, the proposed scale permits to consider the impact of the storage equipment size on the inherent safety of the system. In fact, this scale was used for recalculating the inherent safety index in all the previous optimization cases. Such results are presented in Table 3-16.

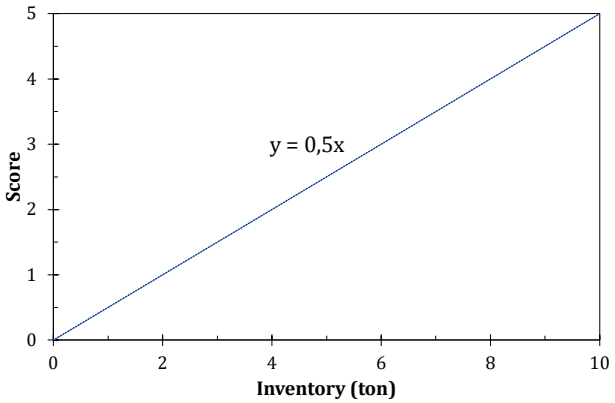

Figure 3-18: Representation of the proposed inventory index for the inherent safety evaluation.

Note that the main trends of results are kept by using the proposed scale, i.e. the inherent safety index increases as the energy system gets bigger. Furthermore, when seasonal storage is included, the new scale enables to discriminate among the cases wherein a different size of the pressurized tank is installed.

Considering these results, the optimization of the inherent safety index was performed by using the proposed scale. Thus, Figure 3-19 shows the optimal configuration of the energy system for each one of the evaluated PV surfaces. Broadly, regarding the surplus electricity storage, this optimization case follows the same pattern as the previous ones, i.e. the hydrogen storage is not used for the smallest area of PV (Figure 3-19a). Moreover, about

the hydrogen supply, the obtained results indicate that the whole demand must be supplied by water electrolysis process. Therefore, neither the reformer nor the anaerobic digester is included within the energy system. This happens because one of the principles of the inherent safety lies on the simplification of the process, so that a safer process is the one with less amount of equipment. In such a way, as the electrolyzer is already installed for converting the surplus electricity into hydrogen, it is used for producing all the required hydrogen. In fact, even though the electrolyzer is not employed in the storage system, it would be the preferred option for obtaining hydrogen instead of reformer. This fact can be verified by comparing the process safety indexes of the electrolyzer and reformer units (Table 3-16). Thus, because of the more intense operating conditions (temperature and pressure), the corresponding value of the reformer is considerably higher than the one of electrolyzer.

Table 3-16: Inherent safety of the energy system using the proposed inventory index for different objective functions.

Equipment	Index	PV area = 5 000 m²				PV area = 7 500 m²				PV area = 10 000 m²			
		TAC	AGE	DEP	WC	TAC	AGE	DEP	WC	TAC	AGE	DEP	WC
Electrolyzer	Chemical	0.2	0.2	0.2	-	0.6	0.5	0.5	0.6	1.0	1.0	1.0	1.2
	Process	3.7	3.7	3.7	-	3.8	3.8	3.8	3.8	3.9	3.9	3.9	3.9
Fuel Cell	Chemical	-	-	-	-	0.5	0.2	0.2	0.8	0.7	0.4	0.4	0.9
	Process	-	-	-	-	3.8	3.7	3.7	3.8	3.8	3.8	3.8	3.8
Digester	Chemical	-	0.1	0.1	-	-	0.1	0.1	-	-	0.1	0.1	-
	Process	-	0.5	0.5	-	-	0.4	0.4	-	-	0.4	0.4	-
Reformer	Chemical	0.2	0.2	0.2	0.2	0.2	0.2	0.2	0.2	0.2	0.2	0.2	0.2
	Process	6.3	6.3	6.3	6.3	6.3	6.3	6.3	6.3	6.3	6.3	6.3	6.3
Hydrogen Tank	Chemical	-	-	-	-	0.1	0.1	0.1	0.2	0.1	0.1	0.1	0.2
	Process	-	-	-	-	4.6	5.4	5.4	7.3	5.0	7.3	7.3	7.3
Total	Chemical	0.4	0.5	0.5	0.2	1.4	1.1	1.1	1.8	1.9	1.8	1.8	2.5
	Process	10.0	10.5	10.5	6.3	18.5	19.6	19.6	21.2	19.0	21.6	21.6	21.3
IST TOTAL		10.4	11.0	11.0	6.5	19.9	20.7	20.7	23.0	20.9	23.4	23.4	23.8

* Objective functions, (TAC) total annualized cost, (AGE) CO_2 emissions, (DEP) grid dependence and (WC) water consumption.

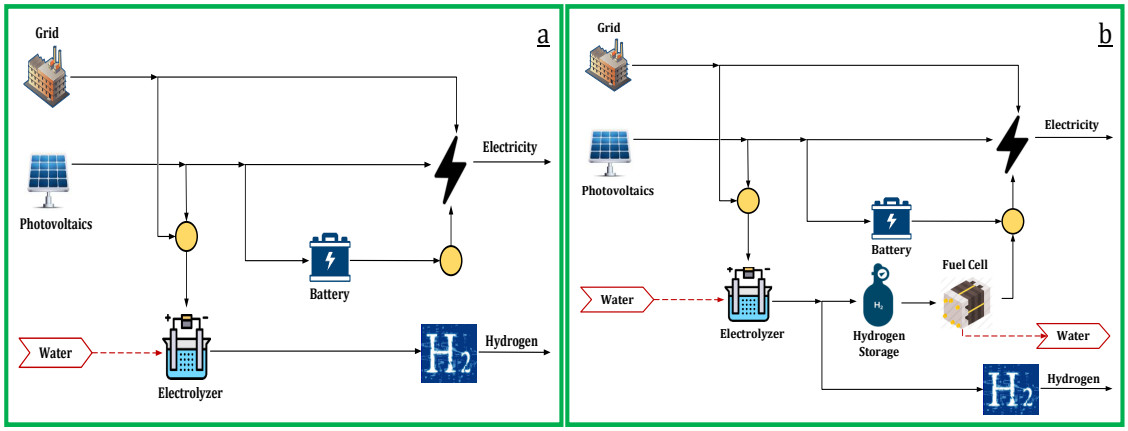

Figure 3-19: Optimal configuration of the distributed energy system for minimizing the inherent safety index. Photovoltaic surface (a) 5000 m² (b) 7500-10000 m².

Table 3-17 shows the results for all the sustainability indicators when the inherent safety index is optimized. As expected, the energy system becomes safer as the size of the plant decreases. In this sense, note that the two indicators of the social dimension are competitive between them since the lowest grid dependence is obtained with the largest PV surface. Also, it is worth to note that the whole of CO_2 emissions is derived of importing electricity from the grid. Moreover, Table 3-18 presents the size and the investment cost of the installed equipment.

Table 3-17: Optimization results of the distributed energy system for minimizing the inherent safety index.

Variable	Area of photovoltaics (m²)		
	5 000	**7 500**	**10 000**
LCOE (€/kWh)	0.47	0.54	0.58
TAC (M€/year)	2.2	2.6	2.8
CAPEX (% TAC)	86	90	92
OPEX (% TAC)	14	10	8
CO_2 emissions (ton/year)	157.2	124.7	89.3
Grid emissions (%)	100	100	100
Process emissions (%)	-	-	-
Biogenic (ton/year)	-	-	-
Water consumption (m³/year)	243.7	276.7	313.6
Electrolysis (%)	100	100	100
Reforming (%)	-	-	-
Digestion (%)	-	-	-
Grid Dependence (%)	57	44	30
Imported electricity (%)	100	100	100
Imported natural gas (%)	-	-	-
Inherent Safety	3.8	12.1	13.4
Chemical Index	0.1	1.5	2.2
Process Index	3.7	10.6	11.2

Table 3-18: Optimal size and investment cost of equipment within the energy system for minimizing the inherent safety index.

Equipment	PV area = 5 000 m²		PV area = 7 500 m²		PV area = 10 000 m²	
	Size	Investment (k€/year)	Size	Investment (k€/year)	Size	Investment (k€/year)
Photovoltaics		103.8		155.8		207.7
Electrolyzer (kW)	394	105.5	1160	310.8	1 640	439.4
Battery (MWh)	30	1 712.8	30	1 712.8	30	1 712.8
Reformer (kW)	-	-	-	-	-	-
Hydrogen Storage (MWh)	-	-	19	12.5	50	34.0
Fuel Cell (kW)	-	-	294	132.7	414	187.3
Digester (kW)	-	-	-	-	-	-

As depicted in Table 3-18 and Figure 3-20, the level of energy stored in the battery reaches up to the maximum capacity for the three surfaces of PV evaluated. Conversely, the size of the pressurized tank is quite far from its upper limit. This occurs because for improving the safety of the process, the system seeks to reduce the inventory of material as much as possible. Indeed, as observed in Figure 3-20b, the amount of stored hydrogen exhibits a behavior characterized by oscillations instead of a seasonal pattern.

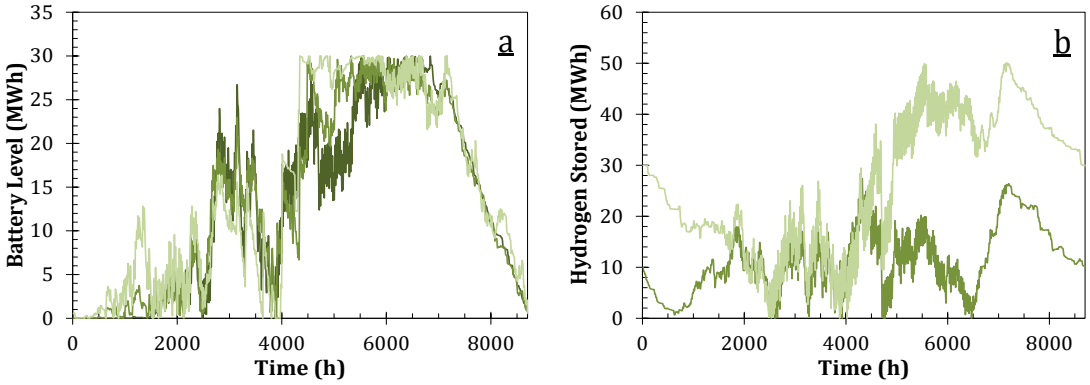

Figure 3-20: Optimal profiles of energy stored. (a) battery, (b) pressurized tank. Photovoltaic surface (—) 5000 m² (hydrogen is not used), (—) 7500 m² and (—) 10000 m².

Otherwise, the need for decreasing the accumulation of hydrogen leads to a high utilization of the power-to-power cycle during sunny periods (Figure 3-21b). Hence, the system promotes the operation of the fuel cell for reducing the capacity of the pressurized tank. In fact, fuel cell supplies between 24-40% of the electricity demands at spring and summer seasons. Moreover, regarding hydrogen demand, Figure 3-22 depicts the distribution of the sources of electricity along the seasons of the year. According to results, the share of PV-based electricity is 12% by using a PV surface of 5000 m², but it could reach up to 60% by installing an area of 10000 m².

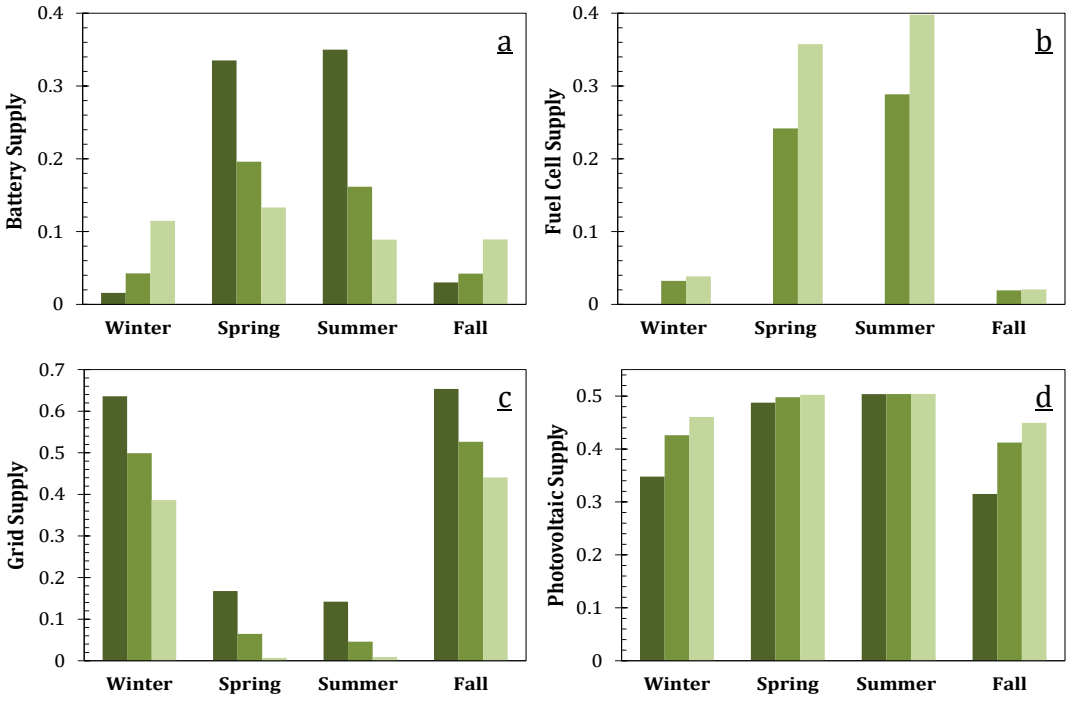

Figure 3-21: Optimal fraction of electricity supplied by the distributed energy system. Photovoltaic surface (■) 5000 m², (■), 7500 m² and (■) 10000 m². Sources (a) battery, (b) fuel cell, (c) grid and (d) photovoltaic panels.

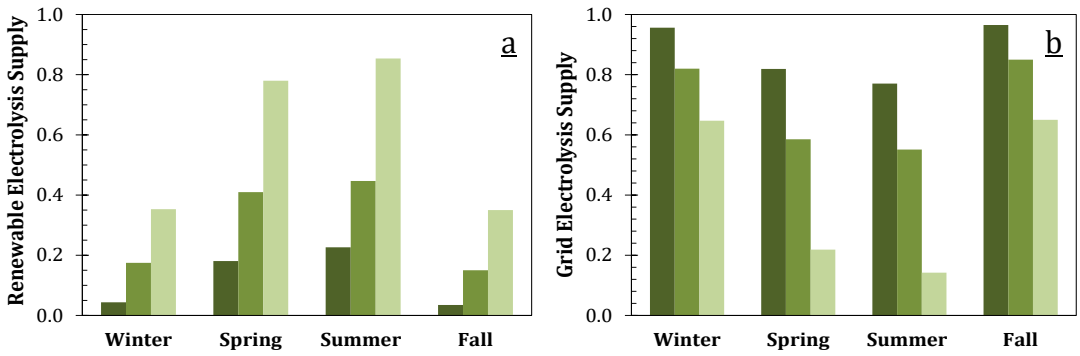

Figure 3-22: Optimal fraction of hydrogen supplied by the distributed energy system. Photovoltaic surface (■) 5000 m², (■), 7500 m² and (■) 10000 m². Sources (a) electrolysis powered by renewable electricity, (b) electrolysis powered by the grid.

3.5 Summary and Conclusions

In this chapter and optimization approach was proposed and implemented for the design and operation of energy systems. The proposed framework was illustrated through a case study based upon the energy system model and the sustainability indicators presented in Chapter 2.

Summarizing, from the optimization results it is noted the significant influence of the evaluated indicator on the design and operation of the energy system. In this respect, from the assessment of the five indicators and the three surfaces of PV, eight energy system configurations were obtained. Then, Figure 3-23 depicts comparatively each one of the optimization results. Such a figure represents normalized values, 1 being the best value (minimum), and 0 the worst value (maximum) of the index. Thus, the farther the vertex of the hexagon is from the center, the better is its performance in the corresponding indicator. For instance, note that the best economic performance corresponds to the PV surface of 5000 m^2. However, this result has one of the poorest yields in the grid dependence (social) and CO_2 emission (environmental) indicators. Additionally, from the figure it is also noted the evolution of the indicators through the different areas of PV. In this regard, the performance on the CO_2 emissions and grid dependence improves as the PV surface gets larger. In contrast, total annualized cost, water consumption and safety indexes get their best performance with the smallest PV surface.

Furthermore, Figure 3-23 also evidences the competitive behavior among the indicators of the sustainability dimensions. This fact highlights the complexity of designing this kind of systems since there is not a single optimal solution for satisfying all the criteria at their best performance. Therefore, it is necessary to include all the sustainability dimensions to identify the trade-offs among them and support the decision-making process during the conceptual design step.

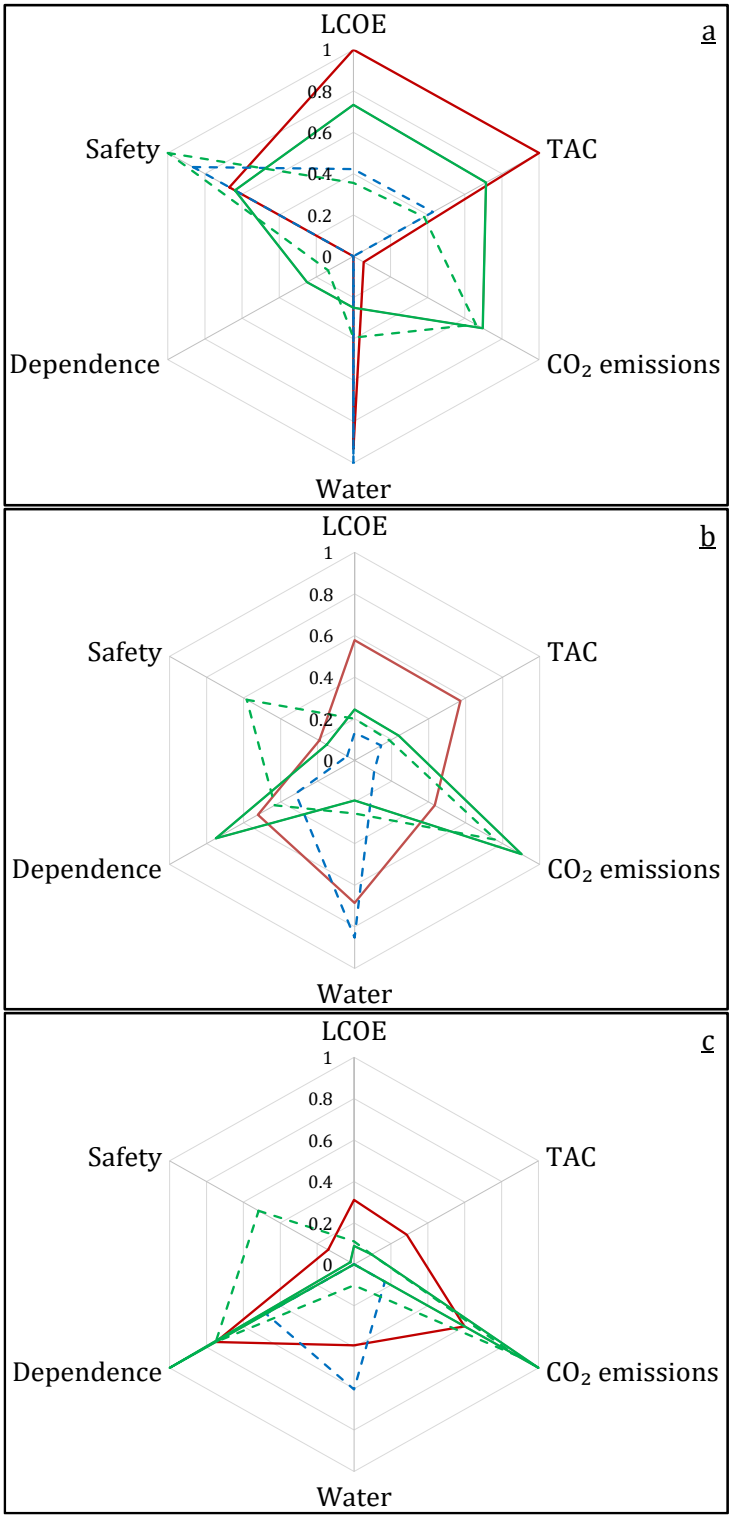

Figure 3-23: Representation of the optimization results. Photovoltaic surface (a) 5000 m², (b), 7500 m² and (c) 10000 m². Objective function (—) total annualized cost, (—) grid dependence, (--) water consumption, (--) inherent safety.

4. Multi-Objective Optimization for the Energy System Design

According to the optimization results presented in the previous chapter, it was evidenced the great impact of the objective function on the optimal design and operation of the energy system. Besides, it was identified the contradictory behavior among the sustainability indicators. Indeed, it was noted that the optimization of one single objective does not enable to satisfy all the sustainability criteria, since improving one objective leads to decrease the performance of another one. Therefore, rather than the individual evaluation of the objectives, the sustainability evaluation requires to consider simultaneously more than one objective, i.e. to address a multi-objective optimization problem. In this regard, this chapter focuses on identifying the relationships between the sustainability criteria through a multi-objective optimization approach. Thus, the chapter is organized as follows. Initially, some general aspects about multi-objective optimization are introduced, and a general overview of the solution methods is presented. Then, based on the energy system model (Chapter 2) and the case study (Chapter 3), four multi-objective optimization problems for the optimal design and operation of the energy system are performed. Such optimization cases include different combinations of the sustainability indicators. Finally, the main results and conclusions are presented.

4.1 Multi-Objective Optimization

4.1.1 General Aspects

The most of engineering applications imply to consider simultaneously more than one objective, i.e. they are multi-objective optimization problems (MOOP). Indeed, this is the case of the process design under sustainability dimensions, since it involves economic, environmental, and social objectives. Often, these objectives are contradictory and therefore competitive among them. Thus, unlike mono-objective optimization problems wherein a unique solution is obtained, multi-objective optimization is characterized by

providing a set of optimal solutions [181,205]. Typically, these results are known as Pareto or non-dominated solutions and represent the trade-offs among the objectives. Mathematically, Pareto solutions constitute a group of equally optimal alternatives, since each one is better than the other in at least one objective. Therefore, by moving across the non-dominated solutions, one objective improves whilst at least one other gets worse [179,181].

It is worth noting that each one of the Pareto solutions has a corresponding point in the decision variables space. Then, multi-objective optimization results consist in a wide range of design and/or operating options to be considered. Thus, from the basis that all those alternatives are equally optimal, the selection of the solution to be implemented relies on the decision-maker (DM) preferences and knowledge [206]. Hence, the role of DM is paramount for performing a multi-objective optimization analysis. In fact, as it will be presented in the next section, the most traditional classification of the solution methods for MOOP is based upon the involvement of DM throughout the solution of the problem [181,205].

4.1.2 Solution Methods

Broadly, multi-objective optimization methods can be divided in two main groups: generating and preference-based methods [181,205]. As aforementioned, these differ in the role of DM. Thus, generating methods are based upon obtaining the set of Pareto solutions without considering the preferences of DM. Then, DM is requested for selecting among the non-dominated alternatives. In this respect, generating methods constitute a great source of information, since they enable to elucidate the compromise among the optimization objectives. Consequently, DM can decide knowing the trade-offs of the criteria. Nonetheless, these methods have some weaknesses related with the massive amount of possible solutions and the computational cost for solving the problem. On the one hand, because the number of Pareto solutions is often too large, and hence difficult to analyze effectively by DM. On the other hand, because the complexity of the problem increases rapidly with the number of objectives, and therefore the computational requirements for obtaining the solution also increase [181,205].

Moreover, preference-based methods entail to use the expertise/knowledge of DM at some stage during the solution of the MOOP. Also, these methods can be sub-divided into two groups: *a priori* and interactive methods. In the former methods, the original MOOP is converted into a single-objective optimization problem and the preferences of DM are used

in its formulation. The goal programming approach is one example of *a priori* methods. Moreover, interactive methods imply to interact with the DM whilst the MOOP is being solved. Examples of this approach are the interactive surrogate worth trade off and the NIMBUS methods [181].

Many methods for solving MOOP imply to transform the original problem into a single-objective one. That is the case of the weighting, epsilon-constraint, and global criterion methods. In general, such methods are simple and effective for solving problems with few objectives. However, they require to solve the optimization problem many times, since only one point of the Pareto set is obtained at a time. Consequently, building an evenly distributed set of non-dominated solutions can be a very time-consuming task. Additionally, as the number of objectives increase, it is more difficult to select suitable values for the weighting and epsilon-constraint methods [181,205].

Moreover, the original MOOP can be addressed by using stochastic techniques and evolutionary algorithms [207]. Broadly, such approaches include Monte Carlo methods and optimization algorithms inspired on biology, physics, and geography. Some examples of these methods are the genetic algorithm, which lies upon the natural selection theory of Darwin; the particle swarm optimization, which is based on the behavior of honeybees; and the simulated annealing, that is inspired on the physical behavior and properties of matter. These approaches do not depend on continuity, derivative conditions and initial points, so that they are suitable for solving problems that could be difficult to address with deterministic methods [207]. Regarding multi-objective optimization, the evolutionary algorithms enable to simultaneously obtain all the set of non-dominated solutions, which provides more information to the DM [181,207].

As noted, there is a wide variety of methods for solving the multi-objective optimization problems. Nevertheless, the exhaustive revision of such approaches is beyond the scope of this work. Accordingly, if required, the reader is referred to the books by Pandu Rangaiah [181], Pandu Rangaiah and Bonilla-Petriciolet [206], Coello Coello et al. [207], Goldberg [208], or the Chapter 6 of the book by Diwekar [205] for a more detailed information.

4.2 Case of Application

The case of application corresponds to that described in section 3.3 of the Chapter 3. As noted, five objective functions are included within the optimization problem for the energy system design under the sustainability dimensions. Such objective functions are the total

annualized cost (J_1), the CO_2 emissions (J_2), the water consumption (J_3), the grid dependence (J_4), and the inherent safety (J_5). According to the results of the previous chapter, it was evidenced the great impact of such indicators on the energy system design. Additionally, in Chapter 2, it was highlighted the need of implementing holistic approaches that include the economy, the ecosystem, and the society along the different stages of engineering projects. Consequently, such focuses require to identify the trade-offs among the sustainability dimensions, rather than concentrating in only one of them.

In this respect, depending on the specific needs of the project or the objectives of decision maker, different combinations of the sustainability indicators could be employed for performing the energy system design. In this line, aiming to illustrate such possibilities, in this work four multi-objective optimization problems are proposed and solved. These cases cover a variety of combinations of the objective functions and enable to obtain insights about the trade-offs among them for the subsequent decision-making process.

Thus, Table 4-1 depicts how the indicators are grouped for addressing the multi-objective optimization. Noted that the problem P1 involves two sub-problems, i.e. the cost against the CO_2 emissions and the cost against the grid dependence. Likewise, P4 also comprises two sub-problems, i.e. the safety against the cost, and the safety against the CO_2 emissions. Meanwhile, problems P2 and P3 include three objectives simultaneously. Moreover, all the constraints are identical to those employed in the mono-objective optimization problems addressed in Chapter 3 (Equations 3.28 to 3.35).

Table 4-1: Multi-objective optimization problems and corresponding indicators for the energy system design.

Problem	Indicators
P1	Cost - CO_2 emissions / Grid dependence
P2	Cost - Water consumption - Grid dependence
P3	Cost – Water consumption - Safety
P4	Safety – Cost / CO_2 emissions

Considering the features of the methods for solving multi-objective optimization problems (section 4.1.2), and the number of objective functions to address, the Non-dominated Sorting Genetic Algorithm (NSGA-II) was selected for solving the proposed optimization problems. Such algorithm was employed through the *gamultiobj* function within MATLAB® software. This algorithm was selected because of it enables to obtain diverse and evenly distributed solutions. Besides, the ready availability and effectiveness of the

algorithm are well documented, as it has been extensively used to solve many optimization problems in chemical engineering [181,206,207,209].

4.2.1 Problem 1: Cost - CO_2 emissions/grid dependence

Figure 4-1 depicts the Pareto fronts for the two multi-objective optimization problems: (i) economic-environmental (Figure 4-1a), and (ii) economic-social (Figure 4-1b). Initially, such problems were solved considering different sizes of the population for the genetic algorithm. In this respect, populations between 500 and 4000 individuals were evaluated to identify the impact of this variable on the Pareto solutions. The corresponding results are presented in Figures C-1 and C-2 of the Annex C. Accordingly, a population of 3000 individuals was selected, since for populations larger than 2000 individuals, no significant impact of this variable is observed on the optimal set of solutions.

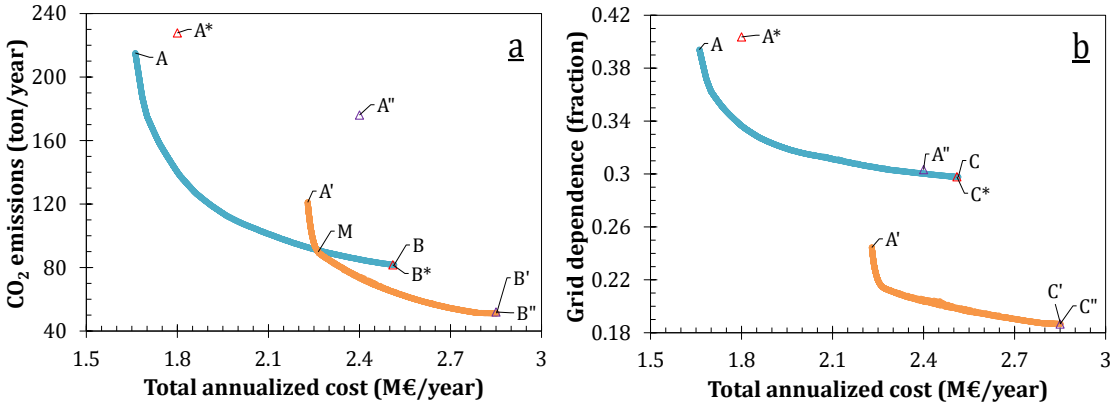

Figure 4-1: Pareto fronts and mono-objective optimization results. (a) CO_2 emission - cost, (b) grid dependence – cost. Photovoltaic surface (● - Δ) 7500 m², (● - Δ) 10000 m². (A – A' – A* - A") optimal cost, (B – B' – B* - B") optimal emission, and (C – C' – C* - C") optimal grid dependence.

First, note that the points A-A'-A"-A* correspond to the best performance from the economic point of view, the points B-B'-B"-B* represent the best solution from the environmental perspective, and the points C-C'-C"-C* represent the social optimum. Among these points, A-A'-B-B'-C-C' correspond to the multi-objective optimization results, whereas the points A"-A*-B"-B*-C"-C* represent the results of the single-objective optimization. Thus, the obtained Pareto fronts reflect the competitive behavior of both pair of objectives, since as the total annualized cost decreases, the CO_2 emissions and the grid dependence get worse. Also, it is worth noting that the economic optimum is not the same for the single and multi-objective optimizations. This fact is observed by comparing the points A and A* for a PV surface of 7500 m², and the points A' and A" for 10000 m². Indeed,

the results from the mono-objective optimizations (A* and A") are dominated points, which suggests that they correspond to a local optimum. Conversely, when the CO_2 emissions and the grid dependence are optimized, the results of the single and multi-objective optimization are identical (B–B*, B'–B", C-C* and C'-C").

Moreover, Figure 4-1 also depicts the influence of the PV surface on the performance of the energy system. In this respect, larger areas of PV enable to achieve lower CO_2 emissions and grid dependence, but also entails a greater economic cost. In general, these results provide a wide range of solutions that can be further evaluated for the DM for their implementation. Interestingly, the results show that there is a zone wherein the PV surface of 7500 m^2 will not be competitive against the area of 10000 m^2. This occurs for the solutions between the points B and M because all of them could be improved in at least one criterion by using a PV surface of 10000 m^2. Mathematically, this implies that the solutions within the MB line are dominated by those obtained with a PV area of 10000 m^2 (line A'B'). In such a way, if the decision maker is willing to invest between 2.3 and 2.5 M€, it would be better to install a PV surface of 10000 instead of 7500 m^2, since for the same cost lower CO_2 emissions and grid dependence could be obtained.

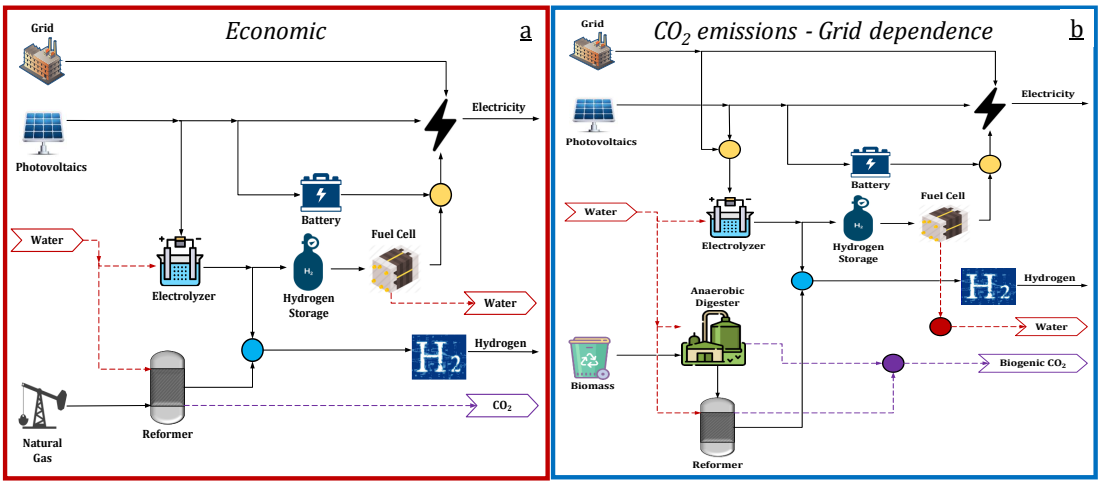

Figure 4-2: Optimal energy system configuration for the extreme points of the Pareto fronts. Objective function (a) total annualized cost, and (b) CO_2 emissions and grid dependence.

Figure 4-2 shows the energy system configuration for the extreme points of the Pareto front, i.e. those obtained from the mono-objective optimization. Note that, from the design perspective, the difference of the energy system structure lies on the source of methane for the reforming process. Thus, when the economic objective is addressed, all the methane is imported from the network (Figure 4-2a). In contrast, if the objective is to reduce the CO_2

emissions or the grid dependence, the reformer reactor is fed with methane from the anaerobic digestion process (Figure 4-2b).

Aiming to elucidate the differences in the design and operating conditions throughout the Pareto fronts, Figure 4-3 presents the installed size and the use of some energy sources as a function of the total annualized cost. As noted in Figures 4-3a and 4-3b, there is a direct relation between the energy storage capacities and the total cost of the system. Then, the best configurations from the economic perspective correspond to those with the smallest storage units. Meanwhile, Figures 4-3c and 4-3d depict the change of the source of methane for the reforming process. As observed, the best performance for the CO_2 emissions and grid dependence indicators is obtained without importing methane from the grid and using the maximum amount available of biomass. Then, as the economic performance improves, the imported natural gas increases and the biomass gets unused, but at the cost of higher CO_2 emissions and grid dependence. Interestingly, note that, whilst the storage capacities are the most influencing variables on the cost criterion, the source of methane has the biggest impact on the emission and grid dependence issues. This fact can be observed by analyzing Figures 4-1 and 4-3. In such a way, going from low emission to low cost, it is observed that the most significative alteration on the slope of the Pareto curves correspond to an important change on the curves of the imported natural gas and the biomass consumption. Roughly, this occurs at a value of 1.9 M€ for a PV surface of 7500 m^2, and at 2.2 M€ when the area of PV is 10000 m^2.

Additionally, as aforementioned, the economic optimum from the multi-objective optimization differs from that obtained through the single-objective optimization. In this regard, the differences in terms of process variables can be noted in Figure 4-3. Again, the points A”-A* represent the single-objective optimization results for the PV surface of 7500 and 10000 m^2, respectively. On the one hand, as observed in Figure 4-3a, multi-objective optimization algorithm finds a solution wherein the required capacity of the battery is smaller with respect to that obtained from the mono-objective optimization. Accordingly, this leads to and energy system with a lower TAC. On the other hand, as noted in Figure 4-3d, single-objective optimization results indicate that biomass is not used at the economic optimum (points A”-A*). Conversely, according to multi-objective optimization results, the economic extremes of the Pareto solutions (A-A’) still include the use of biomass. Consequently, as observed in Figure 4-1, the economic optimum from mono-objective optimization has a poorer performance in the CO_2 emissions and grid dependence indicators.

Moreover, it is also noted that the biomass utilization does not seem to have a great impact on the economic indicator (Figure 4-3d). Therefore, this fact can explain why, even considering different sizes of population (500, 1000, 2000, 3000 and 4000 individuals), multi-objective optimization algorithm does not find a point without including biomass within the energy system.

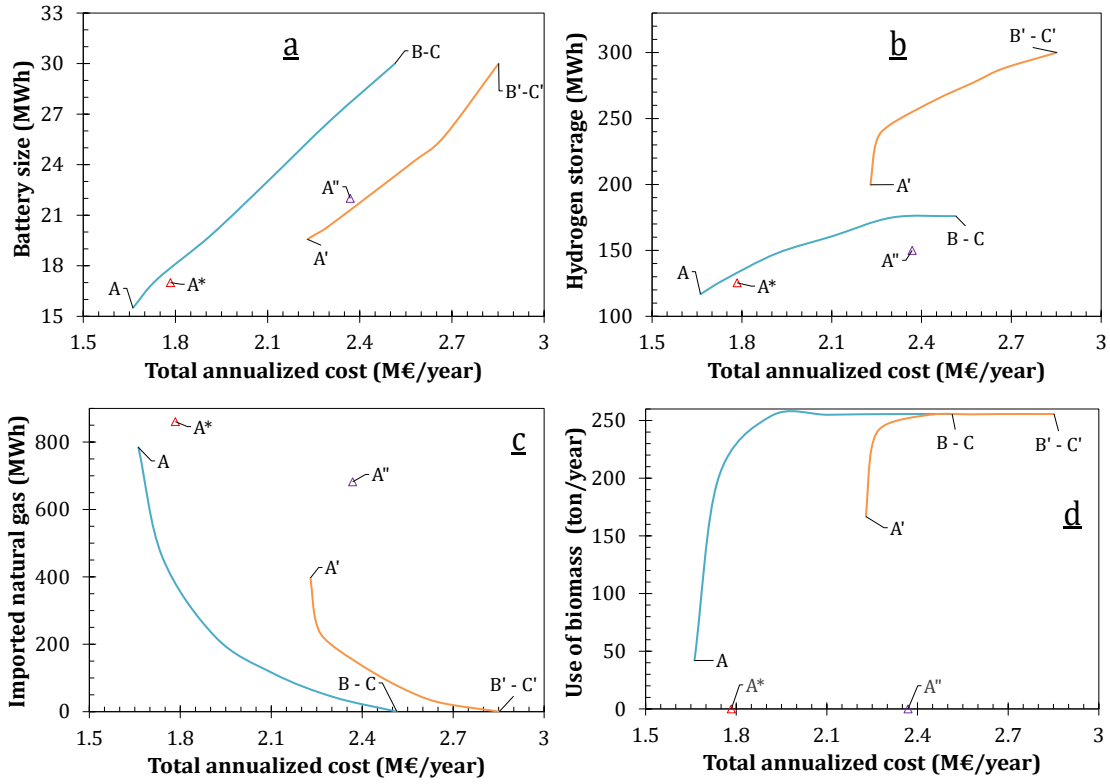

Figure 4-3: Change of design and operation conditions across the Pareto fronts. Photovoltaic surface (— and Δ) 7500 m² and (— and Δ) 10000 m². (a) battery, (b) pressurized tank, (c) imported natural gas, and (d) biomass consumption. (A – A') optimal cost, (B – B') optimal emission, (C – C') optimal grid dependence.

4.2.2 Problem 2: Cost - water consumption - grid dependence

The second multi-objective optimization problem consisted in the simultaneous minimization of the total annualized cost, water consumption and grid dependence. Initially, the problem was solved considering different sizes of population for the genetic algorithm. According to the obtained results, a population of 3000 individuals was selected, since above 2000 individuals, no significant effect on the Pareto solutions was observed. Results of such optimizations are presented in Figure C-3 of the Annex C. Accordingly, Figures 4-4 and 4-5 depicts the obtained Pareto sets considering a PV surface of 7500 and

10000 m², respectively. Such figures include a 3-dimension representation (Figures 4-4a and 4-5a), and the 2-dimension projections for the three evaluated objectives.

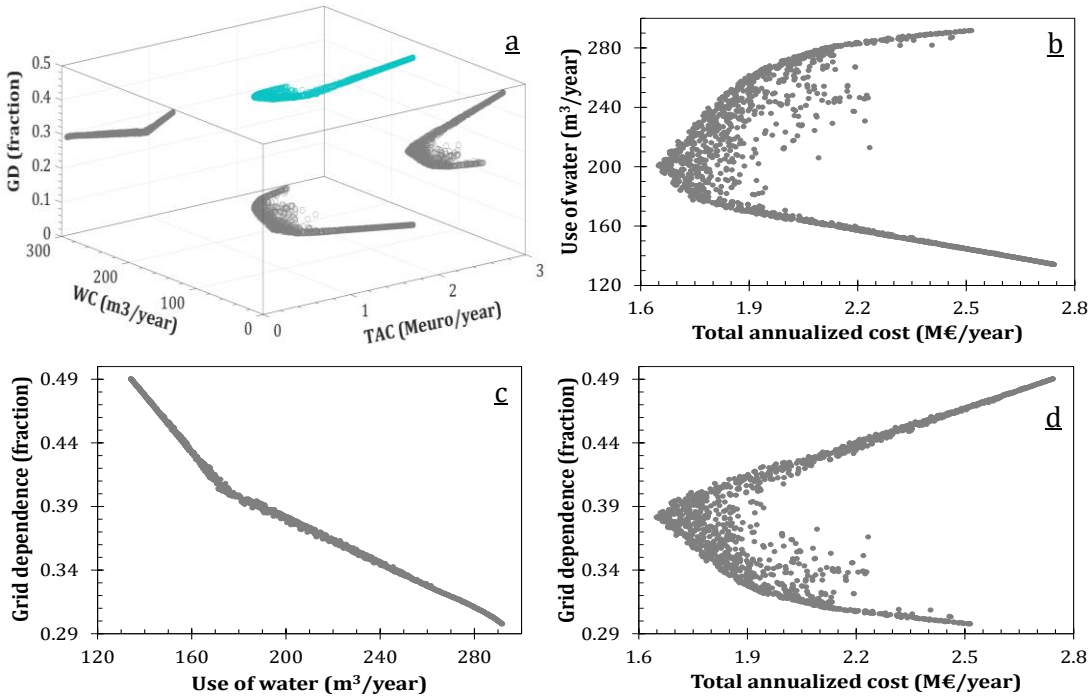

Figure 4-4: Pareto solutions for minimizing the total annualized cost, the water consumption and the grid dependence considering a photovoltaic surface of 7500 m². (●) 3-dimension representation (●) 2-dimension projections.

Results show the trade-offs and the relationships among the objective functions. In fact, it is observed the competition among the three indicators. Thus, the minimum water consumption implies the poorest yield on the cost and self-sufficiency indicators. In the same line, the lowest grid dependence requires the greatest water consumption. According to optimization results, it is also noted that for a given value of the economic indicator (TAC), there is a wide range of possible energy system structures and/or operating policies (Figures 4-4b, 4-4d, 4-5b and 4-5d). Then, for a fixed cost, the selection of the preferred alternative would require defining a value for the water consumption or the grid dependence. Figures 4-4c and 4-5c depict the relation between these two objectives. In this respect, the decision would depend on the specific context conditions and/or decision-maker preferences considering the reliability of the grid and the availability of water. For instance, if the energy system is developed in an isolated location or with regular energy outages, the grid dependence indicator must be privileged to assure the access to energy. Meanwhile, if the project is implemented in an arid zone, or in a place with low water resources, the indicator related to the water consumption will be the most important in the selection of the energy system.

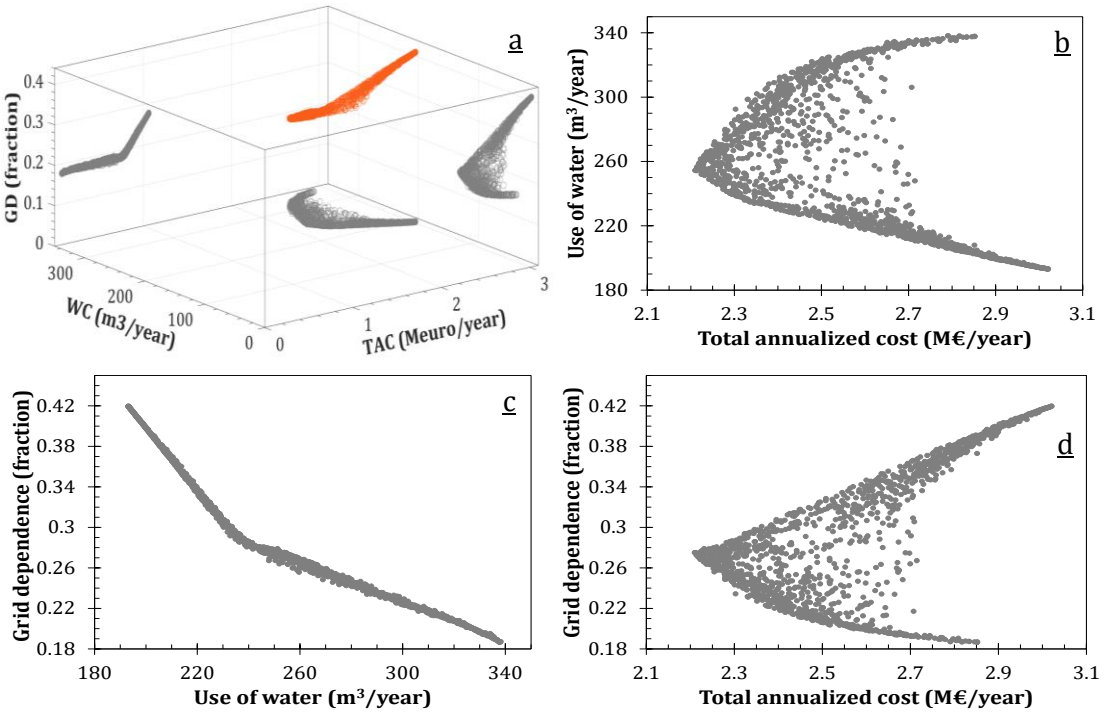

Figure 4-5: Pareto solutions for minimizing the total annualized cost, the water consumption and the grid dependence considering a photovoltaic surface of 10000 m². (●) 3-dimension representation (●) 2-dimension projections.

Figure 4-6 presents the comparison of the Pareto solutions for the two areas of PV evaluated. In those figures, the points A-A', B-B' and C-C' represent the optimal value of the economic, environmental, and social objectives, respectively. In general, the results suggest that the total annualized cost and water consumption indicators improve as the PV surface decreases. Conversely, larger areas of PV favor the energy autonomy. In this respect, note that as the PV surface gets larger, the surplus of electricity increases, and consequently, there is a need of bigger units for energy storage. For the economic and environmental objectives, this implies higher investment cost due to the size of equipment, and more elevated use of water for converting the surplus electricity into hydrogen through the electrolyzer. In contrast, as the area of PV becomes larger, the grid dependence indicator is enhanced, since in such a case, there is a greater amount of energy available from renewables, and therefore less energy must be imported from the grid.

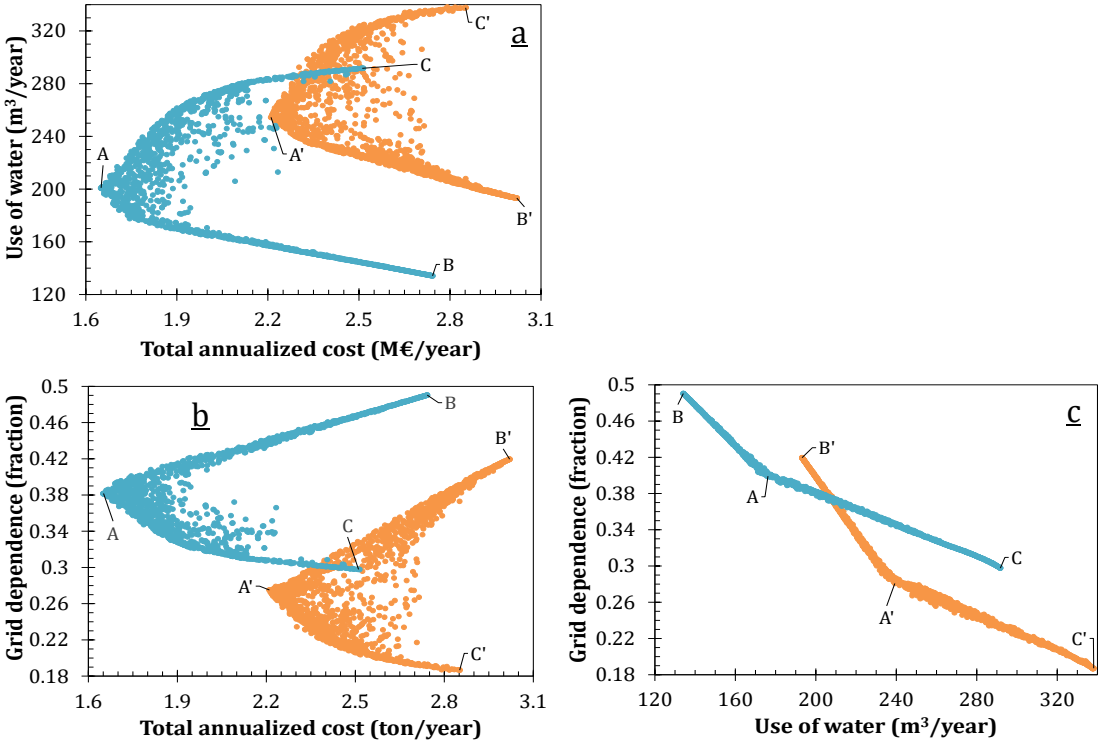

Figure 4-6: 2-dimension projection of the Pareto solutions for minimizing the total annualized cost, the water consumption and the grid dependence. Photovoltaic surface (●) 7500 m², (●) 10000 m². (A – A') optimal cost, (B – B') optimal water consumption, (C – C') optimal grid dependence.

Figure 4-7 depicts the energy system structure when each one of the indicators is evaluated individually. By comparing the optimal configuration from the economic (Figure 4-7a) and environmental perspectives (4-7b), note that both structures involve the same set of equipment for energy conversion and storage. Indeed, according to the flowsheets, the only difference is on the sources for supplying the hydrogen demand. Thus, whilst the economic optimization includes the possibility of providing hydrogen from water electrolysis, the water consumption indicator suggests that all the hydrogen must be supplied via steam methane reforming. In this respect, Figure 4-8 shows the change on the design and operation parameters by going from the economic (A-A') to the environmental (B-B') indicator across the Pareto solutions. On the one hand, as observed in Figures 4-8a and 4-8b, the economic optimum corresponds to the configurations with the smallest size of the storage units. This happens because such devices represent about 60-65% of the CAPEX of the system.

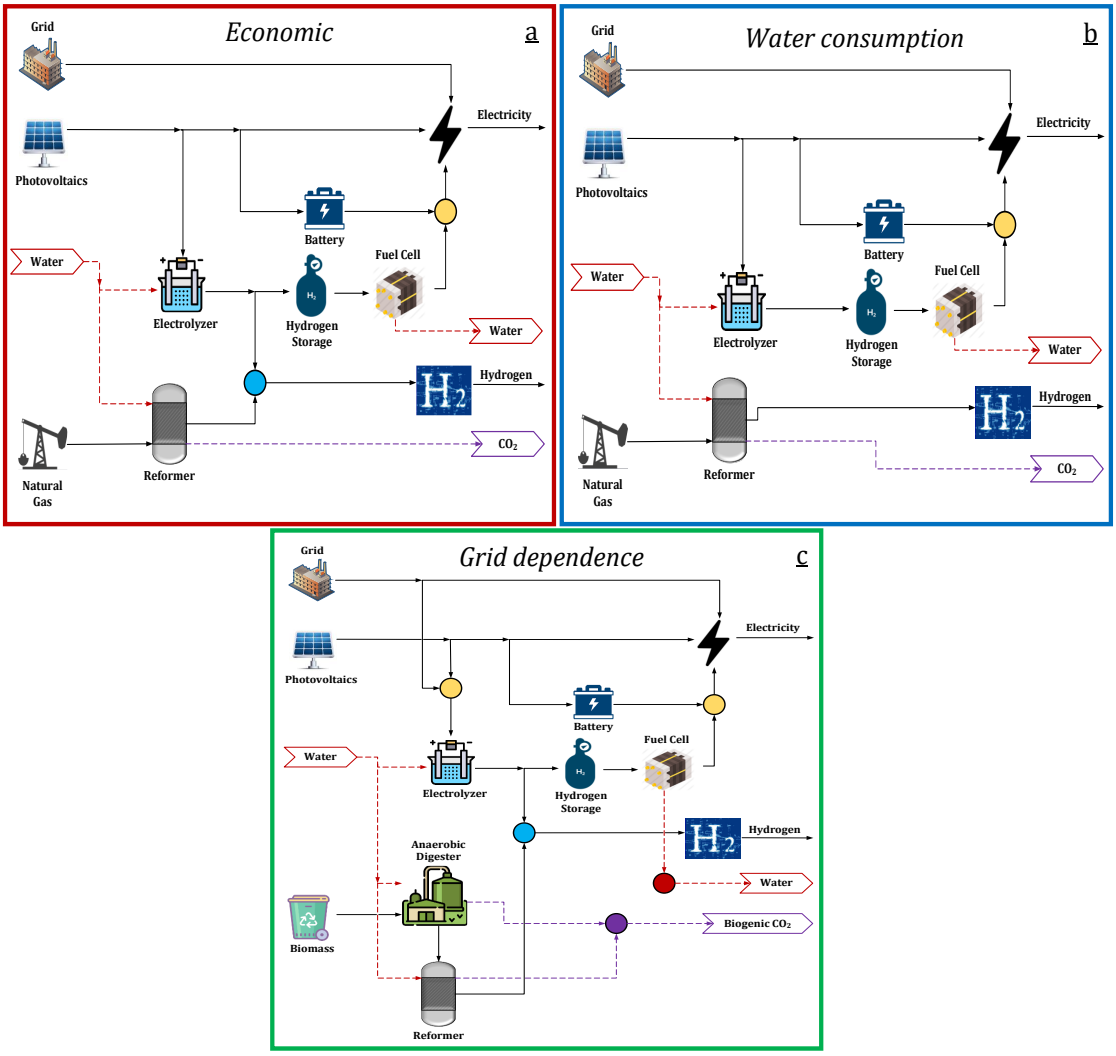

Figure 4-7: Energy system configurations for the extreme points of the Pareto solutions. Objective function (a) total annualized cost, (b) water consumption, and (c) grid dependence.

On the other hand, note that moving towards the optimal value of the water consumption requires to increase the capacity of energy storage (Figures 4-8a and 4-8b) and the amount of natural gas imported from the network (Figure 4-8c). Regarding the energy storage issue, it can be explained by the fact that when the whole system electrolyzer-tank-fuel cell is employed, there is possible to recover the water produced in the fuel cell to be reused in the electrolyzer. Consequently, the net water consumption is lower than that obtained by sending the hydrogen to supply the demand. Besides, the requirement of methane for the reforming process increases as moving towards the minimal water consumption (points B and B'), since the hydrogen supplied by water electrolysis gets lower.

Moreover, the best performance for the grid dependence indicator is obtained by feeding the reforming reactor only with the biomethane produced from the anaerobic digestion process (Figure 4-7c). Accordingly, this configuration corresponds to that without

importing natural gas from the network and with the highest use of biomass, as presented by the points C-C' in the Figures 4-8c and 4-8d.

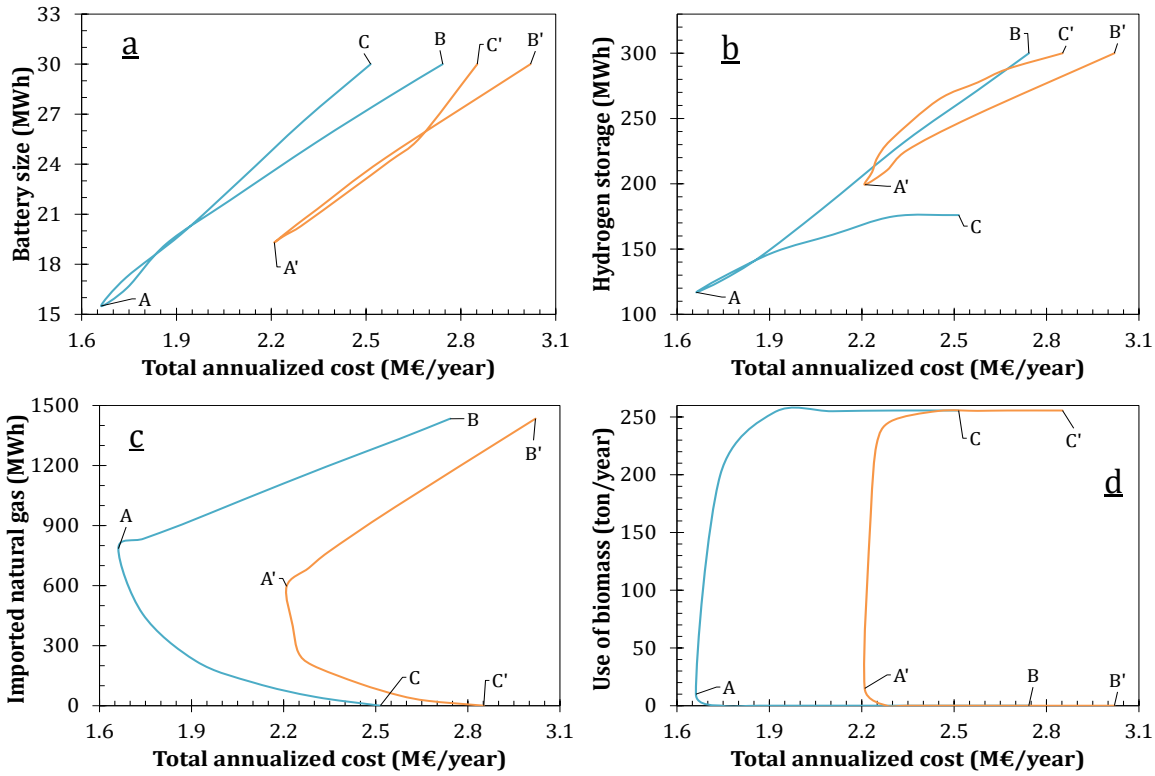

Figure 4-8: Change of design and operation conditions across the Pareto solutions. Photovoltaic surface (—) 7500 m² and (—) 10000 m². (a) battery, (b) pressurized tank, (c) imported natural gas, and (d) biomass consumption. (A – A') optimal cost, (B – B') optimal water consumption, (C – C') optimal grid dependence.

4.2.3 Problem 3: Cost – water consumption - safety

In this optimization problem, the three dimensions of sustainability are evaluated by means of the total annualized cost, water consumption and inherent safety indicators. As before, the first step consisted in performing the optimization by considering different sizes of population for the genetic algorithm. In this case, the evaluated values were 500 and 2000 individuals, and according to the obtained results, no considerable effect of this variable on the set of Pareto solutions was observed. Such results are depicted in Figure C-4 of the Annex C. Consequently, the results corresponding to a population of 2000 individuals were selected for analyzing the multi-objective optimization problem. Thus, Figures 4-9 and 4-10 present the obtained Pareto solutions considering a PV surface of 7500 and 10000 m², respectively.

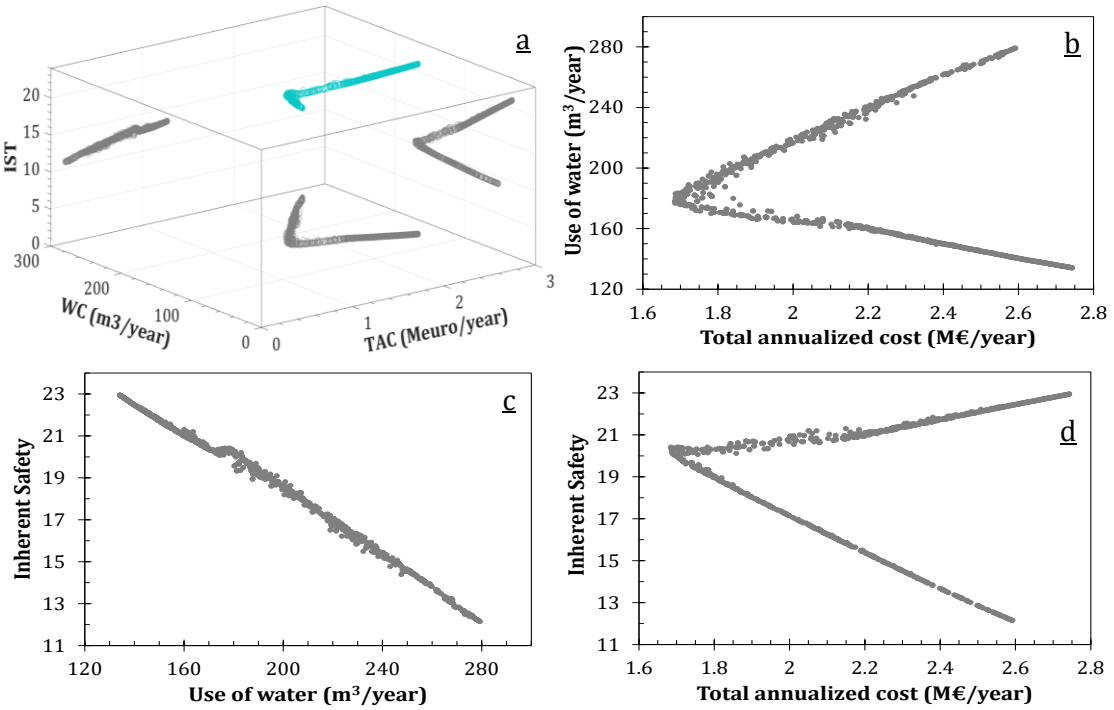

Figure 4-9: Pareto solutions for minimizing the total annualized cost, the water consumption and the inherent safety considering a photovoltaic surface of 7500 m². (●) 3-dimension representation (●) 2-dimension projections.

In general, results show the compromise among the objective functions and their contradictory behavior. As depicted in Figures 4-9(10)b and 4-9(10)d, there are at least two feasible energy system configurations or operating conditions that yield the same performance on the economic indicator. In such a way, the choice of the most suitable option involves the evaluation of the trade-off between the water consumption and safety indicators, which is presented in Figures 4-9(10)c. In those figures, the competition between these two objectives can be noted since the improvement of the safety index requires to increase the use of water.

Moreover, Figure 4-11 illustrates the obtained Pareto solutions for the two areas of PV assessed. In those figures, the points A-A', B-B' and C-C' represent the optimal value of the economic, environmental, and social objectives, respectively. As mentioned in a previous multi-objective optimization problem (P2), the total annualized cost and water consumption indicators improve as the PV surface decreases. Likewise, the safety indicator also gets better for the smaller size of PV, as shown in Figures 4-11b and 4-11c. As aforementioned (P2), as the surface of PV increases, bigger units are required for converting the surplus electricity into hydrogen and for energy storage. Consequently, this leads to an energy system with higher costs, more elevated consumption of water, and more hazardous conditions.

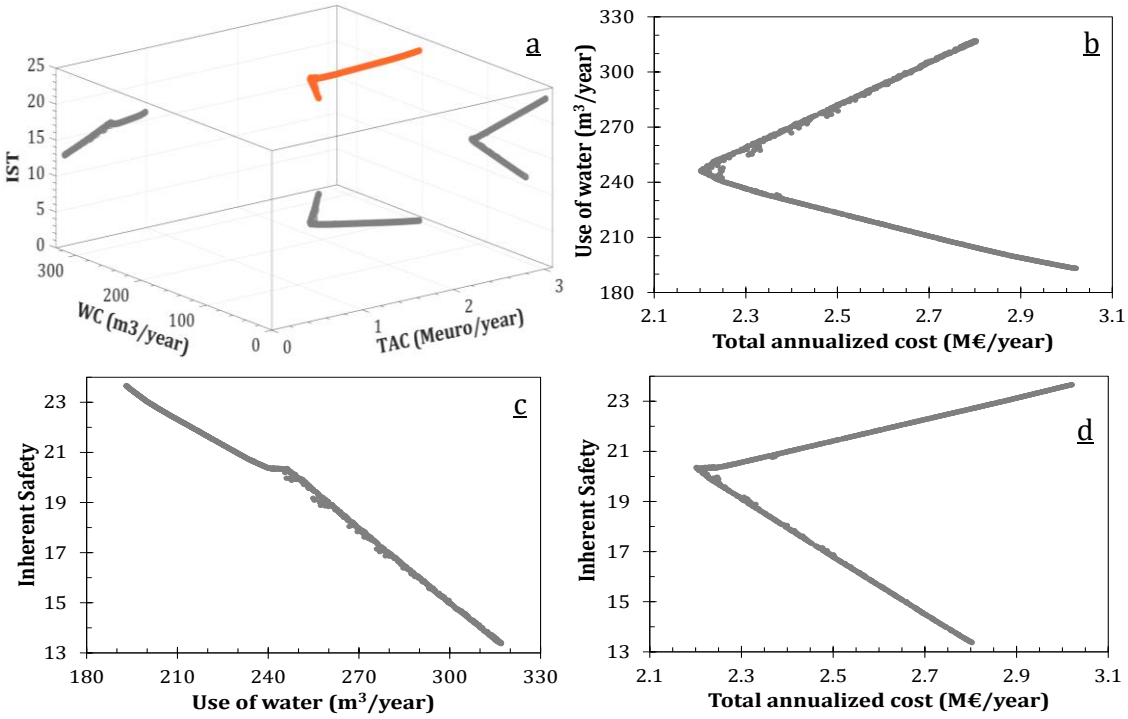

Figure 4-10: Pareto solutions for minimizing the total annualized cost, the water consumption and the inherent safety considering a photovoltaic surface of 10000 m^2. (●) 3-dimension representation (●) 2-dimension projections.

Figure 4-12 shows the configuration of the energy system by considering the three objective functions separately. The comparison between the results of the economic and water consumption indicators was already discussed in the optimization problem P2. Meanwhile, note that the optimization of the safety index implies a new alternative for the energy system configuration (Figure 4-12c). In this regard, aiming to reduce the amount of equipment, the safety indicator suggests a process flowsheet without the reforming reactor. This result can be explained by two facts: (i) because of the intense operating conditions of the reforming process (temperature and pressure), and (ii) because of the electrolyzer is already installed as a part of the hydrogen storage system. Likewise, as the reformer is not used, connection with the natural gas network is not required, since all the hydrogen is obtained via water electrolysis. Additionally, according to the social optimization results, the electrolyzer must be powered by both, the PV and the electricity grid.

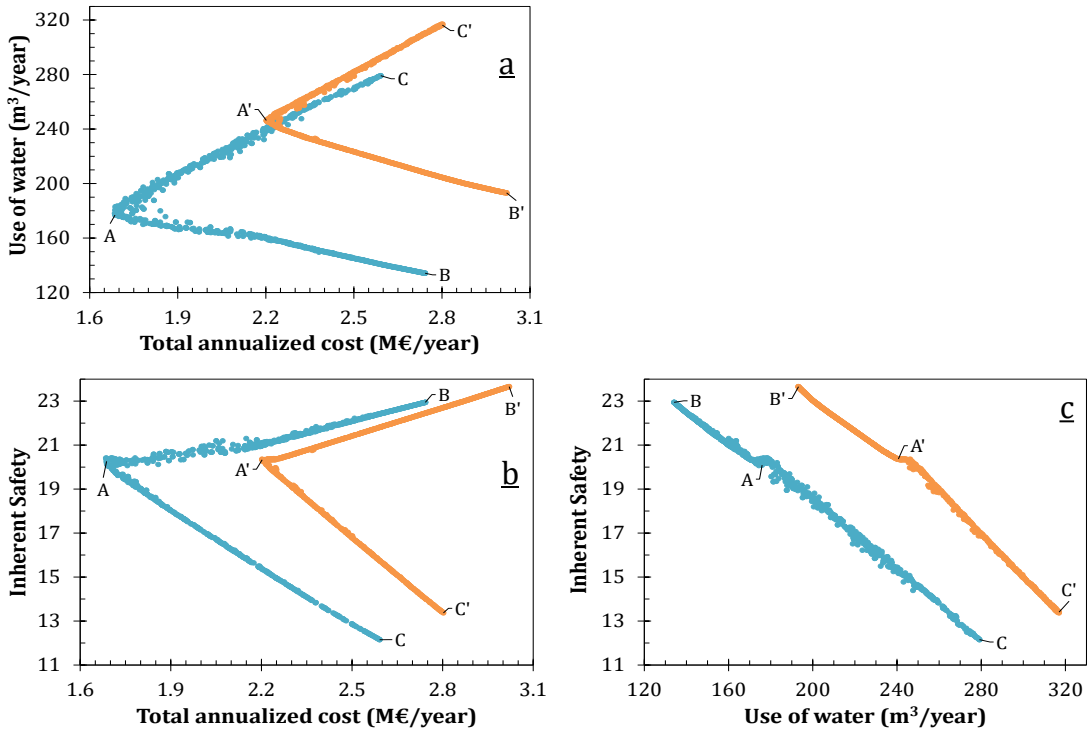

Figure 4-11: 2-dimension projection of the Pareto solutions for minimizing the total annualized cost, the water consumption and the inherent safety. Photovoltaic surface (●) 7500 m², (●) 10000 m². (A – A') optimal cost, (B – B') optimal water consumption, (C – C') optimal inherent safety.

Figure 4-13 illustrate the changes in the design and operating conditions across the Pareto solutions. Going from economic (A – A') to social optimum (C – C'), it is noted that the capacity of the battery increases (Figure 4-13a), whereas the size of the pressurized tank gets smaller (Figure 4-13b). This happens because for improving the safety of the process, the system seeks to reduce the inventory of material (hydrogen) as much as possible, and consequently the battery becomes more used for storing the surplus electricity. Likewise, as moving towards the safest energy system configuration, the reforming reactor gets unused, and hence its installed capacity decreases (Figure 4-13c). At the same time, the electrolyzer is gradually more used for supplying the demand of hydrogen, and consequently, the requirement of importing electricity from the grid increases, as depicted in Figure 4-13d.

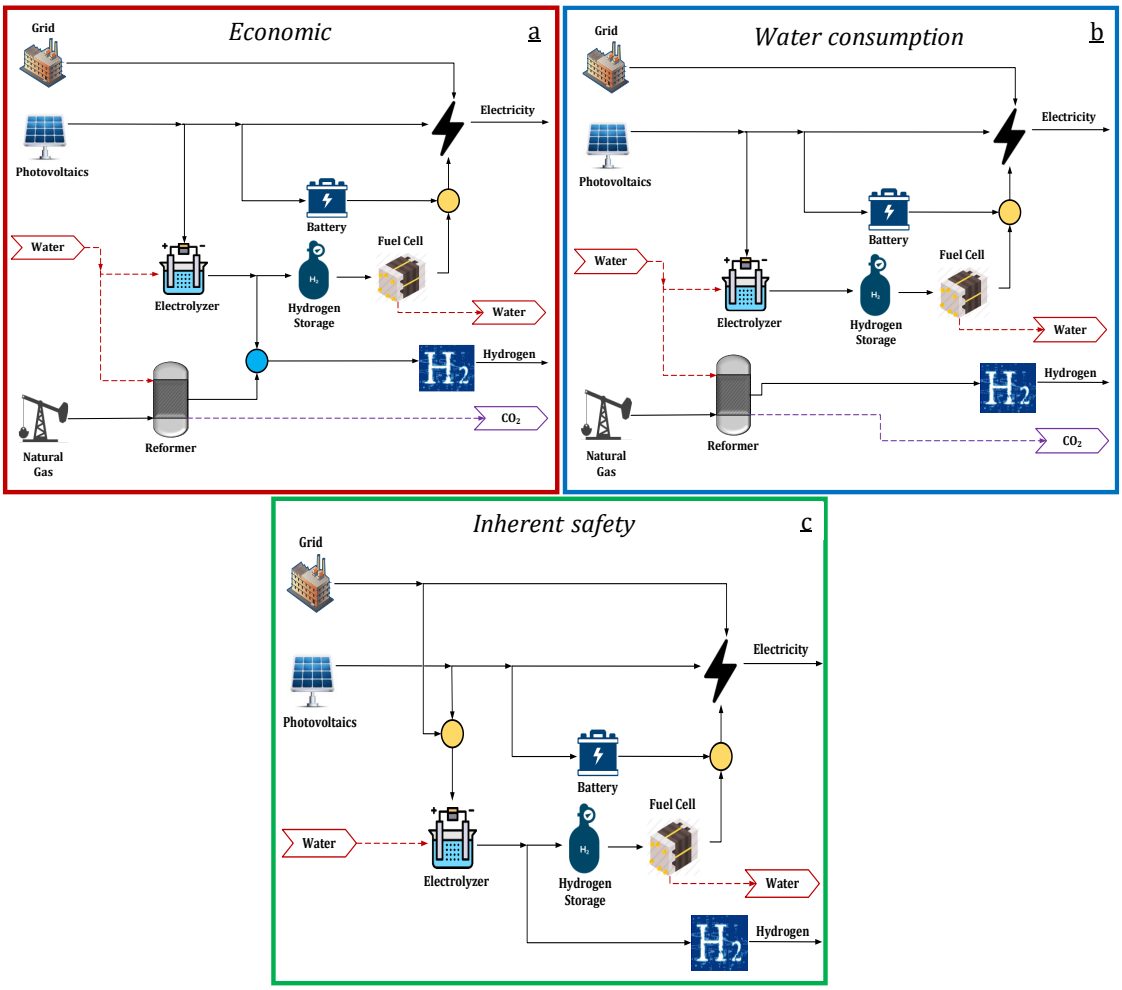

Figure 4-12: Energy system configurations for the extreme points of the Pareto solutions. Objective function (a) total annualized cost, (b) water consumption, and (c) inherent safety.

Interestingly, as shown in Figures 4-11b and 4-11c, the greatest change on the safety index occurs between the economic and social points, i.e. lines AC and A'C' of those figures. Indeed, noted that there is a change in the slope of the curves in Figure 4-11c after the points A and A'. This fact can be explained from the results depicted in Figures 4-13b and 4-13c. As observed, whereas the capacity of the pressurized tank decreases across the lines BA and B'A', the size of the reformer remains constant. This implies that in that zone, only the size of the pressurized tank affects the safety index, which translate into the smaller effect presented in 4-11b and 4-11c. Conversely, in the region represented by lines AC and A'C', the capacity of both the pressurized tank and the reformer reactor decreases, which leads to a bigger impact on the safety of the system.

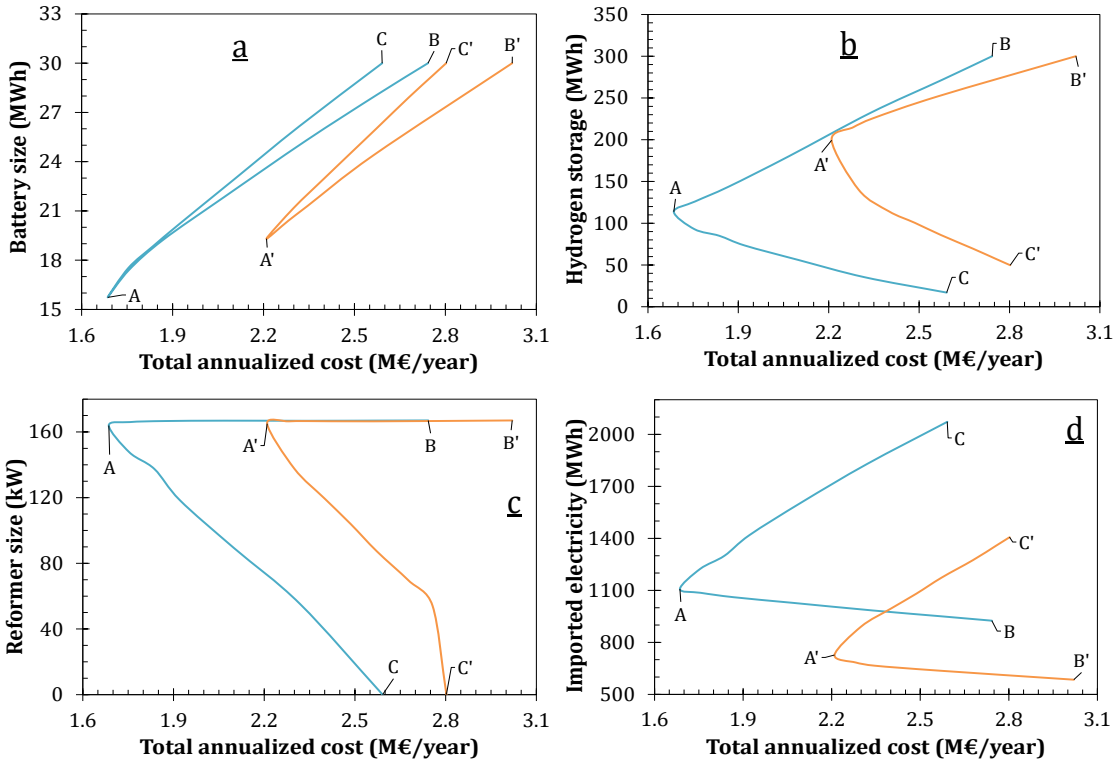

Figure 4-13: Change of design and operating conditions across the Pareto solutions. Photovoltaic surface (—) 7500 m² and (—) 10000 m². (a) battery, (b) pressurized tank, (c) imported natural gas, and (d) imported electricity. (A – A') optimal cost, (B – B') optimal water consumption, (C – C') optimal inherent safety.

4.2.4 Problem 4: Safety – cost/CO_2 emissions

This case comprises two multi-objective optimization problems: (i) the inherent safety against the total annualized cost, and (ii) the inherent safety against the CO_2 emissions. As before, these problems were solved by using a variety of sizes of population for the genetic algorithm. The values considered were 1000, 2000 and 3000 individuals. Results of these optimizations are presented in Figures C-5 and C-6 of the Annex C. According to those results, a population of 2000 individuals was selected for analyzing the multi-objective optimization problems. Figure 4-14 depicts the obtained Pareto front for both optimization cases and the two surfaces of PV evaluated.

Results show the antagonistic behavior of inherent safety index with respect to both the total annualized cost and the CO_2 emissions. Therefore, as the hazardous aspect of the energy system decreases, the cost of the plant (Figure 4-14a) and the emissions (Figure 4-14b) become higher. Figure 4-14 also shows the influence of the PV surface on the Pareto fronts. In this respect, note that the inherent safety improves as the area of PV decreases.

This happens because a smaller PV surface enables to reduce the size of the energy conversion and storage units, which favors the safety of the system.

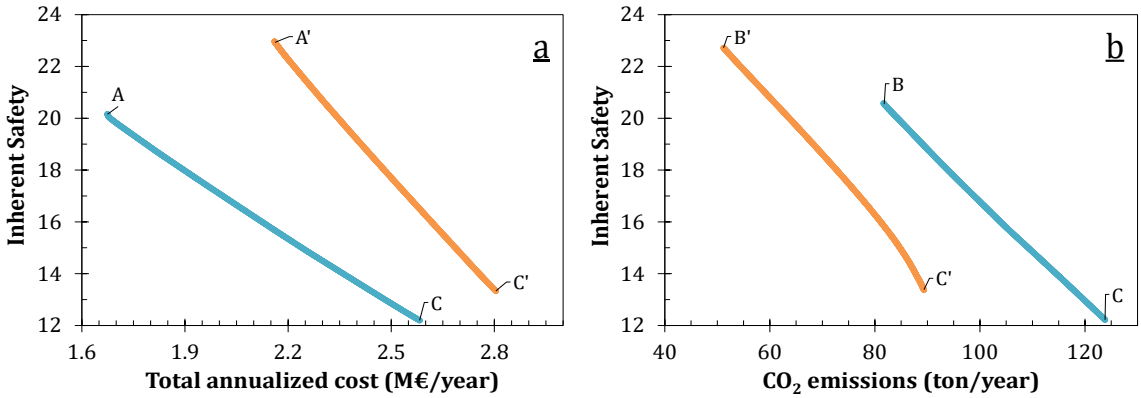

Figure 4-14: Pareto fronts for optimizing the total annualized cost, the CO_2 emissions and the inherent safety. (a) safety - cost, (b) safety – CO_2 emissions. Photovoltaic surface (●) 7500 m², (●) 10000 m². (A – A') optimal cost, (B – B') optimal emission, and (C – C') optimal inherent safety.

Figure 4-15 shows the flowsheet of the energy system when each objective function is independently evaluated. As observed, the topology of the system mainly differs in the energy sources employed for supplying the demand of hydrogen. Thus, the economic objective focuses on producing hydrogen from two process options: (i) the steam methane reforming (using the gas network), and the water electrolysis powered by PV (Figure 4-15a). Meanwhile, the CO_2 emissions indicator suggests including the anaerobic digester for obtaining biogas and subsequently perform the reforming process (Figure 4-15b). Besides, in this case, the electrolyzer is powered by both the electricity grid and the PV. Unlike, the inherent safety index does not include the reforming process within the energy system (Figure 4-15c).

Aiming to elucidate the relation of the optimization objectives in terms of design and/ or operating conditions, Figure 4-16 presents the evolution of such conditions across the Pareto fronts. As mentioned in the optimization problem P3, the relation between the cost and safety indicators can be explained through two process aspects: the size of the units for energy storage, and the sources of hydrogen. In this regard, as noted in Figure 4-16a, the economic objective attempts to reduce the capacity of the battery because of its high investment cost. In contrast, the safety indicator focuses on reducing the amount of hydrogen stored (Figure 4-16c), and the size of the reformer because of its intense operating conditions (Figure 4-16e). Therefore, moving from the safest to the economical

energy system requires to increase the capacity of the pressurized tank, to install and expand the capacity of the reforming reactor, and to decrease the size of the battery.

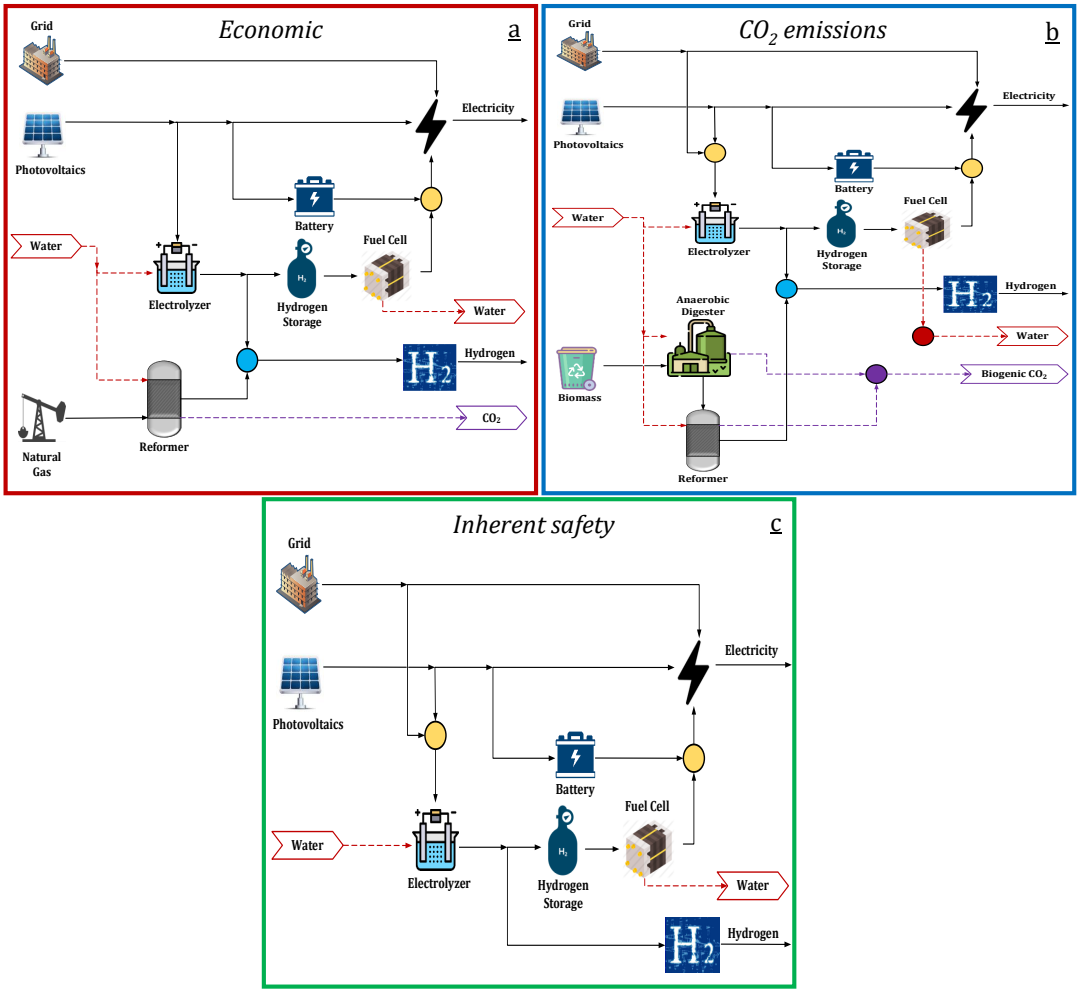

Figure 4-15: Energy system configurations for the extreme points of the Pareto solutions. Objective function (a) total annualized cost, (b) CO_2 emissions, and (c) inherent safety.

Right column in the Figure 4-16 shows the changes of the energy system when the CO_2 emissions and the safety indicators are addressed. Again, the safety index seeks to reduce capacity of the pressurized tank, whereas the environmental indicator requires a large storage capacity for exploiting the energy production from renewables (Figure 4-16b). Moreover, as the safety of the system increases, the electrolyzer becomes the preferred alternative for obtaining hydrogen. Accordingly, the amount of electricity imported from the grid gets higher, as depicted in Figure 4-16d. Thus, as the CO_2 emissions grow, the anaerobic digester and reformer reactor get unused, and hence the use of biomass decreases (Figure 4-16f).

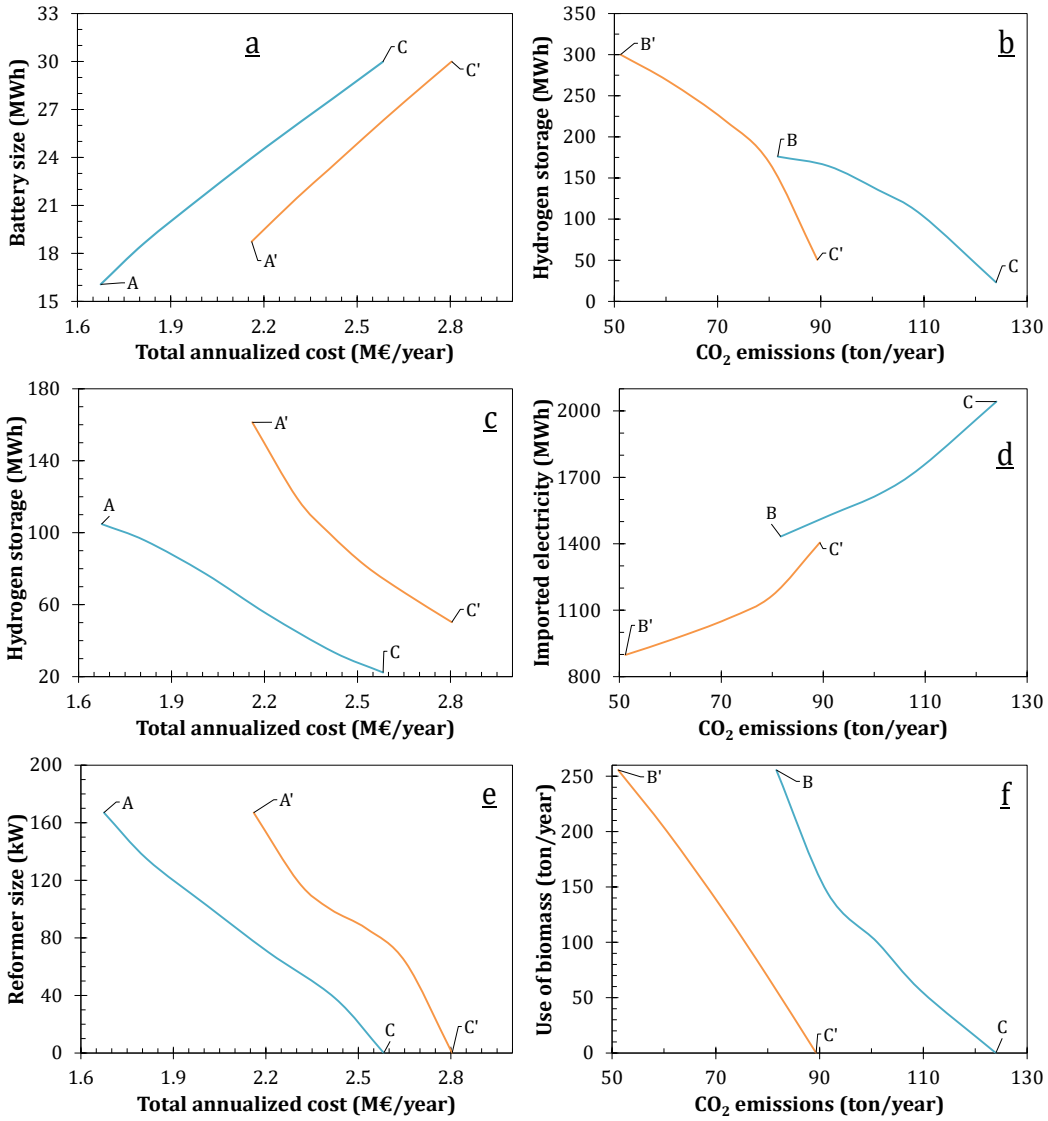

Figure 4-16: Change of design and operating conditions across the Pareto fronts. Photovoltaic surface (—) 7500 m² and (—) 10000 m². Left column (a,c,e) cost vs inherent safety, right column (b,d,f) CO_2 emissions vs inherent safety. (A – A') optimal cost, (B – B') optimal emission, and (C – C') optimal inherent safety.

4.3 Summary

Throughout the previous section, different multi-objective optimization problems were addressed for the energy system design considering the sustainability dimensions. Besides, the obtained Pareto sets were explored for studying the compromises among the criteria, and the evolution of the process variables across the non-dominated solutions. Accordingly, aiming to summarize those findings, this section is dedicated to state the main trends and to identify some general insights for the conceptual design of distributed energy systems.

Thus, Figure 4-17 presents the impact of the analyzed process variables on the sustainability indicators. It is worth to bear in mind that the performance of the indicators improves as their corresponding value decreases. In such a way, ascending and descending arrows represent negative and positive impacts, respectively. For instance, a larger surface of PV enables to reduce the CO_2 emissions and the grid dependence as a higher amount of renewable-based electricity is available. However, this also leads to a more expensive and potentially more hazardous energy system since bigger units for energy conversion and storage are needed. Besides, the performance of the water consumption indicator gets worse because of the amount of water required for converting the surplus electricity into hydrogen also increases.

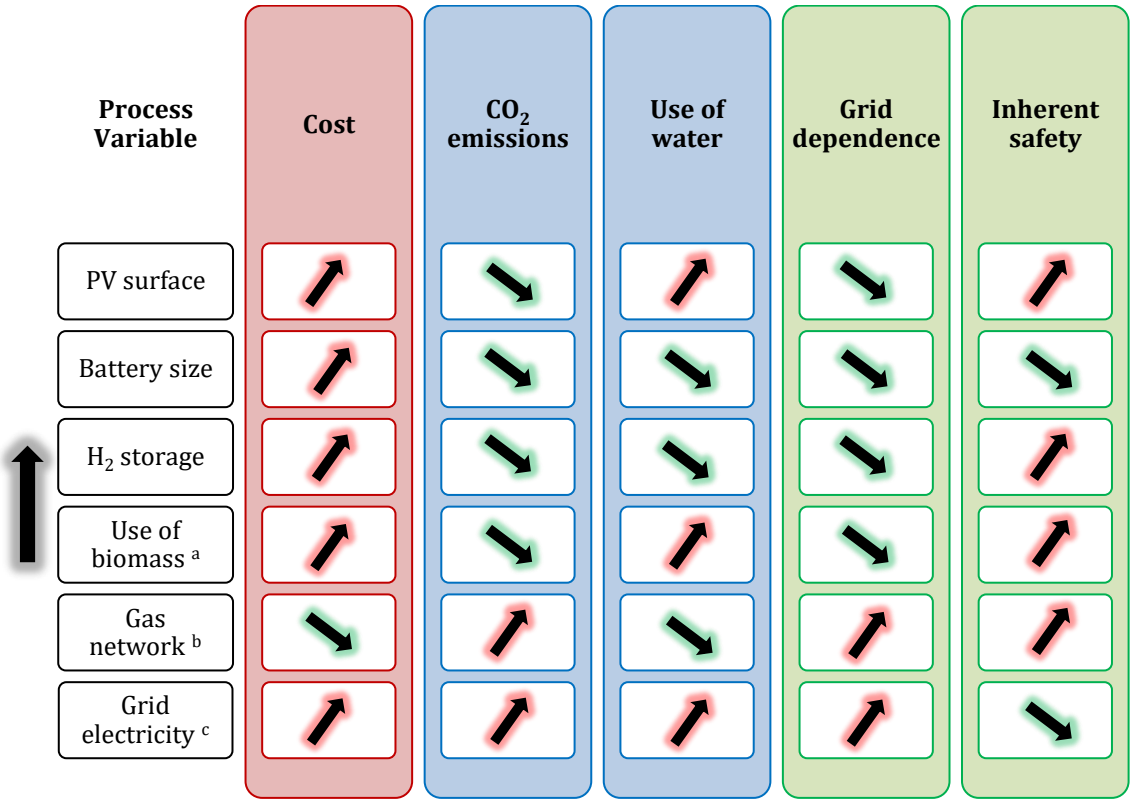

Figure 4-17: Impact of increasing the process variables on the sustainability indicators. (a) the use of biomass entails anaerobic digestion and reforming processes, (b) the gas network is used for steam methane reforming process, (c) grid is used for electrolysis of water.

Regarding the alternatives for electricity storage, it is noted that both options enhance the indicators of the environmental dimension and promote the independence of the system for the energy supply. On the one hand, using energy storage technologies favors the exploitation of renewable-based electricity, since they enable to deal with the mismatch between electricity production and consumption. Thereby, CO_2 emissions and grid dependence indicators are improved because a lower amount of energy must be imported

from the grid. On the other hand, the electrical battery does not require to use water for its operation, and the power-to-power system enables to recover the water from the fuel cell to be reused in the electrolyzer. Consequently, they have a positive impact on the water consumption indicator. Additionally, the obtained results also indicate that the economic aspect is improved by reducing the size of the storage units, which evidences the competition among the sustainability indicators. Moreover, concerning the inherent safety of the system, results suggest reducing capacity of the pressurized tank as it represents the accumulation of a potentially hazardous material.

Otherwise, as observed in Figure 4-17, the impact of the technologies for obtaining hydrogen was also assessed. These alternatives include the use of biomass through the anaerobic digestion and the subsequent reforming process, the steam methane reforming of natural gas from the network, and the electrolysis of water by using electricity from the grid. In this regard, it is worth to note that no technology offers a solution able to simultaneously get the best performance of all the sustainability criteria. For instance, using biomass enables to reduce the CO_2 emissions and the dependence of the main grid, but at the cost of a higher investment, a more elevated water consumption, and riskier process conditions. Meanwhile, the gas network represents a better alternative from the economic point of view as the anaerobic digestion step is not required, and because of the low price of the natural gas. However, this pathway also leads to produce fossil-derived CO_2 emissions, it corresponds to an option highly reliant on the main grid, and it entails the risk associated to the intense process conditions of the reforming reaction. In this respect, it is noted that the safety of the process can be improved by increasing the use of electricity from the grid for producing hydrogen. Nonetheless, in such a way, the performance of the other indicators becomes worse.

4.4 Conclusions

In this chapter the multi-objective optimization was performed for the design and operation of energy systems considering the sustainability dimensions. Altogether, four multi-objective optimization problems were formulated and solved for different combinations of the sustainability indicators. The obtained results elucidate the relationships among the different objective functions and provide a wide spread of optimal system structures and operating conditions. In general, results indicate that the total annualized cost, water consumption, and safety indicators improve as the PV surface decreases. In contrast, larger areas of PV favor the energy autonomy and the CO_2 emissions

reduction. Moreover, for a given PV surface, the obtained Pareto fronts reflects the compromise and the competitive behavior among the sustainability criteria. For instance, as the total annualized cost decreases, the CO_2 emissions and the grid dependence get worse. Besides, the minimum water consumption leads to the poorest yield in the cost and self-sufficiency indicators. Meanwhile, the lowest grid dependence requires the greatest water consumption. Additionally, it was identified that as the hazardous of the energy system decreases, the cost and emissions of the energy system become higher.

Furthermore, the set of Pareto solutions was explored and analyzed for identifying the changes in the design and operating conditions across the optimization results. Overall, these results constitute a valuable information for the subsequent decision-making process, since they depict the trade-off among the sustainability dimensions, and the impact of any decision in terms of the design and operation of the energy system.

5. Optimal Design of Energy Systems in Isolated Zones Using Sustainability Indicators. A Case Study in the Colombian Amazon

In the previous chapters, an optimization-based approach was formulated for the design of distributed energy systems considering the sustainability dimensions. Additionally, the application of the proposed framework was illustrated through a case study located in a neighborhood in France. Taking this into account, this chapter will be focused on two main objectives: (i) to display the flexibility of such an approach, and (ii) to analyze the potential impacts of the implementation of a DES in a completely different context. In this regard, this part of the thesis is dedicated to the design of a DES in the Colombian Amazon region. To do that, initially, a brief context about the energy sector of Colombia is introduced. Thereafter, the case study is presented including the base-case flowsheet, the parameters, and the constraints of the energy system. Subsequently, the optimization problem is formulated according to the specific context conditions. This is followed by the section of results, that comprises both, the mono-objective and multi-objective optimization analysis. Finally, the main conclusions are exposed.

5.1 Colombian Context

Currently, the Colombian energy matrix is strongly dominated by fossil resources since these represent about 92% of the total energy production of the country [210,211]. From this primary exploitation, Colombia exports almost 70% of its energy production in form of coal and oil. The remainder energy (30%) represents the internal consumption [210]. In this respect, around three quarters of the total energy demand of the country are covered by fossil resources, namely oil (37.5%), natural gas (25%) and coal (10.5%). Meanwhile, the share of renewables (27%) is mainly represented by hydropower systems (14%), and bioenergy resources (e.g. biofuels and waste 13%) [212]. Moreover, it is worth to note that the use of coal and oil is concentrated on the supply of fuel and thermal power for the transport and industry sectors, respectively. In contrast, the renewable resources are

focused on the electricity generation. In fact, around 80% of the electricity was produced from renewables in 2017 (mainly hydropower) [210–212].

Broadly, the Colombian electrical infrastructure is divided into the national interconnected grid (NIG), and the non-interconnected zones (NIZ). The former jointly includes companies dedicated to the energy production, transmission, distribution, and commercialization. Hence, this integration enables to provide the electrical service in a reliable way (24h). Conversely, the non-interconnected zones are characterized by local generation plants, intermittent service (6-24h), and high production costs [210]. Figure 5.1 depicts the distribution of the electrical infrastructure across the country. Note that the NIG is concentrated in the central and north region, whereas the non-interconnected zones correspond to the San Andres and Providencia islands, the pacific coast, and the south of the country. Indeed, according to recent reports, the NIZ represent around 52% of the Colombian territory [213].

Figure 5-1: Electrical framework of Colombia. (■) national interconnected system, (■) non-interconnected zones [213].

Nowadays, the electricity provision in NIZ relies on diesel-based generator units, which leads to power systems with high cost (due to the transport of the fuel), low efficiency, and elevated greenhouse gas emissions. In fact, the levelized cost of energy in NIZ can be two or three times higher than the cost in grid connected zones [210]. Consequently, at non-interconnected zones, the electricity tariffs require significant subsidies for allowing the

access of the service to the communities. Aiming to address this issue, the mining and energy planning unit (in spanish UPME) has identified that the implementation of small-scale and renewable-based energy systems could be a reliable and affordable alternative for providing electricity to NIZ [210].

Nevertheless, despite the potential benefits of distributed generation and the renewable resources for supplying energy to the non-interconnected zones, there are some barriers that need to be overcame for the successful deployment of this kind of energy systems. First, the heterogeneity of the zones makes difficult to propose a standard solution for covering the whole territory. Secondly, the experience and information from already executed projects is not properly documented, so that there are no base of knowledge and established models and/or methodologies for the implementation of this kind of systems in the Colombian context. Third, there is a lack of ownership about the technological solutions by the communities. Consequently, further than providing an energetic solution, it is necessary to implement an integrated strategy that supports the improvement of the quality of life of local communities and promotes their participation in the energy projects [210].

Considering the foregoing, the modeling and optimization approach developed in this work could be used as a tool for the preliminary evaluation of decentralized energy systems in the Colombian context. In this respect, the proposed framework has four main features that could be exploited: (i) it enables to assess multiple energy forms, (ii) it includes a variety of criteria for evaluating the performance of the system, (iii) it provides insights for the decision-makers about the trade-offs among the sustainability indicators, and (iv) it could be used as a source of information for promoting the participation of the communities from the early stages of the project.

Accordingly, the next sections of this chapter are dedicated to the early design of a distributed energy system at one isolated zone of Colombia by means of the modeling (Chapter 2 – sections 2.2 and 2.3) and optimization (Chapter 3 – section 3.2) approaches proposed in this work.

5.2 Case Study Definition

The case study was developed considering the conditions of Leticia. This city is the capital of the Amazon department, it is located at the south of the country, and it has a double frontier with Brazil and Peru. The population of Leticia is around 41600 inhabitants, of

which about 37% live in rural zones [213]. Broadly, the Amazon department is characterized for being the home of a great number of indigenous communities. In fact, at Leticia, they represent roughly 43% of total population [214]. As observed in Figure 5-1, Leticia makes part of the non-interconnected zones, so that the electricity supply of the city relies on local diesel generators. Additionally, the population depend upon traditional biomass and liquefied petroleum gas (LPG) for cooking, since they do not have access to the natural gas service which is the main energy source for cooking in Colombia.

Taking this into account, the case study considers a sample of 10% of the population of the city, i.e. around 4160 inhabitants. The evaluated energy sources are solar and biomass (domestic waste), whereas the energy demands are electricity and methane. Wind energy is not assessed because of there is no potential at that zone of the country. Indeed, the south region has the lowest potential across country, with an average wind speed around 1.5-2 m/s [215]. Accordingly, the corresponding base-case flowsheet of the energy system is depicted in Figure 5-2. Note that it does not include connection neither to the electricity grid nor to the gas network, since it is an isolated energy system.

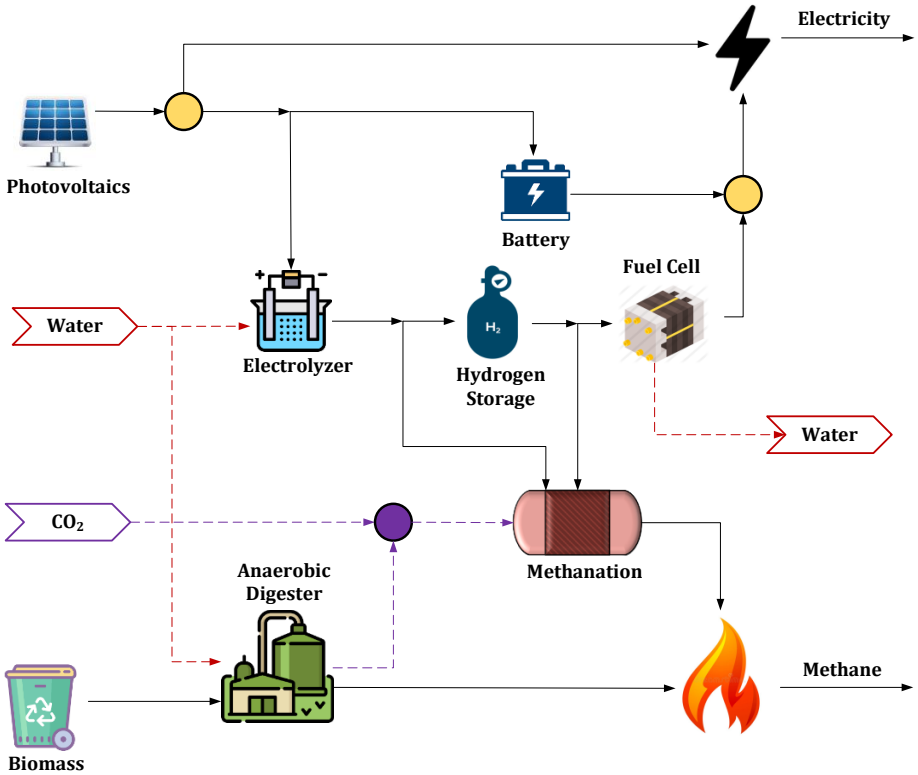

Figure 5-2: Base-case flowsheet of the energy system for the case study in the Colombian Amazon.

Weather data, namely solar irradiance (Figure 5-3a) and ambient temperature (Figure 5-3b) were gathered from Renewables.ninja database [216,217]. Meanwhile, the time-dependent profile of electricity demand (Figure 5-3c) was obtained for 2019 from the data reported by the national monitoring center (in spanish CNM) and the institute for planning and promotion of energy solutions for non-interconnected zones (in spanish IPSE) [213]. The data depicted in Figure 5-3c was obtained assuming that each month has an average day and that all the days have the same behavior, i.e. twelve days were used for representing the whole year. The same approach was used for the demand of methane, which is presented in Figure 5-3d.

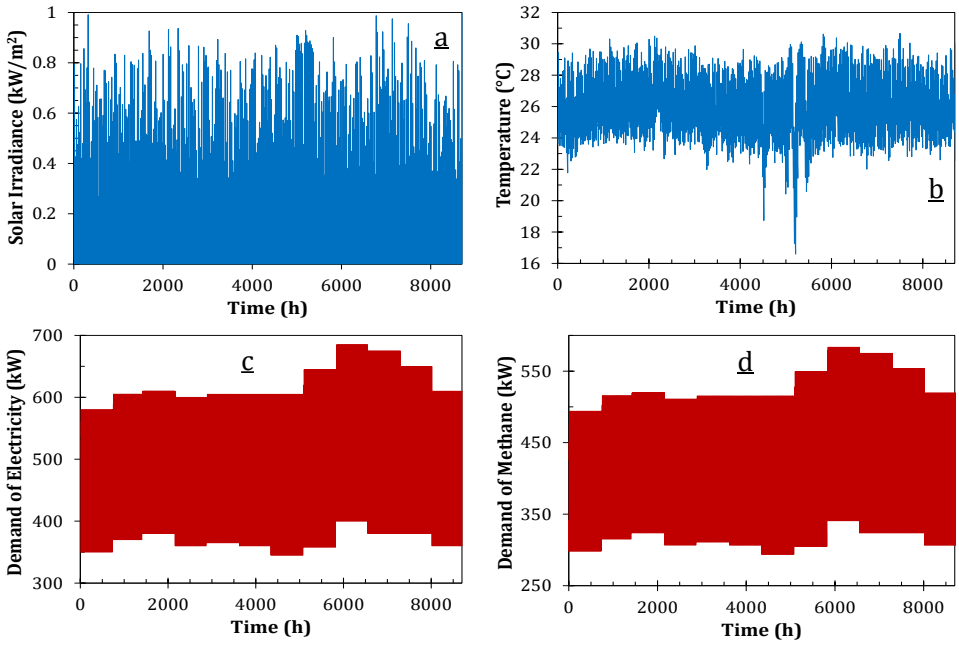

Figure 5-3: Profiles of input data for designing the energy system. (a) Solar radiation, (b) ambient temperature, (c) electricity demand, (d) methane demand.

5.2.1 Parameters

In this study, it was considered that the CO_2 for the methanation reaction can be obtained either from the air or the anaerobic digestion process. Currently, the cost of obtaining CO_2 from the atmosphere is quite uncertain, since literature reports prices ranging from 100 to 1000 USD/ton [218]. Accordingly, a pessimistic value of 460 €/ton (550 USD/ton) for the near term is selected in this work. This source was chosen because it is independent of the location, so that it does not rely on fossil-based plants or industries that release CO_2. Besides, the price of gathering the feedstock for anaerobic digestion process (C_{Bio}) is 0.054 €/kg. Moreover, according to World Bank data, the forest area in Colombia has changed

from 61800 to 58480 ha over this century [219], i.e. the deforestation factor (ω) for this case study is 5.4%. Apart from that, technical and cost parameters for the set of evaluated technologies are presented in Tables 5-1 to 5-3. These include the energy conversion efficiency, lifetime, capital, operation, and maintenance costs, in addition to the operating conditions of each technology.

Table 5-1: Energy conversion efficiencies of the technologies considered in the distributed energy system.

Technology	Value in literature (%)	Selected value (%)	Reference
Photovoltaics	16 – 22	20	[188–190]
Electrolyzer [a]	56 – 69	65	[11,51,191]
Fuel cell [a]	37 – 58	55	[49]
Battery self-discharge (daily)	0.1 – 0.3	0.2	[192]
Battery charge/discharge	75 – 97	95	[69,192,193]
Methanation	77	77	[198]
Anaerobic digestion [b]	0.42 – 0.53	0.48	[126]
Upgrading	99	99	[125]

[a] Polymer electrolyte membrane technology

[b] Using domestic waste (m^3CH_4/kg volatile solid). ≈ 23% of volatile solid in the biomass.

Table 5-2: Cost parameters of energy conversion and storage technologies.

Technology	CAPEX	O&M (% CAPEX)	Lifetime (years)	Reference
Photovoltaics (€/m^2)	220	5	20	[194]
Electrolyzer [a] (€/kW)	1600	2	8	[11,49,195]
Fuel Cell [a] (€/kW)	2700	7	8	[196]
Battery [b] (€/kWh)	520	2	15	[192,193,197]
Pressurized tank (€/kWh)	7.2	5	20	[49]
Methanation (€/kW)	770	4	30	[198]
Anaerobic digestion [c] (€/kW)	1600	2.5	20	[194,199]

[a] Polymer electrolyte membrane technology

[b] Li-ion battery

[c] Includes the upgrading operation

Table 5-3: Operating conditions and heat of reaction of the energy conversion and storage technologies.

Technology	Temperature (°C)	Pressure (MPa)	Heat of Reaction (kJ/mol)	Reference
Electrolyzer	80	4	286	[11,51,160]
Fuel cell	80	4	-286	[11,51]
Pressurized tank	25	4	-	[11,51,160]
Methanation reactor	350	3	-165	[127]
Anaerobic digestion	40	0.1	-	[126]

To consider the impact on the cost of the system due to the characteristics of this case study (isolated zone in a developing country), location factors are included to adjust the capital costs of the plant. These cover contingency, site preparation and startup costs due to the specific location of the project [78,79]. The former is added to account for the uncertainties in the design due to the limited real-world experience with DES in this kind of locations. Accordingly, considering that the system involves non-conventional equipment for Leticia, and that there are no demonstration plants in Colombia, a contingency factor (f_C) of 60% is assumed. Besides, as suggested by Seider et al. [79], a site preparation factor (f_{SP}) of 20% is used because it is a new plant and there is no existing industrial complex in the selected location. Meanwhile, as the energy system employs equipment radically new and there are no skilled people for their installation and operation, a startup factor (f_S) of 30% is used, as recommended by Seider et al. [79]. It is worth to note that the contingency costs are associated to the purchase of the equipment, whereas the site preparation (SPC) and startup costs (SC) are linked to the total fixed capital investment (FCI). Consequently, the Equation 2.43 (Chapter 2) turns into the Equation 5.1.

$$CAPEX = FCI + SPC + SC = FCI(1 + f_{SP} + f_S) \tag{5.1}$$

$$FCI = \sum_{k}^{K} C_k Cap_k CRF_k \,(1 + f_C) \tag{5.2}$$

Moreover, site preparation and startup factors are also included to the cost of capturing CO_2 from the atmosphere. Thus, the adjusted cost corresponds to 690 €/ton. In addition to that, for considering the influence of the economic conditions of Latin America, a discount rate (r) of 12% is used for the assessment of the plant, as suggested in a recent work by Yáñez et al. [220].

5.2.2 Energy System Constraints

As previously discussed in the optimization approach (section 3.2.3), in addition to the energy system model, the maximum capacities of the storage units and the availability of biomass are the constraints of the optimization problem for the energy system design. On the one hand, the upper limits for the battery and hydrogen systems, $S_{B,max}$ and $S_{H2,max}$, were defined according to the electricity consumption profile. In this respect, from the data presented in Figure 5-3c, a daily electricity demand around 12.4 MWh was determined. Thus, considering a battery able to store the equivalent to five days of electricity needs, and a pressurized tank with the capacity of reserving the electricity required for one month,

the upper limits $S_{B,max}$ and $S_{H2,max}$ are 62 MWh and 372 MWh, respectively. On the other hand, the availability of biomass (Bio_D) was estimated considering that in Colombia each inhabitant generates about 277.4 kg/year of domestic waste [221]. From such waste, around 52% corresponds to food and green rubbish that can be used in the digestion process. In such a way, considering the whole city, the biomass available is 6000 ton/year.

5.3 Optimization Problem

According to the optimization approach proposed in section 3.2 of Chapter 3, for the general base-case flowsheet there are eight optimization variables by time step. However, by considering the base-case flowsheet of the case study in Leticia (Figure 5-2), the number of decision variables decreases to three by time step. Besides, the photovoltaic surface (A) was also considered as an optimization variable. Moreover, as the case study focuses on an isolated energy system, the grid dependence indicator is not required since the system must be designed to be fully self-sufficient. Therefore, the optimization problem stated in Equations 3.23-3.35 turned into that presented in Equations 5.3-5.14.

$$Minimize \qquad J_1(u,x,t) = TAC \tag{5.3}$$

$$J_2(u,x,t) = AGE \tag{5.4}$$

$$J_3(u,x,t) = WC \tag{5.5}$$

$$J_5(u,x,t) = IST \tag{5.6}$$

$$Subject\ to \qquad h = f(u(t),x(t),p,t) \quad ,system\ model \tag{5.7}$$

$$0 \leq S_B(t) \leq S_{B,max} \quad ,battery\ storage \tag{5.8}$$

$$S_B(t_0) = S_B(t_f) \quad ,periodicity \tag{5.9}$$

$$0 \leq S_{H2}(t) \leq S_{H2,max} \quad ,hydrogen\ storage \tag{5.10}$$

$$S_{H2}(t_0) = S_{H2}(t_f) \quad ,periodicity \tag{5.11}$$

$$\int_{t0}^{tf} AD_{in}\,dt \leq Bio_D \quad ,biomass\ available \tag{5.12}$$

$$0 \leq u(t) \leq 1 \ ; \ u \ni \{\varphi_1, \delta_1, \sigma_1\}\ and\ A \quad ,decision\ variables \tag{5.13}$$

$$\sum_{i}^{I} S_i(t) = 1 \quad S \ni \{\varphi, \delta, \sigma\} \quad ,consistency \tag{5.14}$$

In these expressions, the performance criteria are the total annualized cost, CO_2 emissions, water consumption and inherent safety. Meanwhile, there are two types of optimization variables. Firstly, the time-dependent ones, which are related to the source of electricity FC_{out} (φ_1), the distribution of surplus electricity production Re_{H2} (δ_1), and the source of methane AD_D (σ_1). Secondly, the photovoltaic surface (A), which does not depend on time.

5.4 Results

This section presents the results of solving the optimization problem formulated in Equations 5.3-5.14 for the case study described in Section 5.2. Initially, the optimization of each criterion individually was addressed. Hence, four optimization problems were solved for minimizing the total annualized cost, the CO_2 emissions, the water consumption, and the inherent safety index. Subsequently, the compromise among the objective functions was investigated through three multi-objective optimization problems by considering different combinations of the sustainability indicators. Likewise to the case study located in Marseille-France, the optimization problem was solved considering a period of one year, and using a time step of 12 hours, i.e. $\Delta t = 12h$, $t_0 = 0h$ and $t_f = 8760h$.

5.4.1 Mono-objective Optimization

Figure 5-4 depicts the optimal configurations of the energy system for each one of the optimization problems. Broadly, obtained results elucidate the influence of the objective function on the optimal design of the energy system. Note that the difference of the system structures lies upon the technologies for electricity storage and for methane production. Interestingly, in all the optimization cases both technologies for energy storage are included. Nevertheless, the use of each one of them is quite different depending on the objective function. Thus, according to results of economic optimization (Figure 5-4a), the system attempts to keep the size of the battery as small as possible, as observed in the profiles presented in Figure 5-5a. This can be explained by comparing the investment costs of the pressurized tank (7.2 €/kWh) and the battery (520 €/kWh). Consequently, as the objective is to minimize the total cost of the energy system, it is crucial to reduce the capacity of the most expensive alternative. Otherwise, regarding to the demand of methane, the obtained results suggest that the anaerobic digestion process is preferred instead of methanation. This occurs because in addition to the methanation reactor itself, the methanation process also requires a source of hydrogen (electrolyzer), and it entails

the cost of capturing CO_2 from the atmosphere. Accordingly, such alternative implies a higher cost than the anaerobic digestion.

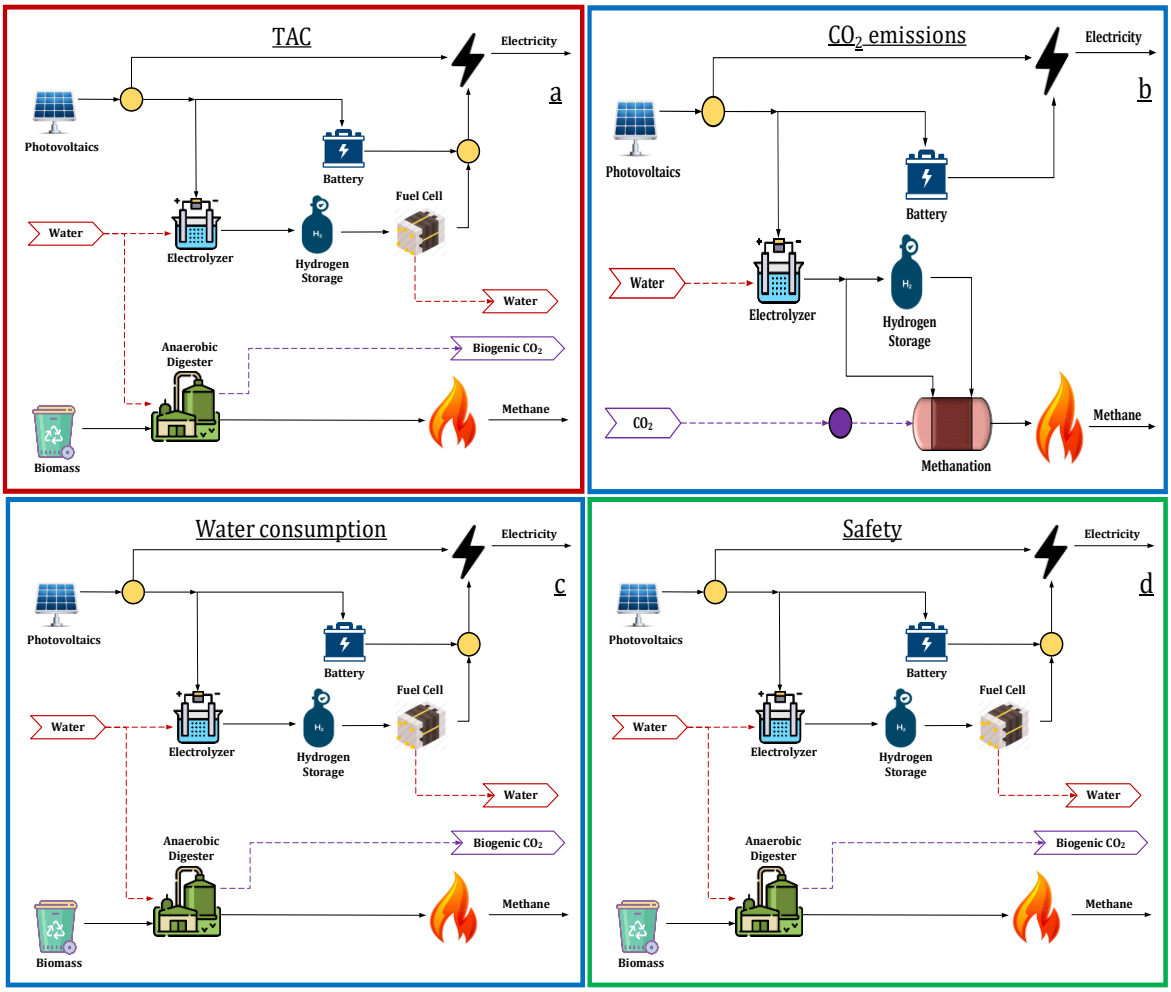

Figure 5-4: Optimal configuration of the distributed energy system for each one of the sustainability criteria.

In contrast, when the CO_2 emission indicator is addressed (Figure 5-4b), the battery is the alternative used for balancing the mismatch between the electricity availability and consumption. Meanwhile, the pressurized tank is fully employed for supplying hydrogen to the methanation reactor. This can be explained by analyzing the sources of methane in terms of CO_2 emissions. In this respect, as the objective is to minimize such indicator, the system privileges the methanation process since it represents an alternative for capturing CO_2 from the atmosphere. Indeed, this operation enables to produce methane with a negative balance of the CO_2 emissions. Therefore, aiming to increase the availability of electricity for water electrolysis and the subsequent methanation, the system employs the battery for the electricity storage because of its high round-trip efficiency.

Interestingly, the energy system flowsheet is the same when water consumption and safety indicators are minimized. This result can be explained through two main facts. On the one hand, regarding the surplus electricity storage, both optimization problems prioritize the utilization of the electrical battery because of it does not imply neither water consumption nor safety risks. Indeed, from a more in-depth analysis, it is noted that the hydrogen storage system is only used because of the battery reaches the maximum capacity imposed in the optimization problem (Figure 5-5a). Moreover, by comparing the profiles of the energy stored of these two optimization cases, it is displayed that the energy system structures are the same, but the sizing of equipment and the operating policies are different. In this respect, the optimization of the water consumption attempts to decrease the employment of the power-to-power system without considering the size of the pressurized tank. Conversely, the minimization of the inherent safety focuses on reducing the inventory of material within the system, which leads to install a pressurized tank as small as possible (green line in Figure 5-5b).

Otherwise, concerning the methane production, optimization results indicate that the anaerobic digester is the best alternative for obtaining methane from the water consumption and safety perspectives. In the former case, this happens because producing 1 MWh of methane by means of methanation process roughly requires 420 L of water (electrolysis). Meanwhile, biomass digestion process demands 264 L of water by 1 MWh of methane. In the latter case, i.e. regarding the safety indicator, the selection lies upon the operating conditions of the alternatives. Thus, as presented in Table 5-3, the methanation reactor operates at more intense conditions than the anaerobic digester. Consequently, aiming to avoid potentially hazardous conditions, the biomass digestion is preferred instead of methanation for supplying the demand of methane.

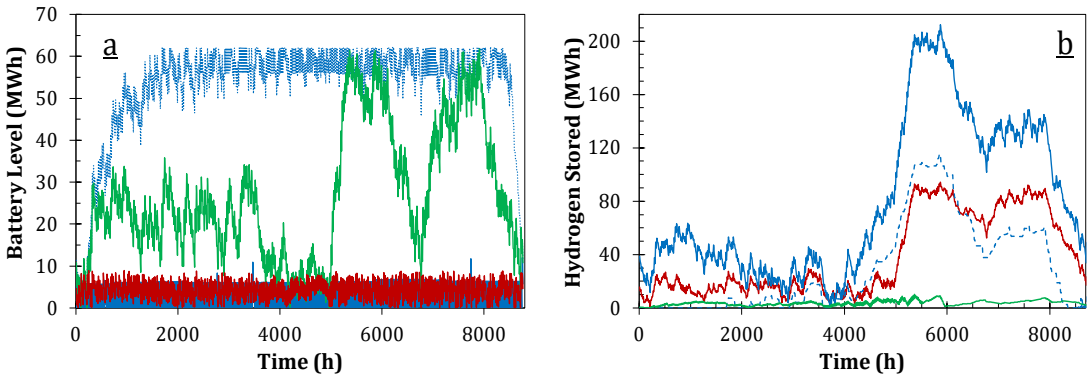

Figure 5-5: Optimal profiles of energy stored. (a) battery, (b) pressurized tank. Objective function (—) total annualized cost, (—) CO_2 emissions, (--) water consumption, and (—) inherent safety.

Optimization results are summarized in Table 5-4. In general, they show the performance of the different energy system configurations over the sustainability indicators. Also, these outcomes indicate the competition among the evaluated criteria. For instance, note that the minimal emission of CO_2 leads to an energy system with the highest consumption of water and the poorest yield in the safety index. Besides, it is worth to point out that the whole CO_2 emissions correspond to those derived from the biomass digestion (biogenic). Indeed, the optimal energy system structure for such indicator leads to a process with negative emissions since CO_2 is captured from the air for the methanation reaction.

Table 5-4: Optimization results for the design of the distributed energy system considering each objective function separately.

Variable	Objective Function			
	TAC	CO_2 emissions	Water consumption	Inherent Safety
LCOE (€/kWh)	0.48	0.94	1.68	1.51
TAC (M€/year)	4.2	8.3	14.7	13.2
CAPEX (% TAC)	93	91	97	97
OPEX (% TAC)	7	9	3	3
CO_2 emissions (ton/year)	23.4	-853.4	23.4	23.4
Biogenic (ton/year)	409.2	-	409.2	409.2
Water consumption (m^3/year)	1 123.4	1 728.6	1 080	1 084
Electrolysis (%)	5.2	100	1.4	1.8
Digestion (%)	94.8	-	98.6	98.2
Inherent Safety	13.8	21.4	15.2	11.9
Chemical Index	1.5	4.1	2.4	0.9
Process Index	12.3	17.3	12.8	11

Moreover, regarding economic indicators, the costs are strongly dominated by the capital expenditures, as these represent more than 90% of the total cost of the energy system. In this respect, Table 5-5 presents the optimal size and investment cost of the technologies installed within the energy system. In fact, such results elucidate that a poor yield in the economic indicator is associated to the installation of a large capacity of battery for electricity storage. For instance, when the water consumption and the inherent safety are optimized, the battery represents around 80% of the investment cost of the plant.

Otherwise, from results depicted in Table 5-5, it is observed the influence of the optimized criteria on the size of the PV. Thus, the problem for the CO_2 minimization leads to the energy system with the largest surface of PV, since in such a case the supply of the whole energy demands (electricity and methane) is based upon that technology (Figure 5-4b). Meanwhile, smaller areas of PV correspond to the energy systems with the largest installed capacities of the battery, as obtained for the water consumption and inherent safety minimization cases. Indeed, that size of the PV surface (≈ 9800 m^2) represents the minimal

required capacity for supplying the demand of electricity. This outcome is explained by the high round-trip efficiency of the electrical battery. Accordingly, the results of the economic optimization show that a larger PV surface is required, as the power-to-power system becomes more used that the battery for the electricity storage (Figure 5-5). This occurs due to the energy losses across the electrolyzer and fuel cell.

Table 5-5: Optimal size and investment cost of equipment within the energy system.

Equipment	TAC		CO_2 emissions		Water consumption		Inherent safety	
	Size	Cost (k€/year)	Size	Cost (k€/year)	Size	Cost (k€/year)	Size	Cost (k€/year)
Photovoltaics (m^2)	10 850	319.4	24 140	710.9	9 720	286.1	9 790	288.3
Electrolyzer (kW)	863	277.8	3 700	1 191	1 336	430.3	489	157.4
Battery (MWh)	9	684.1	12	916.9	62	4 734	61.8	4 715
Methanation (kW)	-	-	554	52.9	-	-	-	-
Tank H_2 (MWh)	95	91.0	213	285.8	115	111.2	10.2	9.8
Fuel Cell (kW)	266	144.3	-	-	516	280.3	125	67.5
Digester (kW)	554	118.6	-	-	554	118.6	554	118.6

Aiming to provide a more comprehensive analysis of these outcomes at the context of Leticia, it is worth to bearing in mind the characteristics of the evaluated case study. More precisely, regarding the economic and CO_2 emissions indicators. First, as aforementioned, Leticia currently depends upon diesel-based units for the electricity supply. In this respect, the mining and energy planning unit (in spanish UPME) estimates that the levelized cost of electricity at NIZ is around three times higher than that of grid connected zones. Hence, considering that for 2019 the grid price was 0.13 €/kWh [222], the cost for a location as Leticia could be about 0.39 €/kWh. Besides, according to Colombian reports, the cost of LGP (which is used for cooking) is roughly 0.018 €/kWh [223]. Consequently, as a reference case, it could be considered that the current LCOE at Leticia is 0.41 €/kWh. Secondly, based upon a typical efficiency for producing electricity through a diesel system (≈ 40 %), and the properties of the fuel [224], i.e. low heating value (42.4 MJ/kg) and emission factor (74.2 $kgCO_2/GJ$), the current CO_2 emissions can be computed. Accordingly, for supplying the electricity needs presented in Figure 5-3c, the corresponding CO_2 emissions are around 3150 $tonCO_2$/year.

Taking this into account, the obtained outcomes represent a preliminary scenario to envisage the potential impacts of replacing the current power plant by a renewable-based energy system. In this respect, according to the results of economic optimization, the LCOE could increase by 17% with respect to the current scenario. Nevertheless, this cost could be reduced through the economy of scale by implementing an energy system for the whole

city (currently 10% of the population was studied). Moreover, regarding the CO_2 emissions, all the obtained configurations enable to avoid the fossil-derived emissions from the diesel units. Indeed, as observed in Table 5-4, around 95% of CO_2 emissions would be biogenic, which are derived from the anaerobic digestion process.

5.4.2 Multi-objective Optimization

According to the results from the mono-objective optimization, it was evidenced the competitive behavior among the evaluated criteria. Thus, by individually evaluating the optimization problems, the yield of one indicator improves but the performance of the other gets worse. Consequently, aiming to address the design of the energy system considering the sustainability dimensions, three multi-objective optimization problems were proposed and solved. These optimization cases include different combinations of the sustainability indicators and enable to identify the compromises among them.

Table 5-6 presents the three multi-objective optimization cases and the associated indicators. Moreover, two different sizes of PV were assessed to evaluate the impact of this variable on the Pareto solutions. In this respect, as obtained from the mono-objective optimization, the minimum PV surface required to supply the electricity demand is around 9800 m^2. Hence, the analyzed areas of PV correspond to 25 and 50% of additional surface with respect to the minimum, i.e. 12250 and 14700 m^2. Nevertheless, the remainder of constraints and decision variables are the same to those presented in Equations 5.7 to 5.14. Again, as in the case study presented in Chapter 4, the multi-objective optimization problems were solved by using the NSGA-II through the *gamultiobj* function within MATLAB® software.

Table 5-6: Multi-objective optimization problems and corresponding indicators for the energy system design.

Problem	Indicators
P1	Cost - CO_2 emissions
P2	Cost - Safety
P3	Cost - CO_2 emissions - Water consumption

- *Problem 1: Cost – CO_2 emissions*

The obtained Pareto fronts are depicted in Figure 5-6. These results correspond to a population of 3000 individuals in the genetic algorithm. Additionally, populations of 1000

and 2000 individuals were assessed to evaluate the impact of this variable on the Pareto solutions. The corresponding outcomes are depicted in Figure C-7 of the Annex C.

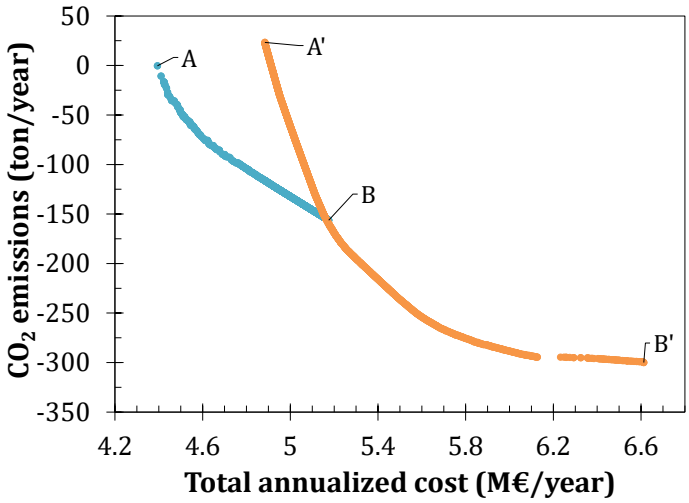

Figure 5-6: Pareto fronts for minimizing the total annualized cost and the CO_2 emissions. Photovoltaic surface (●) 12250 m², (●) 14700 m². (A – A') minimal cost, (B – B') minimal CO_2 emissions.

Broadly, the obtained outcomes indicate the contradictory behavior between the cost and emissions indicators (Figure 5-6). Thus, it is observed that whilst the CO_2 emissions are reduced, the cost of the energy system increases. Besides, results elucidate the influence of the PV surface on the Pareto fronts. In this regard, note that the performance of the economic indicator gets worse as the area of PV grows. This happens because a larger size of PV leads to a higher amount of surplus electricity, and consequently, bigger units are required for energy storage, which translates into more elevated costs. In contrast, a larger PV installation enables to enhance the CO_2 emissions indicator, since in such a case there is a higher amount of renewable-based electricity. Accordingly, low emission levels are achieved as more biomethane can be produced through methanation process, which implies to capture more CO_2 from the air.

Otherwise, Figure 5-7 depicts some of the changes in the design and operating conditions across the Pareto fronts. As already discussed in the mono-objective optimization results, the economic optimization privileges the use of hydrogen for electricity storage because of its lower costs with respect to the battery. Conversely, when the CO_2 emissions are minimized, the battery is employed for electricity storage and hydrogen is focused on producing biomethane by means of the methanation reactor. In such a way, going from the economic (points A and A') to the environmental (points B and B') optimum requires both, to increase the capacity of the battery (Figure 5-7a) and to reduce the size of the fuel cell

(Figure 5-7b). Moreover, as the yield of the emission indicator improves, the share of the methanation reactor for supplying the demand of methane also increases (Figure 5-7c) since that process push up the capture of CO_2 from the atmosphere.

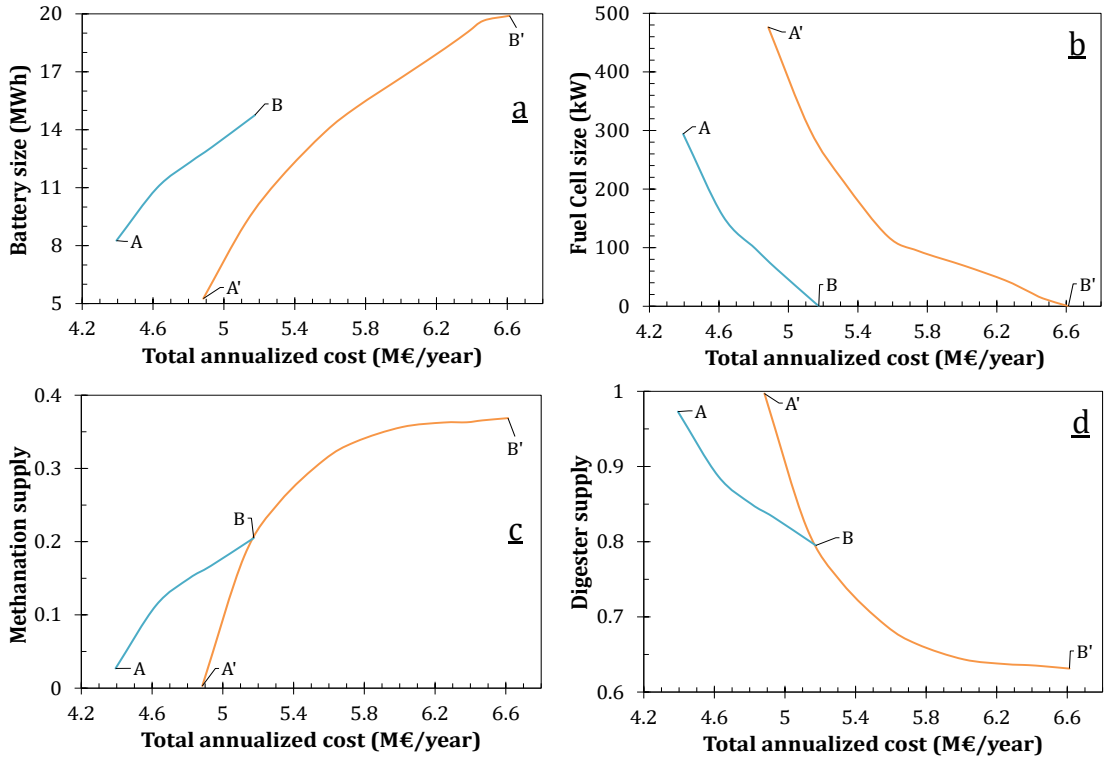

Figure 5-7: Change of design and operating conditions across the Pareto fronts. Photovoltaic surface (—) 12250 m² and (—) 14700 m². (a) battery size, (b) fuel cell size, fraction of methane supplied by (c) methanation and (d) digestion processes. (A – A') minimal cost, (B – B') minimal CO_2 emissions.

It is worth to note that the supply of methane through power-to-gas pathway is limited by the availability of hydrogen obtained from PV-based electricity. Thus, according to the scenarios evaluated, at least 65% of the methane must be obtained from the anaerobic digestion process (Figure 5-7d). Indeed, as obtained in the mono-objective optimization, a PV surface of around 24100 m² is required to produce the whole of methane by means of the power-to-gas route.

- *Problem 2: Cost – Inherent safety*

This multi-objective optimization problem simultaneously addresses the assessment of the total annualized cost and the inherent safety. As in the previous case, the optimization was performed considering different sizes of population for the genetic algorithm. The corresponding results are shown in Figure C-8 of the Annex C. Accordingly, the selected Pareto sets (population of 3000 individuals) for the two PV surfaces are presented in Figure 5-8.

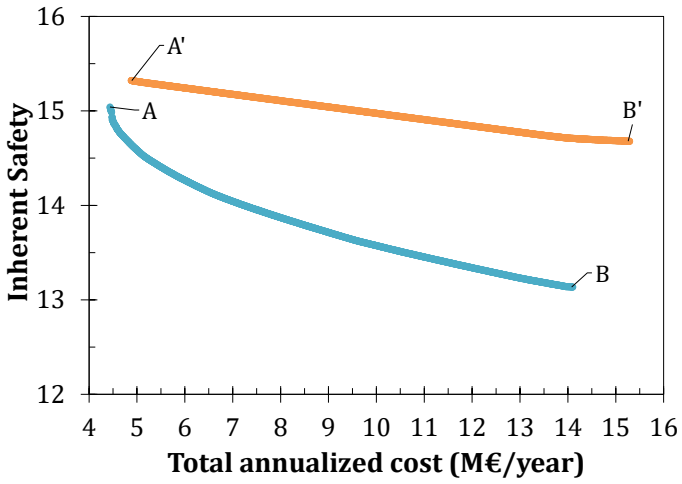

Figure 5-8: Pareto fronts for optimizing the total annualized cost and the inherent safety. Photovoltaic surface (●) 12250 m², (●) 14700 m². (A – A') optimal cost, (B – B') optimal safety.

Results display the competition between the two objectives. Thus, improving the safety of the system requires to elevate the cost of the plant. Besides, it is also noted that the yield of both indicators gets better as the area of PV becomes smaller. This occurs because by reducing the size of PV, the capacity of the energy conversion and storage units is also decreased. Therefore, a smaller area of PV enables to reduce the cost and the hazardous of the energy system.

Moreover, as observed in Figure 5-8, outcomes suggest that the most sensitive impact is on the economic indicator. Indeed, by moving from the economic to the social optimum, the total annualized cost increases near to three times. Conversely, the relative change of the inherent safety index across the Pareto fronts is lower than 15%. This behavior can be explained by analyzing the evolution of one design aspect throughout the set of non-dominated solutions: the capacity of the units for energy storage. In this respect, as presented in the mono-objective optimization results, the economic optimum prioritizes the use of the pressurized tank because of its lower cost, whereas the safety indicator privileges the battery as it does not represent neither chemical nor process risks. Accordingly, as depicted in Figure 5-9, going from the economic to the social optimum implies to increase the capacity of the battery and to reduce the size of the pressurized tank.

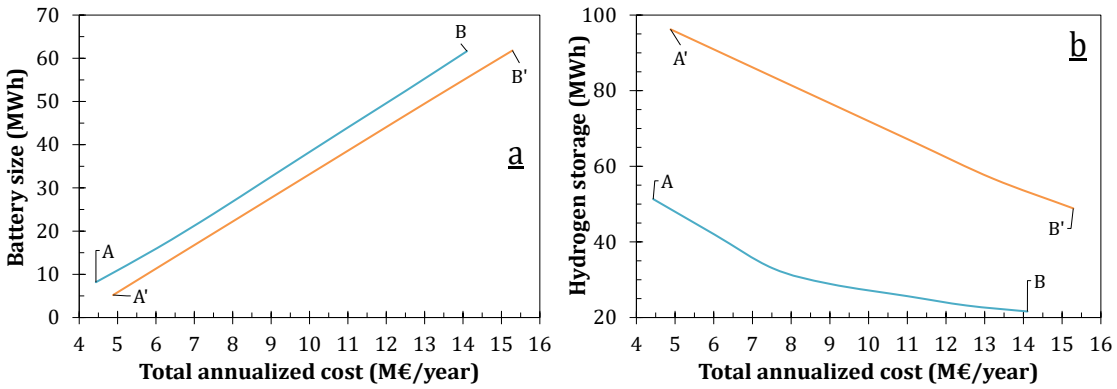

Figure 5-9: Change of design and operating conditions across the Pareto fronts. Photovoltaic surface (—) 12250 m² and (—) 14700 m². (a) battery size, (b) pressurized tank. (A – A') optimal cost, (B – B') optimal safety.

On the one hand, as observed in Figure 5-9a, the size of the battery grows almost six times across the Pareto sets. Besides, according to the results from the single-objective optimizations (Table 5-5), the battery is the most expensive equipment within the energy system. Consequently, by increasing the capacity of the battery, a significant impact on the TAC of the plant is expected, as shown in Figure 5-8. On the other hand, as noted in Figure 5-9b, the safety of the system improves as the size of the pressurized tank decreases. In fact, by moving from the economic to the social optimum, the size of such equipment drops 50%. Nevertheless, the remainder of the system structure remains the same, since the electrolyzer, fuel cell and anaerobic digester are common equipment for the cost and safety optimizations. This fact can be evidenced by comparing the Figure 5-4a and 5-4d. Therefore, as elucidated in Figure 5-8, there is not a significant variation in the value of the safety index throughout the Pareto Front.

- *Problem 3: Cost – CO_2 emissions - Water consumption*

This optimization problem comprises the simultaneous evaluation of three indicators: total annualized cost, CO_2 emissions, and water consumption. As before, the impact of the size of the population in the genetic algorithm was investigated by solving the multi-objective optimization problem for different values of that variable. The values analyzed were 1000, 2000 and 3000 individuals, and the corresponding results are presented in Figure C-9 of the Annex C. Accordingly, a population of 3000 individuals was selected, and the obtained Pareto solutions are depicted in Figures 5-10 and 5-11 for the two sizes of PV evaluated. As noted, those figures include a 3-dimension representation (Figures 5-10a and 5-11a), and the 2-dimension projections for the three assessed objectives.

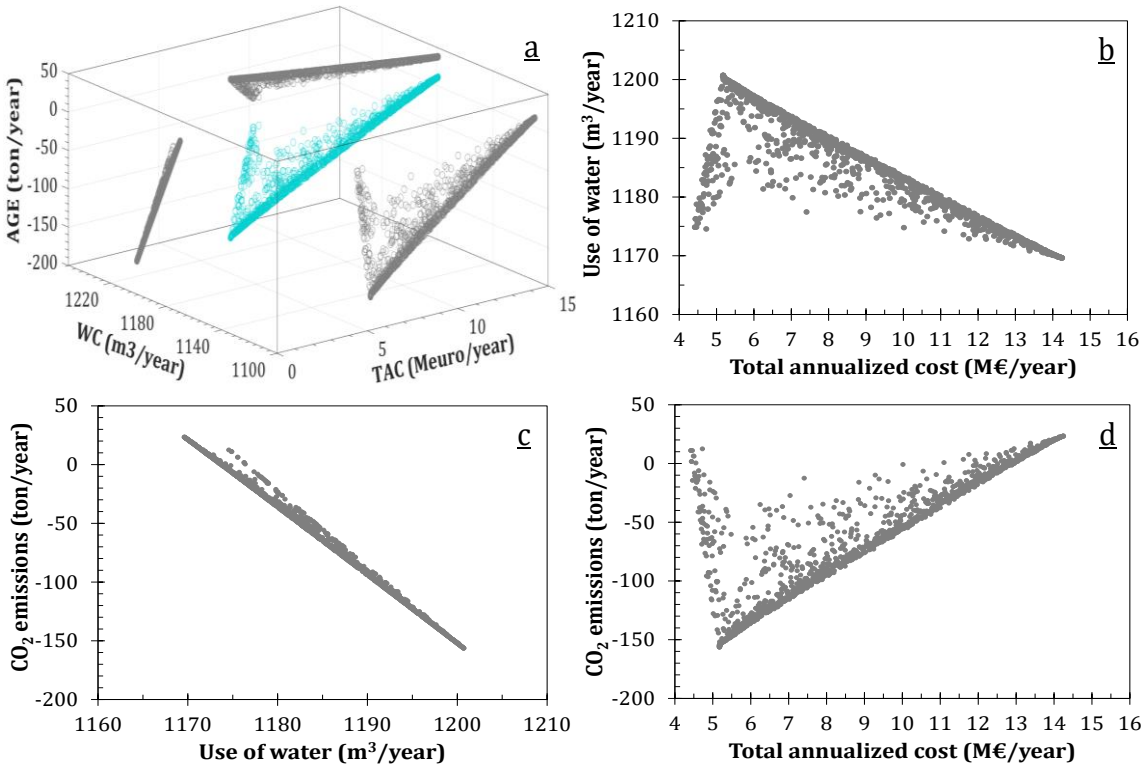

Figure 5-10: Pareto solutions for minimizing the total annualized cost, the CO_2 emissions and the water consumption considering a photovoltaic surface of 12250 m². (●) 3-dimension representation (●) 2-dimension projections.

Broadly, Pareto sets reflect the trade-offs and the contradictory behavior among the three objective functions. Interestingly, results indicate that for a given area of PV, there is a slight opportunity for modifying the performance on the water consumption indicator. This can be appreciated by analyzing the relative change of such indicator throughout the non-dominated solutions with respect to its optimal value from the mono-objective optimization. According to results presented in Table 5-4, the minimal water consumption is 1080 m³/year. Thus, considering the outcomes depicted in Figures 5-10 and 5-11, the relative change of this indicator across de Pareto sets is 3% and 6% for a PV surface of 12250 m² and 14700 m², respectively. In contrast, by doing the same analysis over the other two indicators, it is obtained that the TAC changes by up to 210%, and the CO_2 emissions can vary by up to 37% throughout the Pareto solutions.

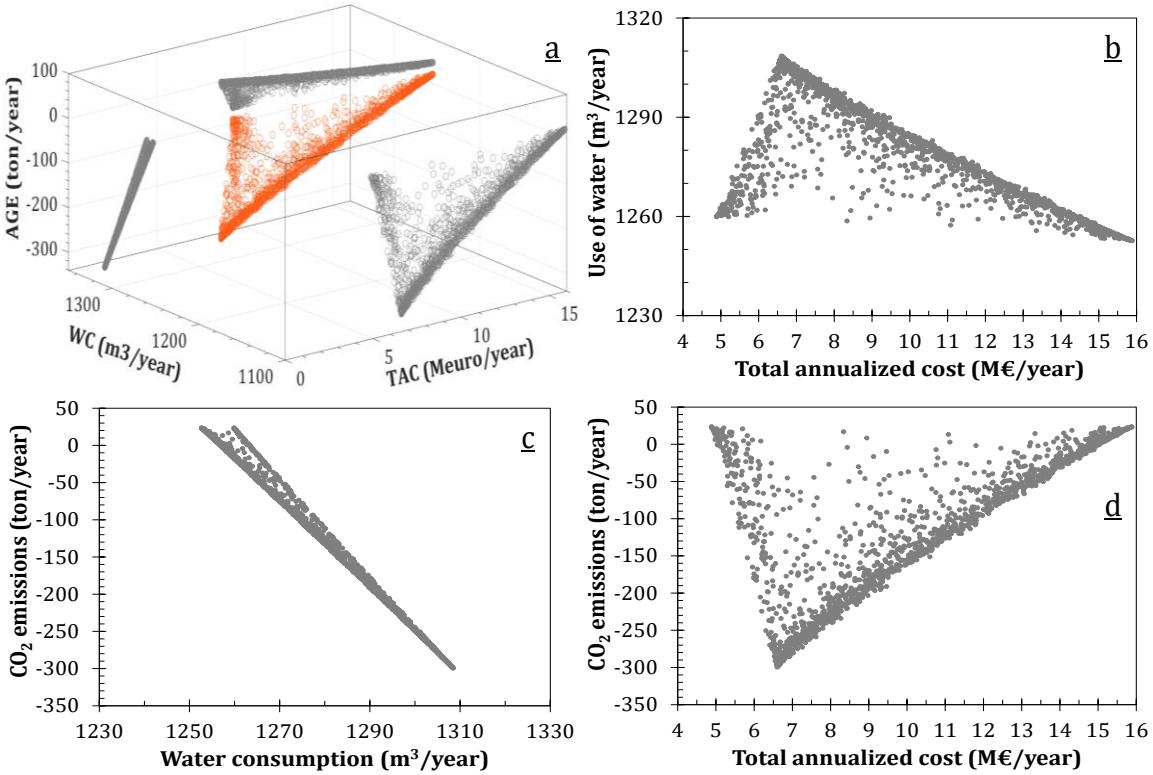

Figure 5-11: Pareto solutions for minimizing the total annualized cost, the CO_2 emissions and the water consumption considering a photovoltaic surface of 14700 m2. (●) 3-dimension representation (●) 2-dimension projections.

Otherwise, Figure 5-12 shows the two-dimension projections of the Pareto sets for the two areas of PV. According to optimization results, the total annualized cost and water consumption indicators improve as the PV surface decreases. Conversely, larger areas of PV enable to obtain a better performance in the CO_2 emissions objective. In this regard, as already discussed in the problem P1, a larger PV surface requires bigger equipment for energy conversion and storage, which leads to higher investment cost. Also, this circumstance entails a growing consumption of water since more electricity must be converted into hydrogen by means of water electrolysis. Meanwhile, as the area of PV becomes larger, there is also a higher amount of electricity available to be used in the methanation reactor, and consequently more CO_2 can be captured from the atmosphere.

Figure 5-13 presents changes in the design and operating conditions across the Pareto solutions. As observed in Figure 5-13a, the installed capacity of the battery consistently increases whilst moving from the points A – A' (economic optimum) to the points C – C' (water consumption optimum). This happens because for decreasing the CO_2 emissions and the use of water of the process, the system prioritizes the use of the battery for electricity storage. In the former case, because this configuration enables to maximize the amount of hydrogen available for methanation process, which leads to promote the capture

of CO_2 from the air. In the latter case, because the battery is an alternative for electricity storage that does not require the utilization of water.

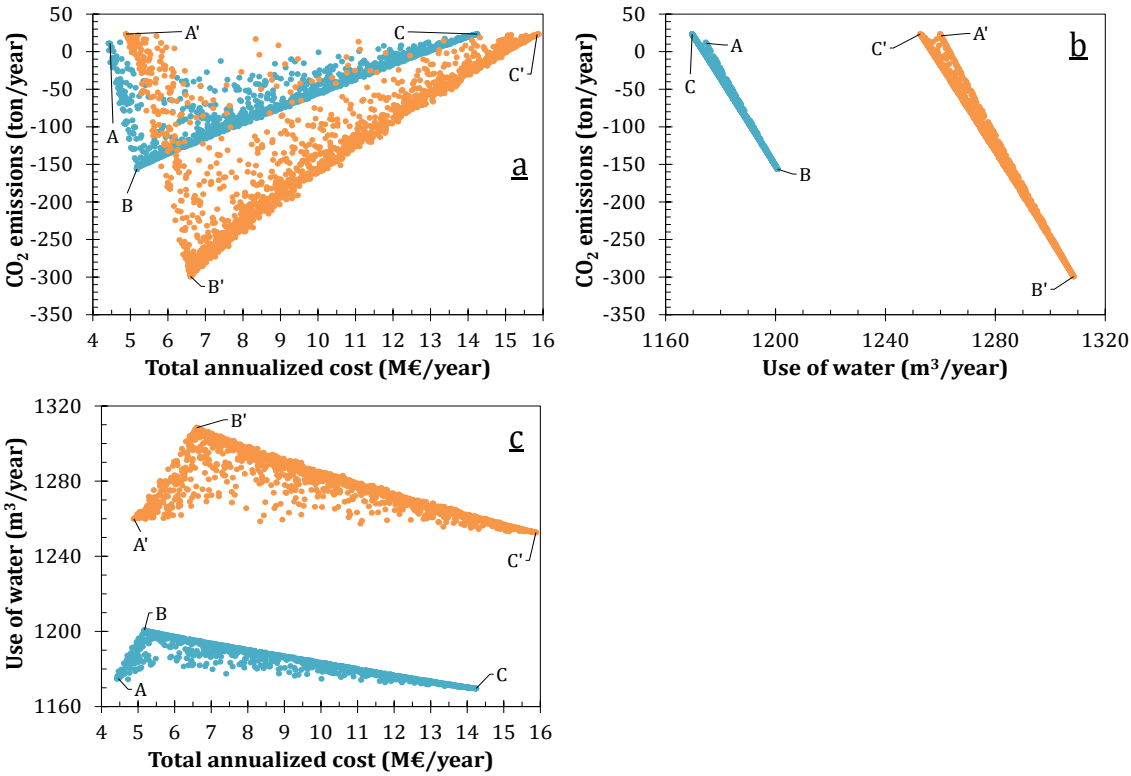

Figure 5-12: 2-dimension projection of the Pareto solutions for minimizing the total annualized cost, the CO_2 emissions and the water consumption. Photovoltaic surface (●) 12250 m², (●) 14700 m². (A – A') minimal cost, (B – B') minimal CO_2 emissions, (C – C') minimal water consumption.

The remainder of relationships between the economic (A – A') and CO_2 emissions optimum (B – B') were already discussed in the multi-objective problem P1. Meanwhile, note that, the size of the fuel cell, and the share of methanation and digester processes for the supply of methane are quite similar to those obtained for the economic optimum. On the one hand, regarding the fuel cell, this occurs because by using the whole system electrolyzer-tank-fuel cell, it is possible to recover the water produced in the fuel cell to be reused in the electrolyzer. Therefore, in such a case the global water consumption is lower than that of using the hydrogen to produce methane. On the other hand, as observed in Figure 5-13d, going towards the minimal water consumption value requires to increase the share of the biomass digestion process in the supply of methane. This alternative is preferred because around 150 L of water can be saved for each MWh of methane produced with respect to the methanation process.

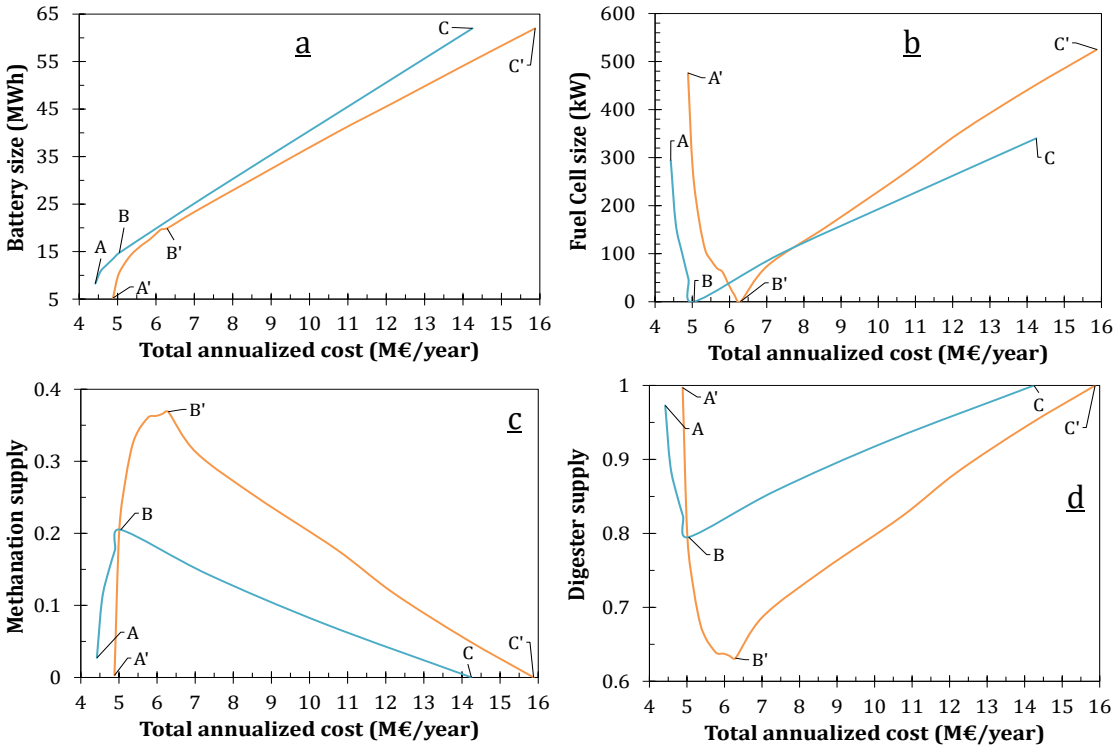

Figure 5-13: Change of design and operating conditions across the Pareto fronts. Photovoltaic surface (—) 12250 m² and (—) 14700 m². (a) battery size, (b) fuel cell size, fraction of methane supplied by (c) methanation and (d) digestion processes. (A – A') minimal cost, (B – B') minimal CO_2 emissions, (C – C') minimal water consumption.

5.5 Summary

Based upon a single and multi-objective optimization approach, the conceptual design of an isolated energy system for a remote location in the Colombian Amazon has been investigated in this chapter. Additionally, the trade-off among the sustainability criteria, and the changes of design and operation conditions across the Pareto solutions were also analyzed. To summarize those findings, Figure 5-14 depicts the impact of the main process variables on the sustainability indicators.

According to the formulation of the optimization problem (section 5.3), the performance of the sustainability indicators improves as their value decreases. Thus, downward arrows (Figure 5-14) represent a positive impact on the corresponding indicator. Through the presented outcomes, it is noted that some trends follow the same behavior to those obtained for the case study located in France (Chapter 4 – section 4.3). For instance, similarly to that case, the CO_2 emissions can be reduced by increasing the availability of PV-based electricity, i.e. installing a larger surface of PV. Nevertheless, this also entails to worse cost, water consumption and inherent safety indicators, since bigger equipment are

required for energy conversion and a higher amount of water is needed for storing the surplus electricity as hydrogen form.

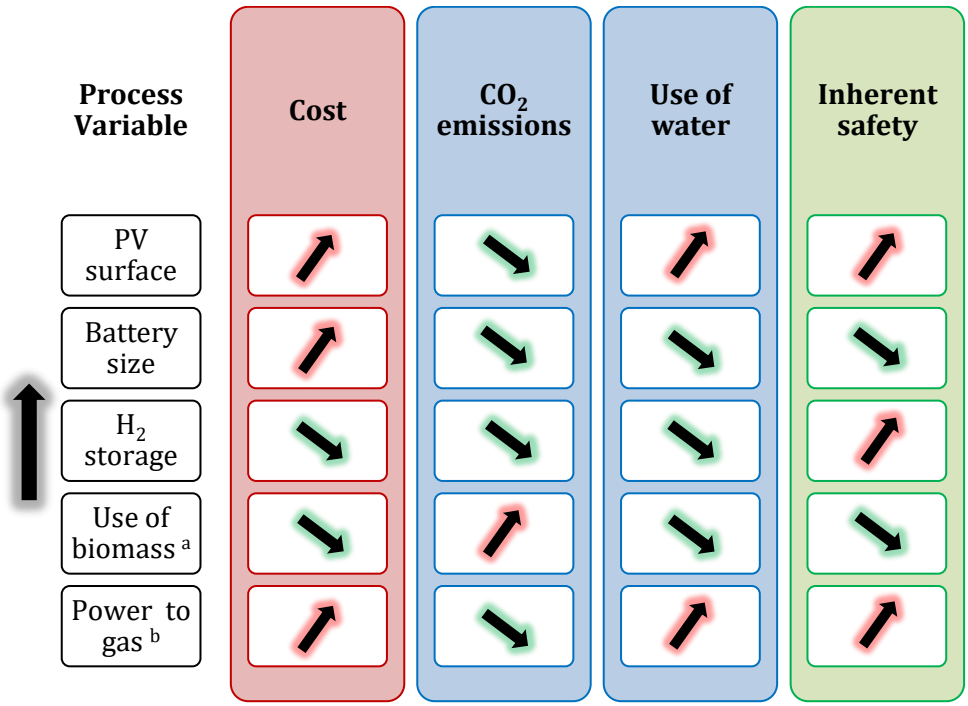

Figure 5-14: Impact of increasing the process variables on the sustainability indicators. (a) biomass is used in the anaerobic digestion process to produce methane (b) power-to-gas involves using a PV-based electrolyzer and the subsequent methanation process.

Moreover, about the alternatives for electricity storage, increasing their installed capacity enhances the yield of the environmental dimension of sustainability. Nonetheless, the results underline the competition between the alternatives when cost and safety aspects are evaluated. Thus, expanding the capacity of the hydrogen storage enables to decrease the investment of the plant, but at the cost of dealing with more hazardous process conditions. In this respect, an interesting difference emerges with respect to the French case study regarding the economic aspect. Indeed, for the case study located in France, the results suggest that the installed capacity of both storage systems must be reduced for improving the economic indicator. This can be explained by analyzing a key difference between the two case studies: the possibility of using energy from the main grid. In such a way, as the case study of France corresponds to a grid-connected energy system, it does not require to have storage units for assuring the energy supply. Consequently, the system can reduce the capacity of such equipment as much as possible, so that the corresponding investment costs can be decreased.

Conversely, the Colombian case study is an isolated energy system since there is no possibility to import energy from the grid. Accordingly, the reliability of the energy supply relies on the use of energy storage units for providing the service when PV electricity is not available. Therefore, as the hydrogen system represents the cheapest option, the best performance on the economic indicator can be obtained by increasing its installed capacity instead of using the electrical battery.

Otherwise, regarding the sources of methane, results shown in Figure 5-14 indicate that the biomass digestion offers the best option for enhancing cost, water consumption and inherent safety indicators. Interestingly, these trends are opposite to those identified for the case study in France. This fact underlines the influence of the context conditions on the selection and the role of technologies within the energy system. Indeed, obtained outcomes suggest that the optimal configuration of the energy system requires to comparatively evaluate the technological options to identify the most suitable solution. For instance, for the French case study, using biomass for producing hydrogen leads to increase the cost and the hazards of the system. On the contrary, for the Colombian case study, the economic and safety issues are improved as the use of biomass becomes greater for producing methane.

In this regard, for producing hydrogen from biomass, anaerobic digestion and steam methane reforming processes are required. Meanwhile, by employing the gas from the network, only the reforming step is needed. Thereby, for the conditions of the case study in France, the use of biomass is not preferred from the economic and safety perspectives, since it entails additional equipment which translates into higher cost and less safe conditions. In contrast, in the Colombian context conditions, biomass is used to produce methane, so that only the anaerobic digester must be employed. In this case, another option is the power-to-gas pathway, which implies the electrolyzer and methanation reactor. Consequently, in such a case, using the anaerobic digester enhances the economic and safety indicators since a lower amount of equipment are required and less intense operating conditions are employed.

5.6 Conclusions

In this chapter the design and operation of a distributed energy system for an isolated community in the Colombian Amazon was studied. The employed framework is an optimization-based approach, which includes to solve single and multi-objective optimization problems for assessing the energy conversion and storage technologies under the sustainability dimensions. Through the obtained results, the impact of the evaluated

criteria on the design and operating conditions of the energy system was investigated. Thus, outcomes indicate that a PV surface of 9800 m^2 is the minimum required for supplying the electricity needs of the considered community (4160 inhabitants). In such a case, the methane demand can be completely covered by means of the anaerobic digestion of domestic waste. Moreover, by installing an area of 24150 m^2, the system can supply both electricity and methane demands via power-to-gas technology. In this case, the system would require to import/capture around 854 tonCO_2/year for the methanation process.

It is worth to note that the obtained results underline the potential of hydrogen as an intermediate to enable the self-sufficiency at tropical and isolated places as the Colombian Amazon. In such a context, as there is no seasonal variation, it is possible to regularly produce hydrogen along the whole year, and consequently to boost the employment of the power-to-gas technology for producing methane based upon PV-electricity. Additionally, this configuration implies either to import or to capture CO_2, which could lead to an energy system with negative CO_2 emissions.

Furthermore, through the multi-objective optimization results, the compromise among the sustainability indicators was displayed. Besides, the implications of the trade-offs in terms of design and operating conditions were explored and analyzed. Thus, the outcomes of this chapter represent a valuable source of information for decision-makers in two main directions: (i) the early design of energy systems in isolated zones, and (ii) the potential utilization of hydrogen for enabling self-sufficiency at remote and tropical zones.

6. Conclusions and Perspectives

6.1 Conclusions

The motivation of this project lied on the necessity of developing methodological tools for the design, analysis, and evaluation of distributed energy systems considering the sustainability dimensions. Thus, as DES are complex socio-technical systems, the main goal of this work was to propose a comprehensive framework that enables: (i) to perform the conceptual design of an energy system for satisfying the needs of the consumers according to the available resources, (ii) to enhance the sustainability performance of the system from early design stages, (iii) to promote the participation of stakeholders, and (iv) to support the decision-making process by analyzing the compromises among the sustainability axes. To do so, four specific objectives were developed throughout the five chapters of this document.

Initially, the current trends in the design of DES were identified. This was performed through a bibliographic analysis that allowed to establish the state of the art about the approaches for the conceptual design of DES. Moreover, considering that hydrogen can play a foremost role in the undergoing energy transition, a particular focus was on those energy systems that include hydrogen as energy carrier. From this analysis, it was elucidated the high involvement of renewable sources in this kind of systems, being the solar, wind, and biomass-based technologies the most used. Besides, it was identified that hydrogen is predominantly employed as a storage medium for mitigating the mismatch between electricity production and consumption. Accordingly, the use of hydrogen is mainly associated to the power-to-power technologies, i.e. electrolyzer, pressurized tank, and fuel cell. The storage of electrical energy in chemical form is positioned as an interesting alternative to batteries, especially when the storage of large amounts of energy and/or during long periods (seasonal storage) is required. In those applications, hydrogen offers an option with reduced self-discharge rate and a lower cost per kWh stored. In addition to that, hydrogen has been seldom considered either as an intermediate for producing biomethane or as a product of the system to be used in mobility. In the former,

hydrogen is obtained via water electrolysis and subsequently is combined with CO_2 to produce methane, in the so-called power-to-gas pathway. In the latter, hydrogen is produced either by means of electrolysis or steam methane reforming processes. For summarizing, as a result of this literature analysis, a paper was published in the *International Journal of Hydrogen Energy* with the following citation:

- Fonseca JD, Camargo M, Commenge JM, Falk L, Gil ID. Trends in design of distributed energy systems using hydrogen as energy vector: A systematic literature review. Int J Hydrogen Energy 2019;44:9486–504. https://doi.org/10.1016/j.ijhydene.2018.09.177.

Then, based upon the results from the previous literature review, a base-case flowsheet for the energy system was proposed including the most common technologies and energy forms. Thus, the configuration considered electricity, hydrogen, and methane as potential energy demands. These can be satisfied either by using renewable resources (biomass, wind, solar) or by importing energy from electricity and natural gas networks. Besides, the electrical battery and hydrogen were included as alternatives for energy storage. Considering the base-case flowsheet, a mathematical model was built for representing the connections among the set of technological units and for describing the operation of the whole system. This model constitutes a basis for the subsequent evaluation of process alternatives, since it enables to predict/understand their behavior and performance in a safe, cheap, and fast way.

Once stated the mass and energy balances that govern the behavior of the energy system, the task of defining the criteria and indicators to evaluate its performance was addressed. Broadly, suitable indicators should enable the discrimination among the evaluated alternatives. Also, they must be easy to analyze, relevant for decision-makers, consistent with the objective and few. In such a way, based upon literature information, six indicators were selected for assessing the sustainability performance of energy systems at conceptual design stage. The selected indicators have four main characteristics: (i) they cover the three sustainability dimensions, (ii) they are directly related with conceptual design decisions, (iii) they can be defined through the information from mass and energy balances, and (iv) they have been identified as relevant for the evaluation of energy systems.

The economic dimension was evaluated through the total annualized cost and the levelized cost of energy. These indicators account for both the investment and operational expenditures, and the minimum price that users would pay for the investor to break even.

Meanwhile, the criteria for assessing the environmental dimension was to minimize the use of water and the CO_2 emissions of the energy system. Accordingly, the yearly CO_2 emissions and water consumption derived from the operation of the energy system were the selected indicators. The analysis of the social dimension was performed under the principle that industrial activities must improve the quality of life, i.e. to have a positive impact on two main aspects: equity and health. Consequently, these issues were addressed through the grid dependency and the inherent safety indicators. The former is associated with the access to affordable, reliable, and modern energy for all, as proposed by United Nations in the sustainable development goals (Goal 7). In this regard, it is essential to ensure that energy is available at a reasonable price, so that the trade-off between this social aspect and the economic indicators is crucial. The latter lies on accounting the inherent risks derived from the operating conditions of technologies and the properties of the chemical compounds used within the energy system.

Based upon the developed energy system model and the selected sustainability indicators, an optimization approach was proposed and implemented for the design and operation of DES. Then, the proposed framework was illustrated through the analysis of a case study. This case of application corresponded to a grid-connected energy system conceived for satisfying the electricity and hydrogen needs of a neighborhood of 1500 inhabitants near to Marseille-France. Additionally, three different scenarios were defined to evaluate the impact of the availability of PV-based electricity on the performance of the system. Given those conditions, five independent optimization problems were formulated and solved for minimizing the total annualized cost, the CO_2 emissions, the water consumption, the grid dependence, and the inherent safety index.

From the optimization results, it was noted the significant influence of the evaluated indicator and the PV surface on the design and operating policy of the energy system. Indeed, from the assessment of the five indicators and the three surfaces of PV, eight different energy system configurations were obtained. According to the results, the performance of the CO_2 emissions and grid dependence improves as the PV-based electricity gets larger. In contrast, total annualized cost, water consumption and safety indexes get their best performance with the smallest PV surface. Moreover, by comparing the obtained outcomes with the performance of a centralized scenario, some additional impacts of the implementation of a DES can be noted. For instance, results indicate that the emission of up to 400 tonCO_2/year can be avoided (with respect to the centralized scenario), and the grid dependency can be reduced to below 20%. Indeed, even with the

smallest area of PV (5000 m^2) and without seasonal energy storage, 25% of the CO_2 emissions can be prevented and near to 40% of self-sufficiency can be achieved.

As a product of this single-optimization analysis, an oral presentation was performed at 17ème Congrès de la Société Française de Génie des Procédés (SFGP2019), and a peer-reviewed article was published in *Energy Journal* with the following citation.

- Fonseca JD, Commenge J-M, Camargo M, Falk L, Gil ID. Multi-criteria optimization for the design and operation of distributed energy systems considering sustainability dimensions. Energy 2021;214. https://doi.org/10.1016/j.energy.2020.118989.

In general, from the solution of these single-optimization problems two main outcomes can be underlined. First, a great knowledge of the system was obtained since the individual evaluation of the indicators allowed to identify and characterize some extreme points of the solution space. Besides, the physical sense behind each one of the eight possible system configurations was explained, and the impact of the availability of renewable-based electricity on the sustainability indicators was analyzed. Secondly, it was elucidated the competition among the evaluated objectives and the complexity of designing this kind of systems, as there is not a single optimal solution for satisfying all the criteria at their best performance. Therefore, it was highlighted the need of exploring the solution space to identify zones of compromise among the sustainability dimensions.

Considering the foregoing, the next step of this research consisted in addressing the conceptual design of DES as a multi-objective optimization problem. Thus, based on the knowledge obtained from the previous single-objective optimization, four multi-objective optimization problems were formulated and solved. These included different combinations of the sustainability indicators. From multi-objective optimization results, the relationships among the objective functions were established, and a wide spread of plausible system configurations and operating conditions were obtained. Broadly, results reflect the compromise and the antagonistic behavior among the sustainability criteria. Thus, it was determined the competition between the total annualized cost and the CO_2 emissions and grid dependence objectives. In such a way, for a given surface of PV, the TAC decreases as the performance in the emissions and self-sufficiency indicators gets worse. Also, it was identified that the water consumption and the grid dependence are contradictory indicators. Likewise, the obtained results depict the competition between the inherent safety index with both the cost and emissions objectives.

Moreover, the Pareto sets were explored and analyzed for identifying the changes in the design and operating conditions throughout the non-dominated solutions. This represents one of the main contributions of this work, since it displays the impact of any decision made over the objective space in terms of design and operation variables. Consequently, these results constitute a valuable information for the subsequent decision-making process.

Summarizing, the proposed framework has four main features: (i) it enables to assess multiple energy forms and technological units, (ii) it includes a variety of criteria for evaluating the performance of the system, (iii) it provides insights for the decision-makers about the trade-offs among the sustainability indicators, and (iv) it could be used as a source of information for promoting the participation of the communities from the early stages of the project.

Taking this into account and to display the flexibility of the proposed approach, a second case study was analyzed in a completely different context. In this case, the objective was to design a self-sufficient energy system with the capacity of supplying the energy needs of a community located in a remote region of the Colombian Amazon. Thus, there are two main differences with respect to the previous case study: (i) this is an isolated energy system, whereas in the French case a grid-connected system was analyzed, and (ii) there is no seasonal variation in the energy demand and availability, since the Colombian Amazon is located in a tropical region. Moreover, to include the specific characteristics of the studied location, cost factors were used to address the socio-technical aspects of installing a DES in this remote zone. These factors incorporate contingency, site preparation and startup costs, which reflect the lack of experience, infrastructure, and skilled people for the implementation of this kind of systems in that location.

According to results, it was determined that at least a PV surface of 9800 m^2 must be installed to satisfy the electricity needs of the considered community (4160 inhabitants). In this case, the demand of methane should be entirely covered by biomethane from an anaerobic digestion process. Nevertheless, by installing an PV area of 24150 m^2, electricity and methane demands can be supplied from PV-based electricity and by using the power-to-gas pathway. In such a case, it is necessary to import/capture around 854 tonCO_2/year for the methanation process. Additionally, these results underline the potential of hydrogen as an intermediate to enable the self-sufficiency at tropical and isolated places as the Colombian Amazon. In such a context, as there is a regular availability of PV-based electricity to obtain hydrogen, the power-to-gas technology seems to be a good alternative for producing methane and to support the self-sufficiency of the system. Furthermore, the

outcomes of this case study highlight the paramount role of the storage technologies in this kind of energy systems. Indeed, storage units are pillars for the reliable operation of an isolated energy system.

Overall, through the analysis of both case studies, it was elucidated that the proposed framework enables to perform a comprehensive analysis for the early design of DES considering the sustainability dimensions. First, a set of relevant indicators were selected and formulated as a function of conceptual design decisions. Then, single-objective optimization allowed to gain a better understanding of the energy system behavior, and to identify the impact of the evaluated criteria on the configuration and operating policy of the energy system. Thereafter, multi-objective optimization allowed to establish the trade-offs among the sustainability indicators and to investigate their corresponding impact in terms of process variables. In such a way, throughout each step, it was illustrated that the proposed approach constitutes a useful tool to perform a sustainability analysis from the early design stages, and that the obtained results represent a source of information that promotes the participation of stakeholders and supports the decision-maker to make an informed decision. Also, it was displayed the flexibility of the proposed framework, so that it could be easily adapted and used for the design of energy system in different context conditions, considering other criteria for evaluation, or including different technological units and energy forms.

6.2 Scientific Products

In addition to this dissertation, other products of this research include the participation in national and international scientific events, training courses, and the publication and submission of peer-reviewed articles.

Scientific Events:

- Oral presentation at 12th European Congress of Chemical Engineering (ECCE12). Florence, September 2019.
- Oral presentation at 17ème Congrès de la Société Française de Génie des Procédés (SFGP2019). Nantes, October 2019.

Training Courses:

- "International Summer School Hydrogen – Hydrogen Technologies in Local Energy Hubs". Nancy, July 2018.

- "Power to molecules (from technology to market uptake)", organized within the framework of the STORE&GO project. Florence, July 2019.

Articles:

- Fonseca JD, Camargo M, Commenge JM, Falk L, Gil ID. Trends in design of distributed energy systems using hydrogen as energy vector: A systematic literature review. Int J Hydrogen Energy 2019;44:9486–504. https://doi.org/10.1016/j.ijhydene.2018.09.177.
- Fonseca JD, Commenge J-M, Camargo M, Falk L, Gil ID. Multi-criteria optimization for the design and operation of distributed energy systems considering sustainability dimensions. Energy 2021;214. https://doi.org/10.1016/j.energy.2020.118989.

6.3 Limitations and Perspectives

Considering the features of the proposed approach and the results obtained through the analysis of the case studies, some limitations and perspectives of future work can be envisaged to support the use of hydrogen as energy vector and the conceptual design of energy systems.

- As stated in the Chapter 2, the proposed energy system model relies on the consideration that the operational conditions of the energy converters are fixed, and the input/output variables are related by means of constant efficiencies and linear expressions. This assumption permits to have a formulation able to capture the key physical features of the technological units, and at the same time, a representation capable to quickly perform the mass and energy balances of the system, as required at conceptual design stage. Nonetheless, even though this approach also enables to ease the subsequent process optimization, it leaves aside the transient behavior of some units, especially those ones with slow dynamics (e.g. digester, reformer). Consequently, once selected the system flowsheet, this issue could be addressed by incorporating mathematical models that enable a more detailed representation of the process units, and thus to perform a more accurate evaluation of the system.
- Another feature of the proposed approach is the resolution time (12 h time steps) used to solve the energy system model and to perform the optimization. As

discussed throughout the document, this time step permits to describe the daily fluctuations of energy demand and availability without penalizing the optimization with a huge quantity of decision variables. Nevertheless, this also implies that the values of all variables remain constant along twelve hours. This can be a critical issue due to the high variability of some data such as the weather conditions and the energy demands. Accordingly, once defined the system flowsheet by using this approach, the energy system structure could be analyzed in-depth by considering smaller time steps. This would enable to obtain a more realistic representation of the system by focusing on the operating aspects, since the system configuration and the size of the equipment would be already defined.

- From the energy system model, it is well noted that there are multiple units which operate at different temperature conditions. Besides, some energy converters are cogeneration units (e.g. fuel cell), and there are operations that imply highly exothermic reactions (e.g. methanation). In such a way, it can be interesting to investigate the heat integration within the energy system, so that the global efficiency of the whole plant could be improved. This would be a challenging task, since it is required to consider the time-dependent behavior of the system, which could lead to new operating strategies.
- In this work the energy systems were designed for a fixed energy demand. Nevertheless, the impact of the energy consumption patterns could be further investigated. For instance, it could be analyzed the effect of implementing energy saving programs on the energy system design. This can be an additional alternative for enhancing the sustainability of the system since the pressure over the capacity of ecosystems for supporting the life and industrial activities could be reduced.
- Regarding the sustainability assessment, different indicators could be evaluated. In this work the CO_2 emissions were evaluated through a gate-to-gate assessment, so that the emissions outside the boundaries of the energy system were not accounted. In this regard, a life cycle analysis could be implemented to obtain a more complete information about the environmental impacts of the energy system. Also, other indicators can be included for the economic and social dimensions, such as the net present value and the job creation.
- Hydrogen technologies have been recognized as a promising alternative to support the energy transition in Europe in the upcoming years. Indeed, huge investments have been decided to boost the technology development. In this work, it was assumed that the selected technologies are already available at commercial level. However, it is not the case for some of the units involved in DES. For example, PEM

electrolyzers are at commercial demonstration level, anerobic digester and Li-ion batteries are broadly deployed in relevant environment, and PV are already competitive and commercial, whereas pressurized tanks for hydrogen storage and steam methane reforming are mature technologies [225,226]. Accordingly, the technological readiness level (TRL) could be further analyzed to consider its impact on the design of the energy system. For instance, for technologies at early demonstration level such as PEM electrolyzers, additional cost for the installation and operation of the equipment could be required. Moreover, an aggregated TRL for the whole system could be calculated from the contribution of each individual equipment and included as objective function to analyze potential perspectives/risks associated to the implementation of some technologies.

- It would be interesting to integrate the decision-maker preferences through a decision-aid making tool. This will enable to rank the obtained Pareto sets and to select the best alternative for the specific context conditions. Moreover, considering that this type of projects involves multiple stakeholders, who often have conflicting objectives. Future studies could investigate the interactive exploration of the Pareto solutions to identify the more suitable zones based on the stakeholders' interests.

Moreover, as stated in Chapter 2, the proposed approach is based upon a deterministic model, i.e. that the whole input data required for the modelling and optimization of the energy system is known without uncertainty. Nevertheless, this represents a limitation of the approach, since there are some input parameters intrinsically uncertain such as the climate conditions (solar irradiance, wind speed), energy demands, and energy prices. Consequently, future work could be undertaken either to analyze the flexibility of the energy system (once designed) to deal with the variations of those data, or to perform the energy system optimization under uncertain conditions (stochastic approach). Some examples of these perspectives are listed below.

- Sensitivity analysis on the performance and cost of equipment to investigate the impact of these variables in terms of design and/or operating conditions of the energy system.
- A long-term analysis to study the effect on the operation of the energy system by changing the amount of energy users over time.

- Probabilistic analysis to investigate accidental failure of equipment, and different scenarios of resources availability and/or energy demands, and their impact on the sustainability criteria.

A. Annex A: Inherent Safety Index

The inherent safety index for evaluating the energy system is calculated as stated by Equations A.1-A.4.

$$IST = \sum_{k}^{K} I_{E,k} \tag{A.1}$$

$$I_{E,k} = I_{C,k} + I_{P,k} \tag{A.2}$$

$$I_{C,k} = \frac{\sum_{n}^{N}(I_{FL,n} + I_{EX,n} + I_{TOX,n} + I_{COR,n})F_n + I_{R,k}\sum_{n}^{N} F_n}{1000} \tag{A.3}$$

$$I_{P,k} = I_{I,k} + I_{T,k} + I_{Pr,k} \tag{A.4}$$

Where, IST is the total inherent safety index, $I_{E,k}$ is the individual equipment safety index, $I_{C,k}$ is the chemical index, and $I_{P,k}$ is the process index of the equipment k. Additionally, $I_{FL,n}$, $I_{EX,n}$, $I_{TOX,n}$ and $I_{COR,n}$ are the flammability, explosiveness, toxicity and corrosiveness scores, respectively. F_n represents the mass flow rate, $I_{R,k}$ is the reaction sore, the subscript n denotes each chemical substance through the equipment k , and the factor 1000 is the basis flow rate. Meanwhile, $I_{I,k}$, $I_{T,k}$ and $I_{Pr,k}$ correspond to the inventory, temperature, and pressure scores, respectively.

- *Chemical Index*

  According to the previous formulation, the chemical index relies upon the flammability, explosiveness, toxicity, and corrosiveness sub-indexes. The scores of such sub-indexes are depicted in Tables A-1 to A-4.

Table A-1: Flammability score [171].

Flammability	Score
Non-flammable	0
Flash point > 55 °C	1
Flash point ≤ 55 °C	2
Flash point < 21 °C	3
Boiling point ≤ 35 °C	4

Table A-2: Explosiveness score [171].

Explosiveness (UEL – LEL)*	Score
Non-explosive	0
0 – 20	1
20 - 45	2
45 - 70	3
70 - 100	4

* (UEL) upper explosive limit, (LEL) lower explosive limit.

Table A-3:Toxicity score [171].

Toxic Limit (ppm)	Score
> 10000	0
≤ 10000	1
≤ 1000	2
≤ 100	3
≤ 10	4
≤ 1	5
≤ 0.1	6

Table A-4: Corrosiveness score [171].

Construction material required	Score
Carbon steel	0
Stainless steel	1
Better material needed	2

Then, considering the scores presented above, and the safety data sheet of the chemical compounds, Table A-5 depicts the obtained chemical sub-indexes.

Table A-5: Chemical sub-indexes for the compounds included within the energy system.

Component	Flammability	Explosiveness	Toxicity	Corrosiveness
Hydrogen	4	4	0	0
Water	0	0	0	0
Carbon dioxide	0	0	1	0
Methane	4	1	0	0

Moreover, regarding the heat of reaction sub-index ($I_{R,k}$), it was determined by means of the relation proposed by Srinivasan and Nhan (Equation A.5) [227]. In that expression, $\Delta H_{R,k}$ represents the heat of the main reaction. The values obtained from Equation A-5 are between 0-1, however the original scale is from 0 to 4. Therefore, aiming to respect the original scale, the result of the Equation A-5 is scaled by multiplying the obtained value by 4.

$$I_{R,k} = 1 - \frac{1}{1 + a\left(\Delta H_{R,k}\right)^{b}} \qquad ; a = 4.47e-5 \; ; b = 2 \tag{A.5}$$

Concerning the mass flow rate (F_n), the selected value corresponds to the maximum flow rate of each compound during the evaluated period.

- *Process Index*

As presented in Equation A.4, the process index depends upon the inventory, temperature, and pressure sub-indexes. The former is determined for each equipment as a function of the amount of material accumulated, as presented in Table A-6.

Table A-6:Inventory index for the inherent safety assessment [171].

Inventory (ton)	Score
0 -1	0
1 – 10	1
10 – 50	2
50 – 200	3
200 – 500	4
500 - 1000	5

Meanwhile, the temperature and pressure sub-indexes were calculated through the relations proposed by Srinivasan and Nhan (Equations A.6 and A.7) [227]. In those expressions, T and P represent the operating temperature and pressure of each equipment.

$$I_{T,k} = \begin{cases} 1 - \exp -(aT - b) & ; a = 0.005, b = 0.125 \quad if \;\; T > 25°C \\ 1 - \exp(aT - b) & ; a = 0.02, b = 0.5 \quad otherwise \end{cases} \tag{A.6}$$

$$I_{Pr,k} = \begin{cases} 1 - \exp -a(P - 1) & ; a = 0.03 \quad if \;\; P > 1atm \\ 1 - \exp a(P - 1) & ; a = 5 \quad otherwise \end{cases} \tag{A.7}$$

As for the case of the heat of reaction sub-index, the values resulting from Equation A.6 and A.7 are between 0-1. Nevertheless, the original scale is from 0 to 4. For that reason, such values are scaled by multiplying the result by 4.

B. Annex B: Energy Storage

As described in the section 3.3.3 of the main document, the pinch analysis was used for defining the maximum capacities of the storage units. Broadly, such approach is based on analyzing the amount of energy stored as a function of time. Thus, Figure B-1 depicts the corresponding GCC for the battery and the pressurized tank units.

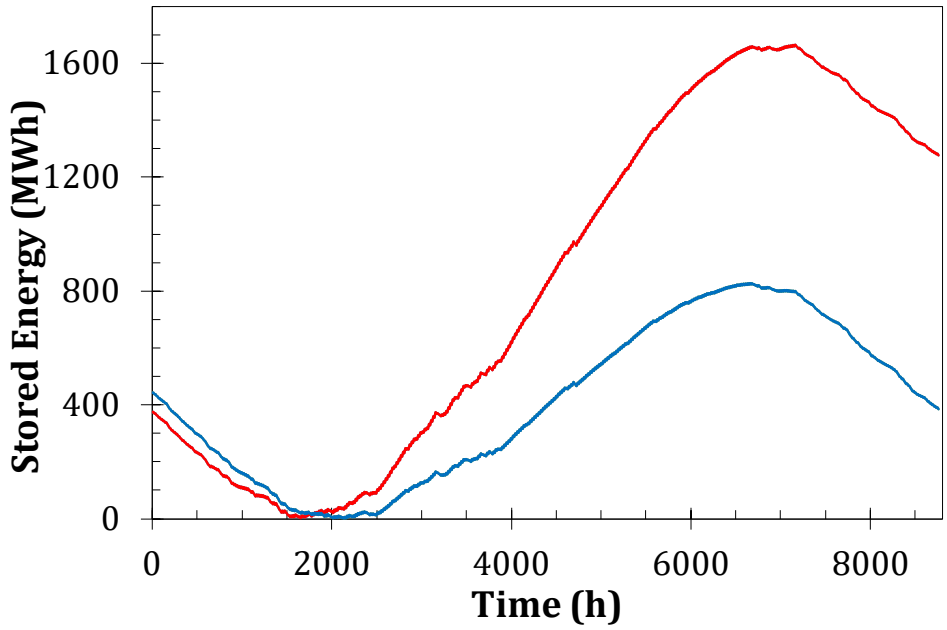

Figure B-1: Grand composite curves considering a photovoltaic surface of 10 000 m². (—) Battery, (—) pressurized tank.

C. Annex C: Multi-objective optimization

- *Case study in France (Chapter 4)*

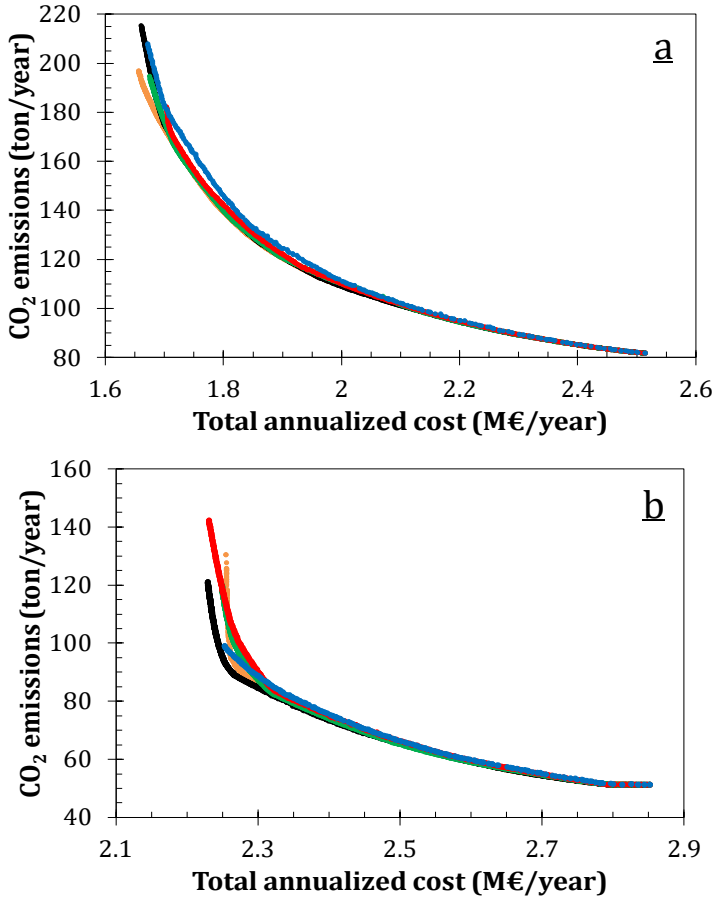

Figure C-1: Pareto solutions for minimizing the total annualized cost and the CO_2 emissions. Population of the genetic algorithm (●) 500 (●) 1000, (●) 2000, (●) 3000 and (●) 4000 individuals. Photovoltaic surface (a) 7500 m², (b) 10000 m².

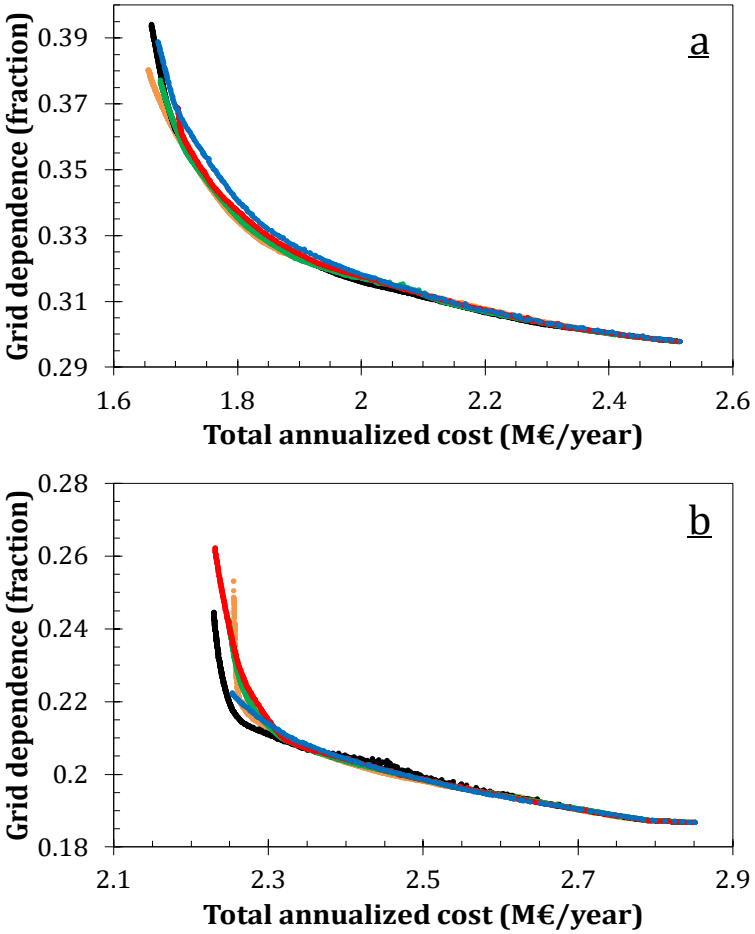

Figure C-2: Pareto solutions for minimizing the total annualized cost and the grid dependence. Population of the genetic algorithm (●) 500 (●) 1000, (●) 2000, (●) 3000 and (●) 4000 individuals. Photovoltaic surface (a) 7500 m², (b) 10000 m².

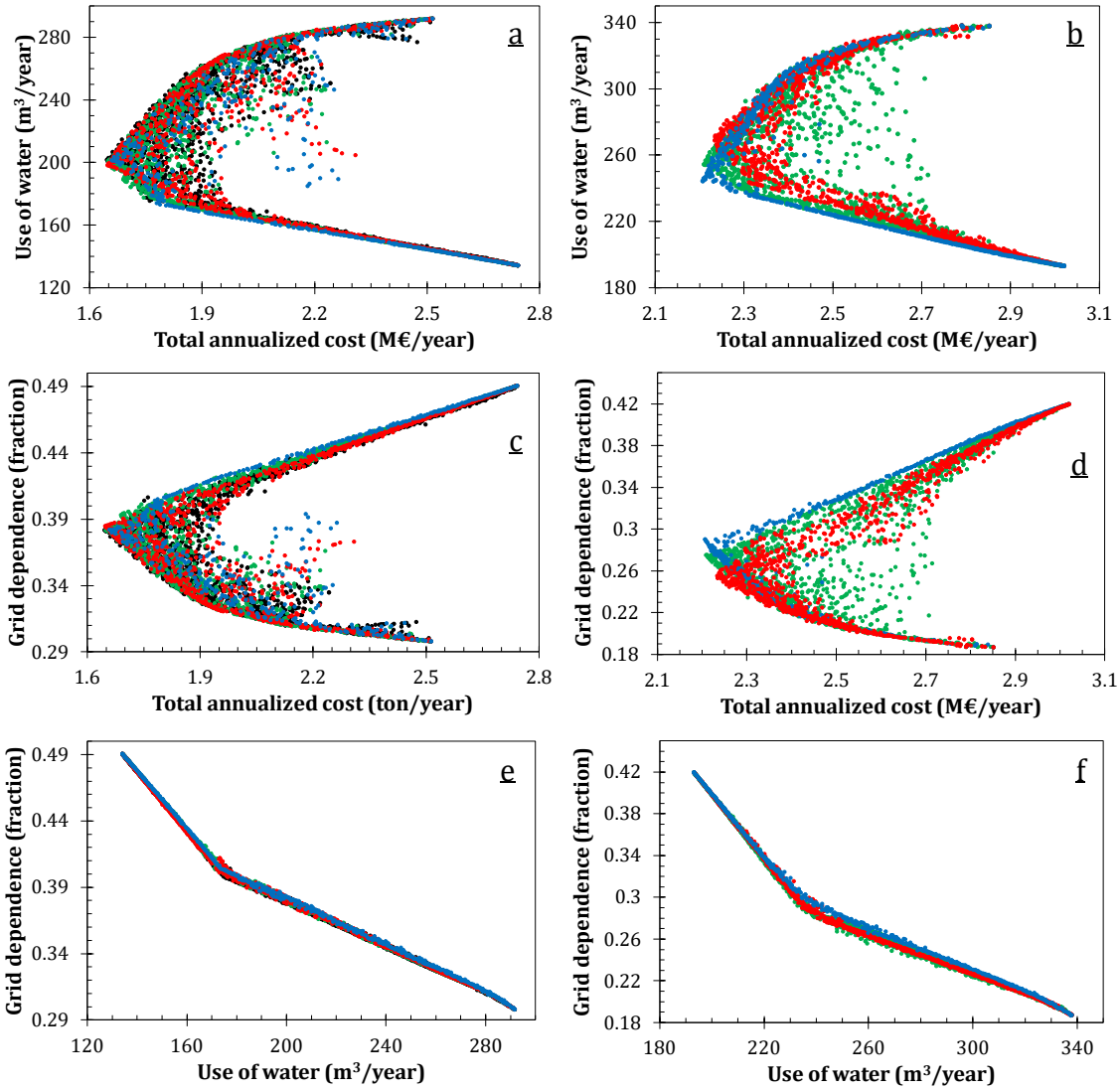

Figure C-3: Pareto solutions for minimizing the total annualized cost, the water consumption, and the grid dependence. Population of the genetic algorithm (●) 1000 (●) 2000, (●) 3000, (●) 4000 Photovoltaic surface: left column (a,c,e) 7500 m², right column (b,d,f) 10000 m².

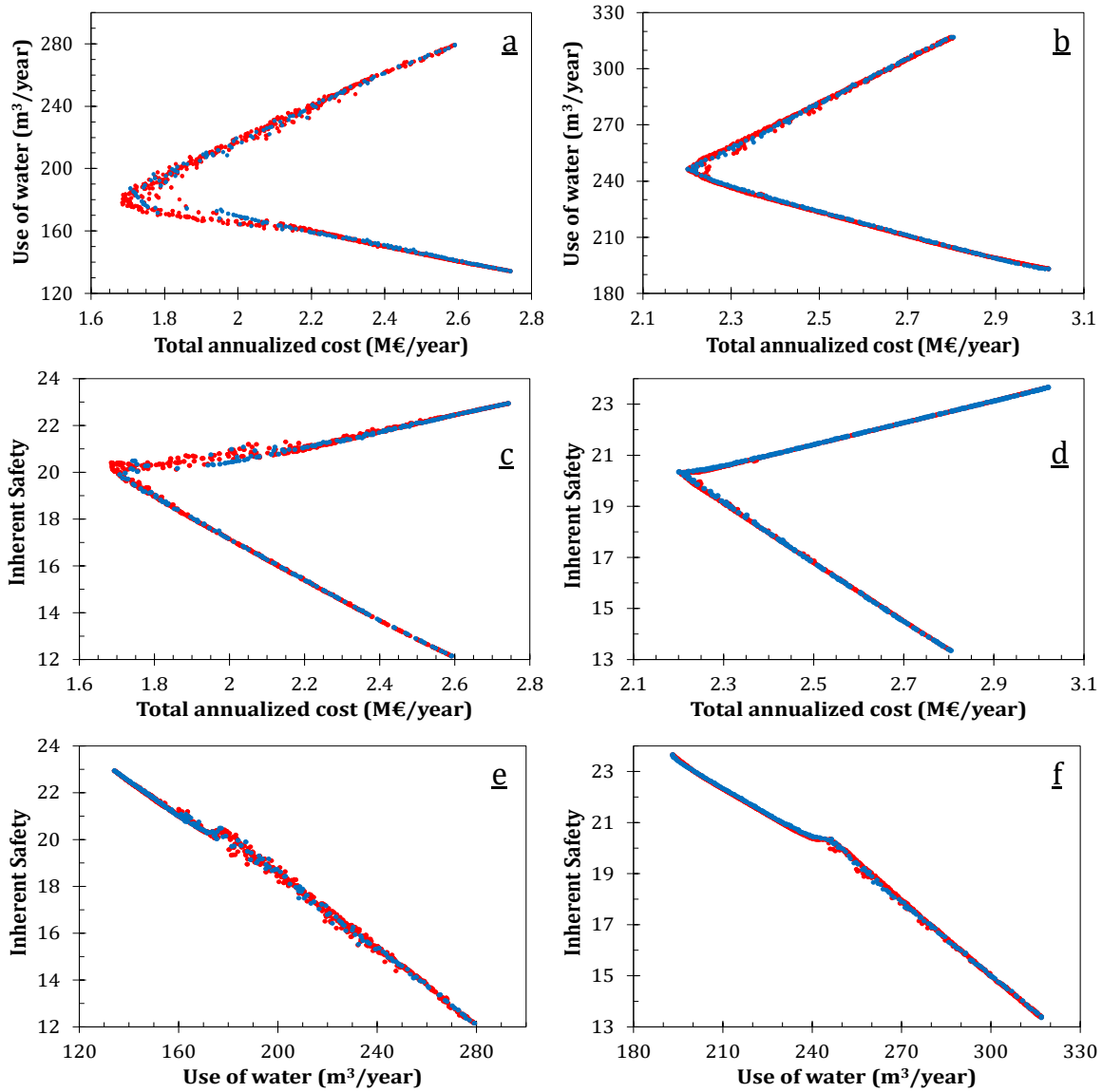

Figure C-4: Pareto solutions for optimizing the total annualized cost, the water consumption, and the inherent safety. Population of the genetic algorithm (●) 500 (●) 2000. Photovoltaic surface: left column (a,c,e) 7500 m², right column (b,d,f) 10000 m².

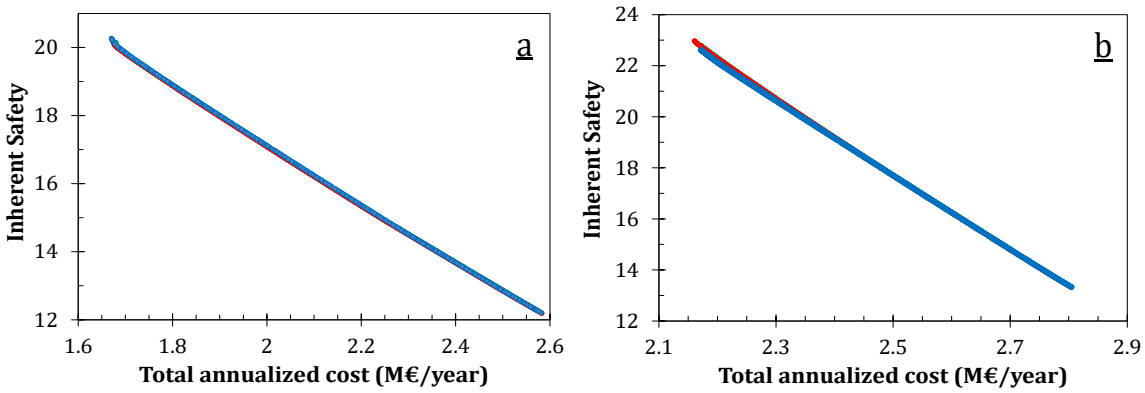

Figure C-5: Pareto solutions for optimizing the total annualized cost and the inherent safety. Population of the genetic algorithm (●) 1000, (●) 2000 and (●) 3000. Photovoltaic surface (a) 7500 m² (b) 10000 m².

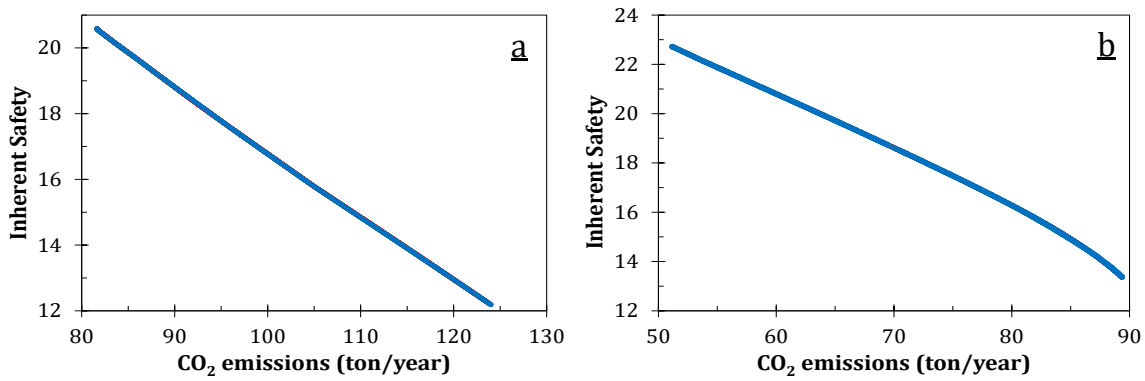

Figure C-6: Pareto solutions for optimizing the CO_2 emissions and the inherent safety. Population of the genetic algorithm (●) 1000, (●) 2000 and (●) 3000. Photovoltaic surface (a) 7500 m² (b) 10000 m².

- *Case study in Colombia (Chapter 4)*

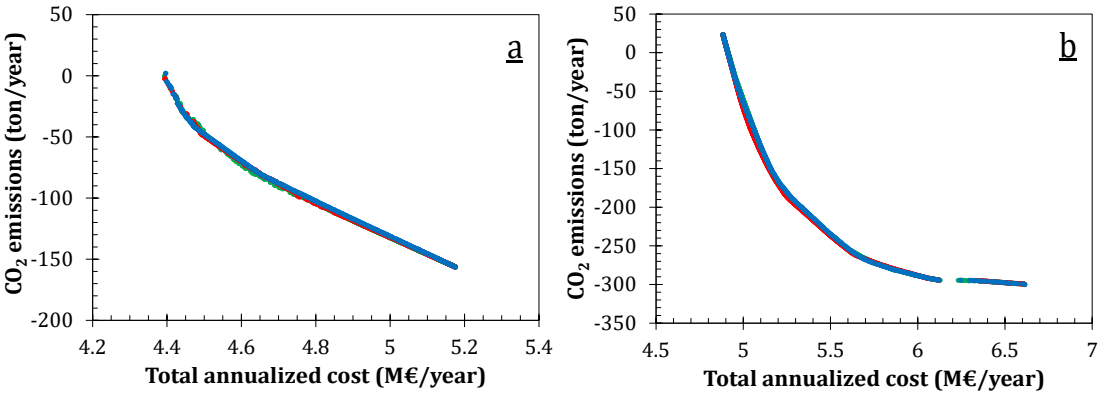

Figure C-7: Pareto solutions for minimizing the total annualized cost and the CO_2 emissions. Population of the genetic algorithm (●) 1000, (●) 2000 and (●) 3000. Photovoltaic surface (a) 12250 m² (b) 14700 m².

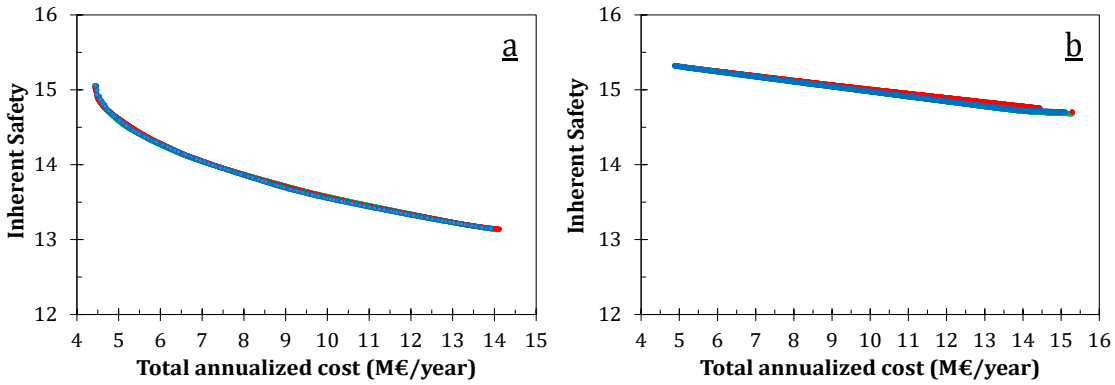

Figure C-8: Pareto solutions for optimizing the total annualized cost and the inherent safety. Population of the genetic algorithm (●) 1000, (●) 2000 and (●) 3000. Photovoltaic surface (a) 12250 m² (b) 14700 m².

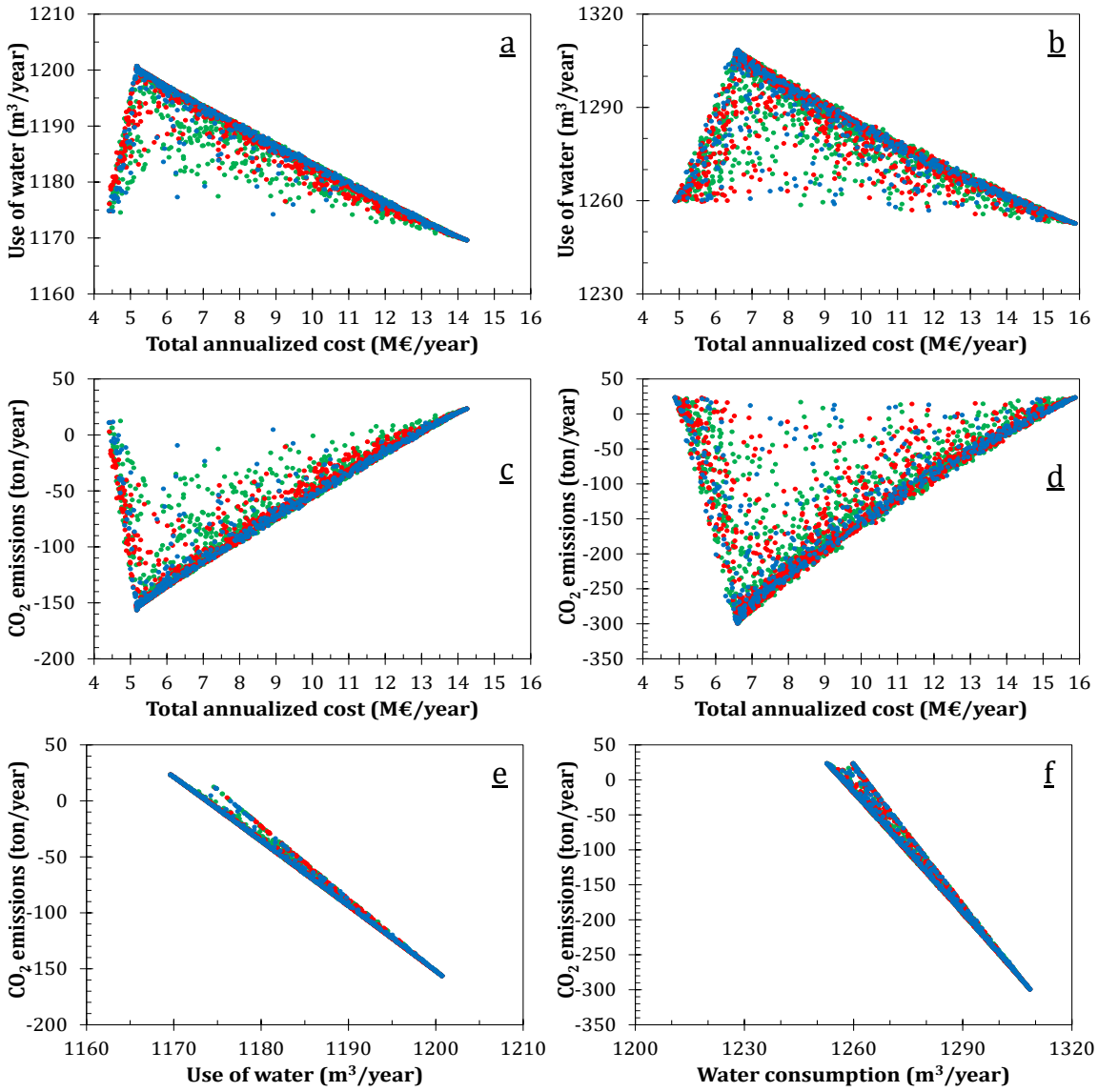

Figure C-9: Pareto solutions for optimizing the total annualized cost, the CO_2 emissions, and the use of water. Population of the genetic algorithm (●) 1000, (●) 2000 and (●) 3000. Photovoltaic surface: left column (a,c,e) 12250 m², right column (b,d,f) 14700 m².

D. Annex D : Résumé en Français

Introduction

L'expansion de l'économie mondiale et la demande croissante de chauffage et de refroidissement ont entraîné une augmentation de 2,3 % de la consommation mondiale d'énergie et de 1,7 % des émissions de CO_2 en 2018 [1]. Ces résultats représentent une préoccupation importante pour le secteur de l'énergie, car les tendances à la hausse des émissions de ces dernières années ne sont pas conformes à l'accord de Paris visant à maintenir l'augmentation de la température mondiale en dessous de 2°C [2]. À cet égard, les principales questions à traiter sont la forte dépendance aux combustibles fossiles et la forte intensité énergétique de certaines industries. En fait, actuellement, environ 82 % des besoins énergétiques mondiaux sont couverts par des sources fossiles [2,3]. En réponse à ce scénario, et pour répondre à l'augmentation continue de la consommation d'énergie et pour atteindre les objectifs environnementaux mondiaux, une transformation énergétique globale est en cours. Ce changement nécessaire repose sur trois piliers principaux : (i) accroître la part des ressources renouvelables, (ii) augmenter la participation de l'électricité à faible teneur en carbone en tant que forme d'énergie d'utilisation finale, et (iii) déployer la production d'énergie distribuée [2–4].

En plus d'atténuer les effets du changement climatique, l'utilisation des énergies renouvelables est stimulée par les préoccupations relatives à la qualité de l'air et à la sécurité énergétique. En ce sens, les sources renouvelables représentent une excellente alternative pour réduire les problèmes de santé liés à la contamination de l'air, pour gérer le caractère limité des sources fossiles et pour fournir de l'électricité aux régions isolées. Dans l'ensemble, la contribution la plus importante des énergies renouvelables se situe dans le secteur de l'électricité, puisqu'en 2018, près de 25 % de la production d'électricité était basée sur les énergies renouvelables [1,2]. En fait, de nos jours, l'électricité apparaît comme l'un des vecteurs énergétiques privilégiés pour soutenir le déploiement des énergies renouvelables et faire face aux défis environnementaux actuels.

La production distribuée fait référence aux systèmes à petite échelle, généralement d'une capacité inférieure à 1000 kW et situés à proximité des consommateurs finaux, c'est-à-dire les systèmes énergétiques distribués/décentralisés (DES) [6,7]. Ce type de centrales énergétiques vise à couvrir les demandes locales, par exemple les bâtiments, les quartiers, les zones isolées, les campus universitaires ou les hôpitaux, en utilisant des sources d'énergie spécifiques sur place. En plus d'une variété de ressources, qui peuvent être renouvelables ou conventionnelles, les DES comprennent des technologies de conversion et de stockage multiples pour répondre à différentes demandes (par exemple, l'électricité, le chauffage, le refroidissement, le carburant). En ce sens, la production distribuée représente un changement de paradigme, les systèmes énergétiques découplés traditionnels étant remplacés par des systèmes comprenant diverses formes d'énergie. La production décentralisée réduit également les pertes d'énergie lors du transport et de la distribution (caractéristique des centrales), encourage l'utilisation des énergies renouvelables (qui dépendent de l'emplacement et ne sont pas facilement transportables), favorise le couplage entre les différentes formes d'énergie, renforce l'autosuffisance énergétique et soutient la sécurité énergétique [7–9].

Parmi la variété des vecteurs énergétiques impliqués dans les DES, l'hydrogène a le potentiel de jouer un rôle clé dans la transition énergétique. L'hydrogène offre une alternative écologique pour toute une série de secteurs, notamment les transports, la chimie et la production d'électricité. C'est un composé polyvalent qui peut être obtenu à partir de diverses sources telles que les combustibles fossiles, les énergies renouvelables, le nucléaire et la biomasse [10]. En outre, l'hydrogène comme moyen de stockage peut améliorer le déploiement des énergies renouvelables en offrant une alternative à moyen (semaines) ou même à long terme (mois) pour compenser l'inadéquation entre la disponibilité de l'électricité et la demande [11,12]. Dans cette application, l'hydrogène offre une option avec un taux d'autodécharge réduit, qui pourrait être reconvertie en électricité si nécessaire, mais aussi en méthane (biométhane) par la voie de la conversion de l'énergie en gaz [13]. Outre le stockage de l'énergie sur de longues périodes, l'hydrogène est une alternative prometteuse pour le transport de l'énergie provenant des énergies renouvelables sur de longues distances. Par exemple, l'hydrogène pourrait être obtenu dans des régions riches en ressources solaires et/ou éoliennes comme l'Amérique latine ou l'Australie, puis être transporté et livré là où cela est nécessaire [11]. D'une manière générale, l'hydrogène peut contribuer à un système énergétique fiable, sûr, résilient et décarbonisé en permettant le couplage des secteurs et en exploitant les synergies entre les différentes formes d'énergie [7,11,12,14].

Malgré les avantages potentiels de l'utilisation de l'hydrogène comme vecteur d'énergie, et en général de la production décentralisée, la conception et l'exploitation de ce type de centrales sont une tâche difficile. Au stade de la conception, l'objectif est de sélectionner les unités de traitement pour la conversion et le stockage de l'énergie, leurs capacités et leurs conditions d'exploitation. En outre, les interconnexions entre ces unités pour la transformation des sources d'énergie en formes d'énergie utiles sont également définies à ce stade. Ainsi, la complexité repose sur trois questions principales : (i) l'incertitude des données d'entrée, (ii) le grand nombre de décisions à prendre, et (iii) la nécessité d'impliquer des objectifs différents et généralement contradictoires. La première est due à la variabilité et à la nature temporelle des sources et des demandes d'énergie, la seconde à la coexistence de multiples technologies de conversion et de stockage de l'énergie et la dernière à la nécessité de développer une industrie mondiale de manière durable [15,16]. La figure D-1 illustre de manière schématique le cadre de la conception des systèmes énergétiques.

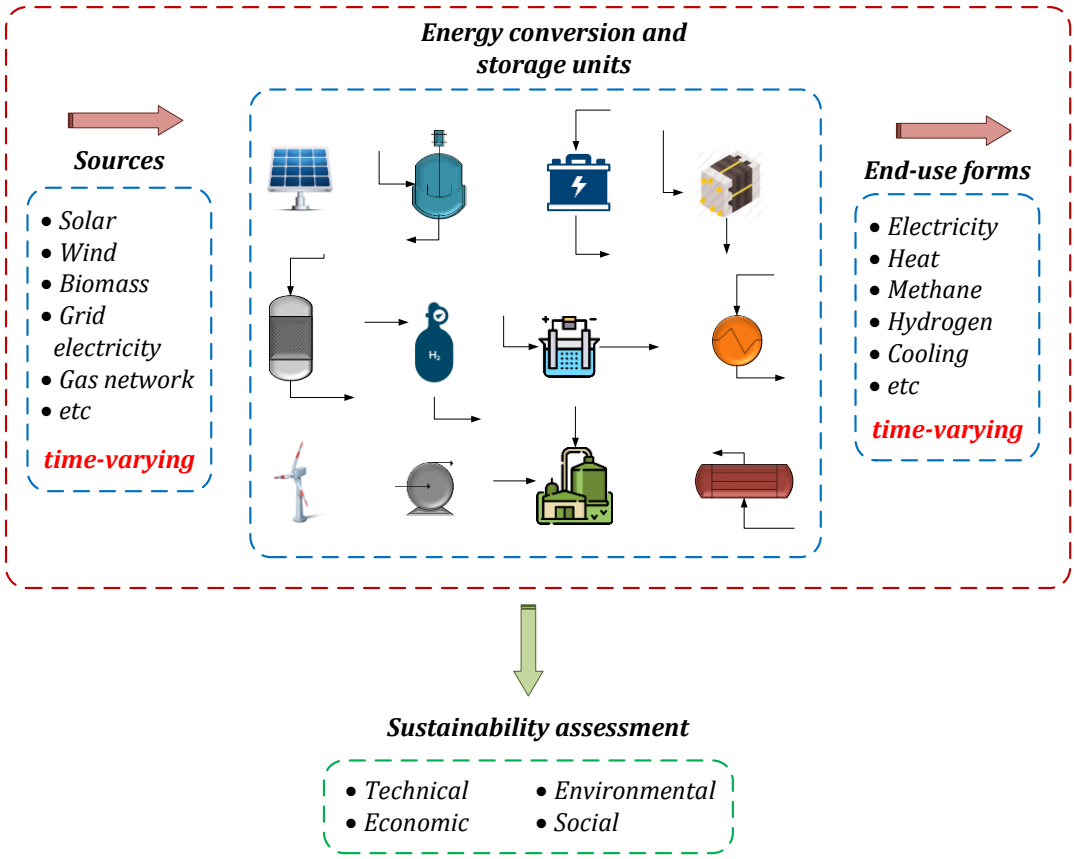

Figure D-1 : Cadre global pour la conception des systèmes énergétiques.

En général, il est bien reconnu que les décisions prises au stade de la conception sont d'une importance capitale parce qu'elles ont le plus grand niveau de liberté et, par conséquent,

la plus grande possibilité d'améliorer les performances de durabilité d'un processus [17–19]. En outre, l'énergie est un élément clé de la vie humaine car elle est le moteur de nombreux aspects de la croissance économique et sociale (par exemple, l'emploi, la production alimentaire, les revenus) [20]. L'utilisation de l'énergie est également liée aux questions environnementales, car elle représente plus des deux tiers des émissions mondiales de gaz à effet de serre [20,21]. En conséquence, l'énergie pourrait être considérée comme le principal défi et la principale opportunité que le monde doit relever pour parvenir à un développement durable [20].

Une stratégie commune d'évaluation des alternatives de processus à l'étape de la conception consiste à utiliser des outils de modélisation et d'optimisation. Les modèles de processus permettent d'effectuer une représentation virtuelle de la réalité, de sorte qu'ils fournissent un moyen peu coûteux, rapide et sûr d'étudier l'impact des décisions de conception sur les performances de durabilité d'un système. Néanmoins, le problème de la conception et du fonctionnement des systèmes énergétiques a potentiellement de nombreuses solutions possibles. D'une part, parce qu'il existe une variété d'unités de traitement et de conditions de fonctionnement qui pourraient être mises en œuvre pour convertir les sources en formes d'énergie requises. D'autre part, parce que l'évaluation de la durabilité implique d'inclure des objectifs multiples et contradictoires, de sorte que la conception et les conditions de fonctionnement du système obtenu pourraient varier en fonction de chaque dimension de la durabilité. De cette manière, énumérer, évaluer et classer toutes les alternatives serait une tâche extrêmement longue. Ensuite, une approche appropriée consiste à utiliser des méthodes mathématiques pour trouver la meilleure solution candidate sans tester explicitement l'ensemble des alternatives, c'est-à-dire pour résoudre un problème d'optimisation.

Les problèmes d'optimisation pour la conception des systèmes énergétiques ont été présentés comme des problèmes multimodaux car ils ont de multiples solutions locales [25]. Il est également reconnu que l'optimisation à objectif unique allège la charge de calcul pour résoudre le problème de conception [24]. Cependant, dans un tel cas, comme l'accent est mis sur un seul critère, le résultat obtenu laisse de côté l'impact des autres critères dans les décisions de conception. À cet égard, l'optimisation mono-objectif semble être une stratégie appropriée pour commencer à connaître l'espace de recherche et pour identifier certains points extrêmes dans les options de conception. Néanmoins, comme nous l'avons déjà dit, l'évaluation de la durabilité repose sur l'équilibre entre les aspects économiques, environnementaux et sociaux, de sorte qu'elle nécessite l'intégration simultanée de

plusieurs critères. En conséquence, la conception durable des systèmes énergétiques se transforme en un problème d'optimisation multi-objectif.

En plus de traiter plusieurs objectifs en même temps, l'optimisation multi-objectif permet d'identifier le compromis entre eux et fournit au décideur une information précieuse pour prendre une décision éclairée. En effet, grâce à l'exploration des compromis entre les dimensions de durabilité, le décideur peut reconnaître l'impact des décisions de conception en termes de variables de conception et de critères de performance.

D'une manière générale, l'état actuel de la littérature montre que la conception des systèmes énergétiques est principalement effectuée sur la base de critères économiques et environnementaux, négligeant ainsi l'impact de la dimension sociale. En fait, lorsqu'ils sont inclus, les aspects sociaux sont pris en compte après pour résoudre le problème d'optimisation, de sorte qu'ils ne constituent pas un critère lors de la conception du système [25]. Néanmoins, en plus d'être économiquement réalisables et respectueuses de l'environnement, les activités industrielles doivent répondre à des exigences sociales, c'est-à-dire améliorer la qualité de vie[26,27]. De plus, même si la conception du système énergétique est avant tout un défi technique, les aspects sociaux peuvent devenir les facteurs les plus importants pour sa mise en œuvre réussie dans la communauté [28].

Les DES se présentent comme des systèmes socio-techniques complexes car ils impliquent différents acteurs en relation étroite avec un ensemble de dispositifs technologiques [29]. À cet égard, il est primordial de promouvoir une participation intense de toutes les parties prenantes et d'intégrer leurs points de vue dans le processus décisionnel [30]. En effet, cette intégration pourrait renforcer l'appropriation des technologies énergétiques par la communauté et avoir un impact positif sur leur mise en œuvre [31,32]. Au contraire, le manque d'implication des parties prenantes peut engendrer une résistance et, par conséquent, limiter le déploiement de solutions technologiques prometteuses [32]. Pour répondre à cette question, il est nécessaire de développer des outils méthodologiques permettant d'analyser ces systèmes socio-techniques dans le cadre du développement durable, c'est-à-dire en considérant leurs aspects économiques, environnementaux et sociaux [24,28,30].

Compte tenu de cela, ce projet devrait fournir un cadre complet pour l'analyse et l'évaluation des systèmes énergétiques distribués en tenant compte des dimensions de durabilité dès les premières étapes de la conception.

Représentation et évaluation du système énergétique

Au stade de la conception, de nombreuses décisions à prendre sont liées à des variables discrètes, telles que l'emplacement des unités de conversion dans le schéma et le choix entre différentes technologies pour une fonction spécifique. Cela conduit à envisager un très large éventail d'alternatives de conception, et contribue par conséquent à la complexité de la tâche de synthèse du processus. Plus précisément, les multiples formes d'énergie incluses dans les DES impliquent une quantité massive d'options pour la transformation et le stockage de l'énergie. Par conséquent, un grand nombre de schémas de processus pourraient être générés. Cependant, la réalisation d'une représentation complète de toutes les technologies disponibles dans les DES, et l'évaluation exhaustive de toutes les configurations de systèmes possibles dépassent le cadre de ce travail.

En tenant compte de cela, un ensemble de technologies candidates a été sélectionné pour construire un schéma de processus de base. Le choix de ce groupe d'unités de conversion et de stockage de l'énergie a été basé sur les résultats de notre étude [11] et sur la littérature concernant la conception des DES. Ainsi, le système énergétique de base considéré dans cette thèse est représenté sur la figure D-2.

Comme l'indique la figure D-2, les sources d'énergie considérées comprennent les ressources solaires, éoliennes et de biomasse, en plus de la possibilité d'importer de l'électricité et du gaz naturel du réseau principal. Ces apports énergétiques sont convertis et/ou gérés au sein du système pour satisfaire la demande d'électricité, d'hydrogène et de méthane. L'électricité est fournie par des panneaux photovoltaïques, des éoliennes ou le réseau électrique. Pour remédier à l'inadéquation entre la disponibilité de l'énergie provenant des énergies renouvelables et la demande, pendant les périodes de forte production d'électricité par des panneaux photovoltaïques ou des éoliennes, le surplus d'énergie peut être stocké dans une batterie électrique ou sous forme d'hydrogène en utilisant un électrolyseur et un réservoir sous pression. Dans cette dernière option de stockage, l'hydrogène peut être reconverti en électricité lorsque cela est nécessaire en utilisant une pile à combustible. En ce qui concerne l'hydrogène, il peut être obtenu par électrolyse de l'eau ou par des procédés de reformage du méthane à la vapeur. Dans le premier cas, le processus est alimenté par de l'électricité renouvelable ou dérivée du réseau, et dans le second cas, on utilise du méthane obtenu par digestion anaérobie ou par le réseau de gaz. En outre, la demande de méthane peut être satisfaite par la transformation de la biomasse, la réaction de méthanisation ou le réseau de gaz naturel. Pour l'unité de méthanisation, les réactifs sont le CO_2 et l'hydrogène provenant de l'électrolyse de l'eau. Le

CO_2 peut être obtenu à partir de diverses sources, y compris des opérations au sein du système telles que la valorisation du biogaz (digestion anaérobie) et la réaction de reformage, mais il peut également être capté dans l'air ou directement importé des rejets de l'industrie (par exemple le ciment).

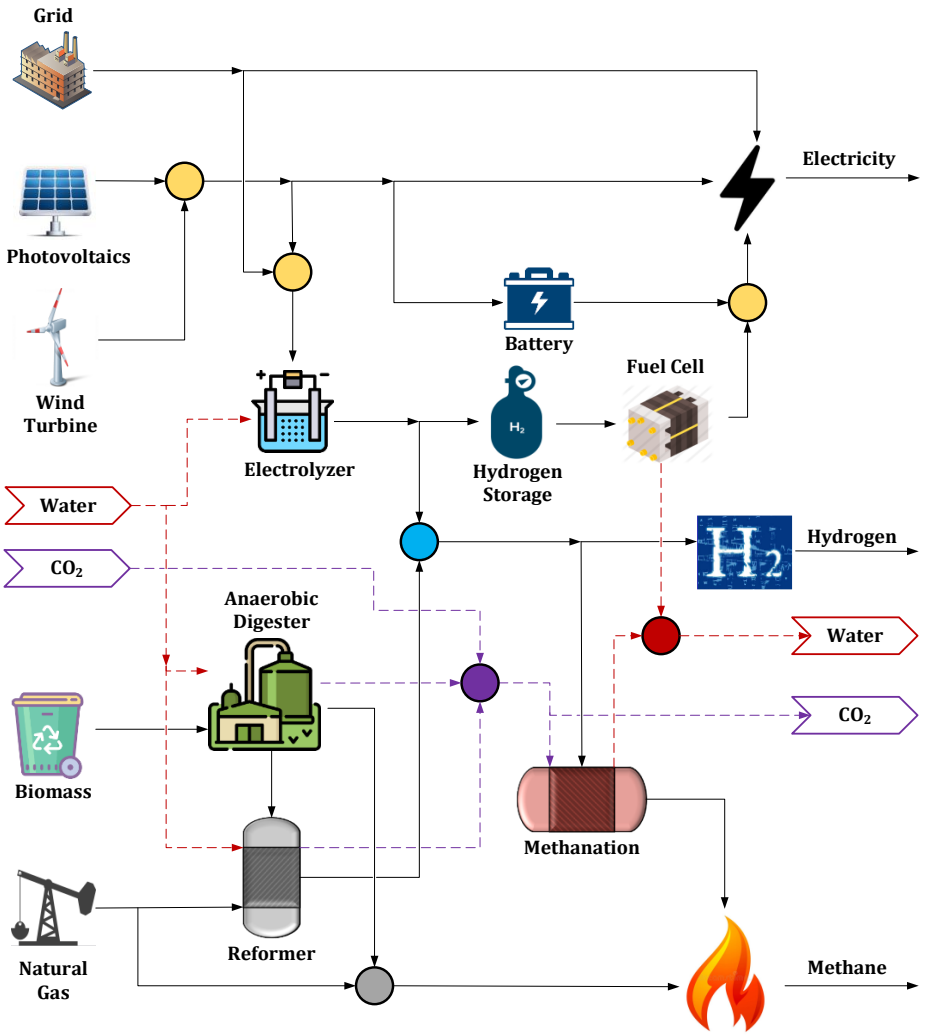

Figure D-2 : Schéma de base du système énergétique. (●) électricité, (●) hydrogène, (●) eau, (●) CO_2, (●) méthane.

Modèle de système énergétique

Le modèle proposé vise à être utilisé pour la conception de systèmes énergétiques. Dans cette optique, l'objectif est de construire une formulation mathématique capable de saisir les principales caractéristiques du système (relations entre les unités de processus, comportement en fonction du temps, stockage d'énergie), puis d'effectuer les bilans de masse et d'énergie pour l'évaluation ultérieure des performances du système. Par

conséquent, le modèle de système énergétique présente quatre caractéristiques principales :

1. Il s'agit d'un modèle d'état pseudo-stationnaire, de sorte que la dépendance temporelle est prise en compte mais que les unités de processus avec des réponses instantanées sont supposées. Par conséquent, l'accumulation dans les convertisseurs d'énergie est négligée. De plus, l'évolution de l'énergie stockée est traitée par la discrétisation de la variable temporelle.
2. Les conditions de fonctionnement des convertisseurs d'énergie sont fixes, puis les variables d'entrée/sortie sont liées au moyen de rendements constants et d'expressions linéaires.
3. Il n'y a pas de pertes d'énergie sur les lignes de connexion.
4. Il s'agit d'un modèle déterministe et toutes les tailles d'équipement sont considérées comme des variables continues.

Évaluation de la durabilité

Le développement durable favorise l'équilibre entre trois aspects : la réussite économique, l'acceptation sociale et la protection de l'environnement [22]. Tout d'abord, la durabilité économique repose sur l'utilisation efficace des matières premières et des ressources naturelles. Par conséquent, l'utilisation de nouvelles technologies et de ressources alternatives, ainsi que le recyclage des déchets sont primordiaux. Deuxièmement, la durabilité sociale est basée sur le bien-être des personnes, la justice sociale et les droits des individus. À cet égard, il est essentiel de tenir compte de la perception du public et de sensibiliser les gens à l'épuisement des ressources fossiles et au changement climatique pour obtenir leur engagement à préserver les ressources naturelles. Enfin, la durabilité environnementale repose sur le maintien de la capacité des écosystèmes à soutenir la vie et l'activité industrielle. Ainsi, l'emploi de ressources renouvelables et la réduction des déchets nocifs pour l'environnement sont les piliers de cet axe [19,22,78]. La figure 2-3 présente une représentation schématique des trois dimensions de la durabilité, également appelée dans la littérature "triple bottom line" (TBL), et de leurs interactions.

Dans ce travail, le choix des indicateurs a été basé sur les informations de la littérature. Ainsi, les indicateurs sélectionnés présentent quatre caractéristiques principales : (i) ils couvrent les trois dimensions de la durabilité, (ii) ils sont directement liés aux décisions de conception, (iii) ils peuvent être définis grâce aux informations provenant des bilans de

masse et d'énergie, et (iv) ils ont été identifiés comme pertinents pour l'évaluation des systèmes énergétiques.

Dimension économique

Dans un marché concurrentiel, la faisabilité économique est vitale pour un nouveau projet. En effet, une viabilité financière défavorable n'est pas durable. À cet égard, les indicateurs de la dimension économique doivent décrire la rentabilité et les coûts du système énergétique. En conséquence, le coût total annualisé (*TAC*) et le coût nivelé de l'énergie (*LCOE)* ont été sélectionnés comme étant les indicateurs les plus pertinents pour évaluer la performance économique des systèmes énergétiques [134,137,138,140–143].

Dimension environnementale

Les systèmes énergétiques conventionnels sont fortement dépendants des combustibles fossiles. En conséquence, l'énergie est le principal facteur de changement climatique, représentant plus de 80 % des émissions de CO_2 en 2018 [21]. Les systèmes énergétiques doivent donc être conçus de manière à réduire ou à éliminer ces rejets, car ils constituent l'une des variables clés pour définir la durabilité d'un processus [137,138,141,143–146].

D'autre part, des milliards de personnes dans le monde manquent encore d'eau potable et d'hygiène ([147]. En outre, les pénuries d'eau dues aux effets du changement climatique font de l'utilisation de l'eau une autre question d'une importance capitale pour l'évaluation des activités industrielles ([144]. Par conséquent, il convient d'éviter les fortes consommations d'eau dans les processus de conversion énergétique, car elles ne sont pas durables [18,134,143,144,148].

En tenant compte de cela, les émissions de CO_2 et la consommation d'eau ont été sélectionnées comme indicateurs pour évaluer la dimension environnementale lors de la conception du système énergétique.

Dimension sociale

Outre la viabilité économique et le respect de l'environnement, les activités industrielles doivent répondre à des exigences sociales, c'est-à-dire améliorer la qualité de vie [26,27]. À cet égard, la perception et l'acceptabilité du public sont d'une importance capitale, car elles peuvent définir si une solution énergétique est mise en œuvre ou non, et représentent le coût immatériel associé à l'image du projet [18,142].

D'une manière générale, la qualité de vie peut être associée à deux aspects principaux : l'équité et la santé. En ce qui concerne l'énergie, l'équité sociale implique le niveau d'équité et d'inclusion pour la distribution des ressources énergétiques [26]. En effet, cette question est abordée dans l'un des objectifs de développement durable proposés par les Nations unies (objectif 7), qui consiste à assurer à tous l'accès à une énergie abordable, fiable, durable et moderne [20]. En outre, l'aspect sanitaire fait référence à la pollution potentielle, aux accidents, aux blessures ou aux décès liés à la production d'énergie. D'une part, la question de la pollution relève généralement de la dimension environnementale, car elle est quantifiée à l'aide de variables telles que les émissions de gaz, les particules ou la contamination de l'eau. D'autre part, les accidents du travail et les risques pour la population sont liés au risque inhérent à l'exploitation des technologies de conversion (par exemple, les conditions de température et de pression) et aux propriétés des composés chimiques (par exemple, l'inflammabilité, la toxicité) utilisés dans les systèmes énergétiques [26,134,137,142,143,148].

En conséquence, la dépendance à l'égard des importations d'énergie et l'indice de sécurité intrinsèque sont les indicateurs choisis pour évaluer la performance du système énergétique.

Optimisation des processus

Étude de cas n° 1 : France

L'étude de cas est une communauté hypothétique de 1500 habitants près de Marseille - France. Ce cas d'application considère le réseau électrique, le photovoltaïque, la biomasse et le réseau de gaz comme des intrants énergétiques. Les demandes énergétiques correspondent à l'électricité et à l'hydrogène. Ainsi, la structure de base du système énergétique peut être réduite (par rapport au cas général, figure D-2) puisque la demande en éoliennes et en méthane n'est pas incluse. Par conséquent, le schéma de base correspondant du système énergétique est illustré à la figure D-3.

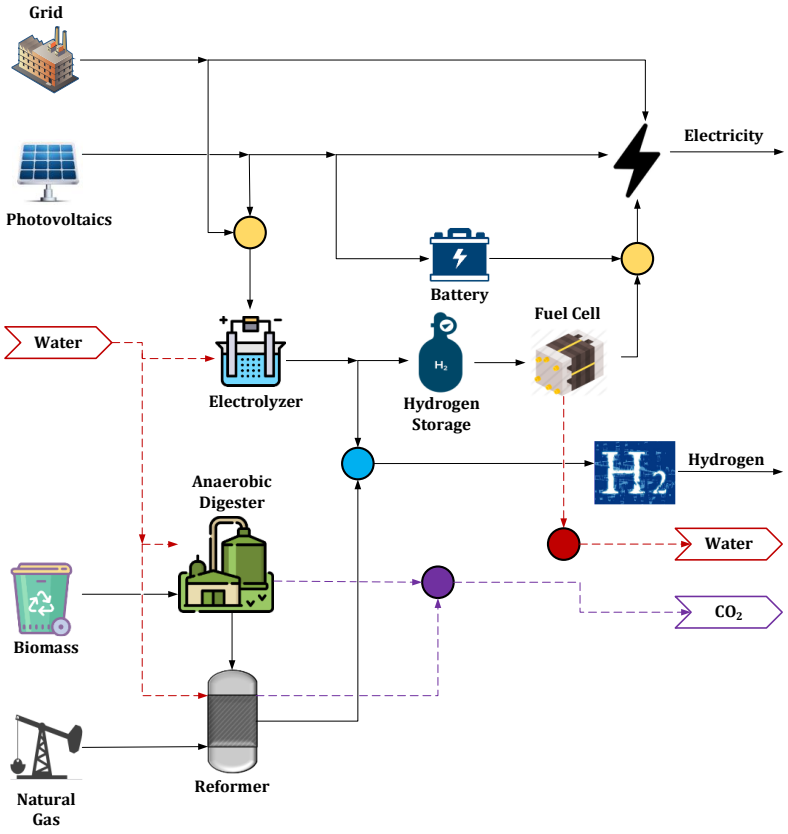

Figure D-3 : Schéma de base du système énergétique pour l'étude de cas.

La figure D-4 illustre les fronts de Pareto pour deux problèmes d'optimisation multi-objectifs : (i) économico-environnemental (figure D-4a), et (ii) économico-social (figure D-4b)

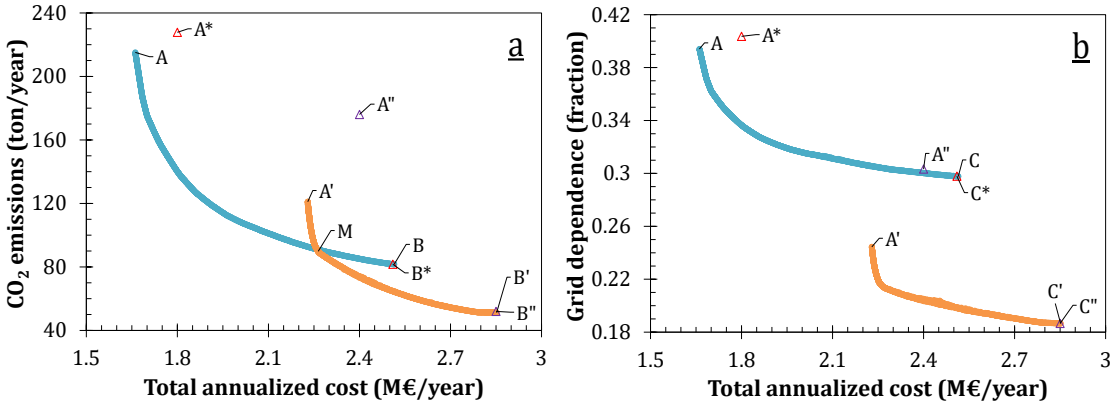

Figure D-4 : Fronts de Pareto et résultats de l'optimisation mono-objectif. (a) Émissions de CO_2 - coût, (b) Dépendance à l'égard du réseau - coût. Surface photovoltaïque (● - Δ) 7500 m², (● - Δ) 10000 m². (A - A' - A* - A") coût optimal, (B - B' - B* - B") émission optimale, et (C - C' - C* - C") dépendance optimale du réseau.

Notons tout d'abord que les points A-A'-A"-A* correspondent à la meilleure performance du point de vue économique, les points B-B'-B"-B* représentent la meilleure solution du

point de vue environnemental, et les points C-C'-C"-C* représentent l'optimum social. Parmi ces points, A-A'-B-B'-C-C' correspondent aux résultats de l'optimisation multi-objectifs, tandis que les points A"-A*-B"-B*-C"-C* représentent les résultats de l'optimisation mono-objectif. Ainsi, les fronts de Pareto obtenus reflètent le comportement concurrentiel des deux paires d'objectifs, puisque plus le coût total annualisé diminue, plus les émissions de CO_2 et la dépendance au réseau s'aggravent. Il convient également de noter que l'optimum économique n'est pas le même pour les optimisations à objectif unique et à objectifs multiples. Ce fait est observé en comparant les points A et A* pour une surface PV de 7500 m^2, et les points A' et A" pour 10000 m^2. En effet, les résultats des optimisations mono-objectives (A* et A") sont des points dominés, ce qui suggère qu'ils correspondent à un optimum local. A l'inverse, lorsque les émissions de CO_2 et la dépendance au réseau sont optimisées, les résultats de l'optimisation mono-objectif et multi-objectifs sont identiques (B-B*, B'-B", C-C* et C'-C").

De plus, la figure D-4 illustre également l'influence de la surface PV sur la performance du système énergétique. À cet égard, des surfaces PV plus grandes permettent de réduire les émissions de CO_2 et la dépendance au réseau, mais entraînent également un coût économique plus élevé. En général, ces résultats fournissent un large éventail de solutions qui peuvent être évaluées plus en détail pour le décideur en vue de leur mise en œuvre. Il est intéressant de noter que les résultats montrent qu'il existe une zone où la surface PV de 7500 m^2 ne sera pas compétitive par rapport à la surface de 10000 m^2. Cela se produit pour les solutions situées entre les points B et M parce que toutes pourraient être améliorées sur au moins un critère en utilisant une surface PV de 10000 m^2. Mathématiquement, cela implique que les solutions situées dans la ligne MB sont dominées par celles obtenues avec une surface PV de 10000 m^2 (ligne A "B"). Ainsi, si le décideur est prêt à investir entre 2,3 et 2,5 millions d'euros, il serait préférable d'installer une surface PV de 10000 m^2 au lieu de 7500 m^2, car pour le même coût, on pourrait obtenir des émissions de CO_2 plus faibles et une dépendance au réseau.

La figure D-5 montre la configuration du système énergétique pour les points extrêmes du front de Pareto, c'est-à-dire ceux obtenus à partir de l'optimisation mono-objectif. Notez que, du point de vue de la conception, la différence de la structure du système énergétique réside dans la source de méthane pour le processus de reformage. Ainsi, lorsque l'objectif économique est abordé, tout le méthane est importé du réseau (figure D-5a). En revanche, si l'objectif est de réduire les émissions de $_{CO2}$ ou la dépendance du réseau, le réacteur du reformeur est alimenté avec du méthane provenant du processus de digestion anaérobie (figure D-5b).

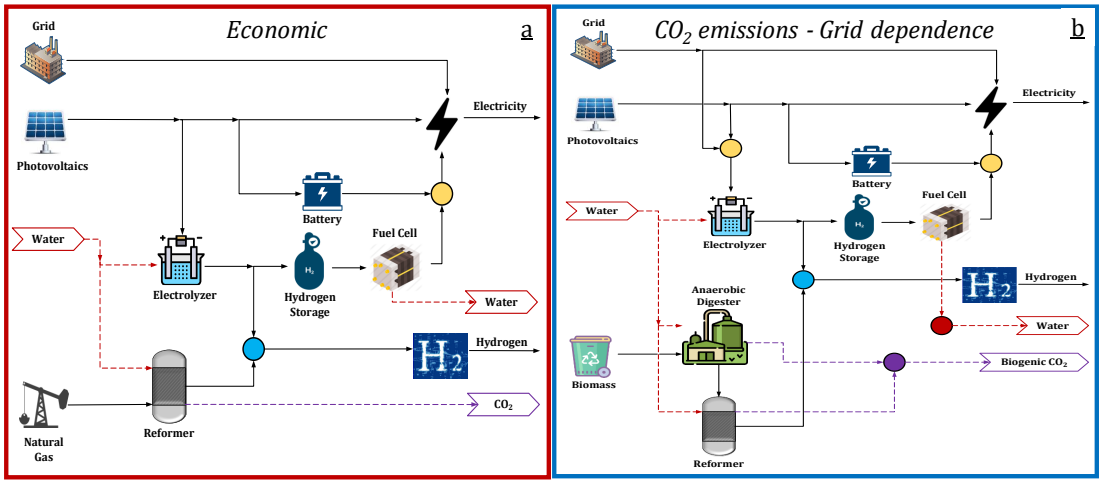

Figure D-5 : Configuration optimale du système énergétique pour les points extrêmes des fronts de Pareto. Fonction objective (a) coût total annualisé, et (b) émissions de CO_2 et dépendance du réseau.

Dans le but d'élucider les différences de conception et de conditions de fonctionnement sur les différents fronts de Pareto, la figure D-6 présente la taille installée et l'utilisation de certaines sources d'énergie en fonction du coût total annualisé. Comme indiqué dans les figures D-6a et D-6b, il existe une relation directe entre les capacités de stockage d'énergie et le coût total du système. Ensuite, les meilleures configurations du point de vue économique correspondent à celles qui ont les plus petites unités de stockage. Les figures D-6c et D-6d illustrent quant à elles le changement de source de méthane pour le processus de reformage. Comme observé, la meilleure performance pour les indicateurs d'émissions de CO_2 et de dépendance au réseau est obtenue sans importer de méthane du réseau et en utilisant la quantité maximale de biomasse disponible. Ensuite, à mesure que la performance économique s'améliore, le gaz naturel importé augmente et la biomasse devient inutilisée, mais au prix d'une augmentation des émissions de CO_2 et de la dépendance au réseau. Il est intéressant de noter que, si les capacités de stockage sont les variables qui influent le plus sur le critère du coût, la source de méthane a l'impact le plus important sur les questions d'émissions et de dépendance au réseau. Ce fait peut être observé en analysant les figures D-4 et D-6. Ainsi, en passant d'une faible émission à un faible coût, on observe que l'altération la plus significative sur la pente des courbes de Pareto correspond à un changement important sur les courbes du gaz naturel importé et de la consommation de biomasse. En gros, cela se produit à une valeur de 1,9 M€ pour une surface PV de 7500 m^2, et à 2,2 M€ lorsque la surface PV est de 10000 m^2.

En outre, comme indiqué précédemment, l'optimum économique de l'optimisation multi-objectifs diffère de celui obtenu par l'optimisation à objectif unique. À cet égard, les différences en termes de variables de processus peuvent être notées dans la figure D-6. Là

encore, les points A"-A* représentent les résultats de l'optimisation à objectif unique pour la surface PV de 7500 et 10000 m², respectivement. D'une part, comme l'observe la figure D-6a, l'algorithme d'optimisation multi-objectifs trouve une solution dans laquelle la capacité requise de la batterie est plus petite par rapport à celle obtenue par l'optimisation mono-objectif. En conséquence, cela conduit à un système énergétique avec un TAC plus faible. D'autre part, comme le montre la figure D-6d, les résultats de l'optimisation mono-objectif indiquent que la biomasse n'est pas utilisée à l'optimum économique (points A"-A*). Inversement, selon les résultats de l'optimisation multi-objectifs, les extrêmes économiques des solutions de Pareto (A-A') incluent toujours l'utilisation de la biomasse. Par conséquent, comme l'observe la figure D-4, l'optimum économique issu de l'optimisation mono-objectif a une performance plus faible dans les indicateurs d'émissions de CO_2 et de dépendance au réseau.

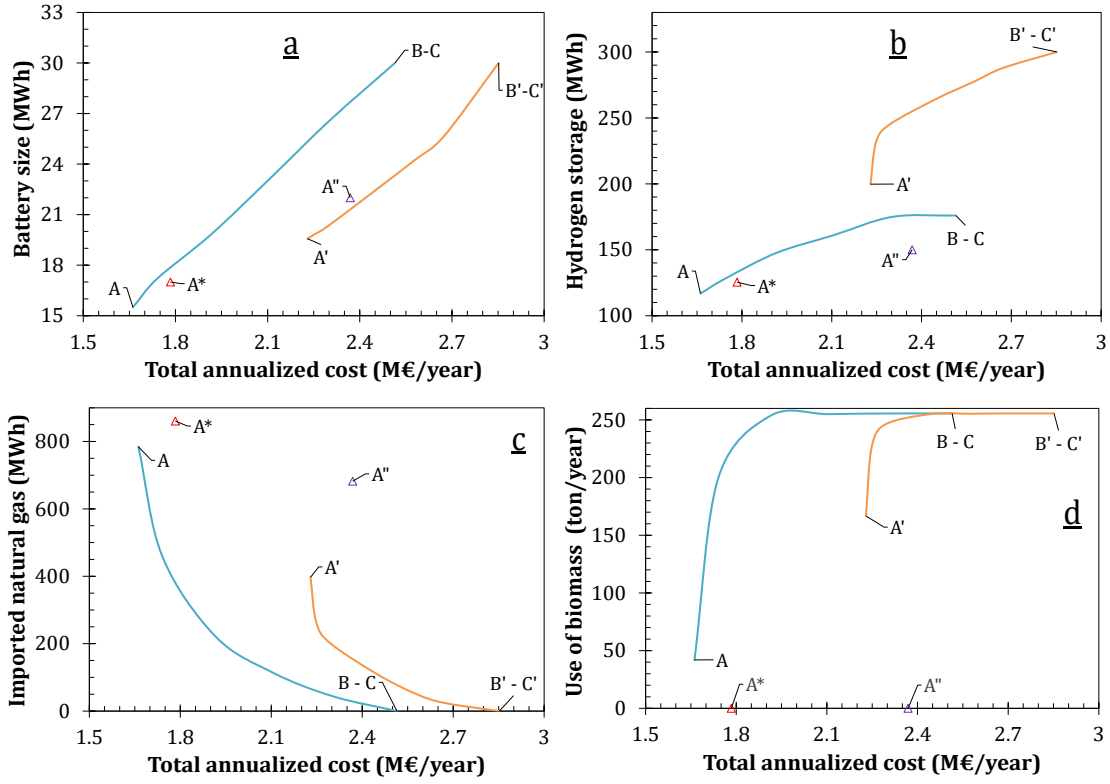

Figure D-6 : Modification des conditions de conception et d'exploitation sur les fronts de Pareto. Surface photovoltaïque (— et Δ) 7500 m² et (— et Δ) 10000 m². (a) batterie, (b) réservoir pressurisé, (c) gaz naturel importé, et (d) consommation de biomasse. (A - A') coût optimal, (B - B') émission optimale, (C - C') dépendance optimale du réseau, (A* - A").

En outre, il est également noté que l'utilisation de la biomasse ne semble pas avoir un grand impact sur l'indicateur économique (figure D-6d). Ce fait peut donc expliquer pourquoi, même en considérant différentes tailles de population (500, 1000, 2000, 3000 et 4000

individus), l'algorithme d'optimisation multi-objectifs ne trouve pas de point sans inclure la biomasse dans le système énergétique.

En plus du problème d'optimisation précédent, trois autres scénarios à objectifs multiples ont été évalués en incluant différentes combinaisons d'indicateurs de durabilité. Les résultats obtenus élucident les relations entre les différentes fonctions objectives et fournissent un large éventail de structures de systèmes et de conditions de fonctionnement optimales. En général, les résultats indiquent que le coût total annualisé, la consommation d'eau et les indicateurs de sécurité s'améliorent à mesure que la surface PV diminue. En revanche, des surfaces PV plus grandes favorisent l'autonomie énergétique et la réduction des émissions de CO_2. De plus, pour une surface PV donnée, les fronts de Pareto obtenus reflètent le compromis et le comportement concurrentiel parmi les critères de durabilité. Par exemple, à mesure que le coût total annualisé diminue, les émissions de CO_2 et la dépendance au réseau s'aggravent. De plus, la consommation minimale d'eau conduit au plus faible rendement sur les indicateurs de coût et d'autosuffisance. Par ailleurs, la plus faible dépendance au réseau exige la plus grande consommation d'eau. De plus, il a été identifié que plus le danger du système énergétique diminue, plus le coût et les émissions du système énergétique augmentent.

En outre, l'ensemble des solutions de Pareto a été exploré et analysé pour identifier les changements dans la conception et les conditions d'exploitation à travers les résultats de l'optimisation. Dans l'ensemble, ces résultats constituent une information précieuse pour le processus décisionnel ultérieur, car ils décrivent le compromis entre les dimensions de durabilité et l'impact de toute décision en termes de conception et d'exploitation du système énergétique.

Étude de cas n° 2 : Colombie

L'étude de cas porte sur un échantillon de 10 % de la population de la ville de Leticia, soit environ 4160 habitants. Les sources d'énergie évaluées sont l'énergie solaire et la biomasse (déchets domestiques), tandis que les demandes énergétiques sont l'électricité et le méthane. L'énergie éolienne n'est pas évaluée car il n'y a pas de potentiel dans cette zone du pays. En effet, la région sud a le plus faible potentiel du pays, avec une vitesse moyenne du vent d'environ 1,5-2 m/s [215]. En conséquence, le schéma de base correspondant du système énergétique est représenté dans la figure D-7. Notez qu'il n'inclut pas la connexion ni au réseau électrique ni au réseau de gaz, puisqu'il s'agit d'un système énergétique isolé.

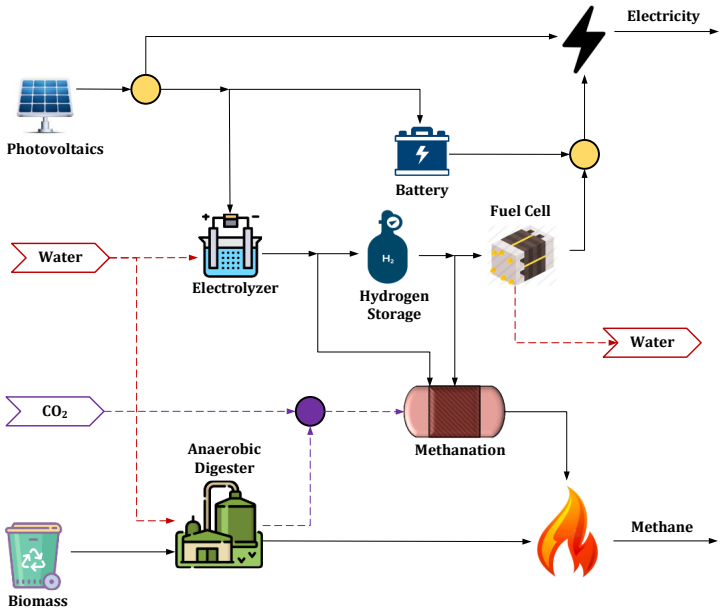

Figure D-7 : Schéma de base du système énergétique pour l'étude de cas en Amazonie colombienne.

La figure D-8 illustre les configurations optimales du système énergétique pour chacun des problèmes d'optimisation. De manière générale, les résultats obtenus permettent d'élucider l'influence de la fonction objectif sur la conception optimale du système énergétique. Notez que la différence entre les structures du système repose sur les technologies de stockage de l'électricité et de production de méthane. Il est intéressant de noter que dans tous les cas d'optimisation, les deux technologies de stockage de l'énergie sont incluses. Néanmoins, l'utilisation de chacune d'entre elles est très différente selon la fonction objective. Ainsi, selon les résultats de l'optimisation économique (figure D-8a), le système tente de maintenir la taille de la batterie aussi petite que possible. Cela peut s'expliquer en comparant les coûts d'investissement du réservoir sous pression (7,2 €/kWh) et de la batterie (520 €/kWh). Par conséquent, comme l'objectif est de minimiser le coût total du système énergétique, il est crucial de réduire la capacité de l'alternative la plus coûteuse. Sinon, en ce qui concerne la demande de méthane, les résultats obtenus suggèrent que le processus de digestion anaérobie est préférable à la méthanisation. En effet, en plus du réacteur de méthanisation lui-même, le processus de méthanisation nécessite également une source d'hydrogène (électrolyseur), et il implique le coût de la capture du CO_2 de l'atmosphère. Par conséquent, cette alternative implique un coût plus élevé que la digestion anaérobie.

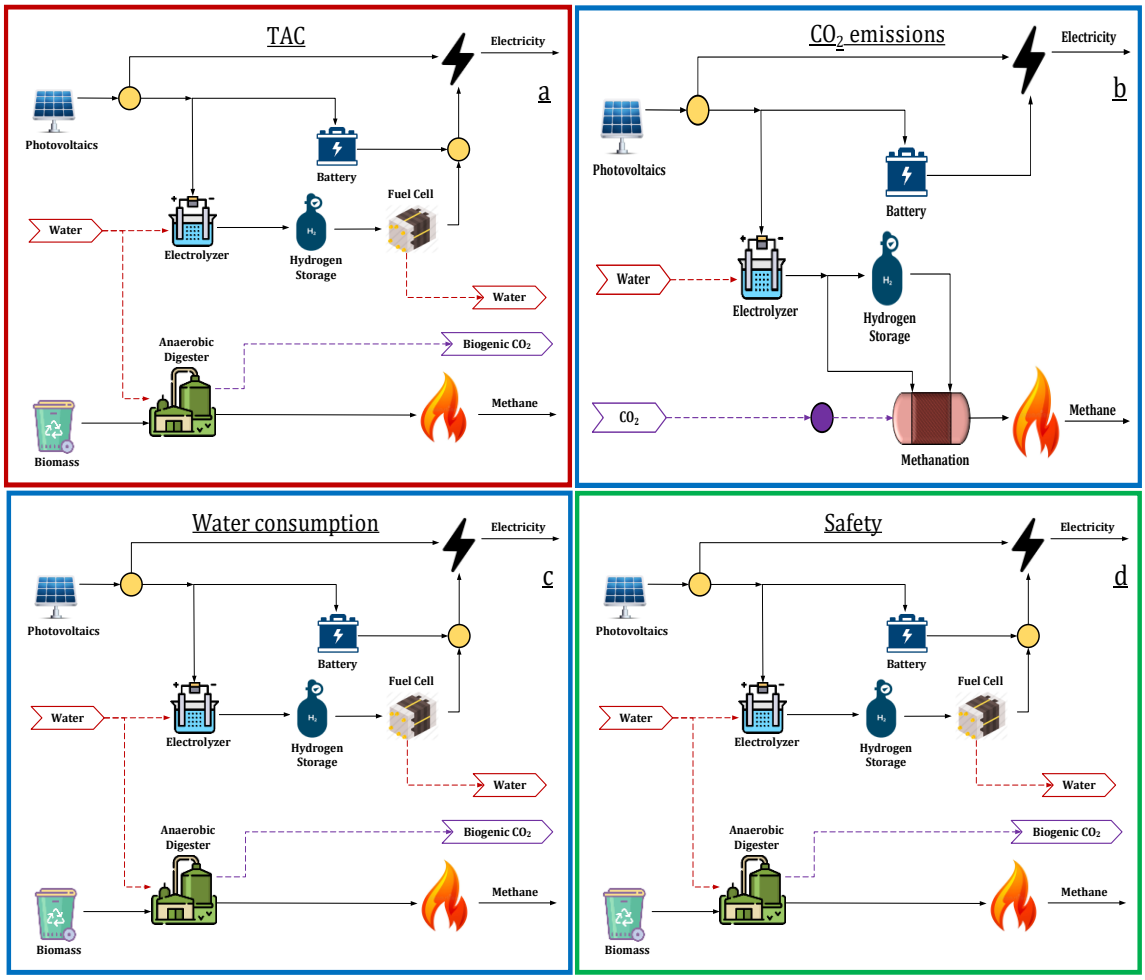

Figure D-8 : Configuration optimale du système énergétique distribué pour chacun des critères de durabilité.

En revanche, lorsque l'indicateur d'émission de CO_2 est pris en compte (figure D-8b), la batterie est l'alternative utilisée pour compenser le décalage entre la disponibilité et la consommation d'électricité. En attendant, le réservoir pressurisé est pleinement utilisé pour alimenter en hydrogène le réacteur de méthanisation. Cela peut s'expliquer par l'analyse des sources de méthane en termes d'émissions de CO_2. À cet égard, l'objectif étant de minimiser cet indicateur, le système privilégie le processus de méthanisation car il représente une alternative pour capturer le CO_2 de l'atmosphère. En effet, cette opération permet de produire du méthane avec un bilan négatif des émissions de CO_2. Par conséquent, dans le but d'augmenter la disponibilité de l'électricité pour l'électrolyse de l'eau et la méthanisation qui s'ensuit, le système utilise la batterie pour le stockage de l'électricité en raison de son rendement élevé aller-retour.

Il est intéressant de noter que le schéma du système énergétique est le même lorsque la consommation d'eau et l'indicateur de sécurité sont minimisés. Ce résultat peut s'expliquer

par deux faits principaux. D'une part, en ce qui concerne le stockage de l'électricité excédentaire, les deux problèmes d'optimisation donnent la priorité à l'utilisation de la batterie électrique car elle n'implique ni consommation d'eau ni risques de sécurité. En effet, d'après une analyse plus approfondie, on constate que le système de stockage d'hydrogène n'est utilisé que parce que la batterie atteint la capacité maximale imposée dans le problème d'optimisation. De plus, en comparant les profils de l'énergie stockée de ces deux cas d'optimisation, on constate que les structures du système énergétique sont les mêmes, mais que le dimensionnement des équipements et les politiques d'exploitation sont différents. À cet égard, l'optimisation de la consommation d'eau tente de réduire l'emploi du système de production d'énergie sans tenir compte de la taille du réservoir sous pression. À l'inverse, la minimisation de la sécurité inhérente se concentre sur la réduction du stock de matériel dans le système, ce qui conduit à installer un réservoir pressurisé aussi petit que possible.

D'autre part, en ce qui concerne la production de méthane, les résultats de l'optimisation indiquent que le digesteur anaérobie est la meilleure alternative pour obtenir du méthane du point de vue de la consommation d'eau et de la sécurité. Dans le premier cas, cela se produit parce que pour produire 1 MWh de méthane au moyen du processus de méthanisation, il faut environ 420 litres d'eau (électrolyse). En revanche, le processus de digestion de la biomasse nécessite 264 litres d'eau par MWh de méthane. Dans ce dernier cas, c'est-à-dire en ce qui concerne l'indicateur de sécurité, la sélection repose sur les conditions de fonctionnement des alternatives. Ainsi, le réacteur de méthanisation fonctionne dans des conditions plus intenses que le digesteur anaérobie. Par conséquent, afin d'éviter des conditions potentiellement dangereuses, la digestion de la biomasse est préférée à la méthanisation pour satisfaire la demande de méthane.

De plus, la figure D-9 illustre les fronts de Pareto obtenus en considérant un problème d'optimisation multi-objectifs entre les indicateurs de coût et d'émissions de CO_2. En général, les résultats obtenus indiquent le comportement contradictoire entre les indicateurs de coûts et d'émissions (figure D-9). Ainsi, on observe que si les émissions de CO_2 sont réduites, le coût du système énergétique augmente. En outre, les résultats élucident l'influence de la surface PV sur les fronts de Pareto. A cet égard, il faut noter que la performance de l'indicateur économique s'aggrave à mesure que la surface du PV augmente. Cela se produit parce qu'une plus grande surface de PV entraîne une plus grande quantité d'électricité excédentaire, et par conséquent, des unités plus grandes sont nécessaires pour le stockage de l'énergie, ce qui se traduit par des coûts plus élevés. En revanche, une installation photovoltaïque de plus grande taille permet d'améliorer

l'indicateur des émissions de CO_2, car dans ce cas, la quantité d'électricité produite à partir de sources renouvelables est plus importante. En conséquence, de faibles niveaux d'émission sont atteints car une plus grande quantité de biométhane peut être produite par le processus de méthanisation, ce qui implique de capturer plus de CO_2 dans l'air.

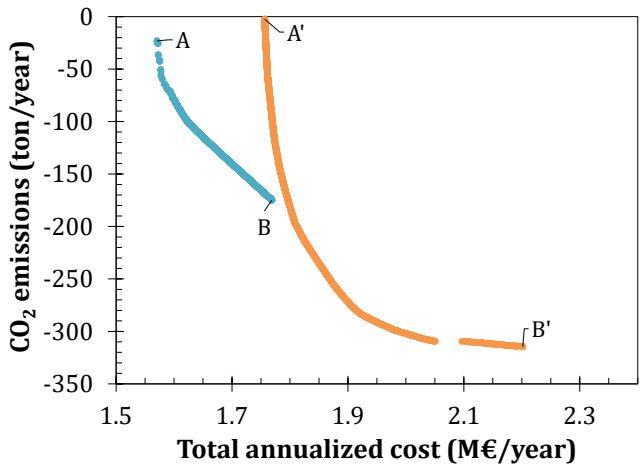

Figure D-9 : Fronts de Pareto pour minimiser le coût total annualisé et les émissions de CO_2. Surface photovoltaïque (●) 12250 m², (●) 14700 m². (A - A') coût minimal, (B - B') émissions de CO_2 minimales.

Sinon, la figure D-10 illustre certains des changements dans la conception et les conditions de fonctionnement sur les fronts de Pareto. Comme déjà évoqué dans les résultats de l'optimisation mono-objectif, l'optimisation économique privilégie l'utilisation de l'hydrogène pour le stockage de l'électricité en raison de ses coûts inférieurs par rapport à la batterie. À l'inverse, lorsque les émissions de CO_2 sont réduites au minimum, la batterie est utilisée pour le stockage de l'électricité et l'hydrogène se concentre sur la production de biométhane au moyen du réacteur de méthanisation. De cette manière, passer de l'optimum économique (points A et A') à l'optimum environnemental (points B et B') nécessite à la fois d'augmenter la capacité de la batterie (figure D-10a) et de réduire la taille de la pile à combustible (figure D-10b). En outre, à mesure que le rendement de l'indicateur d'émission s'améliore, la part du réacteur de méthanisation pour répondre à la demande de méthane augmente également (figure D-10c), car ce processus favorise le captage du CO_2 de l'atmosphère.

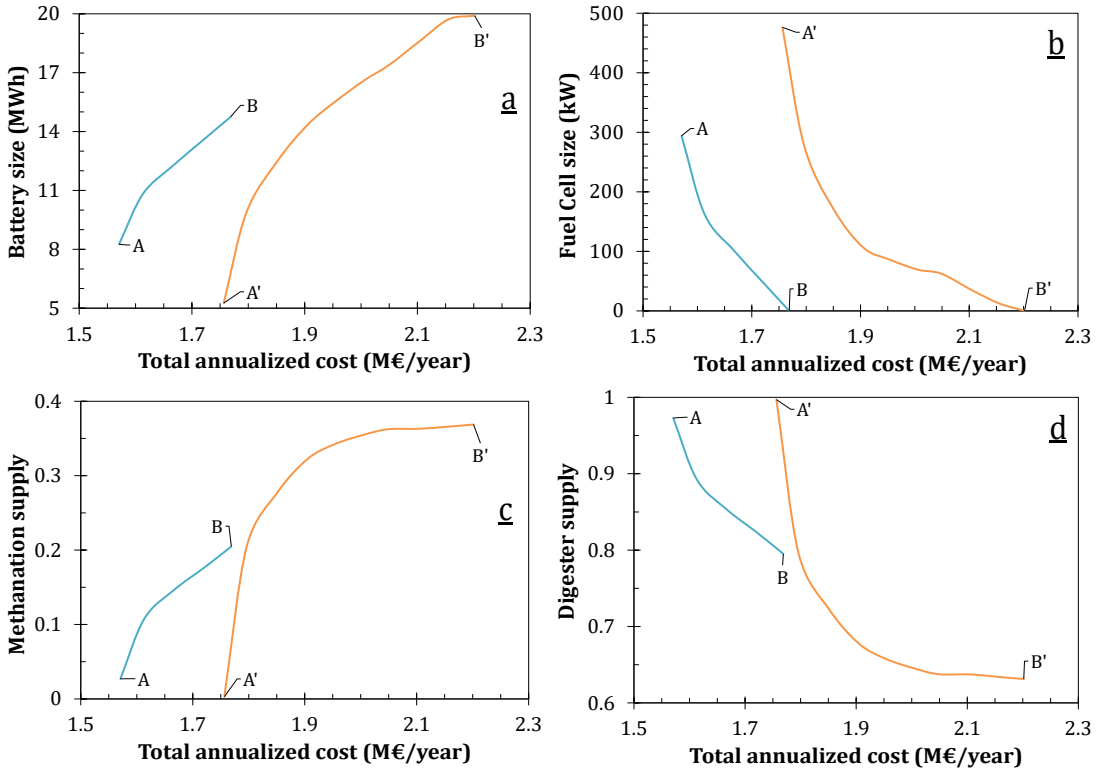

Figure D-10 : Modification de la conception et des conditions de fonctionnement sur les fronts de Pareto. Surface photovoltaïque (—) 12250 m² et (—) 14700 m². (a) taille de la batterie, (b) taille de la pile à combustible, fraction du méthane fournie par (c) les processus de méthanisation et (d) de digestion. (A - A') coût minimal, (B - B') émissions minimales de CO_2.

Il convient de noter que l'approvisionnement en méthane par la voie de la conversion de l'énergie électrique en gaz est limité par la disponibilité de l'hydrogène obtenu à partir de l'électricité produite par les systèmes photovoltaïques. Ainsi, selon les scénarios évalués, au moins 65 % du méthane doit être obtenu par le processus de digestion anaérobie (figure D-10d). En effet, comme obtenu dans l'optimisation mono-objectif, une surface PV d'environ 24100 m² est nécessaire pour produire la totalité du méthane par la voie "power-to-gas".

Grâce aux résultats obtenus, l'impact des critères évalués sur la conception et les conditions de fonctionnement du système énergétique a été étudié. Ainsi, les résultats indiquent qu'une surface PV de 9800 m² est le minimum requis pour répondre aux besoins en électricité de la communauté considérée (4160 habitants). Dans ce cas, la demande de méthane peut être entièrement couverte par la digestion anaérobie des déchets domestiques. En outre, en installant une surface de 24150 m², le système peut répondre à la fois aux demandes d'électricité et de méthane grâce à la technologie "power-to-gas".

Dans ce cas, le système nécessiterait d'importer/capturer environ 854 tonnes de CO_2/an pour le processus de méthanisation.

Il convient de noter que les résultats obtenus soulignent le potentiel de l'hydrogène en tant qu'intermédiaire pour permettre l'autosuffisance dans des endroits tropicaux et isolés comme l'Amazonie colombienne. Dans un tel contexte, comme il n'y a pas de variations saisonnières, il est possible de produire régulièrement de l'hydrogène tout au long de l'année, et donc de stimuler l'emploi de la technologie "power-to-gas" pour la production de méthane à partir d'électricité photovoltaïque. De plus, cette configuration implique soit d'importer soit de capturer du CO_2, ce qui pourrait conduire à un système énergétique avec des émissions de CO_2 négatives.

En outre, grâce aux résultats de l'optimisation multi-objectifs, le compromis entre les indicateurs de durabilité a été affiché. En outre, les implications des compromis en termes de conception et de conditions d'exploitation ont été explorées et analysées. Ainsi, les résultats représentent une source d'information précieuse pour les décideurs dans deux directions principales : (i) la conception des systèmes énergétiques dans les zones isolées, et (ii) l'utilisation potentielle de l'hydrogène pour permettre l'autosuffisance dans les zones éloignées et tropicales.

Conclusions

La motivation de ce projet repose sur la nécessité de développer des outils méthodologiques pour la conception, l'analyse et l'évaluation des systèmes d'énergie distribués en tenant compte des dimensions de durabilité. Ainsi, comme les DES sont des systèmes socio-techniques complexes, l'objectif principal de ce travail était de proposer un cadre global qui permette (i) d'effectuer la conception d'un système énergétique pour satisfaire les besoins des consommateurs en fonction des ressources disponibles, (ii) d'améliorer la performance de durabilité du système dès les premières étapes de la conception, (iii) de promouvoir la participation des parties prenantes, et (iv) de soutenir le processus décisionnel en analysant les compromis entre les axes de durabilité.

Dans l'ensemble, l'analyse de deux études de cas a permis d'établir que le cadre proposé permet d'effectuer une analyse complète pour la conception initiale du DES en tenant compte des dimensions de durabilité. Tout d'abord, un ensemble d'indicateurs pertinents a été sélectionné et formulé en fonction des décisions de conception. Ensuite, l'optimisation à objectif unique a permis de mieux comprendre le comportement du système énergétique et d'identifier l'impact des critères évalués sur la configuration et la politique d'exploitation

du système énergétique. Par la suite, l'optimisation multi-objectifs a permis d'établir les compromis entre les indicateurs de durabilité et d'étudier leur impact correspondant en termes de variables de processus. De cette manière, tout au long de chaque étape, il a été démontré que l'approche proposée constitue un outil pour réaliser une analyse de durabilité dès les premières étapes de la conception, et que les résultats obtenus représentent une source d'information qui favorise la participation des parties prenantes et aide le décideur à prendre une décision éclairée. Il a également été démontré la flexibilité du cadre proposé, de sorte qu'il peut être facilement adapté et utilisé pour la conception de systèmes énergétiques dans différentes conditions de contexte, en tenant compte d'autres critères d'évaluation, ou en incluant différentes unités technologiques et formes d'énergie.

References

[1] International Energy Agency (IEA). Global Energy & CO2 Status Report. 2019.

[2] International Renewable Energy Agency (IRENA). Global Energy transformation:A roadmap to 2050. Abu Dhabi: 2018.

[3] REN21. Renewables 2019 Global Status Report. Paris: 2019.

[4] International Energy Agency (IEA). Status of Power System Transformation 2019: Power System Flexibility. 2019.

[5] U.S. Energy Information Administration. International Energy Outlook 2019. Washington: 2019.

[6] Alanne K, Saari A. Distributed energy generation and sustainable development. Renew Sustain Energy Rev 2006;10:539–58. https://doi.org/10.1016/j.rser.2004.11.004.

[7] Fonseca JD, Camargo M, Commenge JM, Falk L, Gil ID. Trends in design of distributed energy systems using hydrogen as energy vector: A systematic literature review. Int J Hydrogen Energy 2019;44:9486–504. https://doi.org/10.1016/j.ijhydene.2018.09.177.

[8] Bouffard F, Kirschen DS. Centralised and distributed electricity systems. Energy Policy 2008;36:4504–8. https://doi.org/10.1016/j.enpol.2008.09.060.

[9] Shivarama Krishna K, Sathish Kumar K. A review on hybrid renewable energy systems. Renew Sustain Energy Rev 2015;52:907–16. https://doi.org/10.1016/j.rser.2015.07.187.

[10] Mazloomi K, Gomes C. Hydrogen as an energy carrier: Prospects and challenges. Renew Sustain Energy Rev 2012;16:3024–33. https://doi.org/10.1016/j.rser.2012.02.028.

[11] International Energy Agency (IEA). The Future of Hydrogen. 2019.

[12] Parra D, Valverde L, Pino FJ, Patel MK. A review on the role, cost and value of hydrogen energy systems for deep decarbonisation. Renew Sustain Energy Rev 2019;101:279–94. https://doi.org/10.1016/j.rser.2018.11.010.

[13] Nastasi B, Lo Basso G. Hydrogen to link heat and electricity in the transition towards future Smart Energy Systems. Energy 2016;110:5–22.

https://doi.org/10.1016/j.energy.2016.03.097.

[14] Dincer I, Acar C. Smart energy solutions with hydrogen options. Int J Hydrogen Energy 2018;43:8579–99. https://doi.org/10.1016/j.ijhydene.2018.03.120.

[15] Liu P, Georgiadis MC, Pistikopoulos EN. An energy systems engineering approach for the design and operation of microgrids in residential applications. Chem Eng Res Des 2013;91:2054–69. https://doi.org/10.1016/j.cherd.2013.08.016.

[16] Mavromatidis G, Orehounig K, Bollinger LA, Hohmann M, Marquant JF, Miglani S, et al. Ten questions concerning modeling of distributed multi-energy systems. Build Environ 2019;165:106372. https://doi.org/10.1016/j.buildenv.2019.106372.

[17] Argoti A, Orjuela A, Narváez PC. Challenges and opportunities in assessing sustainability during chemical process design. Curr Opin Chem Eng 2019;26:96–103. https://doi.org/10.1016/j.coche.2019.09.003.

[18] Ruiz-Mercado GJ, Smith RL, Gonzalez MA. Sustainability indicators for chemical processes: I. Taxonomy. Ind Eng Chem Res 2012;51:2309–28. https://doi.org/10.1021/ie102116e.

[19] Ruiz-mercado G, Cabezas H. Sustainability in the Design, Synthesis and Analysis of Chemical Engineering Processes. Elsevier - Butterworth-Heinemann; 2016.

[20] United Nations. Sustainable Development Goals. Goal 7 Afford Clean Energy 2020. https://www.un.org/sustainabledevelopment/energy/ (accessed May 12, 2020).

[21] International Energy Agency (IEA). CO2 emmisions from fuel combustion - Highlights. 2019.

[22] Dimian AC, Bildea CS, Kiss AA. Integrated Design and Simulation of Chemical Processes. Second edi. Amsterdam: Elsevier B.V; 2014.

[23] Bakshi BR, Fiksel J. The quest for sustainability: Challenges for process systems engineering. AIChE J 2003;49:1350–8. https://doi.org/10.1002/aic.690490602.

[24] Azapagic A, Stamford L, Youds L, Barteczko-Hibbert C. Towards sustainable production and consumption: A novel DEcision-Support Framework IntegRating Economic, Environmental and Social Sustainability (DESIRES). Comput Chem Eng 2016;91:93–103. https://doi.org/10.1016/j.compchemeng.2016.03.017.

[25] Frangopoulos CA. Recent developments and trends in optimization of energy systems. Energy 2018;164:1011–20. https://doi.org/10.1016/j.energy.2018.08.218.

[26] International Atomic Energy Agency (IAEA), United Nations Department of Economic and Social Affairs, International Energy Agency (IEA), EUROSTAT, European Environment Agency. Energy Indicators for Sustainable Development :

Guidelines and Methodologies. 2005.

[27] García-Serna J, Pérez-Barrigón L, Cocero MJ. New trends for design towards sustainability in chemical engineering: Green engineering. Chem Eng J 2007;133:7–30. https://doi.org/10.1016/j.cej.2007.02.028.

[28] Weinand JM, Scheller F, McKenna R. Reviewing energy system modelling of decentralized energy autonomy. Energy 2020;203:117817. https://doi.org/10.1016/j.energy.2020.117817.

[29] Koirala BP, Koliou E, Friege J, Hakvoort RA, Herder PM. Energetic communities for community energy: A review of key issues and trends shaping integrated community energy systems. Renew Sustain Energy Rev 2016;56:722–44. https://doi.org/10.1016/j.rser.2015.11.080.

[30] Campos-Guzmán V, García-Cáscales MS, Espinosa N, Urbina A. Life Cycle Analysis with Multi-Criteria Decision Making: A review of approaches for the sustainability evaluation of renewable energy technologies. Renew Sustain Energy Rev 2019;104:343–66. https://doi.org/10.1016/j.rser.2019.01.031.

[31] Berka AL, Creamer E. Taking stock of the local impacts of community owned renewable energy: A review and research agenda. Renew Sustain Energy Rev 2018;82:3400–19. https://doi.org/10.1016/j.rser.2017.10.050.

[32] Sheikh NJ, Kocaoglu DF, Lutzenhiser L. Social and political impacts of renewable energy: Literature review. Technol Forecast Soc Change 2016;108:102–10. https://doi.org/10.1016/j.techfore.2016.04.022.

[33] World Health Organization (WHO). WHO Coronavirus Disease (COVID-19) Dashboard 2020. https://covid19.who.int/ (accessed June 15, 2020).

[34] International Energy Agency (IEA). Global Energy Review 2020. 2020.

[35] International Energy Agency (IEA). World Energy Outlook 2017 2017. http://www.iea.org/weo2017/ (accessed April 8, 2018).

[36] Chicco G, Mancarella P. Distributed multi-generation: A comprehensive view. Renew Sustain Energy Rev 2009;13:535–51. https://doi.org/10.1016/j.rser.2007.11.014.

[37] Siemens. Ventotene an off-the-grid Italian island 2020. https://new.siemens.com/global/en/products/energy/references/ventotene.html (accessed June 16, 2020).

[38] Siemens. Driving zero fossil fuels for Galápagos 2020. https://new.siemens.com/global/en/products/energy/references/galapagos.html

(accessed June 16, 2020).

[39] Hydro Tasmania. Hybrid Energy Solutions - Success stories 2020. https://www.hydro.com.au/clean-energy/hybrid-energy-solutions/success-stories (accessed June 16, 2020).

[40] Innovation and Networks Executive Agency (INEA). Supporting Innovative Solutions for Smart Grids and Storage. 2019.

[41] Geidl M, Koeppel G, Favre-Perrod P. The Energy Hub – A powerful concept for future energy systems. Third Annu. Carnegie Mellon Conf. Electr. Ind., 2007. https://doi.org/http://dx.doi.org/10.1016/j.solener.2010.12.027.

[42] Geidl M. Integrated Modeling and Optimization of Multi-Carrier Energy Systems. ETH Zurich, 2007. https://doi.org/10.3929/ethz-a-005377890.

[43] Manfren M, Caputo P, Costa G. Paradigm shift in urban energy systems through distributed generation: Methods and models. Appl Energy 2011;88:1032–48. https://doi.org/10.1016/j.apenergy.2010.10.018.

[44] Adil AM, Ko Y. Socio-technical evolution of Decentralized Energy Systems: A critical review and implications for urban planning and policy. Renew Sustain Energy Rev 2016;57:1025–37. https://doi.org/10.1016/j.rser.2015.12.079.

[45] Mancarella P. MES (multi-energy systems): An overview of concepts and evaluation models. Energy 2014;65:1–17. https://doi.org/10.1016/j.energy.2013.10.041.

[46] Mohammadi M, Noorollahi Y, Mohammadi-ivatloo B, Yousefi H. Energy hub: From a model to a concept – A review. Renew Sustain Energy Rev 2017;80:1512–27. https://doi.org/10.1016/j.rser.2017.07.030.

[47] Rong A, Lahdelma R. Role of polygeneration in sustainable energy system development challenges and opportunities from optimization viewpoints. Renew Sustain Energy Rev 2016;53:363–72. https://doi.org/10.1016/j.rser.2015.08.060.

[48] Manwell JF. Hybrid Energy Systems. Encycl Energy 2004:215.

[49] International Energy Agency (IEA). Technology Roadmap: Hydrogen and Fuel Cells. 2015. https://doi.org/10.1007/SpringerReference_7300.

[50] Nastasi B, Lo Basso G. Power-to-Gas integration in the Transition towards Future Urban Energy Systems. Int J Hydrogen Energy 2017;42:23933–51. https://doi.org/10.1016/j.ijhydene.2017.07.149.

[51] International Renewable Energy Agency (IRENA). Hydrogen From Renewable Power: Technology outlook for the energy transition. 2018.

[52] Stolten D, Emonts B. Hydrogen Science and Engineering. vol. 1. Weinheim: Wiley

VCH; 2016. https://doi.org/10.1017/CBO9781107415324.004.

[53] Subramani V, Basile A. Compendium of Hydrogen Energy. vol. 1 Hydrogen. Elsevier; 2015.

[54] Squadrito G, Andaloro L, Ferraro M, Antonucci V. Advances in Hydrogen Production, Storage and Distribution. 2014. https://doi.org/10.1533/9780857097736.3.451.

[55] Chen J, Yan L, Song W, Xu D. Methane steam reforming thermally coupled with catalytic combustion in catalytic microreactors for hydrogen production. Int J Hydrogen Energy 2017;42:664–80. https://doi.org/10.1016/j.ijhydene.2016.12.114.

[56] Dincer I, Zamfirescu C. Sustainable hydrogen production. vol. 305. Weinheim: Elsevier Inc.; 2004. https://doi.org/10.1126/science.1103197.

[57] Garcia DA, Barbanera F, Cumo F, Di Matteo U, Nastasi B. Expert opinion analysis on renewable hydrogen storage systems potential in Europe. Energies 2016;9. https://doi.org/10.3390/en9110963.

[58] Valladares M-R de. Global Trends and Outlook for Hydrogen. 2017.

[59] Liu K, Song C, Subramani V. Hydrogen and Syngas Production and Purification Technologies. New Jersey: Wiley - AIChE; 2010. https://doi.org/10.1002/9780470561256.

[60] Luz Silveira J. Sustainable Hydrogen Production Processes. Switzertland: Springer; 2017. https://doi.org/10.1007/978-3-319-41616-8.

[61] Susastriawan AAP, Saptoadi H, Purnomo. Small-scale downdraft gasifiers for biomass gasification: A review. Renew Sustain Energy Rev 2017;76:989–1003. https://doi.org/10.1016/j.rser.2017.03.112.

[62] Luque R, Lin CSK, Clark J, Wilson K. Handbook of Biofuels Production. Elsevier Ltd; 2016. https://doi.org/10.1016/B978-0-08-100455-5.00010-2.

[63] Nikolaidis P, Poullikkas A. A comparative overview of hydrogen production processes. Renew Sustain Energy Rev 2017;67:597–611. https://doi.org/10.1016/j.rser.2016.09.044.

[64] Dincer I, Acar C. Review and evaluation of hydrogen production methods for better sustainability. Int J Hydrogen Energy 2014;40:11094–111. https://doi.org/10.1016/j.ijhydene.2014.12.035.

[65] Dincer I, Acar C. Innovation in hydrogen production. Int J Hydrogen Energy 2017;42:14843–64. https://doi.org/10.1016/j.ijhydene.2017.04.107.

[66] da Silva Veras T, Mozer TS, da Costa Rubim Messeder dos Santos D, da Silva César A. Hydrogen: Trends, production and characterization of the main process worldwide. Int J Hydrogen Energy 2017;42:2018–33. https://doi.org/10.1016/j.ijhydene.2016.08.219.

[67] Barthelemy H, Weber M, Barbier F. Hydrogen storage: Recent improvements and industrial perspectives. vol. 42. Elsevier Ltd; 2017. https://doi.org/10.1016/j.ijhydene.2016.03.178.

[68] Ajanovic A, Hiesl A, Haas R. On the role of storage for electricity in smart energy systems. Energy 2020;200:117473. https://doi.org/10.1016/j.energy.2020.117473.

[69] Aneke M, Wang M. Energy storage technologies and real life applications – A state of the art review. Appl Energy 2016;179:350–77. https://doi.org/10.1016/j.apenergy.2016.06.097.

[70] Viswanathan B. Energy Sources: Fundamentals of Chemical Conversion Processes and Applications. 2016. https://doi.org/10.1080/00908310490450836.

[71] Baetcke L, Kaltschmitt M. Hydrogen storage for mobile application: Technologies and their assessment. Elsevier Ltd.; 2018. https://doi.org/10.1016/B978-0-12-811197-0.00005-1.

[72] Zhang YH, Jia ZC, Yuan ZM, Yang T, Qi Y, Zhao DL. Development and Application of Hydrogen Storage. J Iron Steel Res Int 2015;22:757–70. https://doi.org/10.1016/S1006-706X(15)30069-8.

[73] Najjar YSH. Hydrogen safety: The road toward green technology. Int J Hydrogen Energy 2013;38:10716–28. https://doi.org/10.1016/j.ijhydene.2013.05.126.

[74] Royle M, Willoughby D. The safety of the future hydrogen economy. Process Saf Environ Prot 2011;89:452–62. https://doi.org/10.1016/j.psep.2011.09.003.

[75] Saffers JB, Molkov V V. Hydrogen safety engineering framework and elementary design safety tools. Int J Hydrogen Energy 2014;39:6268–85. https://doi.org/10.1016/j.ijhydene.2013.06.060.

[76] Douglas JM. Conceptual Design Of Chemical Processes. Singapore: McGRAW-HILL; 1988.

[77] Biegler LT, Grossmann IE, Westerberg AW. Systematic Methods of Chemical Process Design. New Jersey: Prentice Hall; 1999.

[78] Smith R. Chemical Process Design and Integration. John Wiley & Sons, Ltd; 2005.

[79] Seider WD, Lewin DR, Seader JD, Widagdo S, Gani R, Ng KM. Product and Process Design Principles: Synhtesis, Analysis and Evaluation. Fourth edi. New York: Wiley;

2017.

[80] Karmellos M, Georgiou PN, Mavrotas G. A comparison of methods for the optimal design of Distributed Energy Systems under uncertainty. Energy 2019;178:318–33. https://doi.org/10.1016/j.energy.2019.04.153.

[81] Akbari K, Jolai F, Ghaderi SF. Optimal design of distributed energy system in a neighborhood under uncertainty. Energy 2016;116:567–82. https://doi.org/10.1016/j.energy.2016.09.083.

[82] Gabrielli P, Fürer F, Mavromatidis G, Mazzotti M. Robust and optimal design of multi-energy systems with seasonal storage through uncertainty analysis. Appl Energy 2019;238:1192–210. https://doi.org/10.1016/j.apenergy.2019.01.064.

[83] Kang J, Wang S. Robust optimal design of distributed energy systems based on life-cycle performance analysis using a probabilistic approach considering uncertainties of design inputs and equipment degradations. Appl Energy 2018;231:615–27. https://doi.org/10.1016/j.apenergy.2018.09.144.

[84] Mavromatidis G, Orehounig K, Carmeliet J. Design of distributed energy systems under uncertainty: A two-stage stochastic programming approach. Appl Energy 2018;222:932–50. https://doi.org/10.1016/j.apenergy.2018.04.019.

[85] Jing R, Wang M, Zhang Z, Wang X, Li N, Shah N, et al. Distributed or centralized? Designing district-level urban energy systems by a hierarchical approach considering demand uncertainties. Appl Energy 2019;252:113424. https://doi.org/10.1016/j.apenergy.2019.113424.

[86] Mehleri ED, Sarimveis H, Markatos NC, Papageorgiou LG. A mathematical programming approach for optimal design of distributed energy systems at the neighbourhood level. Energy 2012;44:96–104. https://doi.org/10.1016/j.energy.2012.02.009.

[87] Yang Y, Zhang S, Xiao Y. An MILP (mixed integer linear programming) model for optimal design of district-scale distributed energy resource systems. Energy 2015;90:1901–15. https://doi.org/10.1016/j.energy.2015.07.013.

[88] Khalid F, Dincer I, Rosen MA. Analysis and assessment of an integrated hydrogen energy system. Int J Hydrogen Energy 2016;41:7960–7. https://doi.org/10.1016/j.ijhydene.2015.12.221.

[89] Schütz T, Hu X, Fuchs M, Müller D. Optimal design of decentralized energy conversion systems for smart microgrids using decomposition methods. Energy 2018;156:250–63. https://doi.org/10.1016/j.energy.2018.05.050.

[90] Pan G, Gu W, Wu Z, Lu Y, Lu S. Optimal design and operation of multi-energy system with load aggregator considering nodal energy prices. Appl Energy 2019;239:280–95. https://doi.org/10.1016/j.apenergy.2019.01.217.

[91] Dorotić H, Pukšec T, Duić N. Economical, environmental and exergetic multi-objective optimization of district heating systems on hourly level for a whole year. Appl Energy 2019;251:113394. https://doi.org/10.1016/j.apenergy.2019.113394.

[92] Dorotić H, Pukšec T, Duić N. Multi-objective optimization of district heating and cooling systems for a one-year time horizon. Energy 2019;169:319–28. https://doi.org/10.1016/j.energy.2018.11.149.

[93] Maroufmashat A, Sattari S, Roshandel R, Fowler M, Elkamel A. Multi-objective Optimization for Design and Operation of Distributed Energy Systems through the Multi-energy Hub Network Approach. Ind Eng Chem Res 2016;55:8950–66. https://doi.org/10.1021/acs.iecr.6b01264.

[94] Falke T, Krengel S, Meinerzhagen AK, Schnettler A. Multi-objective optimization and simulation model for the design of distributed energy systems. Appl Energy 2016;184:1508–16. https://doi.org/10.1016/j.apenergy.2016.03.044.

[95] Gabrielli P, Gazzani M, Martelli E, Mazzotti M. Optimal design of multi-energy systems with seasonal storage. Appl Energy 2018;219:408–24. https://doi.org/10.1016/j.apenergy.2017.07.142.

[96] Fazlollahi S, Becker G, Ashouri A, Maréchal F. Multi-objective, multi-period optimization of district energy systems: IV - A case study. Energy 2015;84:365–81. https://doi.org/10.1016/j.energy.2015.03.003.

[97] Rieder A, Christidis A, Tsatsaronis G. Multi criteria dynamic design optimization of a small scale distributed energy system. Energy 2014;74:230–9. https://doi.org/10.1016/j.energy.2014.06.007.

[98] Pelet X, Favrat D, Leyland G. Multiobjective optimisation of integrated energy systems for remote communities considering economics and CO2 emissions. Int J Therm Sci 2005;44:1180–9. https://doi.org/10.1016/j.ijthermalsci.2005.09.006.

[99] Li L, Mu H, Li N, Li M. Economic and environmental optimization for distributed energy resource systems coupled with district energy networks. Energy 2016;109:947–60. https://doi.org/10.1016/j.energy.2016.05.026.

[100] Di Somma M, Yan B, Bianco N, Graditi G, Luh PB, Mongibello L, et al. Design optimization of a distributed energy system through cost and exergy assessments. Energy Procedia 2017;105:2451–9. https://doi.org/10.1016/j.egypro.2017.03.706.

[101] Fazlollahi S, Mandel P, Becker G, Maréchal F. Methods for multi-objective investment and operating optimization of complex energy systems. Energy 2012;45:12–22. https://doi.org/10.1016/j.energy.2012.02.046.

[102] Ren H, Zhou W, Nakagami K, Gao W, Wu Q. Multi-objective optimization for the operation of distributed energy systems considering economic and environmental aspects. Appl Energy 2010;87:3642–51. https://doi.org/10.1016/j.apenergy.2010.06.013.

[103] Di Somma M, Yan B, Bianco N, Luh PB, Graditi G, Mongibello L, et al. Multi-objective operation optimization of a Distributed Energy System for a large-scale utility customer. Appl Therm Eng 2016;101:752–61. https://doi.org/10.1016/j.applthermaleng.2016.02.027.

[104] Di Somma M, Graditi G, Heydarian-Forushani E, Shafie-khah M, Siano P. Stochastic optimal scheduling of distributed energy resources with renewables considering economic and environmental aspects. Renew Energy 2018;116:272–87. https://doi.org/10.1016/j.renene.2017.09.074.

[105] Dufo-López R, Bernal-Agustín JL. Multi-objective design of PV-wind-diesel-hydrogen-battery systems. Renew Energy 2008;33:2559–72. https://doi.org/10.1016/j.renene.2008.02.027.

[106] Eriksson ELV, Gray EMA. Optimization of renewable hybrid energy systems – A multi-objective approach. Renew Energy 2019;133:971–99. https://doi.org/10.1016/j.renene.2018.10.053.

[107] Jing R, Wang M, Zhang Z, Liu J, Liang H, Meng C, et al. Comparative study of posteriori decision-making methods when designing building integrated energy systems with multi-objectives. Energy Build 2019;194:123–39. https://doi.org/10.1016/j.enbuild.2019.04.023.

[108] Jing R, Wang M, Liang H, Wang X, Li N, Shah N, et al. Multi-objective optimization of a neighborhood-level urban energy network: Considering Game-theory inspired multi-benefit allocation constraints. Appl Energy 2018;231:534–48. https://doi.org/10.1016/j.apenergy.2018.09.151.

[109] Simeoni P, Nardin G, Ciotti G. Planning and design of sustainable smart multi energy systems. The case of a food industrial district in Italy. Energy 2018;163:443–56. https://doi.org/10.1016/j.energy.2018.08.125.

[110] El-Emam RS, Dincer I. Assessment and Evolutionary Based Multi-Objective Optimization of a Novel Renewable-Based Polygeneration Energy System. J Energy

Resour Technol 2016;139:012003. https://doi.org/10.1115/1.4033625.

[111] Al Rafea K, Elsholkami M, Elkamel A, Fowler M. Integration of Decentralized Energy Systems with Utility-Scale Energy Storage through Underground Hydrogen-Natural Gas Co-Storage Using the Energy Hub Approach. Ind Eng Chem Res 2017;56:2310–30. https://doi.org/10.1021/acs.iecr.6b02861.

[112] AlRafea K, Fowler M, Elkamel A, Hajimiragha A. Integration of renewable energy sources into combined cycle power plants through electrolysis generated hydrogen in a new designed energy hub. Int J Hydrogen Energy 2016;41:16718–28. https://doi.org/10.1016/j.ijhydene.2016.06.256.

[113] Ahmadi P, Dincer I, Rosen M a. Thermoeconomic multi-objective optimization of a novel biomass-based integrated energy system. Energy 2014;68:958–70. https://doi.org/10.1016/j.energy.2014.01.085.

[114] Vafaei M, Kazerani M. Optimal unit-sizing of a wind-hydrogen-diesel microgrid system for a remote community. IEEE PES Trondheim PowerTech Power Technol. a Sustain. Soc. POWERTECH 2011, 2011, p. 1–7. https://doi.org/10.1109/PTC.2011.6019412.

[115] Friedler F, Fan LT. P-graph Intoduction 2020. http://p-graph.com/introduction/ (accessed July 1, 2020).

[116] Friedler F, Varga JB, Fan LT. Decision-mapping: A tool for consistent and complete decisions in process synthesis. Chem Eng Sci 1995;50:1755–68. https://doi.org/10.1016/0009-2509(95)00034-3.

[117] Rasmuson A, Andresson B, Olsson L, Ronnie A. Mathematical Modeling in Chemical Engineering. New York: Cambidge University Press; 2014. https://doi.org/10.1017/CBO9781107415324.004.

[118] Ferrareso Lona LM. A Step by Step Approach to the Modeling of Chemical Engineering Processes. Springer; 2018. https://doi.org/10.1007/978-3-319-66047-9.

[119] Ravindran A, Ragsdell KM, Reklaitis G V. Engineering Optimization: Methods and Applications. Second Edi. New Jersey: John Wiley & Sons, Inc.; 2006. https://doi.org/10.1002/9780470117811.

[120] Martin M. Introduction to Software for Chemical Engineers. First. Taylor & Francis; 2014. https://doi.org/10.1201/b17150-8.

[121] Mavromatidis G. MODEL - BASED DESIGN OF DISTRIBUTED URBAN ENERGY SYSTEMS UNDER UNCERTAINTY. ETH Zurich, 2017.

[122] Zendehboudi S, Rezaei N, Lohi A. Applications of hybrid models in chemical,

petroleum, and energy systems: A systematic review. Appl Energy 2018;228:2539–66. https://doi.org/10.1016/j.apenergy.2018.06.051.

[123] Skoplaki E, Palyvos JA. On the temperature dependence of photovoltaic module electrical performance: A review of efficiency/power correlations. Sol Energy 2009;83:614–24. https://doi.org/10.1016/j.solener.2008.10.008.

[124] Baghaee HR, Mirsalim M, Gharehpetian GB, Talebi H a. Reliability/cost-based multi-objective Pareto optimal design of stand-alone wind/PV/FC generation microgrid system. Energy 2016;115:1022–41. https://doi.org/10.1016/j.energy.2016.09.007.

[125] Thrän D, Billig E, Persson T, Svensson M, Daniel-Gromke J, Ponitka J, et al. Biomethane Status and Factors Affecting Market Development and Trade. 2014.

[126] Pramanik SK, Suja FB, Zain SM, Pramanik BK. The anaerobic digestion process of biogas production from food waste: Prospects and constraints. Bioresour Technol Reports 2019;8:100310. https://doi.org/10.1016/j.biteb.2019.100310.

[127] Götz M, Lefebvre J, Mörs F, McDaniel Koch A, Graf F, Bajohr S, et al. Renewable Power-to-Gas: A technological and economic review. Renew Energy 2016;85:1371–90. https://doi.org/10.1016/j.renene.2015.07.066.

[128] Sidkar SK. Sustainable Development and Sustainability Metrics. AIChE J 2003;49:1928–32.

[129] Azapagic A, Perdan S. Indicators of Sustainable Development for Industry: A General Framework. Process Saf Environ Prot 2000;78:243–61. https://doi.org/http://dx.doi.org/10.1205/095758200530763.

[130] Kurka T, Blackwood D. Participatory selection of sustainability criteria and indicators for bioenergy developments. Renew Sustain Energy Rev 2013;24:92–102. https://doi.org/10.1016/j.rser.2013.03.062.

[131] Bautista S, Narvaez P, Camargo M, Chery O, Morel L. Biodiesel-TBL+: A new hierarchical sustainability assessment framework of PC&I for biodiesel production - Part i. Ecol Indic 2016;60:84–107. https://doi.org/10.1016/j.ecolind.2015.06.020.

[132] Liu G. Development of a general sustainability indicator for renewable energy systems: A review. Renew Sustain Energy Rev 2014;31:611–21. https://doi.org/10.1016/j.rser.2013.12.038.

[133] Pavlovskaia E. Sustainability criteria: their indicators, control, and monitoring (with examples from the biofuel sector). Environ Sci Eur 2014;26:1–12.

https://doi.org/10.1186/s12302-014-0017-2.

[134] Shaaban M, Scheffran J. Selection of sustainable development indicators for the assessment of electricity production in Egypt. Sustain Energy Technol Assessments 2017;22:65–73. https://doi.org/10.1016/j.seta.2017.07.003.

[135] Buchholz T, Luzadis VA, Volk TA. Sustainability criteria for bioenergy systems: results from an expert survey. J Clean Prod 2009;17:S86–98. https://doi.org/10.1016/j.jclepro.2009.04.015.

[136] Bautista S, Enjolras M, Narvaez P, Camargo M, Morel L. Biodiesel-triple bottom line (TBL): A new hierarchical sustainability assessment framework of principles criteria & indicators (PC&I) for biodiesel production. Part II-validation. Ecol Indic 2016;69:803–17. https://doi.org/10.1016/j.ecolind.2016.04.046.

[137] Stamford L, Azapagic A. Sustainability indicators for the assessment of nuclear power. Energy 2011;36:6037–57. https://doi.org/10.1016/j.energy.2011.08.011.

[138] Stamford L, Azapagic A. Life cycle sustainability assessment of electricity options for the UK. Int J Energy Res 2012;33. https://doi.org/10.1002/er.2962.

[139] Anastas PT, Zimmerman JB. Design through the 12 principles of green engineering. Environ Sci Technol 2003;35:94A-101A. https://doi.org/10.1109/EMR.2007.4296421.

[140] Afgan NH, Carvalho MG. Sustainability assessment of hydrogen energy systems. Int J Hydrogen Energy 2004;29:1327–42. https://doi.org/10.1016/j.ijhydene.2004.01.005.

[141] Strantzali E, Aravossis K. Decision making in renewable energy investments: A review. Renew Sustain Energy Rev 2016;55:885–98. https://doi.org/10.1016/j.rser.2015.11.021.

[142] Santoyo-Castelazo E, Azapagic A. Sustainability assessment of energy systems: Integrating environmental, economic and social aspects. J Clean Prod 2014;80:119–38. https://doi.org/10.1016/j.jclepro.2014.05.061.

[143] Abu-Rayash A, Dincer I. Sustainability assessment of energy systems: A novel integrated model. J Clean Prod 2019;212:1098–116. https://doi.org/10.1016/j.jclepro.2018.12.090.

[144] Evans A, Strezov V, Evans TJ. Assessment of sustainability indicators for renewable energy technologies. Renew Sustain Energy Rev 2009;13:1082–8. https://doi.org/10.1016/j.rser.2008.03.008.

[145] Afgan NH, Carvalho MG. Sustainability assessment of a hybrid energy system. Energy Policy 2008;36:2903–10. https://doi.org/10.1016/j.enpol.2008.03.040.

[146] Neves AR, Leal V. Energy sustainability indicators for local energy planning: Review of current practices and derivation of a new framework. Renew Sustain Energy Rev 2010;14:2723–35. https://doi.org/10.1016/j.rser.2010.07.067.

[147] United Nations. Sustainable Development Goals. Goal 6 Ensure Access to Water Sanit All 2020. https://www.un.org/sustainabledevelopment/water-and-sanitation/ (accessed May 16, 2020).

[148] Moslehi S, Arababadi R. Sustainability Assessment of Complex Energy Systems Using Life Cycle Approach-Case Study: Arizona State University Tempe Campus. Procedia Eng 2016;145:1096–103. https://doi.org/10.1016/j.proeng.2016.04.142.

[149] Vasco-Correa J, Khanal S, Manandhar A, Shah A. Anaerobic digestion for bioenergy production: Global status, environmental and techno-economic implications, and government policies. Bioresour Technol 2018;247:1015–26. https://doi.org/10.1016/j.biortech.2017.09.004.

[150] Lin L, Shah A, Keener H, Li Y. Techno-economic analyses of solid-state anaerobic digestion and composting of yard trimmings. Waste Manag 2019;85:405–16. https://doi.org/10.1016/j.wasman.2018.12.037.

[151] Yoshida H, Gable JJ, Park JK. Evaluation of organic waste diversion alternatives for greenhouse gas reduction. Resour Conserv Recycl 2012;60:1–9. https://doi.org/10.1016/j.resconrec.2011.11.011.

[152] Surendra KC, Takara D, Hashimoto AG, Khanal SK. Biogas as a sustainable energy source for developing countries: Opportunities and challenges. Renew Sustain Energy Rev 2014;31:846–59. https://doi.org/10.1016/j.rser.2013.12.015.

[153] Law BE, Harmon ME. Forest sector carbon management, measurement and verification, and discussion of policy related to climate change. Carbon Manag 2011;2:73–84. https://doi.org/10.4155/cmt.10.40.

[154] Mitchell SR, Harmon ME, O'Connell KEB. Carbon debt and carbon sequestration parity in forest bioenergy production. GCB Bioenergy 2012;4:818–27. https://doi.org/10.1111/j.1757-1707.2012.01173.x.

[155] Agostini A, Giuntoli J, Boulamanti A. Carbon accounting of forest bioenergy: conclusions and recommendations from a critical literature review. Luxembourg: 2014. https://doi.org/10.2788/29442.

[156] Klöpffer W, Grahl B. Life Cycle Assessment (LCA): A Guide to Best Practice. Weinheim: Wiley VCH; 2014.

[157] International Standard Organization. Environmental Management - Life Cycle

Assessment - Principles and Framework (ISO 14040:2006) 2006.

[158] Reiter G, Lindorfer J. Global warming potential of hydrogen and methane production from renewable electricity via power-to-gas technology. Int J Life Cycle Assess 2015;20:477–89. https://doi.org/10.1007/s11367-015-0848-0.

[159] DNV GL. Power-to-Gas project in Rozenburg, The Netherlands. Groningen: 2015.

[160] Association française pour l'hydrogene et les piles à combustible (AFHYPAC). Production D'Hydrogene Par Electrolyse De L'Eau. vol. Fiche 3.2. 2019.

[161] Mikhail J, Gallego-schmid A, Stamford L, Azapagic A. Design and environmental sustainability assessment of small-scale off-grid energy systems for remote rural communities. Appl Energy 2020;258:114004. https://doi.org/10.1016/j.apenergy.2019.114004.

[162] Gallego Carrera D, Mack A. Sustainability assessment of energy technologies via social indicators: Results of a survey among European energy experts. Energy Policy 2010;38:1030–9. https://doi.org/10.1016/j.enpol.2009.10.055.

[163] Ribeiro F, Ferreira P, Araújo M. The inclusion of social aspects in power planning. Renew Sustain Energy Rev 2011;15:4361–9. https://doi.org/10.1016/j.rser.2011.07.114.

[164] Rösch C, Bräutigam K, Kopfmüller J, Stelzer V, Lichtner P. Indicator system for the sustainability assessment of the German energy system and its transition. Energy Sustain Soc 2017;7:1–13. https://doi.org/10.1186/s13705-016-0103-y.

[165] Rae C, Bradley F. Energy autonomy in sustainable communities - A review of key issues. Renew Sustain Energy Rev 2012;16:6497–506. https://doi.org/10.1016/j.rser.2012.08.002.

[166] Athar M, Shariff AM, Buang A. A review of inherent assessment for sustainable process design. J Clean Prod 2019;233:242–63. https://doi.org/10.1016/j.jclepro.2019.06.060.

[167] Roy N, Eljack F, Jiménez-Gutiérrez A, Zhang B, Thiruvenkataswamy P, El-Halwagi M, et al. A review of safety indices for process design. Curr Opin Chem Eng 2016;14:42–8. https://doi.org/10.1016/j.coche.2016.07.001.

[168] Song D, Yoon ES, Jang N. A framework and method for the assessment of inherent safety to enhance sustainability in conceptual chemical process design. J Loss Prev Process Ind 2018;54:10–7. https://doi.org/10.1016/j.jlp.2018.02.006.

[169] Rahman M, Heikkilä AM, Hurme M. Comparison of inherent safety indices in process concept evaluation. J Loss Prev Process Ind 2005;18:327–34. https://doi.org/10.1016/j.jlp.2005.06.015.

[170] Jafari MJ, Mohammadi H, Reniers G, Pouyakian M, Nourai F, Torabi SA, et al. Exploring inherent process safety indicators and approaches for their estimation: A systematic review. J Loss Prev Process Ind 2018;52:66–80. https://doi.org/10.1016/j.jlp.2018.01.013.

[171] Heikkilä AM. Inherent safety in process plant design. An index-based approach. Helsinki University of Technology, 1999.

[172] Kletz T, Amyotte P. Process plants: A handbook for inherently safer design. Second. Boca Raton: CRC Press; 2010. https://doi.org/10.1201/9781439804568.

[173] Li X, Zanwar A, Jayswal A, Lou HH, Huang Y. Incorporating exergy analysis and inherent safety analysis for sustainability assessment of biofuels. vol. 50. 2011. https://doi.org/10.1021/ie101660q.

[174] Park S, Xu S, Rogers W, Pasman H, El-Halwagi MM. Incorporating inherent safety during the conceptual process design stage: A literature review. J Loss Prev Process Ind 2020;63:104040. https://doi.org/10.1016/j.jlp.2019.104040.

[175] Laurence D. Quantifying inherent safety of chemical process routes. Loughborough University of Technology, 1996.

[176] Gangadharan P, Singh R, Cheng F, Lou HH. Novel Methodology for Inherent Safety Assessment in the Process Design Stage. Ind Eng Chem Res 2013;52:5921–33. https://doi.org/10.1021/ie303163y.

[177] Edgar TF, Himmelblau DM. Optimization of Chemical Process. Second. New York: McGRAW-HILL; 2001.

[178] Sioshansi R, Conejo AJ. Optimization in Engineering: Models and Algorithms. vol. 120. Springer; 2017. https://doi.org/10.1007/978-3-319-56769-3.

[179] Dutta S. Optimization in Chemical Engineering. Delhi: Cambridge University Press; 2016.

[180] Floudas CA. Nonlinear and Mixed-Integer Optimization: Fundamentals and Applications. Oxford University Press; 1995.

[181] Pandu Rangaiah G. Multi-objective Optimization: Techniques and Applications in Chemical Engineering. Singapore: World Scientific Publishing; 2009. https://doi.org/10.1007/978-1-84800-382-8_2.

[182] Goderbauer S, Comis M, Willamowski FJL. The synthesis problem of decentralized energy systems is strongly NP-hard. Comput Chem Eng 2019;124:343–9. https://doi.org/10.1016/j.compchemeng.2019.02.002.

[183] Solcast. Solar Forecasting & Solar Irradiance Data 2019. https://solcast.com/

(accessed June 16, 2019).

[184] Open Data Réseaux Énergies (ODRÉ). Consommation quotidienne brute (2012 à 2019) 2019.

[185] Ministère de la Transition Écologique et Solidaire. Données et études statistiques Pour le changement climatique, l'énergie, l'environnement, le logement, et les transports 2019. https://www.statistiques.developpement-durable.gouv.fr/prix-de-lenergie-0?rubrique=22 (accessed April 3, 2019).

[186] (ADEME) Agence de l'Environnement et de la Maîtrise de l'Energie. Données - Base Carbone. Bilans GES 2019. http://www.bilans-ges.ademe.fr/ (accessed December 15, 2019).

[187] Angelonidi E, Smith SR. A comparison of wet and dry anaerobic digestion processes for the treatment of municipal solid waste and food waste. Water Environ J 2015;29:549–57. https://doi.org/10.1111/wej.12130.

[188] WINAICO. Photovoltaic Modules. Prod Datasheets 2019. http://www.winaico.com/photovoltaik/modules/wsp-m6-perc-mono/ (accessed September 4, 2019).

[189] Mitsubishi Electric. Solar Solutions. Specif Sheets 2019. https://www.mitsubishielectricsolar.com/products/residential/solar_modules (accessed September 4, 2019).

[190] LG Electronics Inc. Solar - Products. Sol Bus Div 2019. https://www.lg.com/global/business/solar (accessed September 4, 2019).

[191] Buttler A, Spliethoff H. Current status of water electrolysis for energy storage, grid balancing and sector coupling via power-to-gas and power-to-liquids: A review. Renew Sustain Energy Rev 2018;82:2440–54. https://doi.org/10.1016/j.rser.2017.09.003.

[192] Luo X, Wang J, Dooner M, Clarke J. Overview of current development in electrical energy storage technologies and the application potential in power system operation. Appl Energy 2015;137:511–36. https://doi.org/10.1016/j.apenergy.2014.09.081.

[193] Parra D, Swierczynski M, Stroe DI, Norman SA, Abdon A, Worlitschek J, et al. An interdisciplinary review of energy storage for communities: Challenges and perspectives. Renew Sustain Energy Rev 2017;79:730–49. https://doi.org/10.1016/j.rser.2017.05.003.

[194] International Renewable Energy Agency (IRENA). Renewable Power Generation Costs in 2018. Abu Dhabi: 2019.

[195] Parra D, Patel MK. Techno-economic implications of the electrolyser technology and size for power-to-gas systems. Int J Hydrogen Energy 2016;41:3748–61. https://doi.org/10.1016/j.ijhydene.2015.12.160.

[196] Korner A. Technology Roadmap: Hydrogen and Fuel Cells (Technical Annex). 2015. https://doi.org/10.1007/SpringerReference_7300.

[197] International Renewable Energy Agency (IRENA). Electricity Storage and Renewables: Costs and Markets to 2030. Abu Dhabi: 2017.

[198] International Energy Agency (IEA). IEA G20 Hydrogen report: Assumptions. 2019.

[199] International Renewable Energy Agency (IRENA). Renewable Energy Technologies: Cost Analysis Series. 2012.

[200] Chen H, Ngoc T, Yang W, Tan C, Li Y. Progress in electrical energy storage system : A critical review. Prog Nat Sci 2009;19:291–312. https://doi.org/10.1016/j.pnsc.2008.07.014.

[201] Bandyopadhyay S. Design and optimization of isolated energy systems through pinch analysis. Asia-Pacific J Chem Eng 2011:518–26. https://doi.org/10.1002/apj.

[202] (ADEME) Agence de l'Environnement et de la Maîtrise de l'Energie. MODECOM 2017 Campagne nationale de caractérisation des déchets ménagers et assimilés. Angers: 2019.

[203] (ADEME) Agence de l'Environnement et de la Maîtrise de l'Energie. Déchets Chiffres-clés. Angers: 2018.

[204] Agora Energiewende. Recent Electricity Data. Power Price Emiss 2020. https://www.agora-energiewende.de/en/service/recent-electricity-data/chart/power_price_emission/01.01.2018/31.12.2018/ (accessed June 8, 2020).

[205] Diwekar U. Introduction to Applied Optimization. Second edi. Springer; 2008. https://doi.org/10.1007/978-0-387-73669-3.

[206] Pandu Rangaiah G, Bonilla-Petriciolet A. Multi-Objective Optimization in Chemical Engineering: Developments and Applications. John Wiley & Sons, Ltd; 2013. https://doi.org/10.6028/jres.090.045.

[207] Coello Coello CA, Lamont GB, Veldhuizen DA Van, Goldberg DE, Koza JR. Evolutionary Algorithms for Solving Multi-Objective Problems. Second edi. Springer; 2007. https://doi.org/10.1007/978-0-387-36797-2.

[208] Goldberg DE. Genetic Algorithms in Search, Optimization & Machine Learning. Addison-Wesley Publishing Company; 1989.

[209] Cui Y, Geng Z, Zhu Q, Han Y. Review: Multi-objective optimization methods and application in energy saving. Energy 2017;125:681–704. https://doi.org/10.1016/j.energy.2017.02.174.

[210] Unidad de Planeación Minero Energética (UPME). Integración de las energías renovables no convencionales en Colombia. Bogotá: 2015. https://doi.org/10.1017/CBO9781107415324.004.

[211] International Energy Agency (IEA). IEA Atlas of Energy 2020. http://energyatlas.iea.org/#!/profile/WORLD/COL (accessed August 7, 2020).

[212] International Energy Agency (IEA). IEA Country Profiles - Colombia. Key Energy Stat 2020. https://www.iea.org/countries/Colombia (accessed August 7, 2020).

[213] Centro Nacional de Monitoreo (CNM). Telemetria - Informes Mensuales 2019. http://190.216.196.84/cnm/ (accessed June 9, 2020).

[214] Sistema de Informacion Ambiental Territorial de la Amazonia Colombiana (SIAT-AC). Informacion de Referencia 2020. http://siatac.co/web/guest/inicio/siatac (accessed June 10, 2020).

[215] Ministerio de Ambiente y Desarrollo Sostenible. Estado del Ambiente y los Recursos Naturales Renovables. 2019.

[216] Staffell I, Pfenninger S. Using bias-corrected reanalysis to simulate current and future wind power output. Energy 2016;114:1224–39. https://doi.org/10.1016/j.energy.2016.08.068.

[217] Pfenninger S, Staffell I. Long-term patterns of European PV output using 30 years of validated hourly reanalysis and satellite data. Energy 2016;114:1251–65. https://doi.org/10.1016/j.energy.2016.08.060.

[218] Broehm M, Strefler J, Bauer N. Techno-Economic Review of Direct Air Capture Systems for Large Scale Mitigation of Atmospheric CO2. SSRN Electron J 2015:1–28. https://doi.org/10.2139/ssrn.2665702.

[219] World Bank. Country Profile: Colombia 2020. https://databank.worldbank.org/views/reports/reportwidget.aspx?Report_Name=CountryProfile&Id=b450fd57&tbar=y&dd=y&inf=n&zm=n&country=COL (accessed July 12, 2020).

[220] Yáñez E, Ramírez A, Núñez-López V, Castillo E, Faaij A. Exploring the potential of carbon capture and storage-enhanced oil recovery as a mitigation strategy in the Colombian oil industry. Int J Greenh Gas Control 2020;94:102938. https://doi.org/10.1016/j.ijggc.2019.102938.

[221] Kaza S, Yao L, Bhada-Tata P, Van Woerden F. What a Waste 2.0: A Global Snapshot

of Solid Waste Management to 2050. Urban Dev. Ser., Washington: World Bank Group; 2018.

[222] Unidad de planeación Minero Energética (UPME). Precios energía eléctrica - comparación paises 2020. https://www1.upme.gov.co/InformacionCifras/Paginas/precios-energia-electrica-comparacion-paises.aspx (accessed July 22, 2020).

[223] Ecopetrol. Precios históricos - GLP 2020. https://www.ecopetrol.com.co/wps/portal/Home/es/GruposInteres/Servicios/Precioshistoricos/glp (accessed July 22, 2020).

[224] Unidad de planeación Minero Energética (UPME). Aplicación - Calculadora de Emisiones 2020. http://www.upme.gov.co/Calculadora_Emisiones/aplicacion/calculadora.html# (accessed July 22, 2020).

[225] International Energy Agency (IEA). Special Report on Clean Energy Innovation: Accelerating technology progress for a sustainable future. 2020.

[226] International Energy Agency (IEA). ETP Clean Energy Technology Guide 2020. https://www.iea.org/articles/etp-clean-energy-technology-guide (accessed November 10, 2020).

[227] Srinivasan R, Nhan NT. A statistical approach for evaluating inherent benign-ness of chemical process routes in early design stages. Process Saf Environ Prot 2008;86:163–74. https://doi.org/10.1016/j.psep.2007.10.011.